

Introduction to Superconductivity

USQIS Summer School
DOE National Quantum Information Science Research Centers

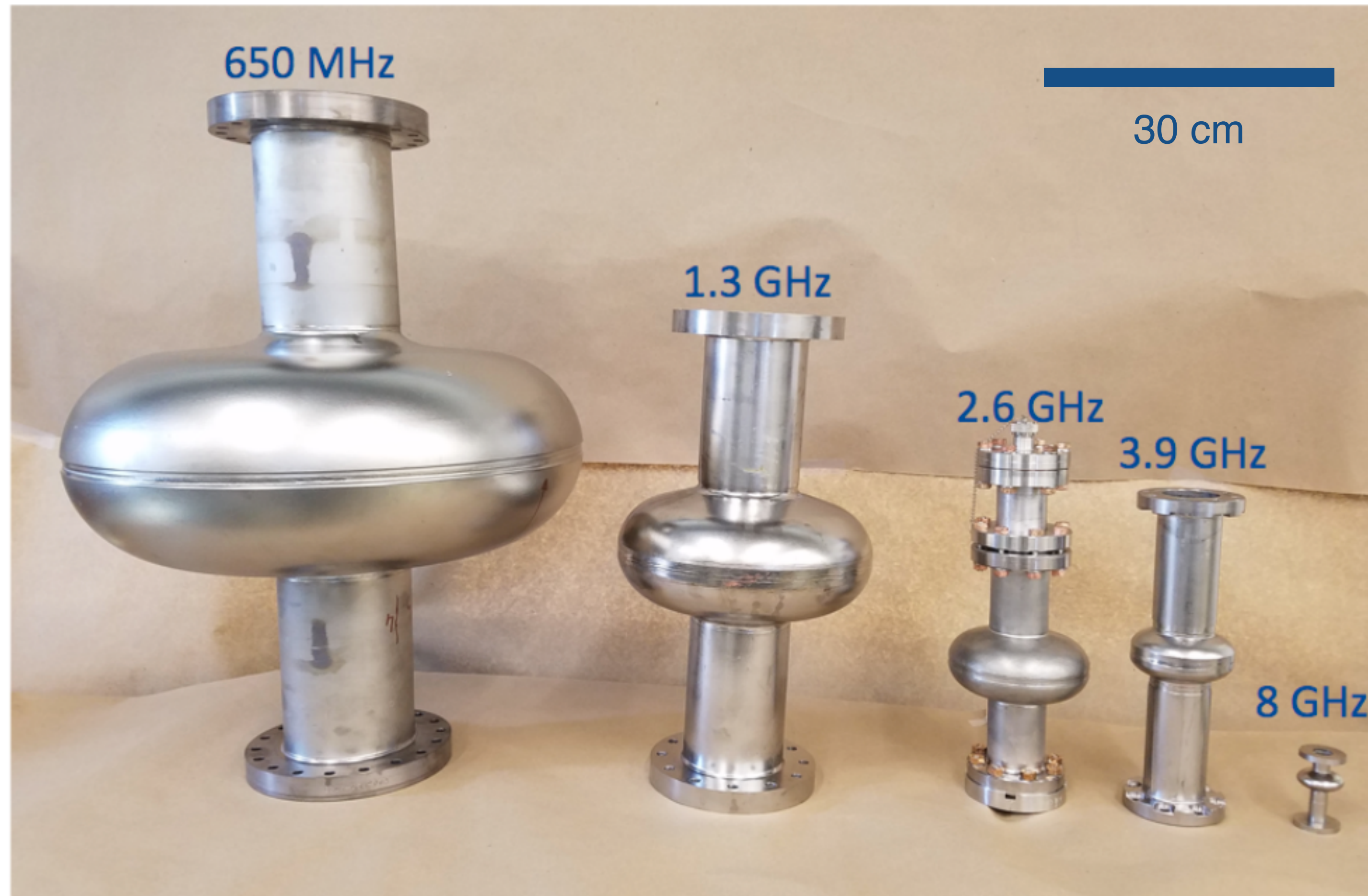


Jim Sauls

Hearne Institute of Theoretical Physics
Department of Physics and Astronomy
Louisiana State University, Baton Rouge LA

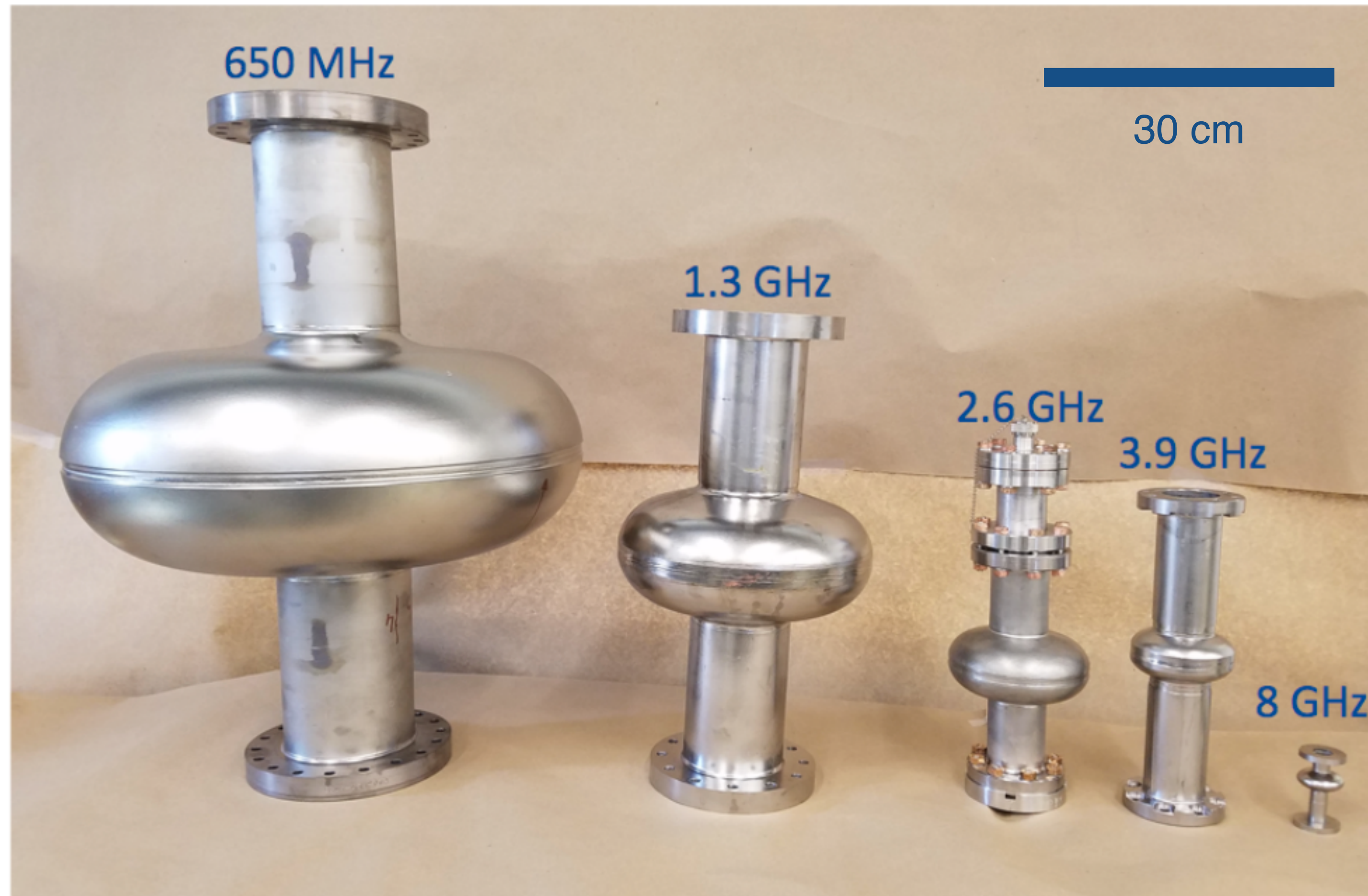


Niobium Superconducting RF (SRF) cavities



Niobium Superconducting RF (SRF) cavities

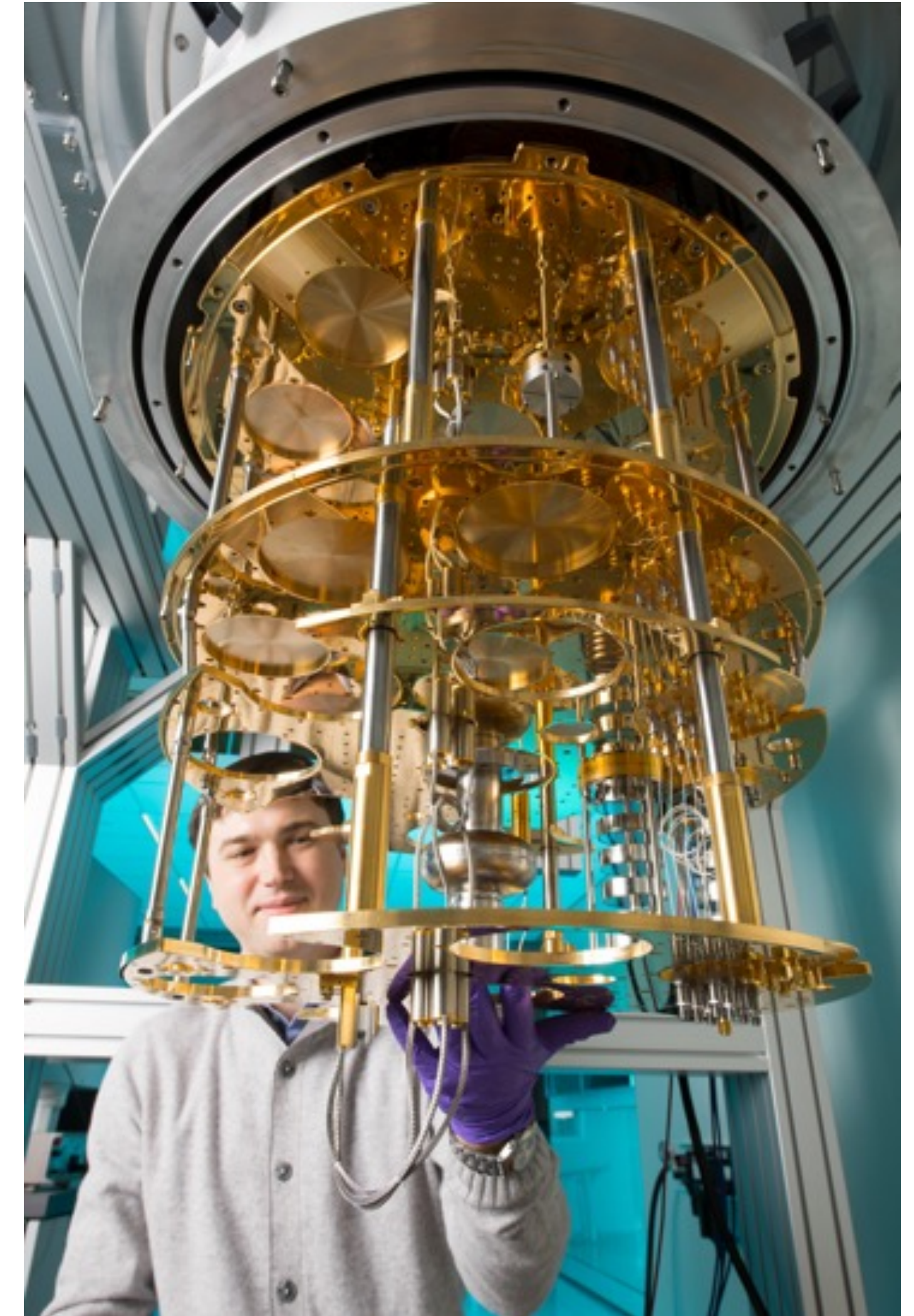
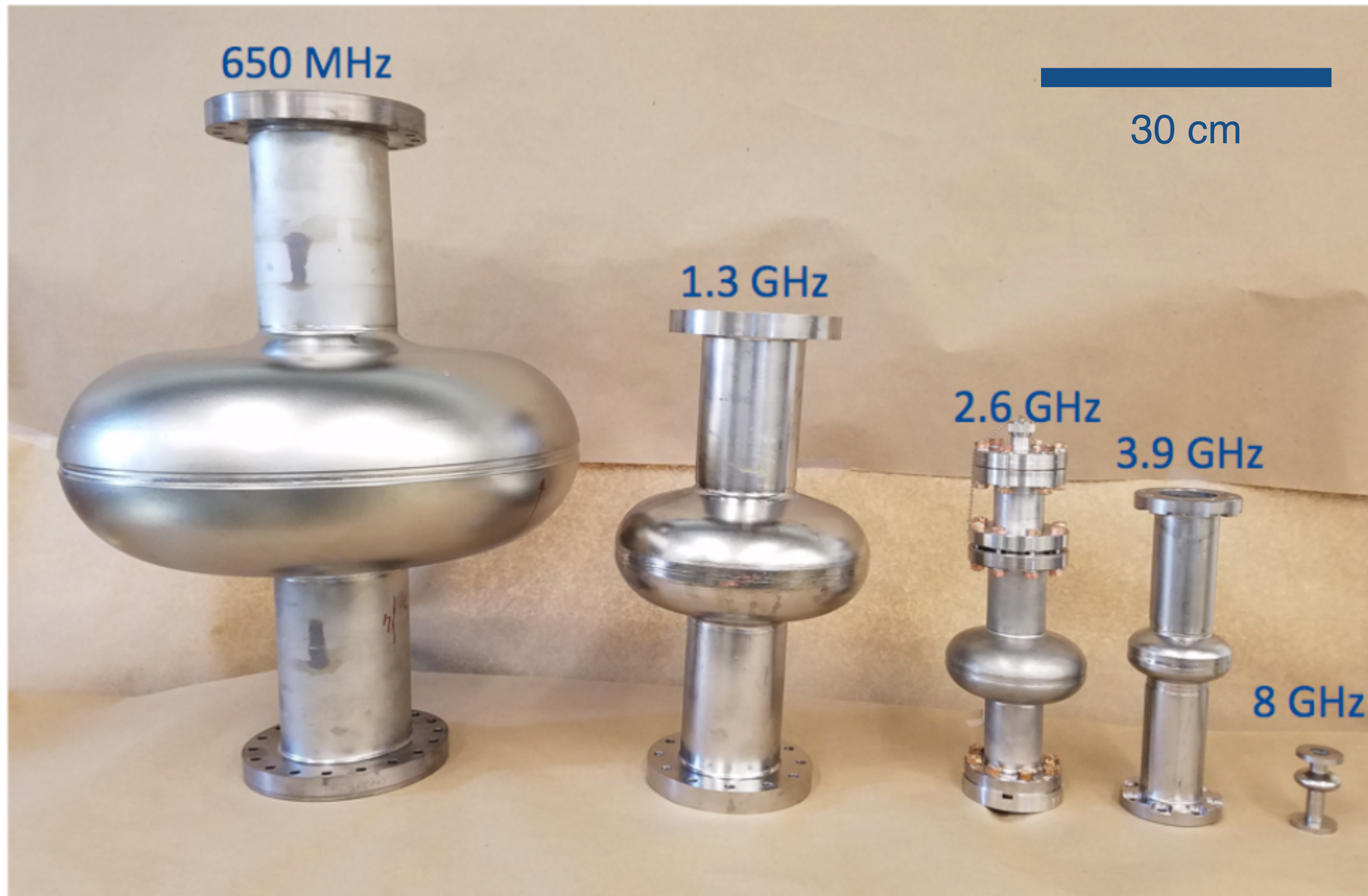
When cooled to temperatures well below the onset of superconductivity ...



Niobium SRF cavities are the most efficient
Electromagnetic resonators that have been engineered

Niobium Superconducting RF (SRF) cavities

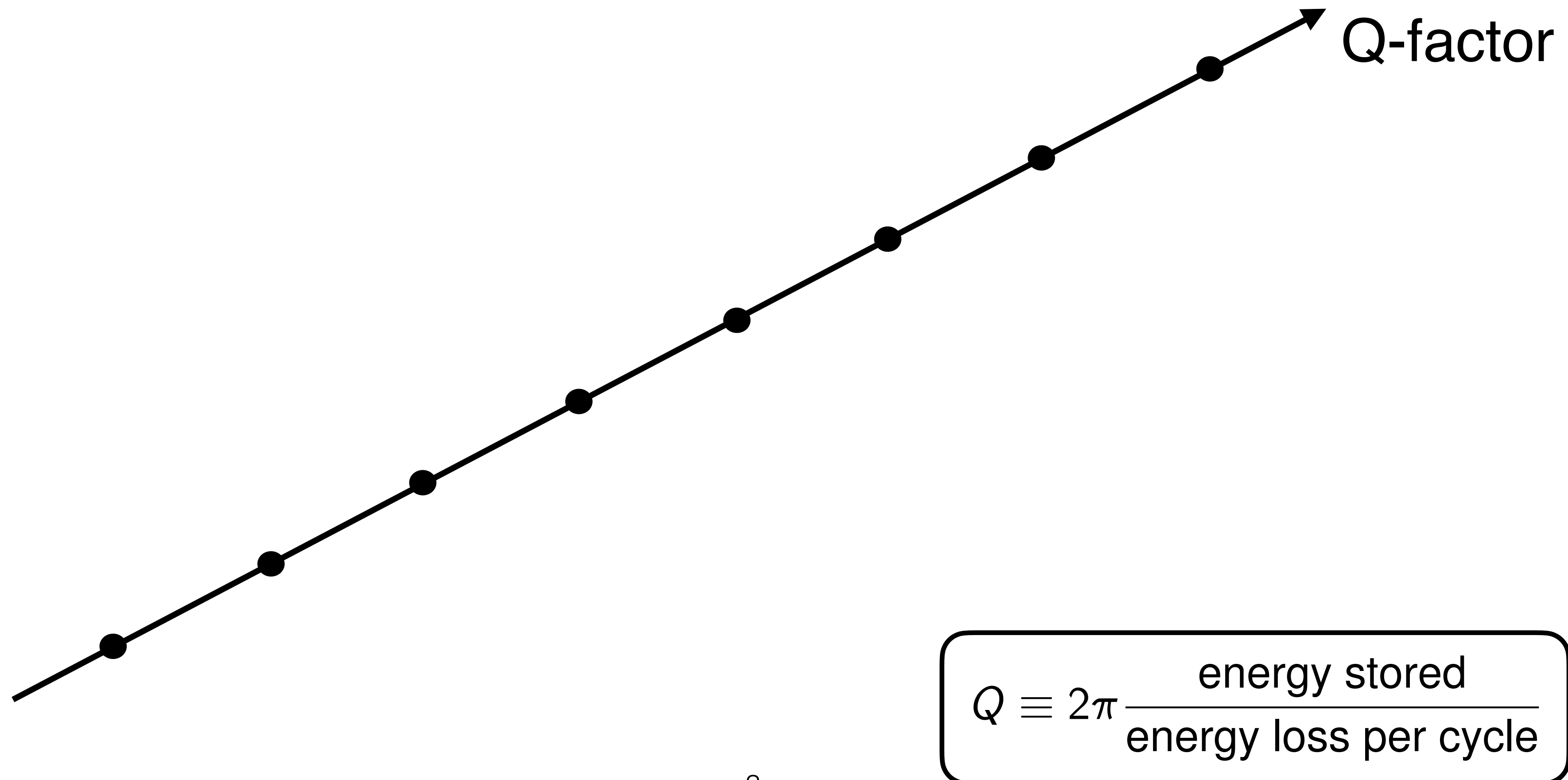
When cooled to temperatures well below the onset of superconductivity ...



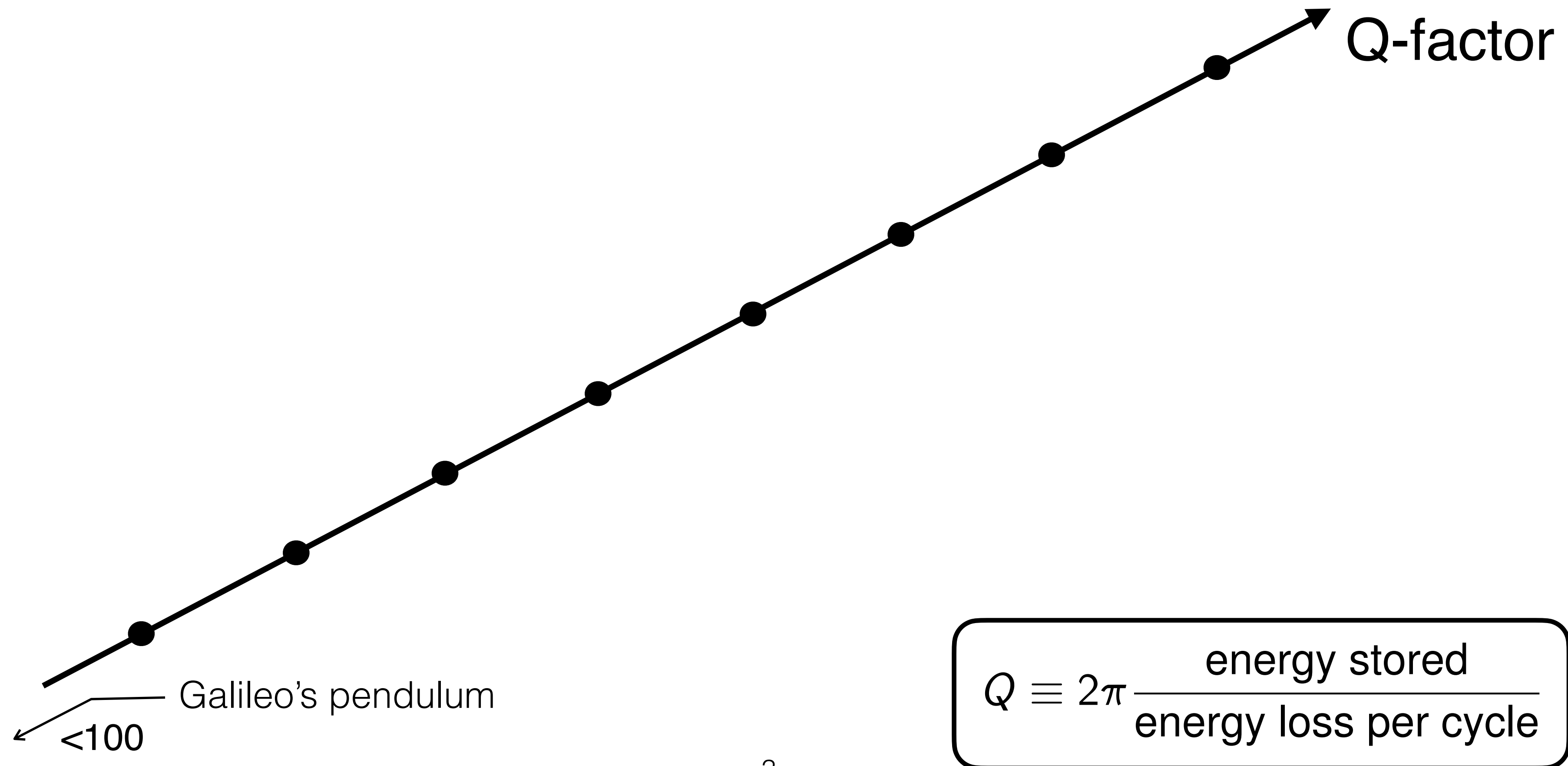
Niobium SRF cavities are the most efficient
Electromagnetic resonators that have been engineered

For quantum applications superconducting devices
are cooled in Helium dilution refrigerators down to
~10 milli-Kelvin above absolute zero

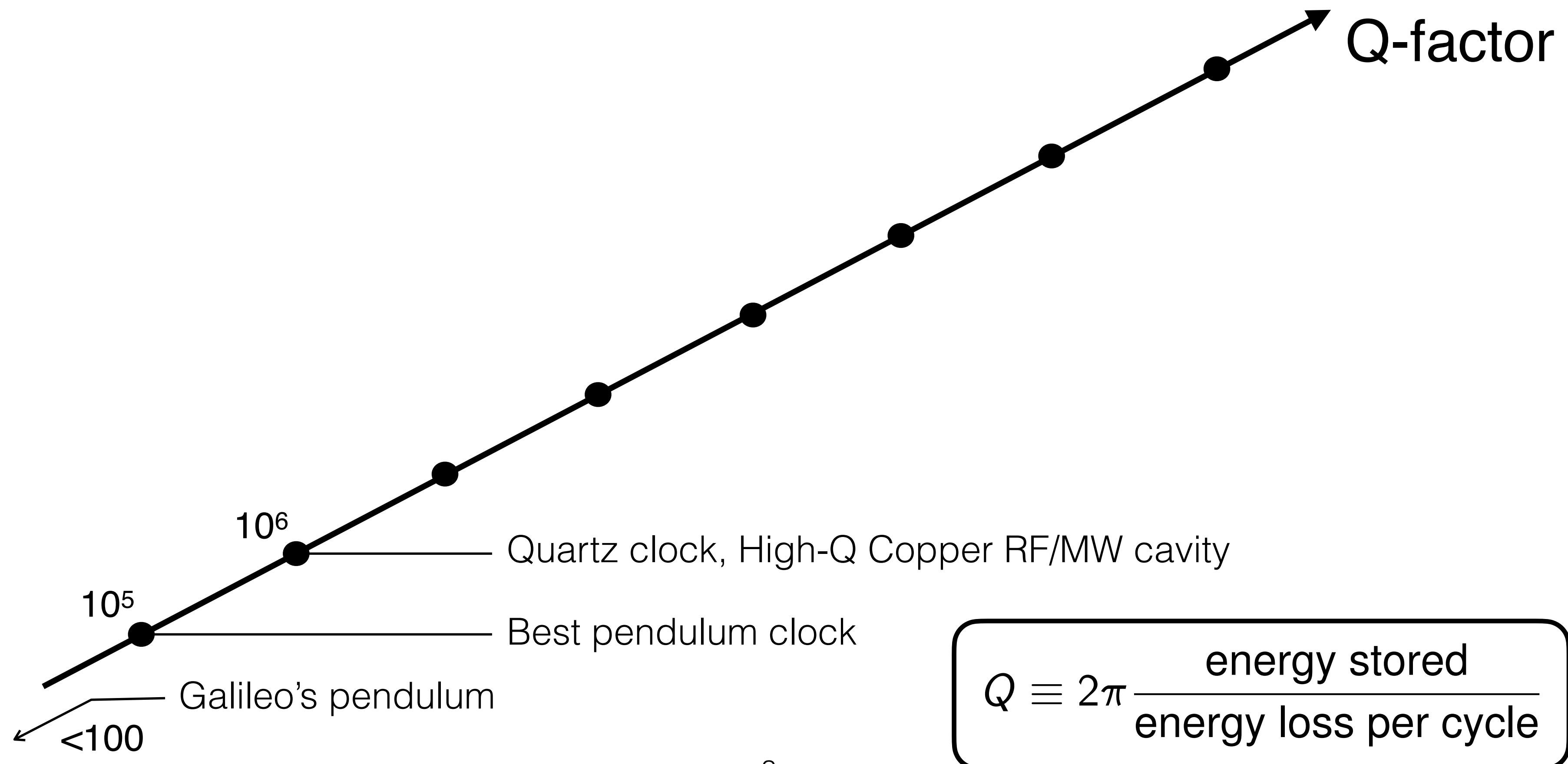
Superconducting RF (SRF) cavities is the most efficient engineered oscillator



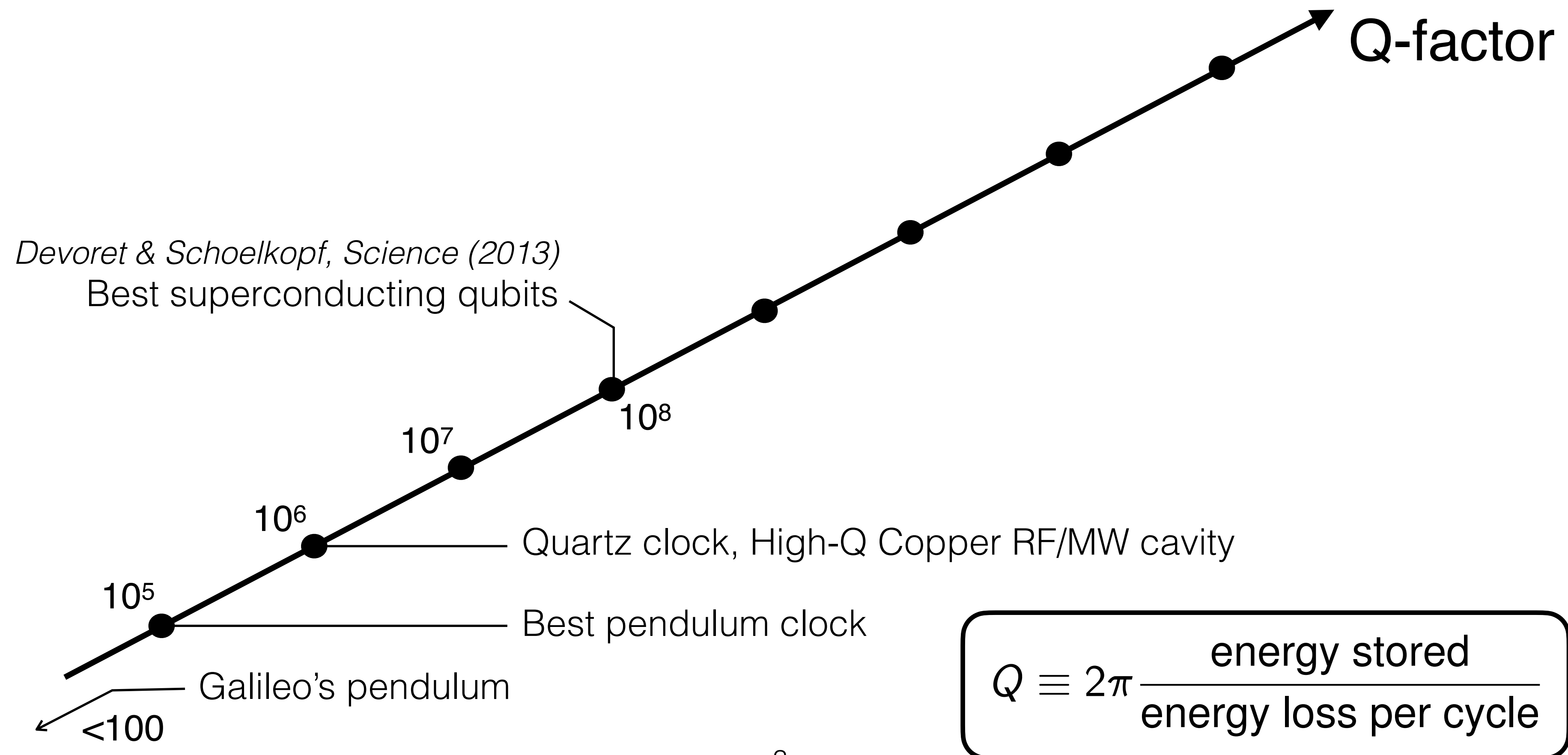
Superconducting RF (SRF) cavities is the most efficient engineered oscillator



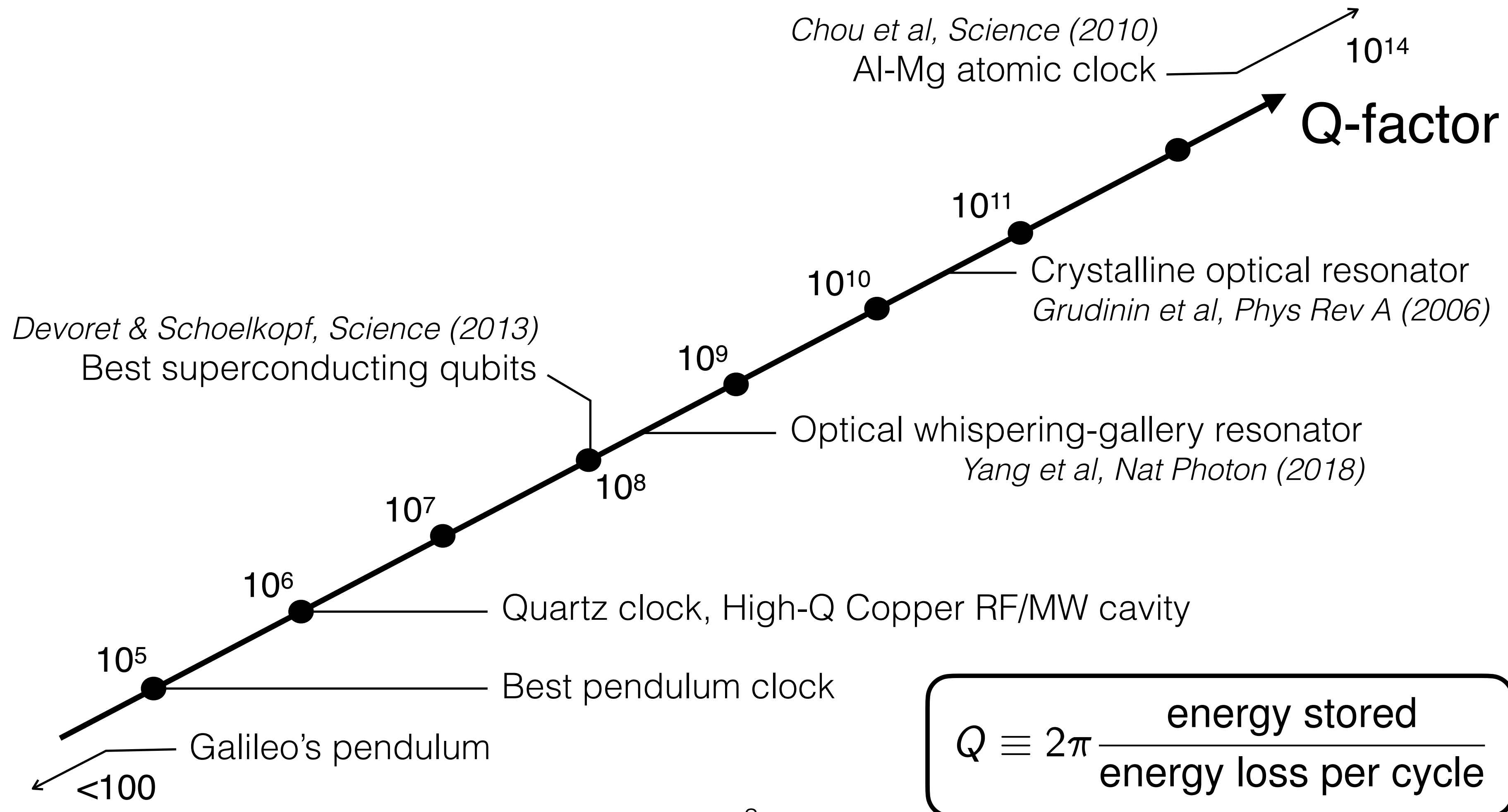
Superconducting RF (SRF) cavities is the most efficient engineered oscillator



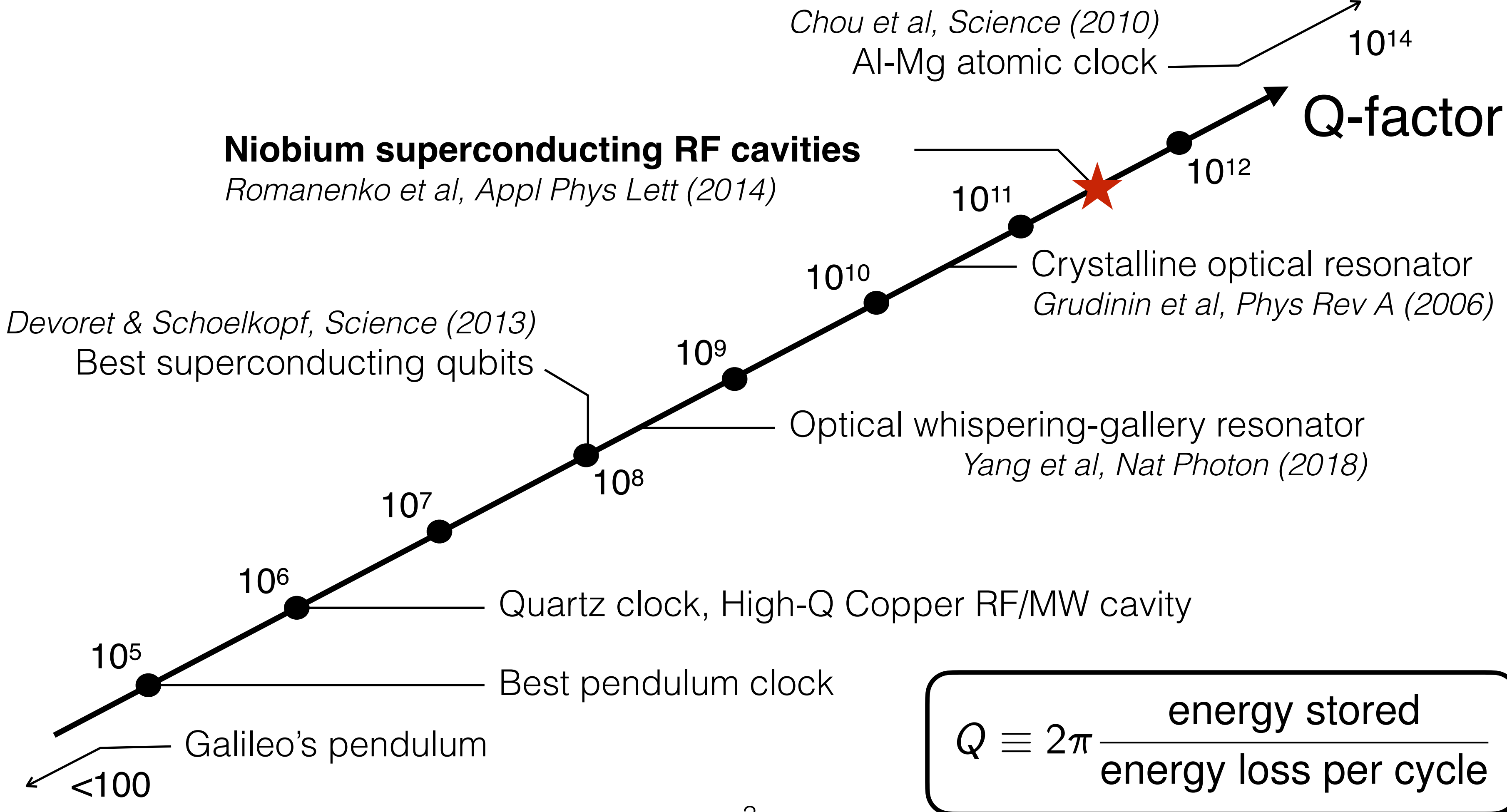
Superconducting RF (SRF) cavities is the most efficient engineered oscillator



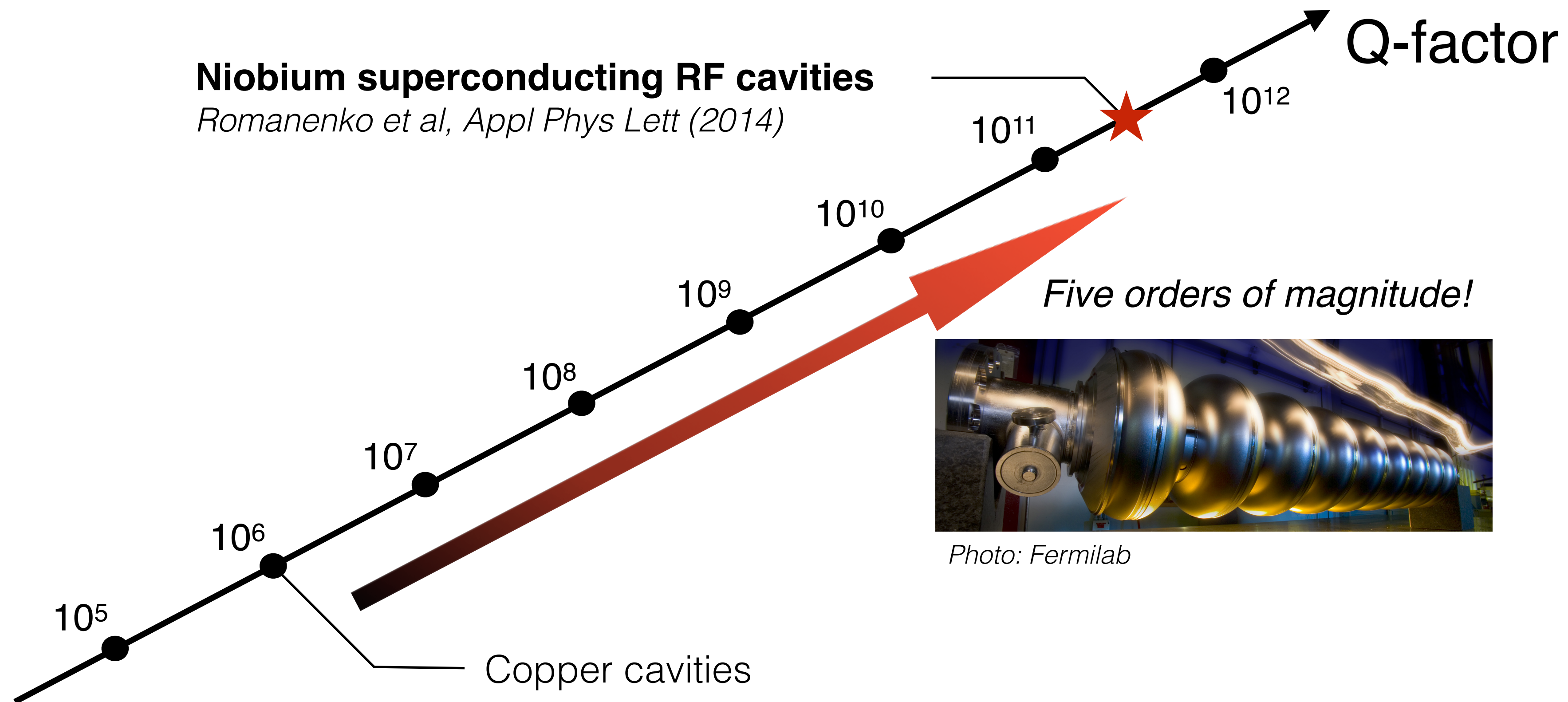
Superconducting RF (SRF) cavities is the most efficient engineered oscillator



Superconducting RF (SRF) cavities is the most efficient engineered oscillator



100,000 times more efficient than Cu-based RF technology



How efficient is $Q = 2 \times 10^{11}$?

How efficient is $Q = 2 \times 10^{11}$?

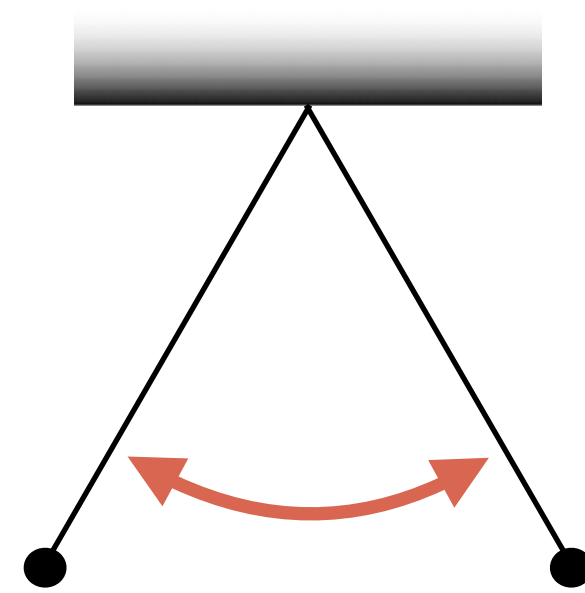
Galileo's pendulum would still be swinging if it were as efficient as today's best oscillators

1600AD

Scientific work on pendulum started



Galileo



Pendulum

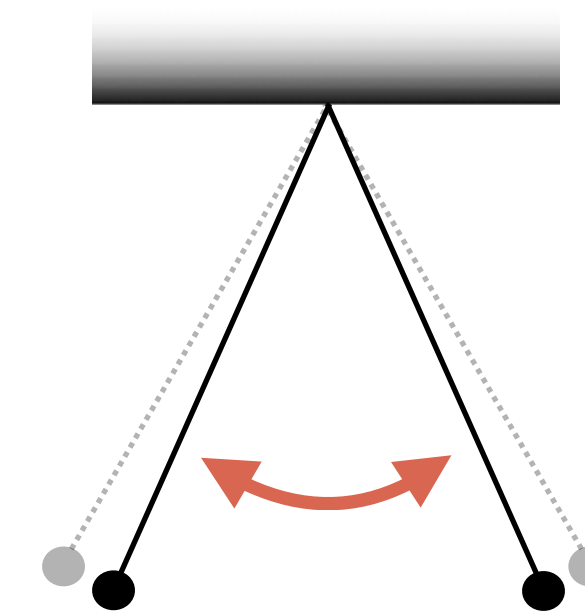
400
years


Today



Galileo

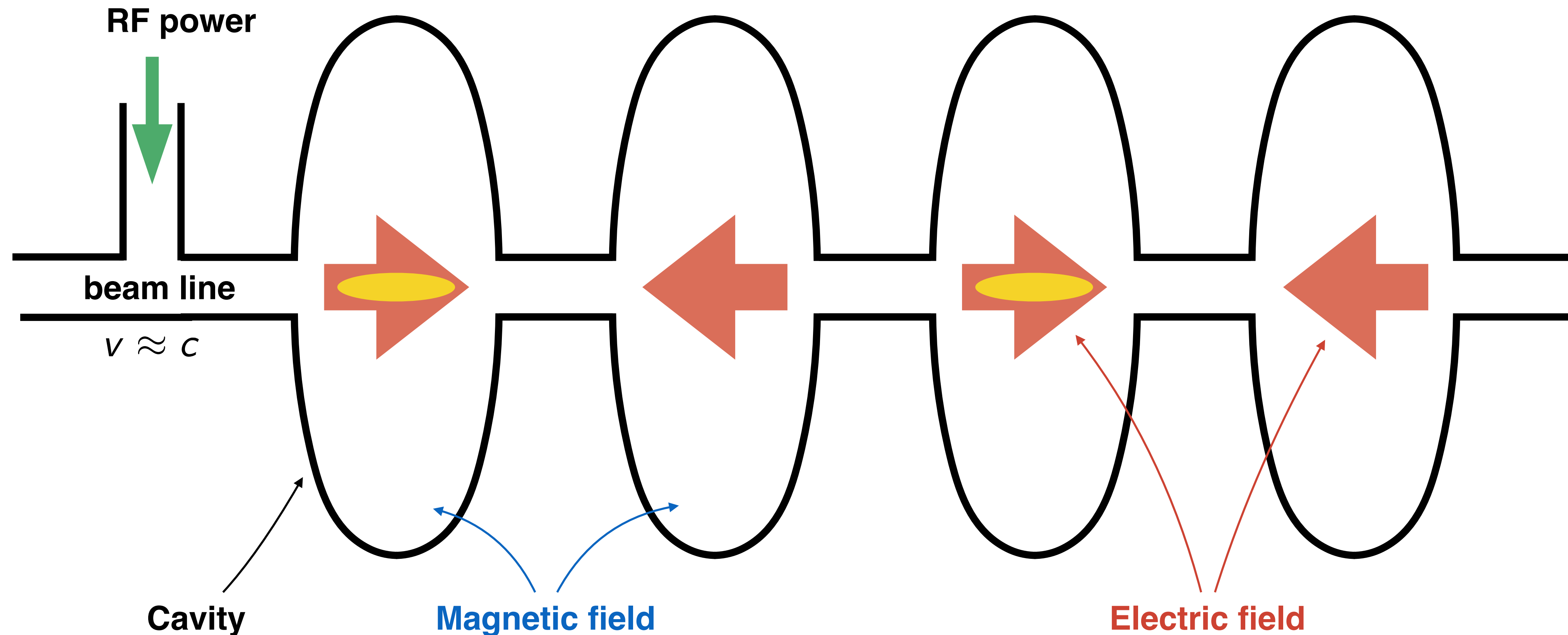
*Lost ~20% of
its amplitude*



Pendulum

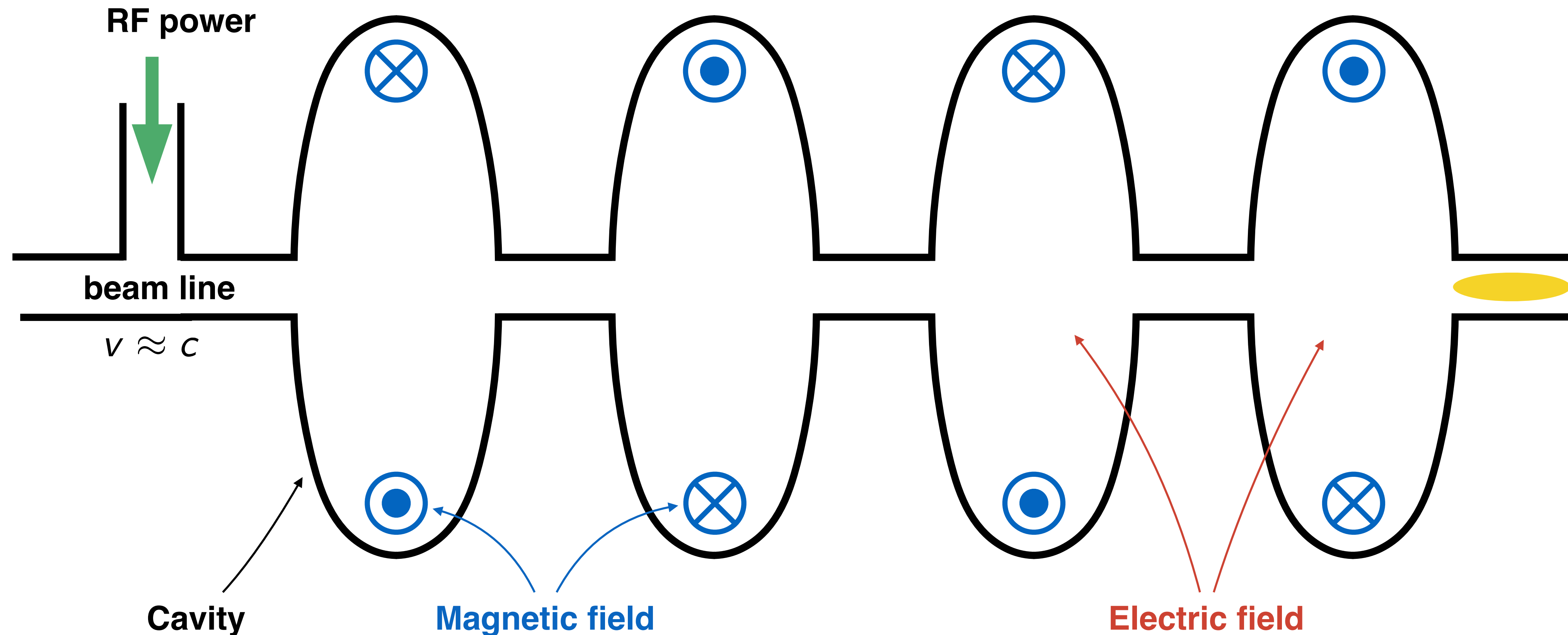
SRF cavities provide an effective method to accelerate charged particles to high energies

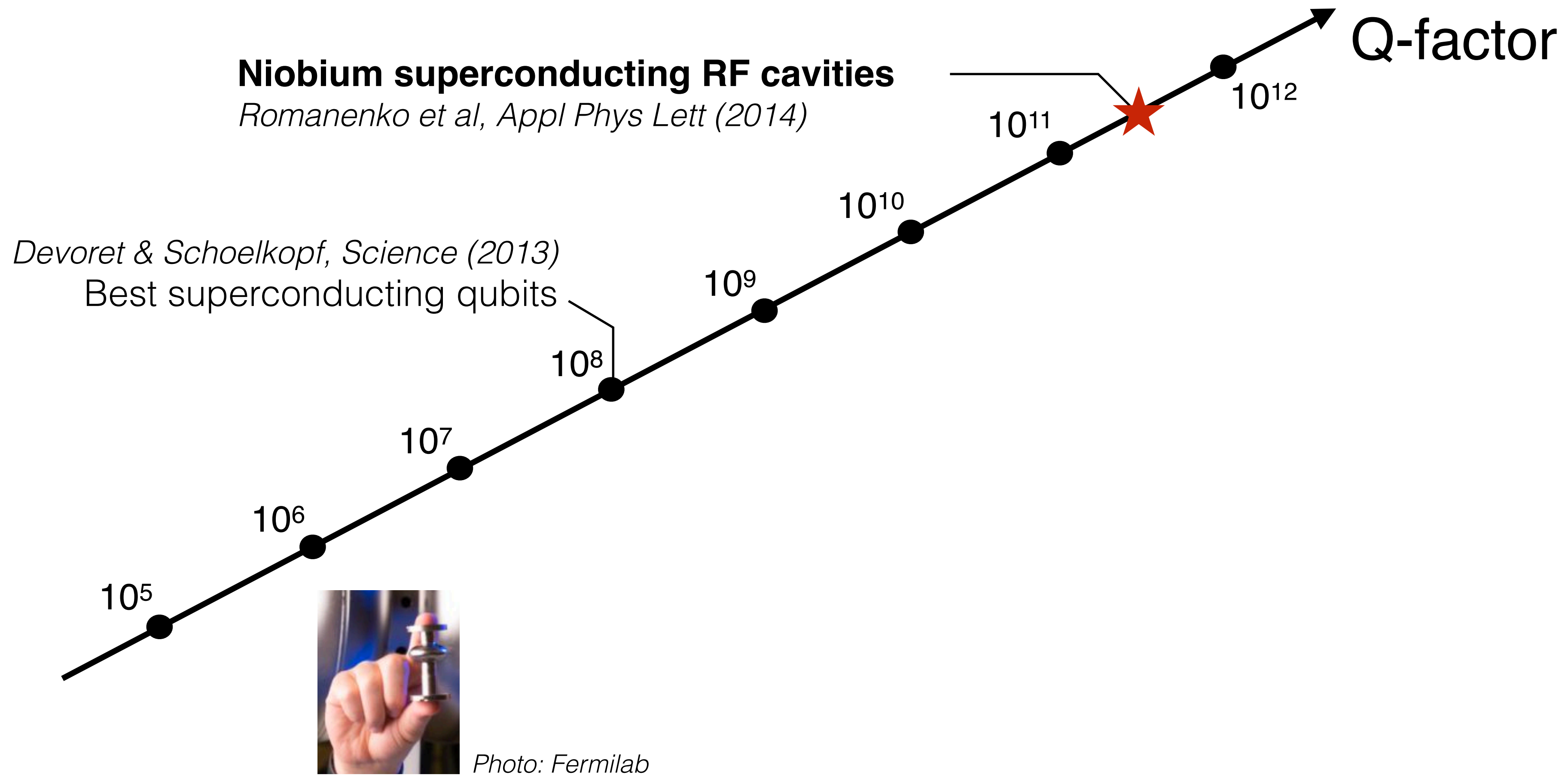
Cross section of linear accelerator



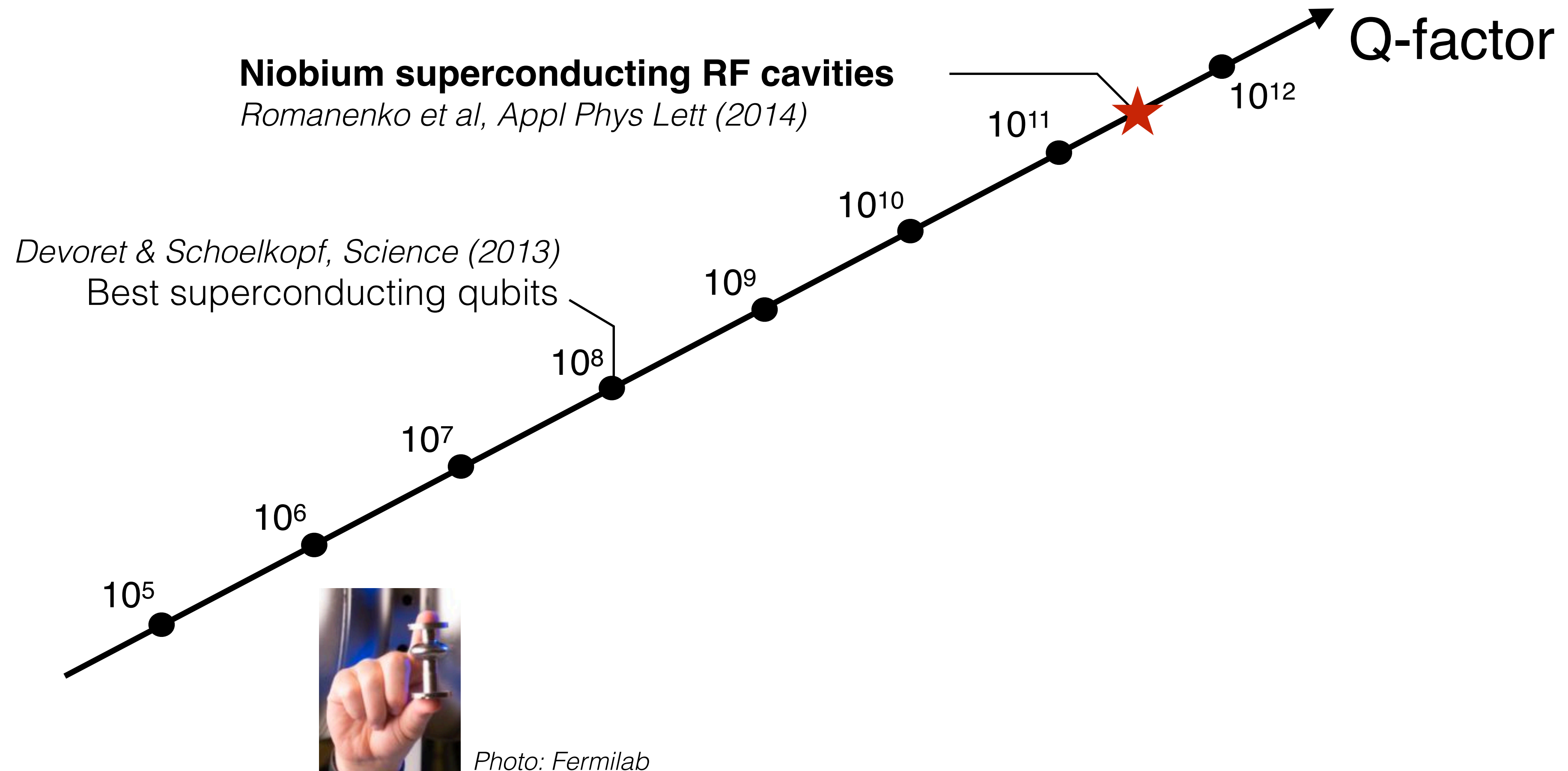
SRF cavities provide an effective method to accelerate charged particles to high energies

Cross section of linear accelerator



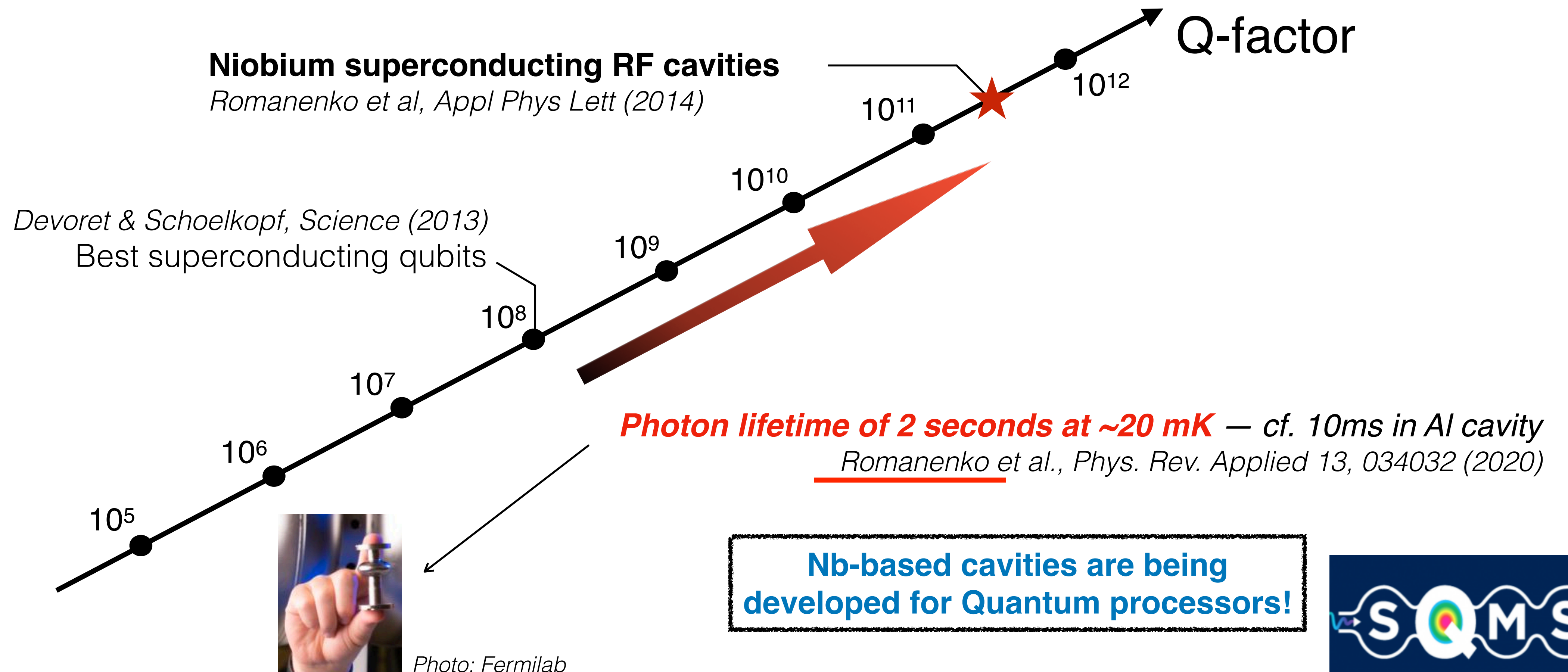


SRF Cavities in the Quantum Regime



SRF Cavities in the Quantum Regime

Nb SRF improved *photon* lifetimes by *a factor of 1,000!*



What else can we do with high Q Superconducting Resonators?

Look for rare events using
microwave photons

- ❖ Dark Matter Searches
- ❖ Tests of Low-Energy QED



❖ What are the key properties of superconductors?

❖ What are the key properties of superconductors?

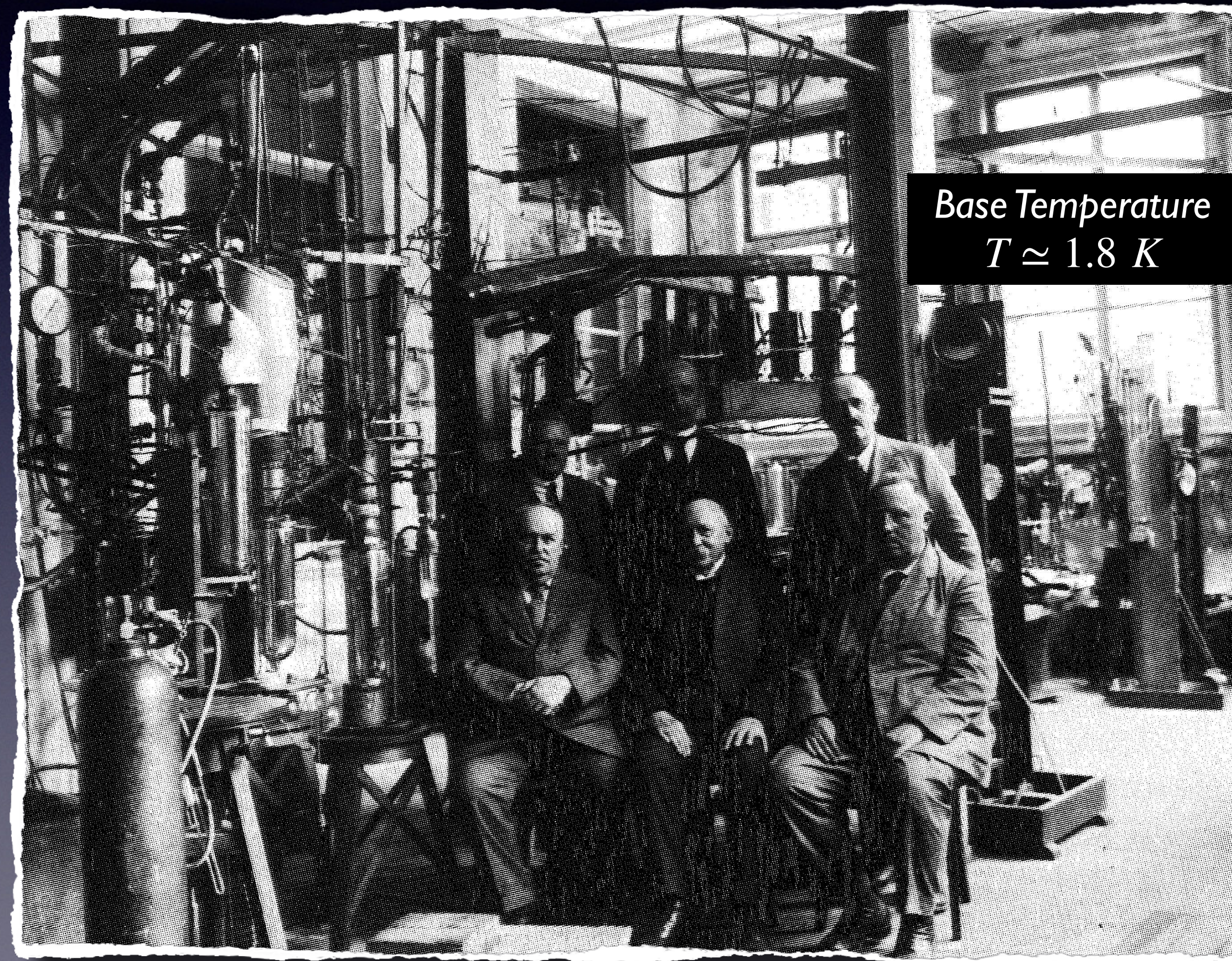
❖ How does superconductivity lead to high Q microwave resonators?

- ❖ What are the key properties of superconductors?
- ❖ How does superconductivity lead to high Q microwave resonators?
- ❖ What are some of the challenges to improving superconducting quantum devices for processors and sensors?

H. Kamerlingh Onnes' Laboratory

Leiden Institute of Physics

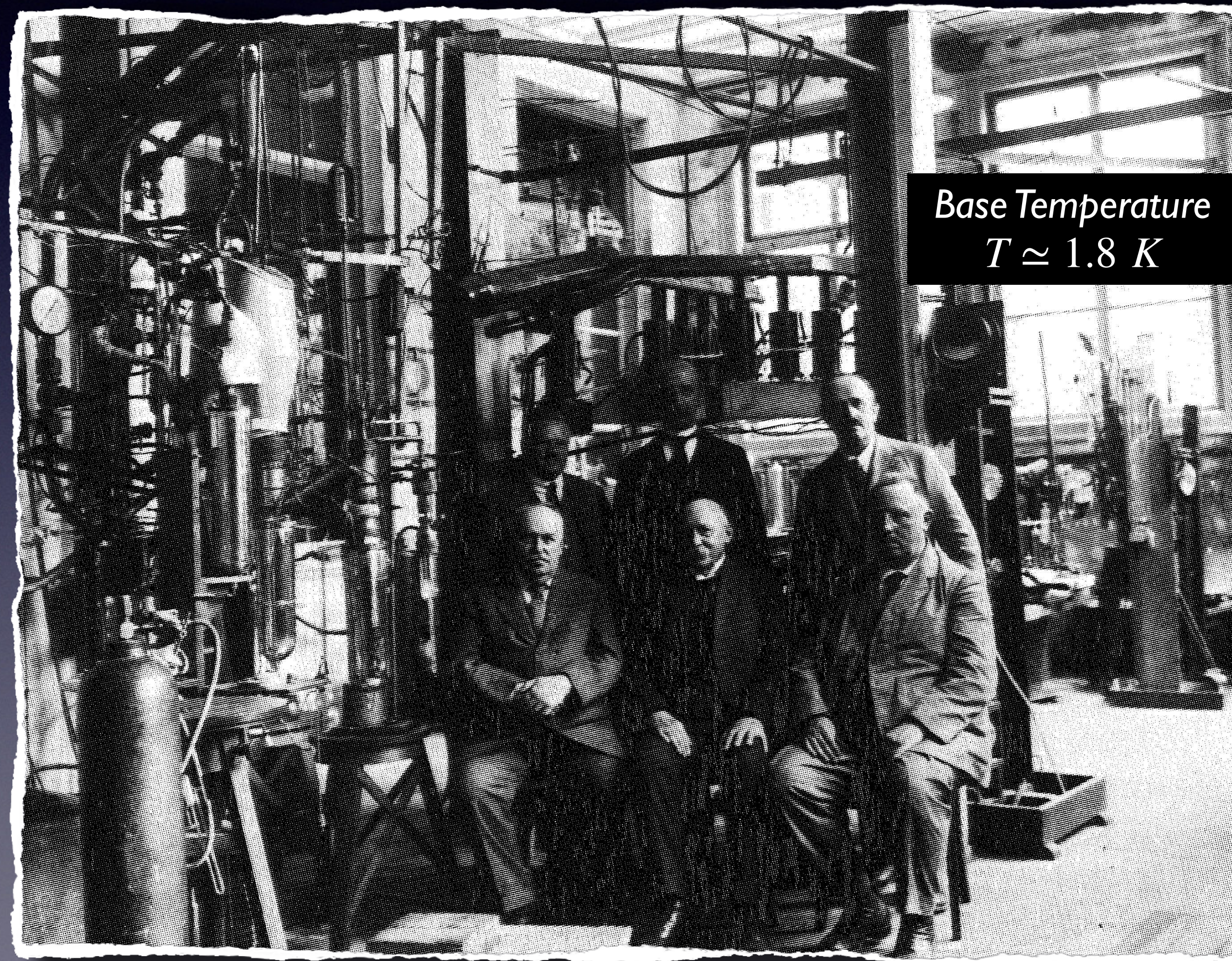
✓ 1908 - Liquefied Helium - New Era in Low Temperature Physics



H. Kamerlingh Onnes' Laboratory

Leiden Institute of Physics

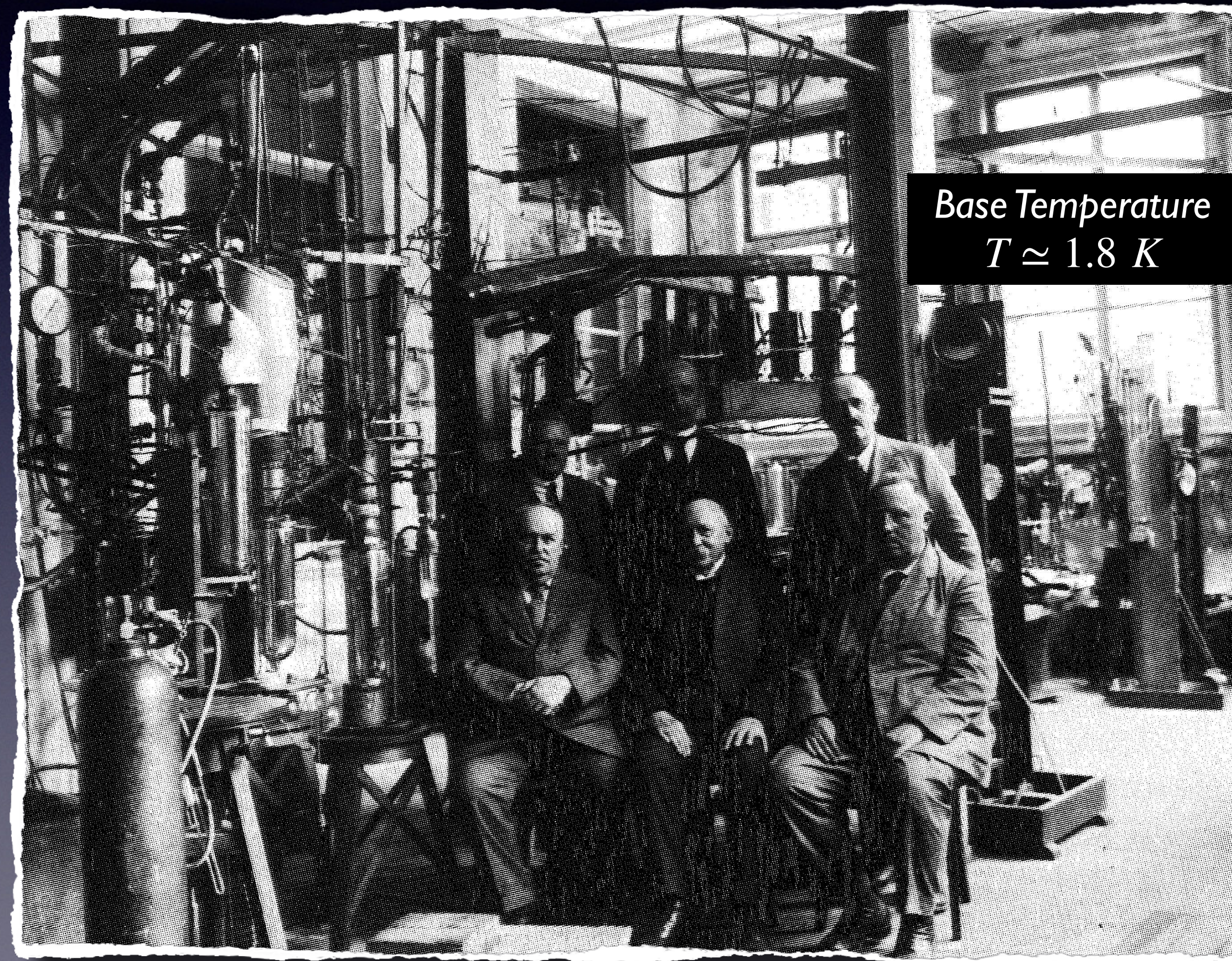
- ✓ 1908 - Liquified Helium - New Era in Low Temperature Physics
- ✓ 1910 - Low Temperature Resistance of Metals



H. Kamerlingh Onnes' Laboratory

Leiden Institute of Physics

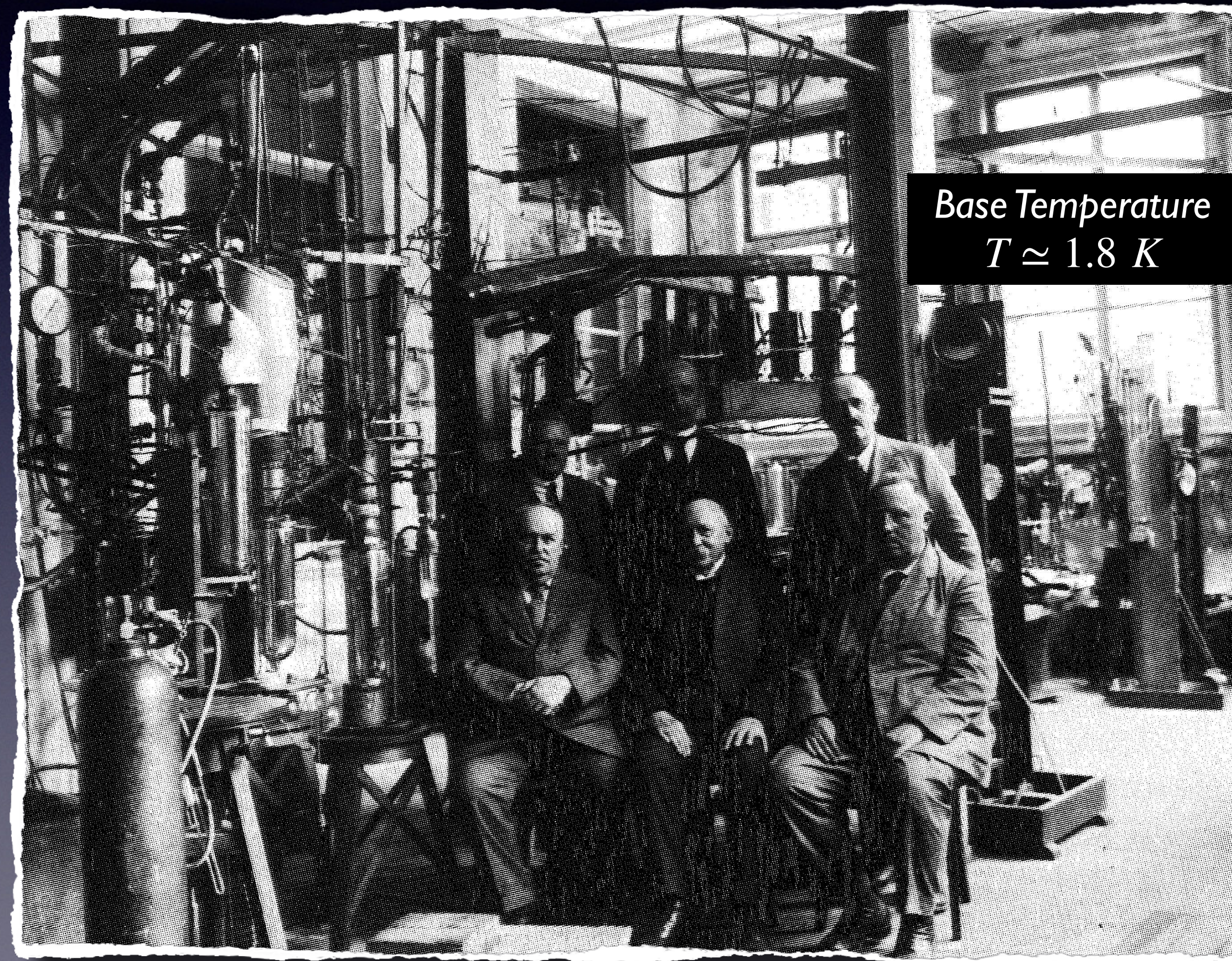
- ✓ 1908 - Liquefied Helium - New Era in Low Temperature Physics
- ✓ 1910 - Low Temperature Resistance of Metals
- ✓ 1911 - Discovered Superconductivity in Hg, Pb, Sn



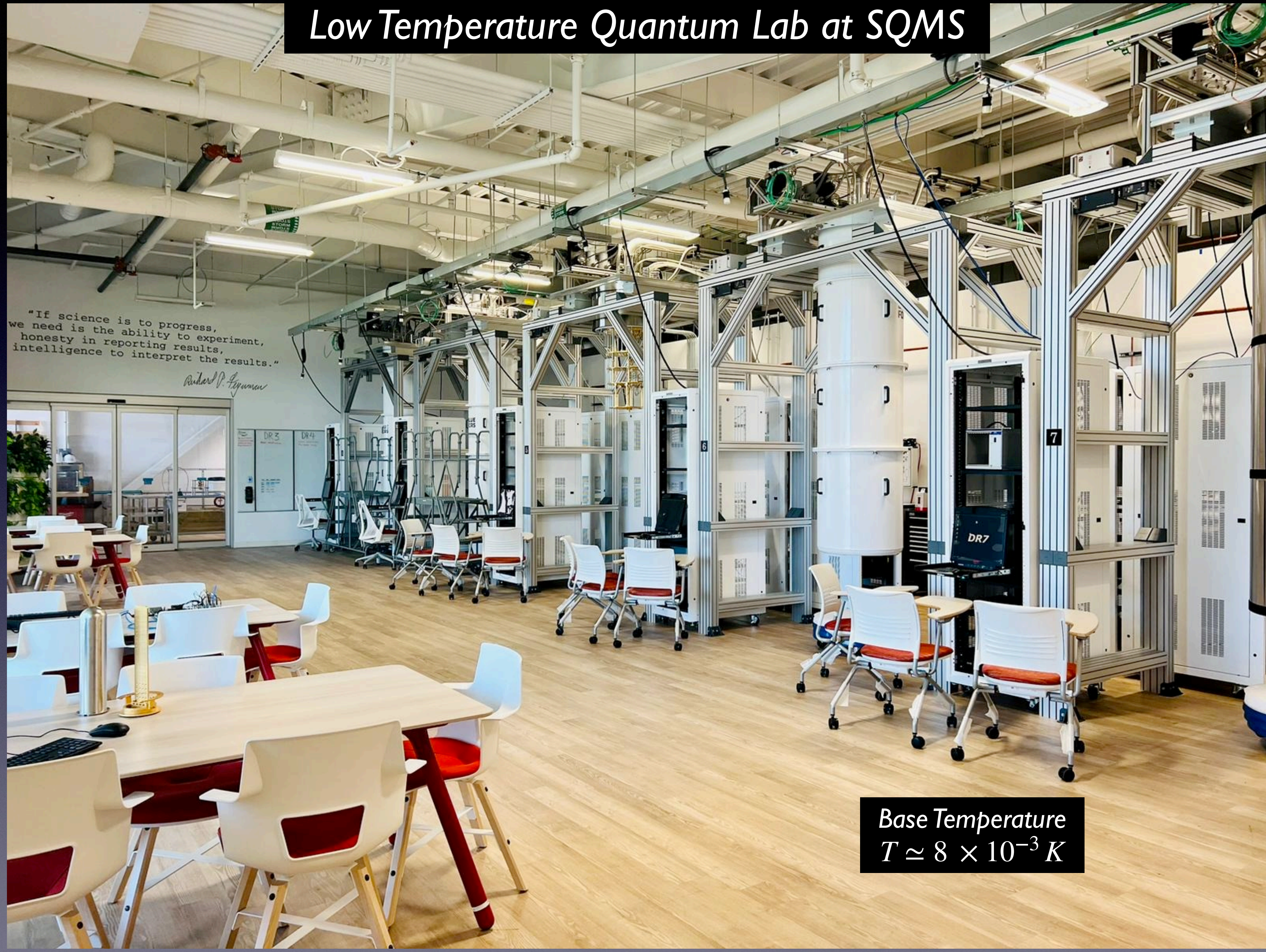
H. Kamerlingh Onnes' Laboratory

Leiden Institute of Physics

- ✓ 1908 - Liquefied Helium - New Era in Low Temperature Physics
- ✓ 1910 - Low Temperature Resistance of Metals
- ✓ 1911 - Discovered Superconductivity in Hg, Pb, Sn
- ✓ 1914 - Demonstrated Persistent Currents in a Pb ring.



Low Temperature Quantum Lab at SQMS



"If science is to progress,
we need is the ability to experiment,
honesty in reporting results,
intelligence to interpret the results."
Richard P. Feynman

Base Temperature
 $T \simeq 8 \times 10^{-3} K$

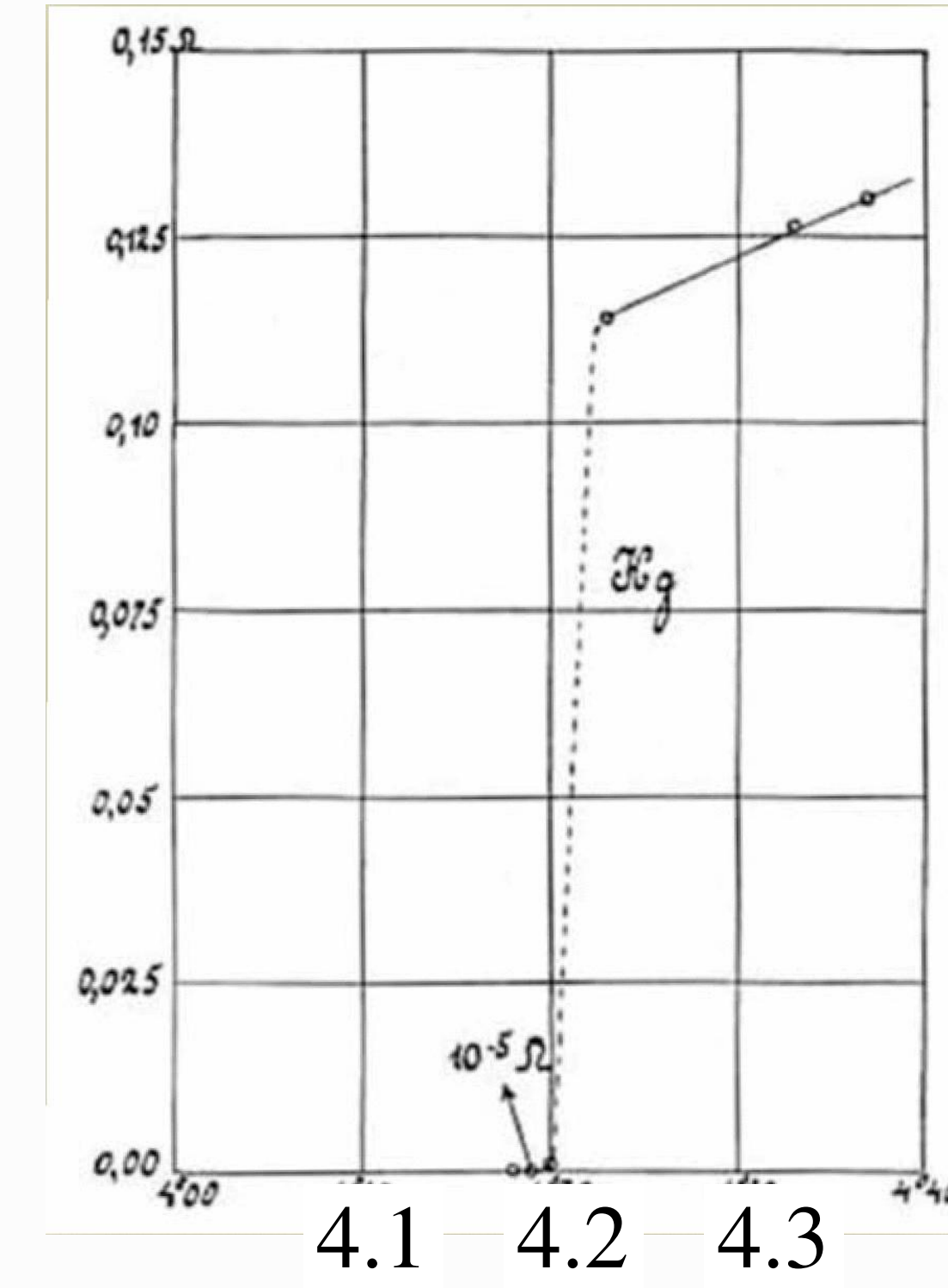
The Discovery of Superconductivity

Kammerlingh Onnes Laboratory, Leiden, April 8, 1911

Physics Today, September 2010, by Dirk van Delft and Peter Kes

- ▶ The experiment was started at 7am. Kamerlingh Onnes arrived when helium circulation began at 11:20am.
- ▶ The resistance of the mercury fell with the falling temperature. Soon after noon the gas thermometer denoted 5Kelvin.
- ▶ Then the team started to reduce the vapor pressure of the helium, and it began to evaporate rapidly. They measured its specific heat and stopped at a vapor pressure of 197 mmHg (0.26 atmospheres), corresponding to about 3K.
- ▶ Exactly at 4pm, the resistances of the gold and mercury were determined again. The latter was, in the historic entry, Mercury practically zero.

$R [\Omega]$



$T [K]$

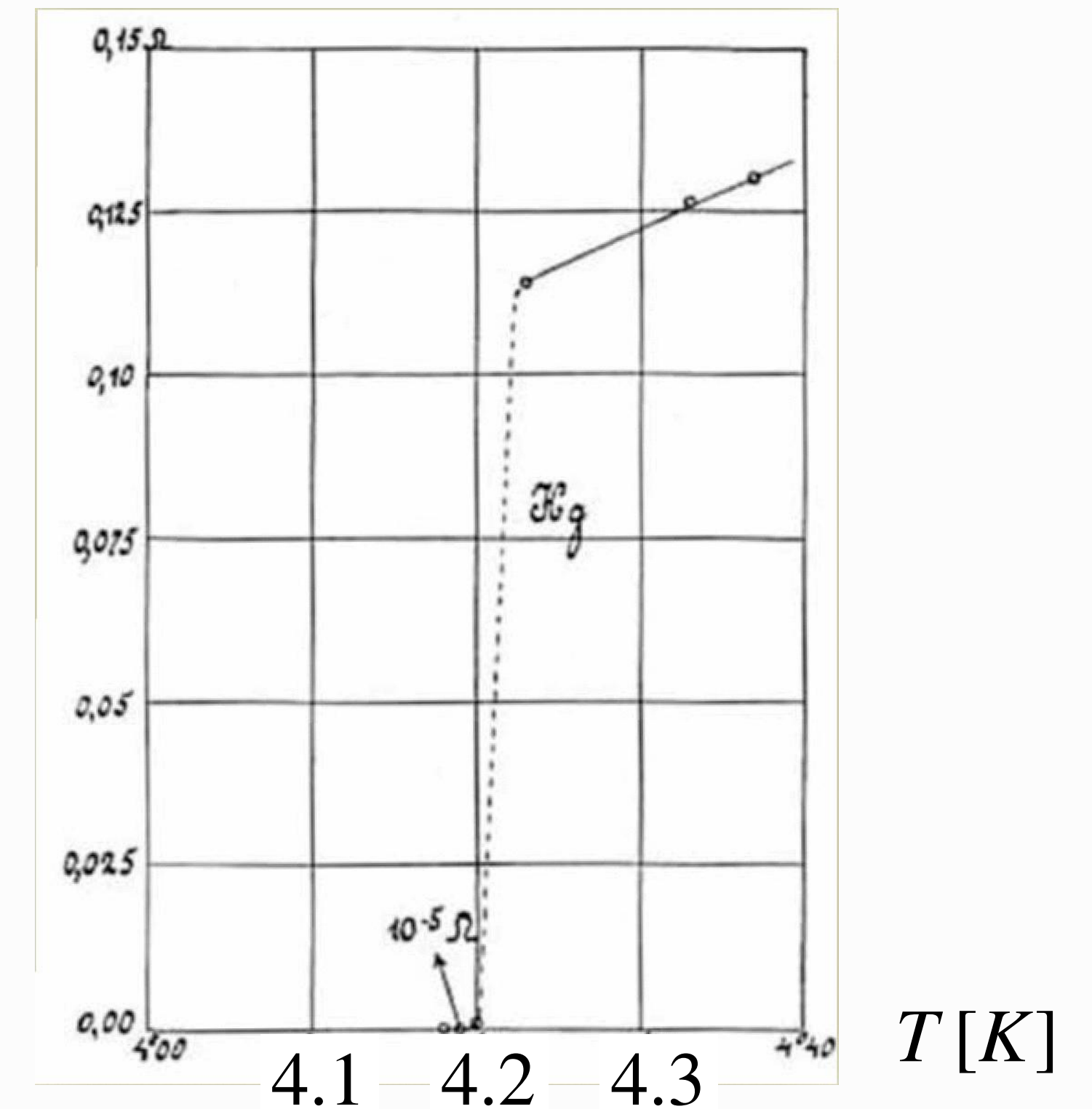
The Discovery of Superconductivity

Kammerlingh Onnes Laboratory, Leiden, April 8, 1911

Physics Today, September 2010, by Dirk van Delft and Peter Kes

- ▶ The experiment was started at 7am. Kamerlingh Onnes arrived when helium circulation began at 11:20am.
- ▶ The resistance of the mercury fell with the falling temperature. Soon after noon the gas thermometer denoted 5Kelvin.
- ▶ Then the team started to reduce the vapor pressure of the helium, and it began to evaporate rapidly. They measured its specific heat and stopped at a vapor pressure of 197 mmHg (0.26 atmospheres), corresponding to about 3K.
- ▶ Exactly at 4pm, the resistances of the gold and mercury were determined again. The latter was, in the historic entry, Mercury practically zero.

$R [\Omega]$



$T [K]$

- ▶ ... At the end of the day, Kamerlingh Onnes finished with an intriguing notebook entry: Dorsman [who had controlled and measured the temperatures] really had to hurry to make the observations. The temperature had been surprisingly hard to control. **Just before the lowest temperature [about 1.8 K] was reached, the boiling suddenly stopped and was replaced by evaporation in which the liquid visibly shrank. So, a remarkably strong evaporation at the surface.**

Without realizing the origin, the Leiden team had observed rapid heat transfer in the superfluid phase of liquid helium below 2.2 K discovered by J.F. Allen, A. D. Misener and P. Kapitza in 1937. [Nature, 141, 74 (1938)]

Elemental Superconductors

KNOWN SUPERCONDUCTIVE ELEMENTS

■ BLUE = AT AMBIENT PRESSURE
■ GREEN = ONLY UNDER HIGH PRESSURE

1A	1	H	IIA											IIIA	IVA	VA	VIA	VIIA	0	2	He
	2	3	4											5	6	7	8	9	10		
		Li	Be											B	C	N	O	F	Ne		
	3	11	12											13	14	15	16	17	18		
		Na	Mg	IIIB	IVB	VB	VIB	VII B	VII		IB	II B	Al	Si	P	S	Cl	Ar			
	4	19	20	21	22	23	24	25	26	27	28	29	30	31	32	33	34	35	36		
		K	Ca	Sc	Ti	Y	Cr	Mn	Fe	Co	Ni	Cu	Zn	Ga	Ge	As	Se	Br	Kr		
	5	37	38	39	40	41	42	43	44	45	46	47	48	49	50	51	52	53	54		
		Rb	Sr	Y	Zr	Nb	Mo	Tc	Ru	Rh	Pd	Ag	Cd	In	Sn	Sb	Te	I	Xe		
	6	55	56	57	72	73	74	75	76	77	78	79	80	81	82	83	84	85	86		
		Cs	Ba	*La	Hf	Ta	W	Re	Os	Ir	Pt	Au	Hg	Tl	Pb	Bi	Po	At	Rn		
	7	87	88	89	104	105	106	107	108	109	110	111	112								
		Fr	Ra	+Ac	Rf	Ha	106	107	108	109	110	111	112								

SUPERCONDUCTORS.ORG

* Lanthanide Series	58	59	60	61	62	63	64	65	66	67	68	69	70	71
	Ce	Pr	Nd	Pm	Sm	Eu	Gd	Tb	Dy	Ho	Er	Tm	Yb	Lu
+ Actinide Series	90	91	92	93	94	95	96	97	98	99	100	101	102	103
	Th	Pa	U	Np	Pu	Am	Cm	Bk	Cf	Es	Fm	Md	No	Lr

- ▶ Lowest T_c Elemental Superconductor: Rh: $T_c = 0.32 \times 10^{-3} K$
- ▶ Highest T_c Elemental Superconductor: Nb: $T_c = 9.33 K$
- ▶ Highest T_c Superconducting Compound: $(\text{Hg}_{0.8}\text{Tl}_{0.2})\text{Ba}_2\text{Ca}_2\text{Cu}_3\text{O}_{8.33}$: $T_c = 138 K$

Elemental Superconductors

KNOWN SUPERCONDUCTIVE ELEMENTS

■ BLUE = AT AMBIENT PRESSURE
■ GREEN = ONLY UNDER HIGH PRESSURE

1A	1	H	IIA											IIIA	IVA	VA	VIA	VIIA	0	2	He
	1	3	4											5	6	7	8	9	10		
	2	Li	Be											B	C	N	O	F	Ne		
	3	11	12	III B	IV B	V B	VI B	VII B	VIII B	IX B	X B	13	14	15	16	17	18				
	4	19	20	21	22	23	24	25	26	27	28	29	30	31	32	33	34	35	36		
	5	37	38	39	40	41	42	43	44	45	46	47	48	49	50	51	52	53	54		
	6	55	56	*La	72	73	74	75	76	77	78	79	80	81	82	83	84	85	86		
	7	87	88	+Ac	104	105	106	107	108	109	110	111	112								
		Fr	Ra		Rf	Ha	106	107	108	109	110	111	112								

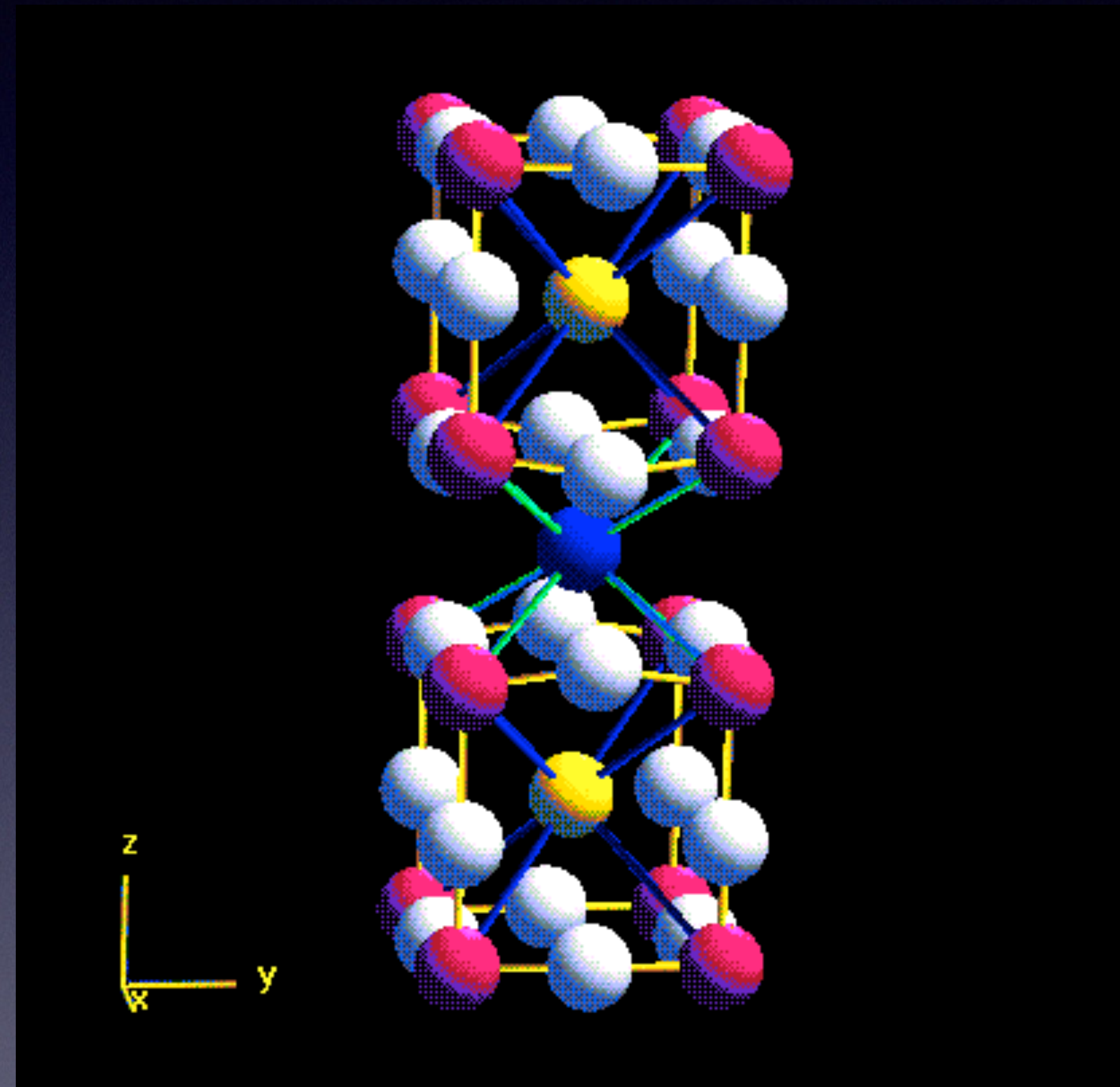
SUPERCONDUCTORS.ORG

* Lanthanide Series	58	59	60	61	62	63	64	65	66	67	68	69	70	71
	Ce	Pr	Nd	Pm	Sm	Eu	Gd	Tb	Dy	Ho	Er	Tm	Yb	Lu
+ Actinide Series	90	91	92	93	94	95	96	97	98	99	100	101	102	103
	Th	Pa	U	Np	Pu	Am	Cm	Bk	Cf	Es	Fm	Md	No	Lr

- ▶ Lowest T_c Elemental Superconductor: Rh: $T_c = 0.32 \times 10^{-3} K$
- ▶ Highest T_c Elemental Superconductor: Nb: $T_c = 9.33 K$
- ▶ Highest T_c Superconducting Compound: $(\text{Hg}_{0.8}\text{Tl}_{0.2})\text{Ba}_2\text{Ca}_2\text{Cu}_3\text{O}_{8.33}$: $T_c = 138 K$

High Tc Superconductors

$Y_{0.5}Lu_{0.5}Ba_2Cu_3O_7$	107 K
$(Y_{0.5}Tm_{0.5})Ba_2Cu_3O_7$	105 K
$(Y_{0.5}Gd_{0.5})Ba_2Cu_3O_7$	97 K
$Y_2CaBa_4Cu_7O_{16}$	97 K
$Y_3Ba_4Cu_7O_{16}$	96 K
$NdBa_2Cu_3O_7$	96 K
$Y_2Ba_4Cu_7O_{15}$	95 K
$GdBa_2Cu_3O_7$	94 K
$YBa_2Cu_3O_7$	92 K
$TmBa_2Cu_3O_7$	90 K
$YbBa_2Cu_3O_7$	89 K
$YSr_2Cu_3O_7$	62 K



<http://superconductors.org/>

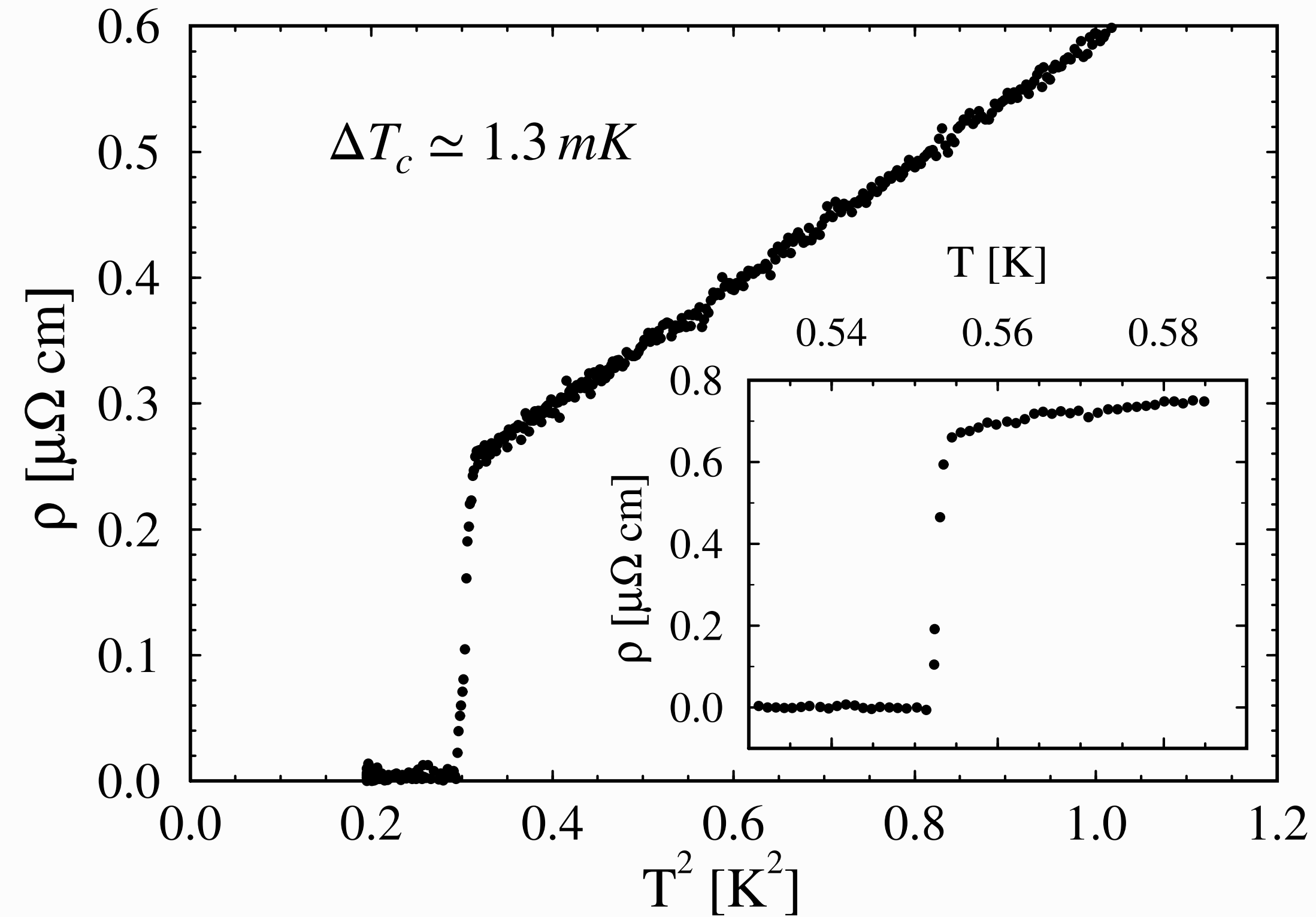
$Bi_{1.6}Pb_{0.6}Sr_2Ca_2Sb_{0.1}Cu_3O_y$	115 K
$Bi_2Sr_2Ca_2Cu_3O_{10}^{***}$	110 K
$Bi_2Sr_2CaCu_2O_9^{***}$	110 K
$Bi_2Sr_2(Ca_{0.8}Y_{0.2})Cu_2O_8$	95-96K
$Bi_2Sr_2CaCu_2O_8$	91-92K

$(Hg_{0.8}Tl_{0.2})Ba_2Ca_2Cu_3O_{8.33}$	138 K*
$HgBa_2Ca_2Cu_3O_8$	133-135 K
$HgBa_2Ca_3Cu_4O_{10+}$	125-126 K
$HgBa_2(Ca_{1-x}Sr_x)Cu_2O_{6+}$	123-125 K
$HgBa_2CuO_{4+}$	94-98 K

<http://phycomp.technion.ac.il/~ira/superconductors.html>

Superconductivity in Single Crystals of UPt₃

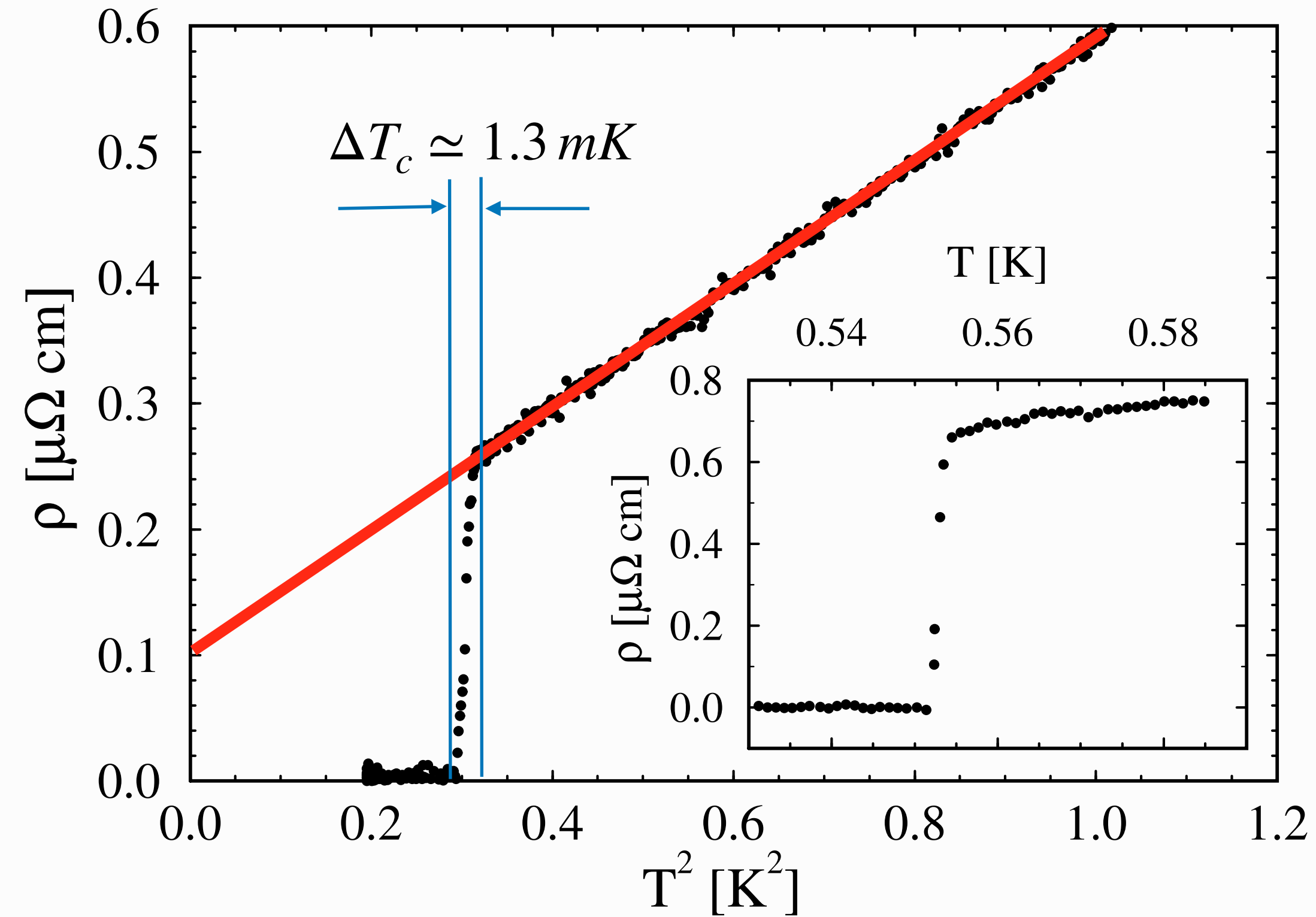
J.B. Kycia et al., Phys. Rev. B 58, R603 (1998).



- ▶ Resistivity of UPt₃ annealed at 900°C. $\rho = \rho_0 + AT^2$
- ▶ $T_c = 552 \text{ mK}$ Inset: Superconducting transition for a sample annealed at 800°C. The transition *width* is 1.3 mK.

Superconductivity in Single Crystals of UPt_3

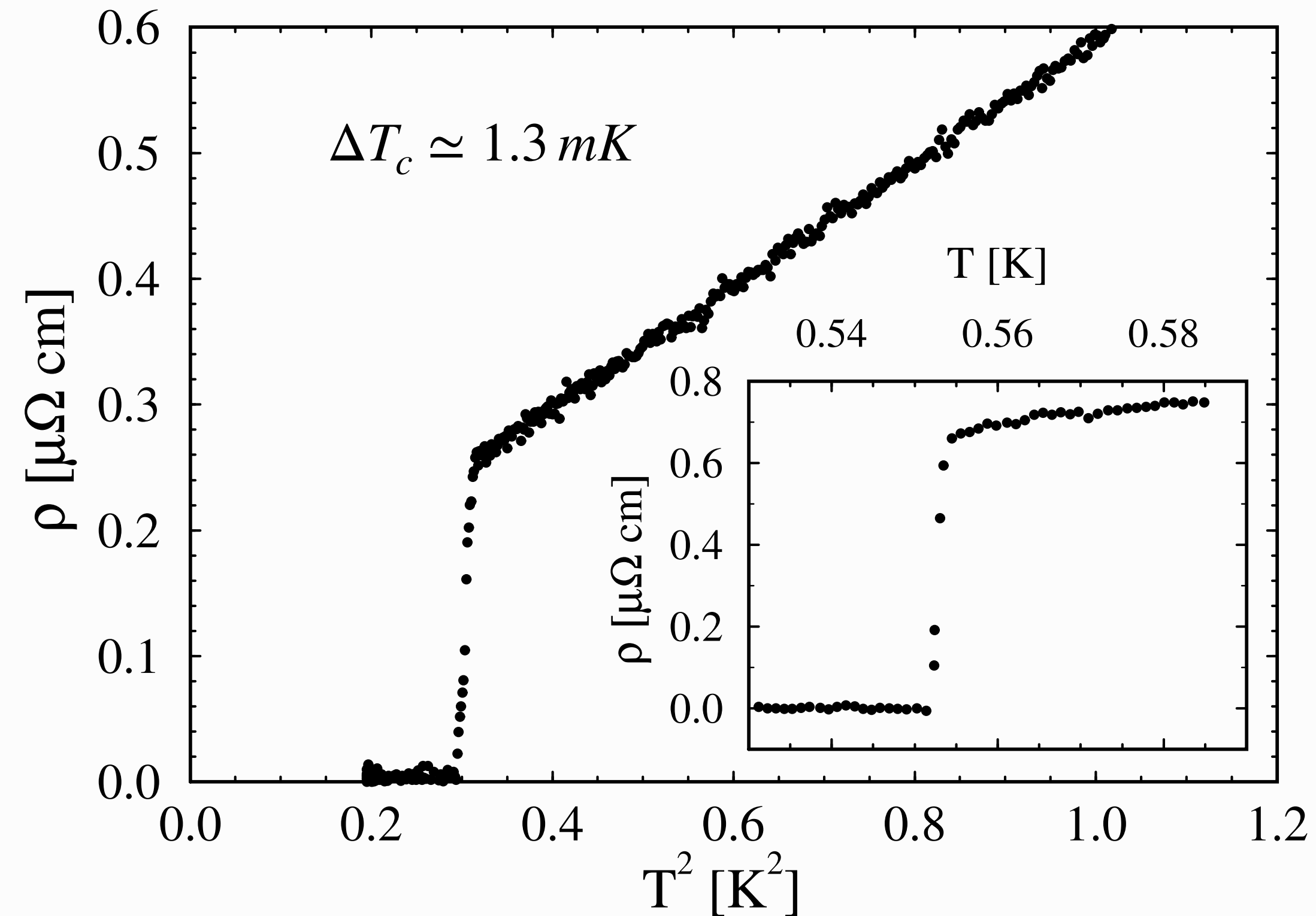
J.B. Kycia et al., Phys. Rev. B 58, R603 (1998).



- ▶ Resistivity of UPt_3 annealed at 900°C . $\rho = \rho_0 + AT^2$
- ▶ $T_c = 552 \text{ mK}$ Inset: Superconducting transition for a sample annealed at 800°C . The transition *width* is 1.3 mK .

Superconductivity in Single Crystals of UPt_3

J.B. Kycia et al., Phys. Rev. B 58, R603 (1998).

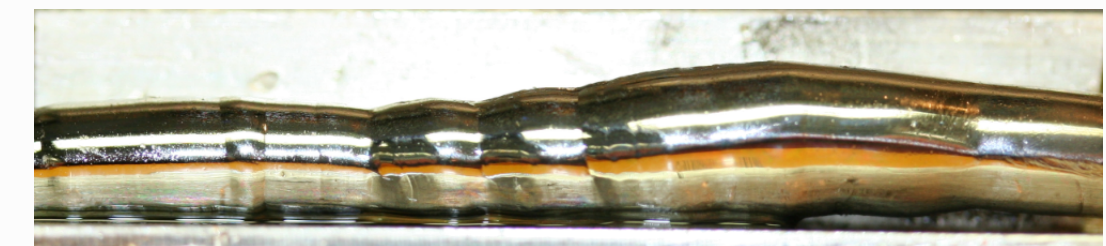


▶ Resistivity of UPt_3 annealed at 900°C . $\rho = \rho_0 + AT^2$

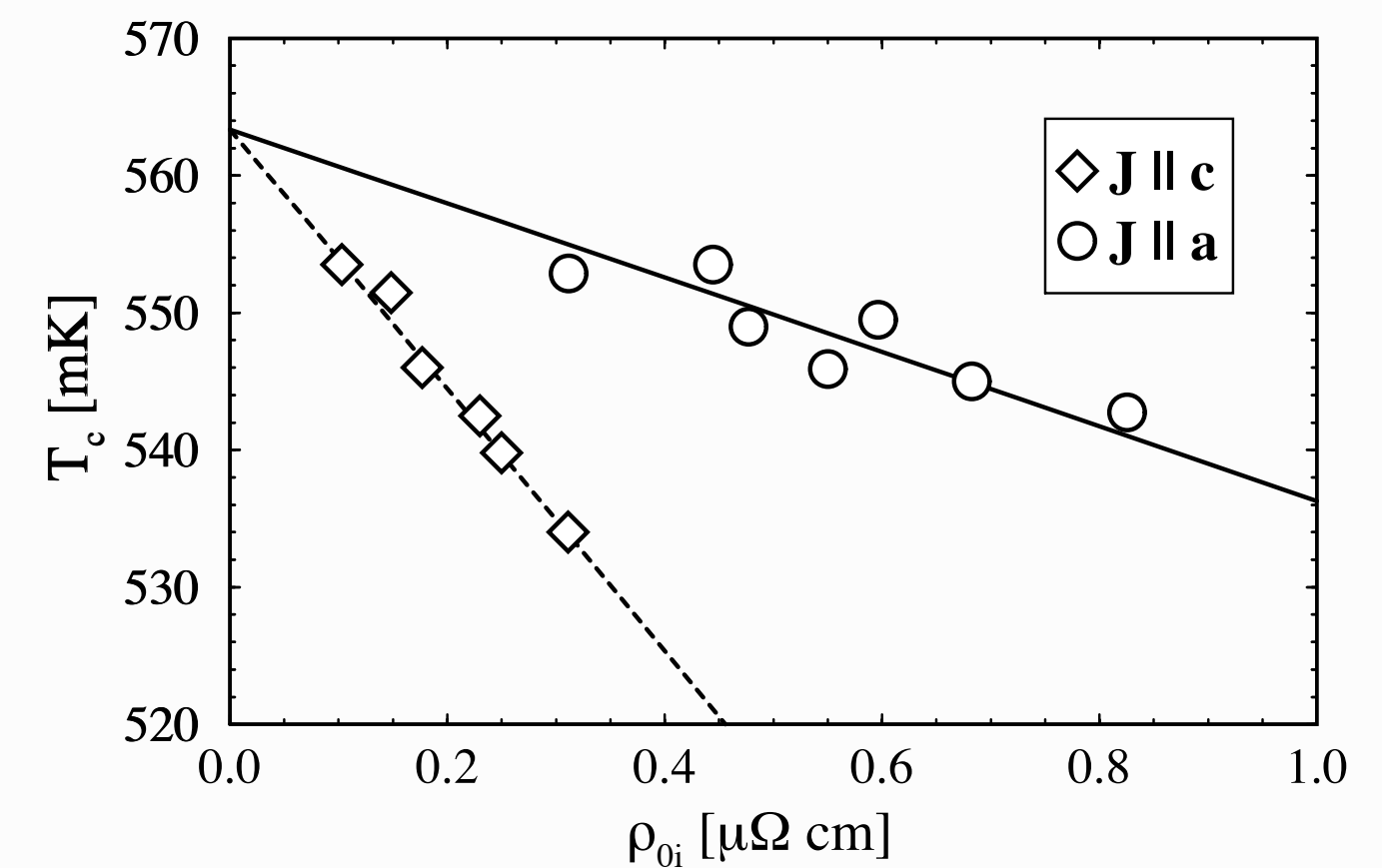
▶ $T_c = 552\text{ mK}$ Inset: Superconducting transition for a sample annealed at 800°C . The transition *width* is 1.3 mK .

▶ $RRR \equiv \rho(300\text{ K})/\rho(T \rightarrow 0)$

▶ UPt_3 Crystal ($RRR \approx 1500$)



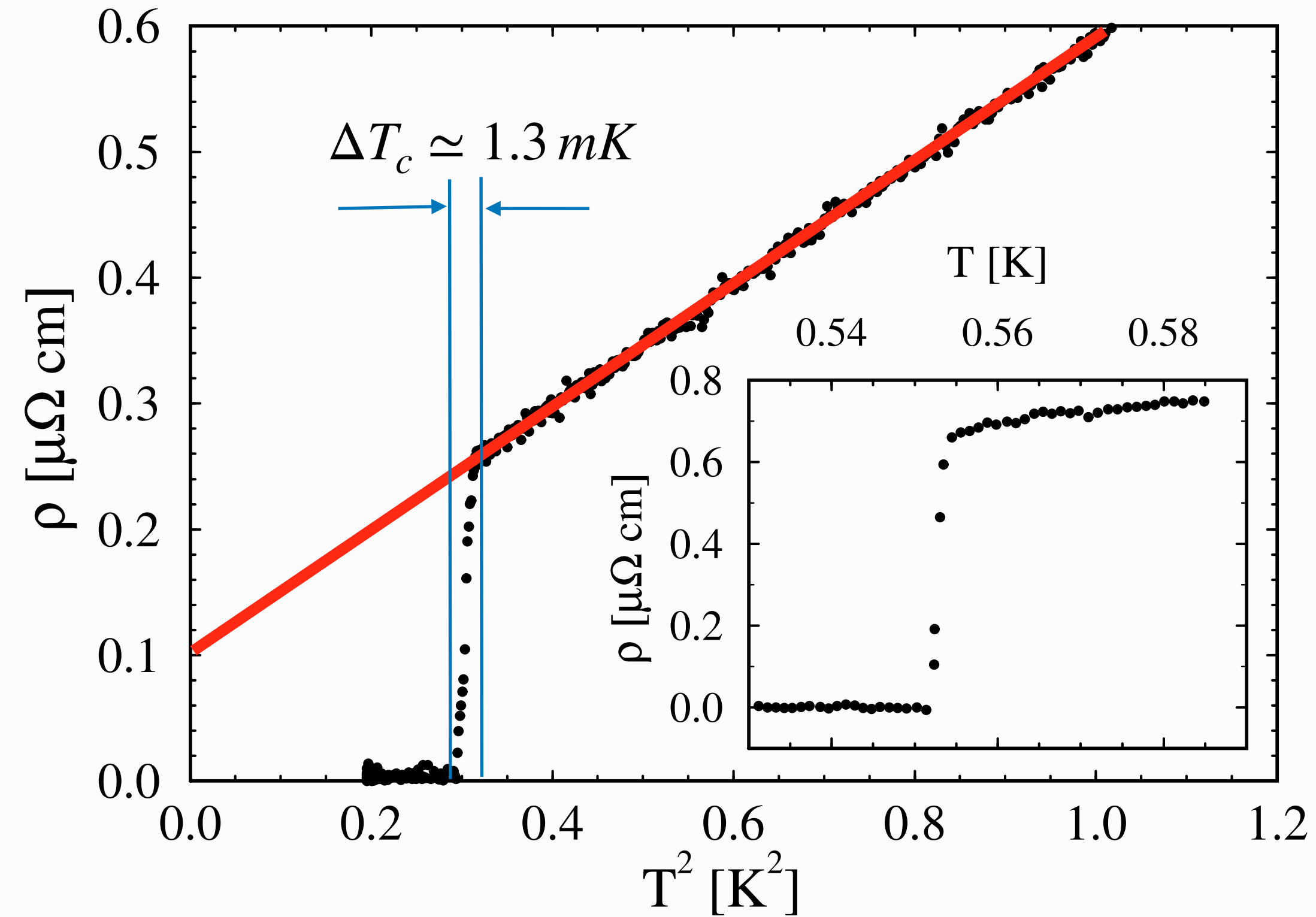
T_c vs. residual resistivity



▶ Superconductivity in UPt_3 is very sensitive to disorder!

Superconductivity in Single Crystals of UPt_3

J.B. Kycia et al., Phys. Rev. B 58, R603 (1998).

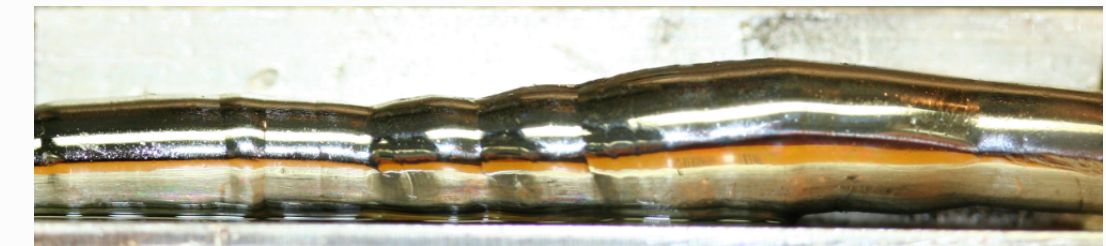


▶ Resistivity of UPt_3 annealed at 900°C . $\rho = \rho_0 + AT^2$

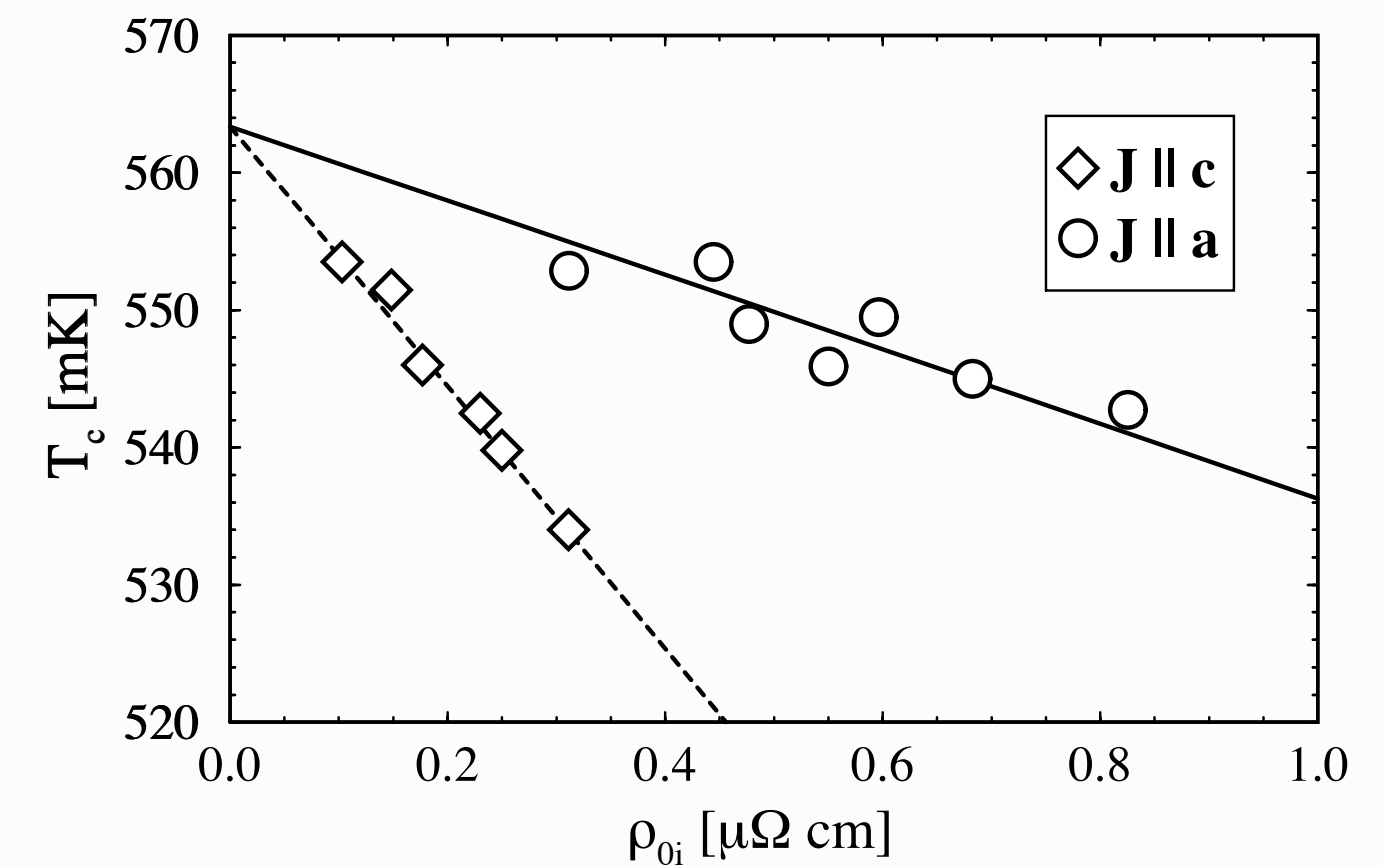
▶ $T_c = 552\text{ mK}$ Inset: Superconducting transition for a sample annealed at 800°C . The transition *width* is 1.3 mK .

▶ $RRR \equiv \rho(300\text{ K})/\rho(T \rightarrow 0)$

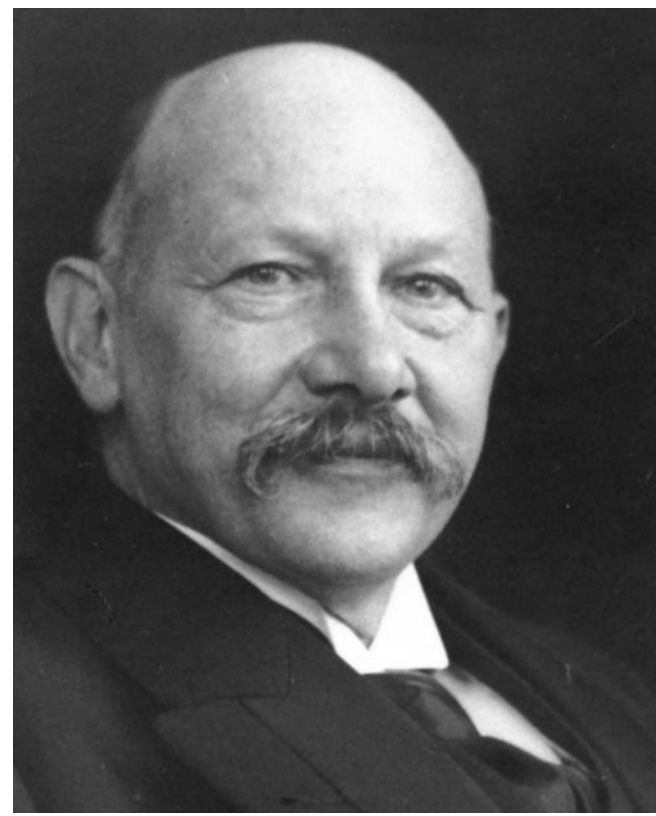
▶ UPt_3 Crystal ($RRR \approx 1500$)



T_c vs. residual resistivity



▶ Superconductivity in UPt_3 is very sensitive to disorder!



✓ 1911 - Superconductivity of Hg $T < 4.2\text{K}$

Kamerlingh Onnes

Supercurrents can
persist in
metastable states



Kamerlingh Onnes

- ✓ 1911 - Superconductivity of Hg $T < 4.2\text{K}$
- ✓ 1913 - Persistent Currents in a Pb ring

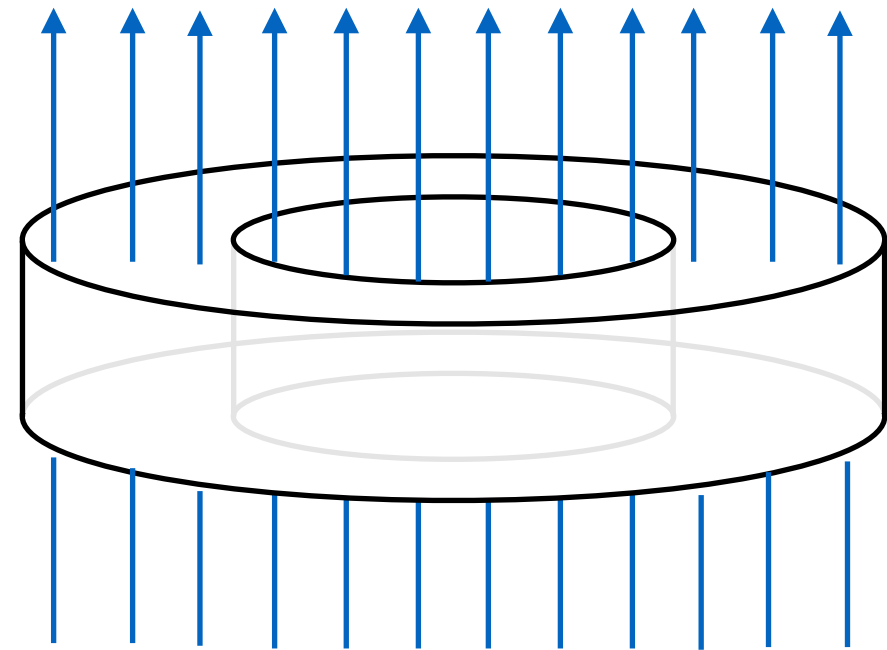
Supercurrents can
persist in
metastable states



Kamerlingh Onnes

- ✓ 1911 - Superconductivity of Hg $T < 4.2\text{K}$
- ✓ 1913 - Persistent Currents in a Pb ring

applied B-field



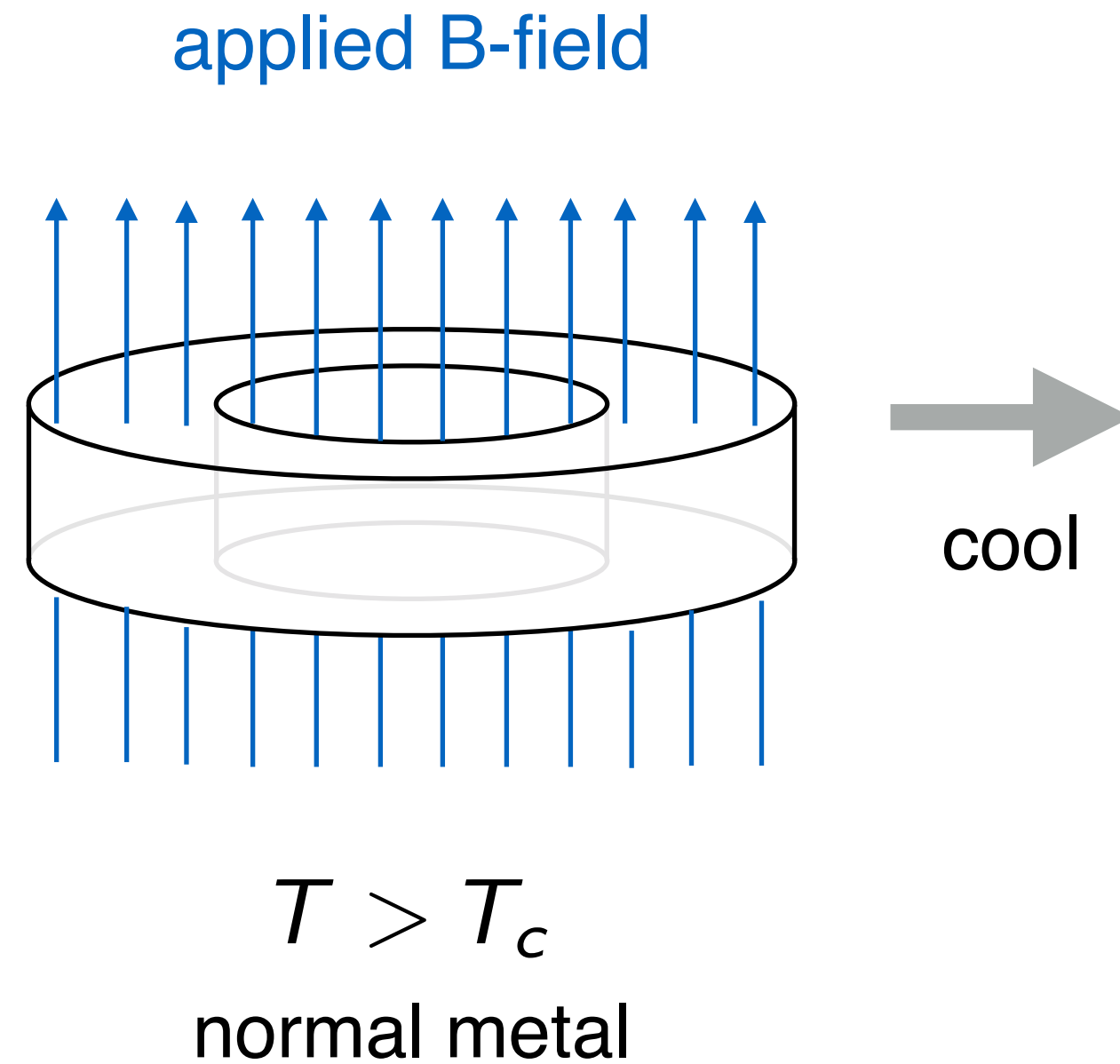
$T > T_c$
normal metal

Supercurrents can persist in *metastable* states



Kamerlingh Onnes

- ✓ 1911 - Superconductivity of Hg $T < 4.2\text{K}$
- ✓ 1913 - Persistent Currents in a Pb ring



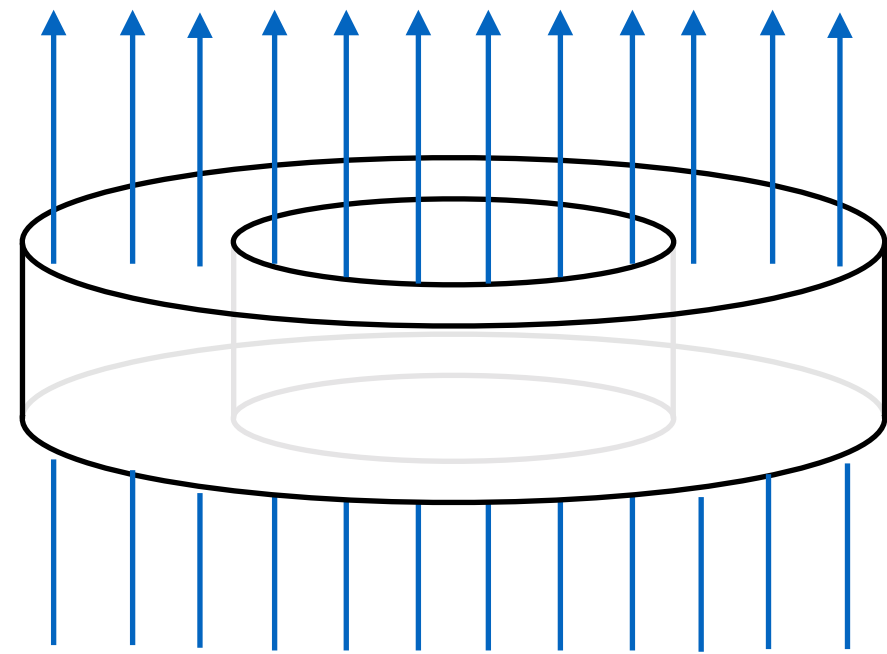
Supercurrents can persist in *metastable* states



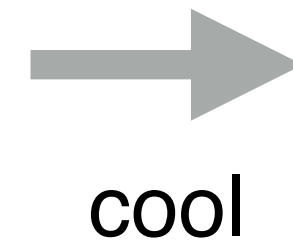
Kamerlingh Onnes

- ✓ 1911 - Superconductivity of Hg $T < 4.2\text{K}$
- ✓ 1913 - Persistent Currents in a Pb ring

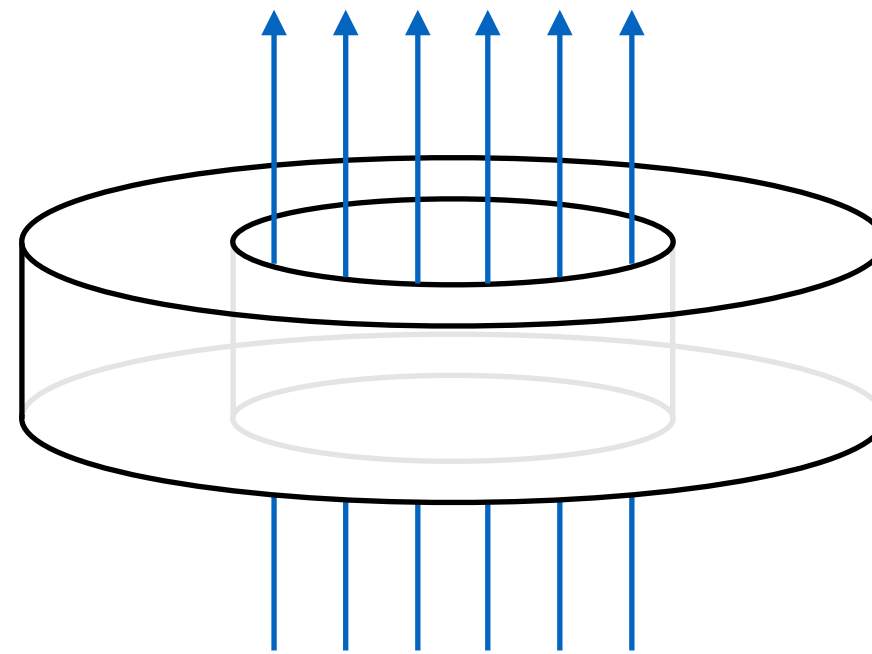
applied B-field



$T > T_c$
normal metal



applied B-field



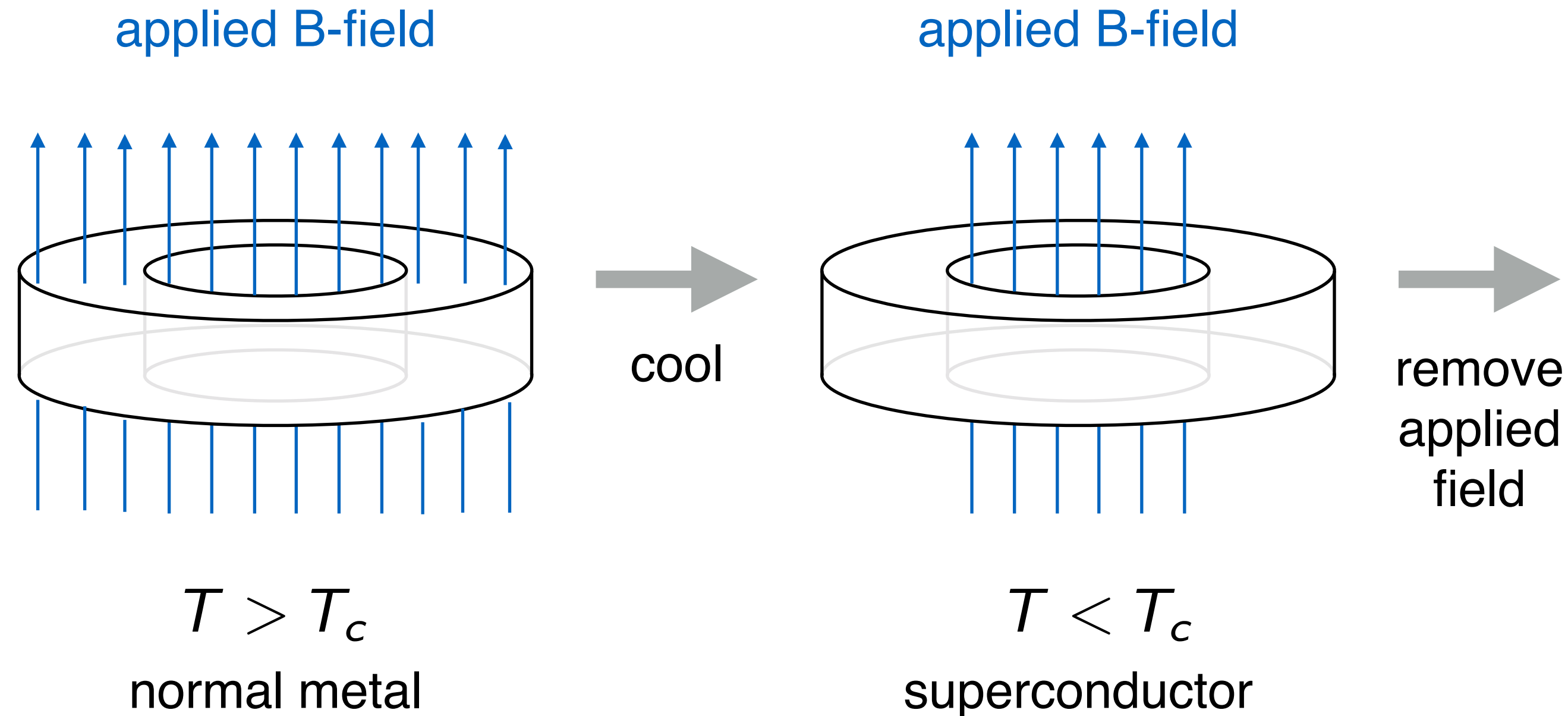
$T < T_c$
superconductor

Supercurrents can persist in *metastable* states



Kamerlingh Onnes

- ✓ 1911 - Superconductivity of Hg $T < 4.2\text{K}$
- ✓ 1913 - Persistent Currents in a Pb ring

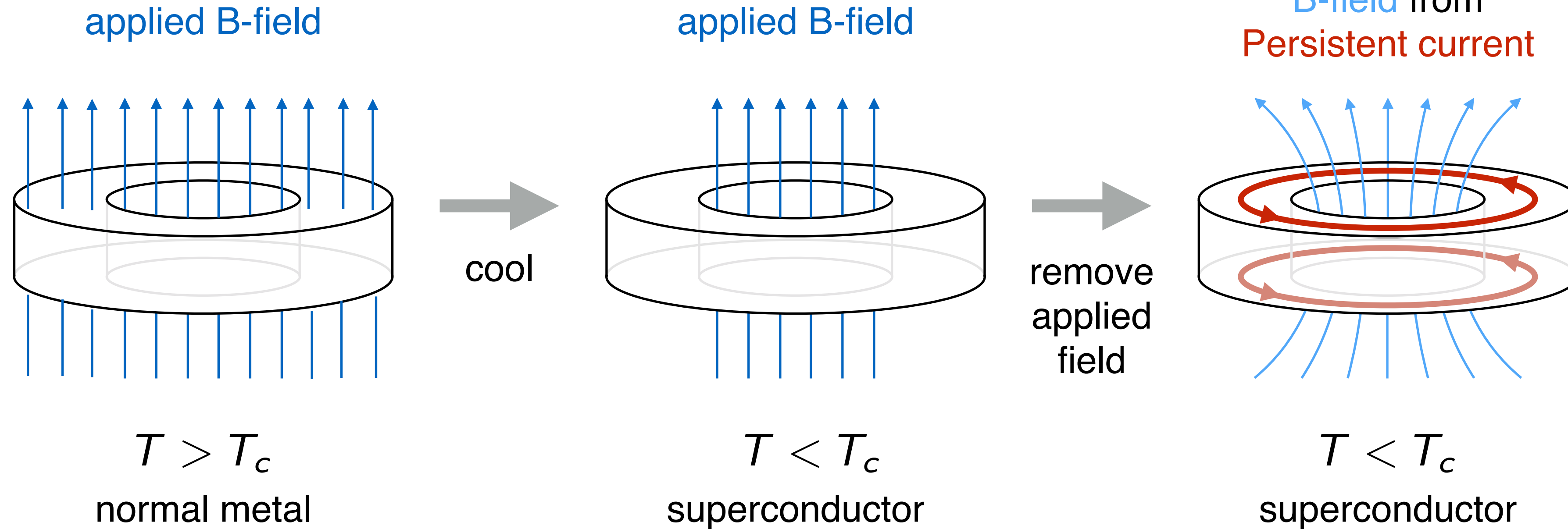


Supercurrents can persist in *metastable* states



Kamerlingh Onnes

- ✓ 1911 - Superconductivity of Hg $T < 4.2\text{K}$
- ✓ 1913 - Persistent Currents in a Pb ring

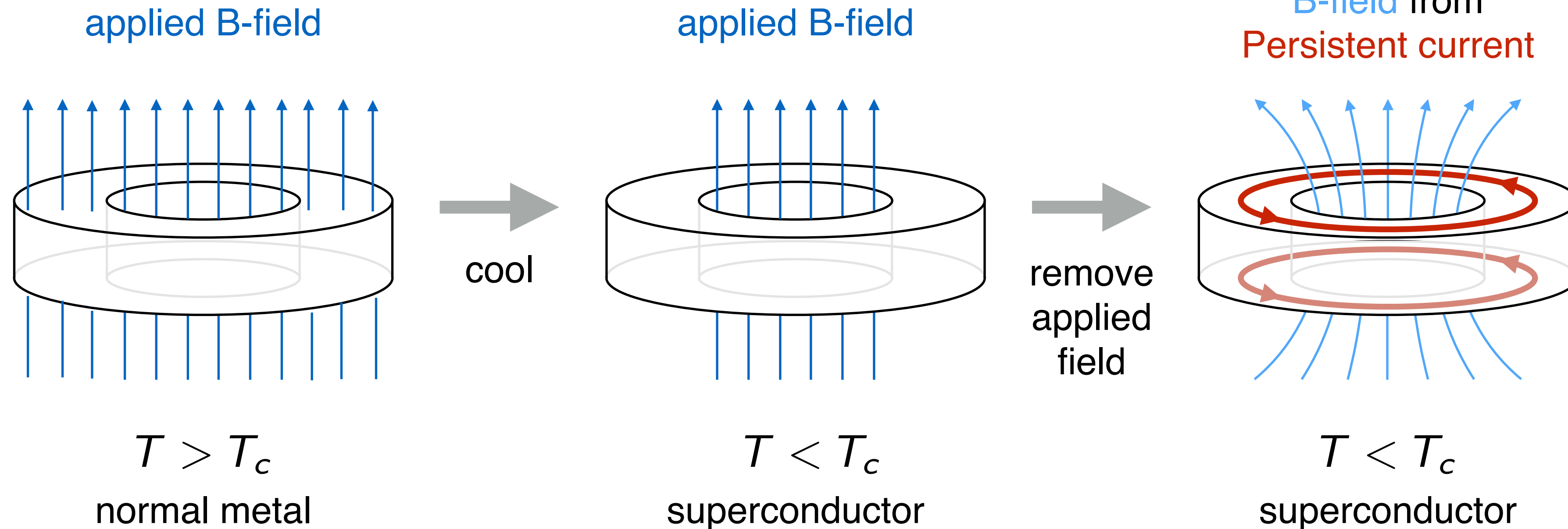


Supercurrents can persist in *metastable* states



Kamerlingh Onnes

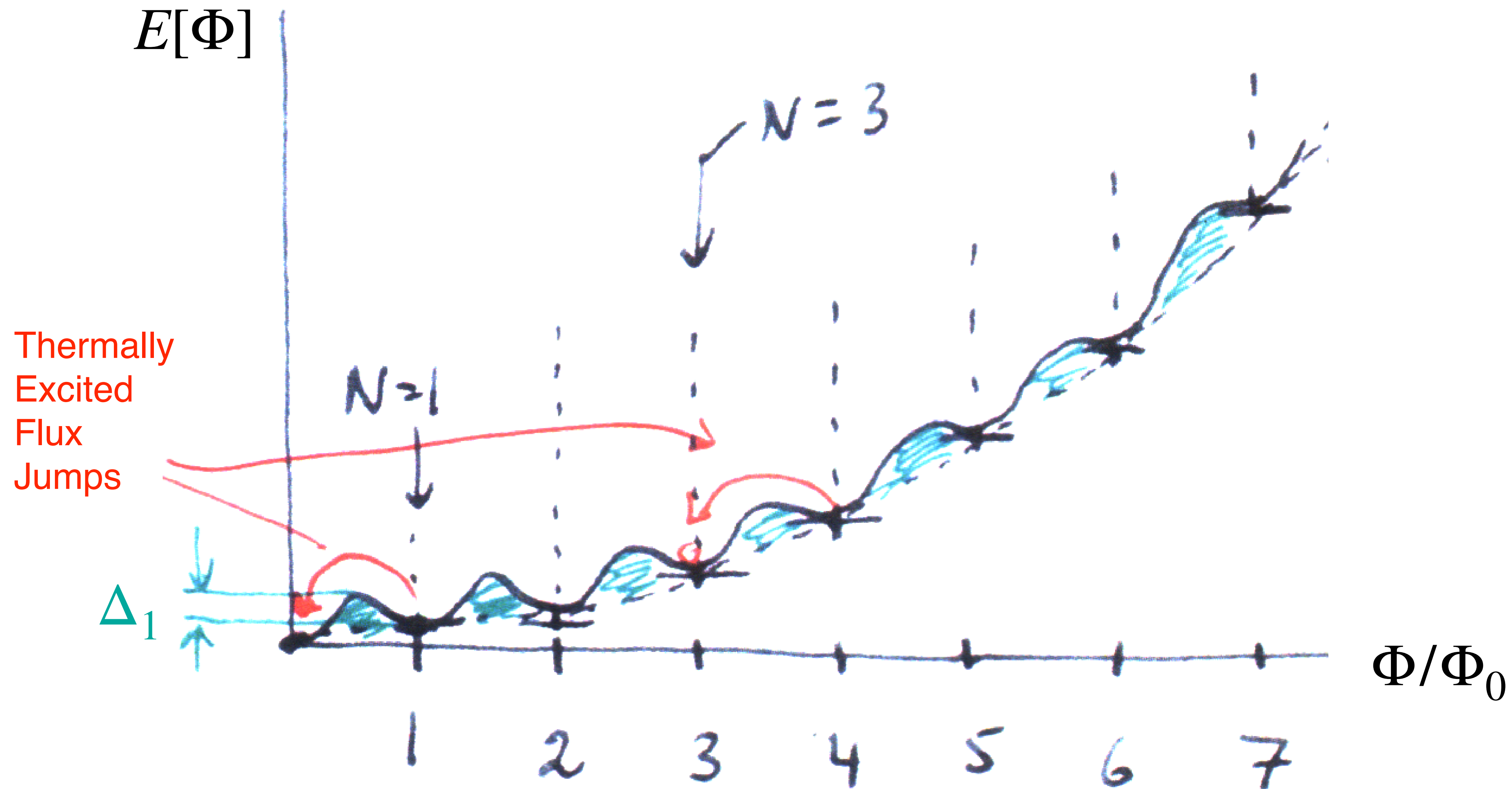
- ✓ 1911 - Superconductivity of Hg $T < 4.2\text{K}$
- ✓ 1913 - Persistent Currents in a Pb ring



❖ *File & Mills, Phys Rev Lett 10, 93 (1963) - $\tau > 10^5$ yr*

❖ *Quinn & Ittner, J. Appl. Phys. 33, 748 (2004) - $\rho(T < T_c) < 3.6 \times 10^{-23} \Omega - cm$*

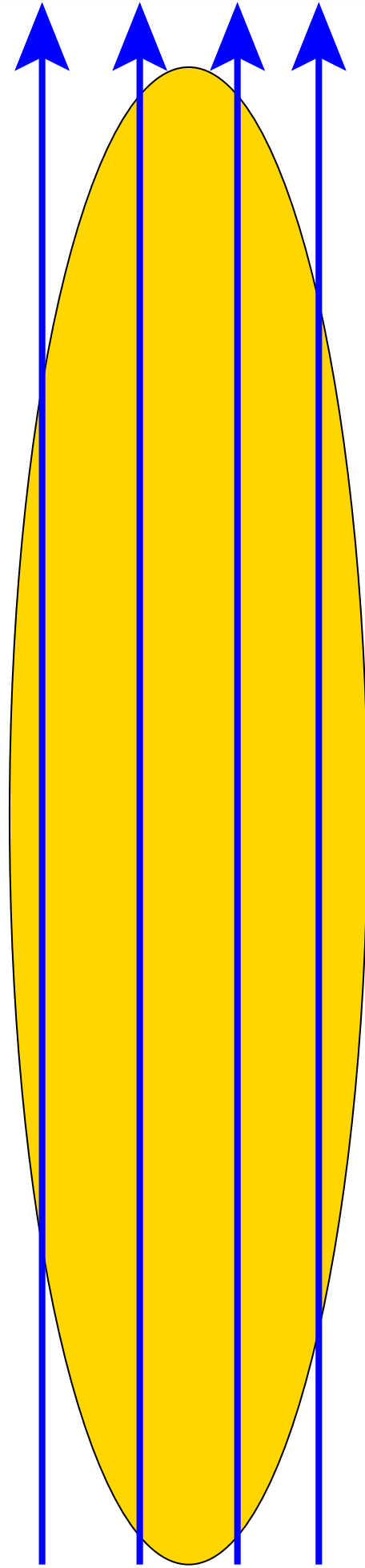
Energy Landscape of Current Carrying States of a Toroidal Ring



❖ Metastable Persistent Current States protected by a large activation barrier

Perfect Diamagnetism

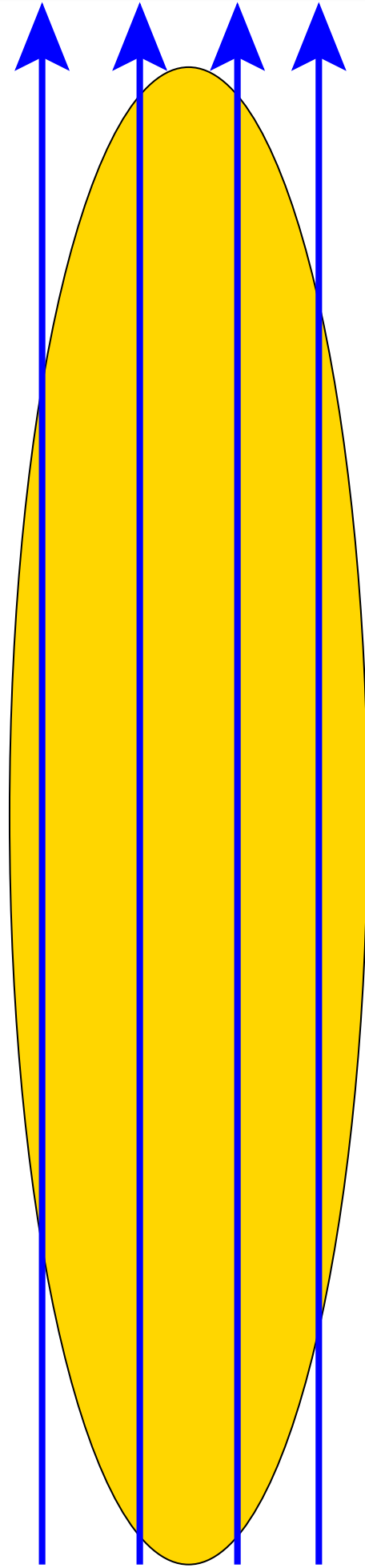
1933 - Walther Meissner & Robert Ochsenfeld, T.U. Munich



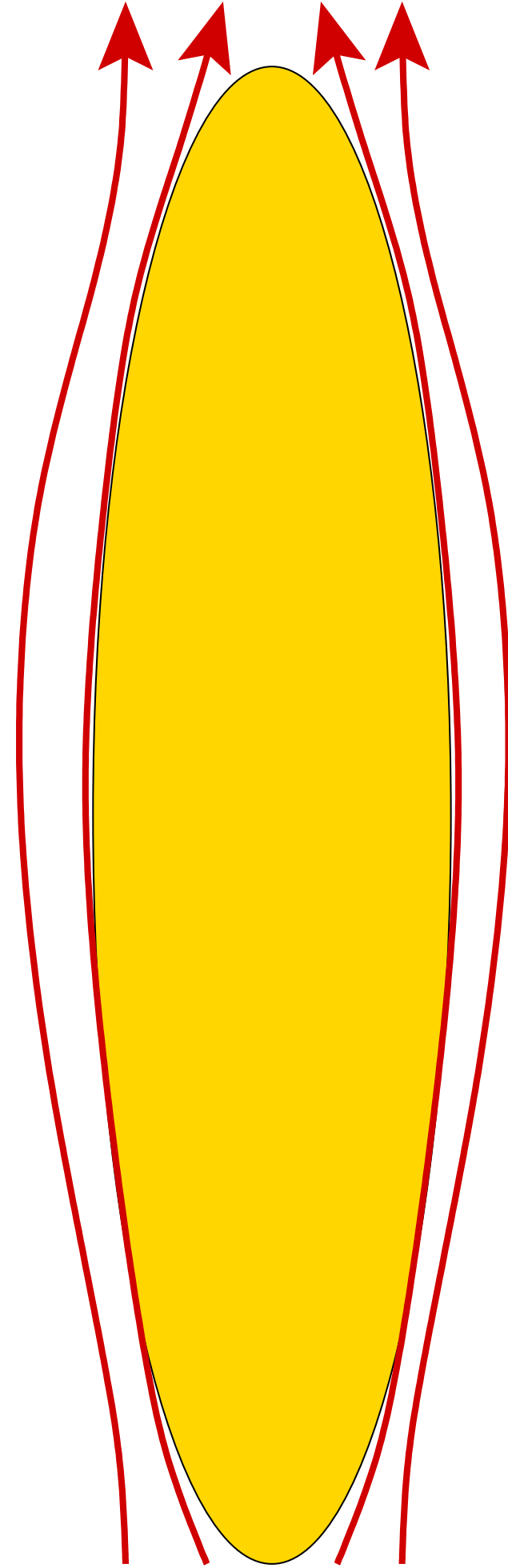
$$T > T_c$$
$$B = H$$

Perfect Diamagnetism

1933 - Walther Meissner & Robert Ochsenfeld, T.U. Munich



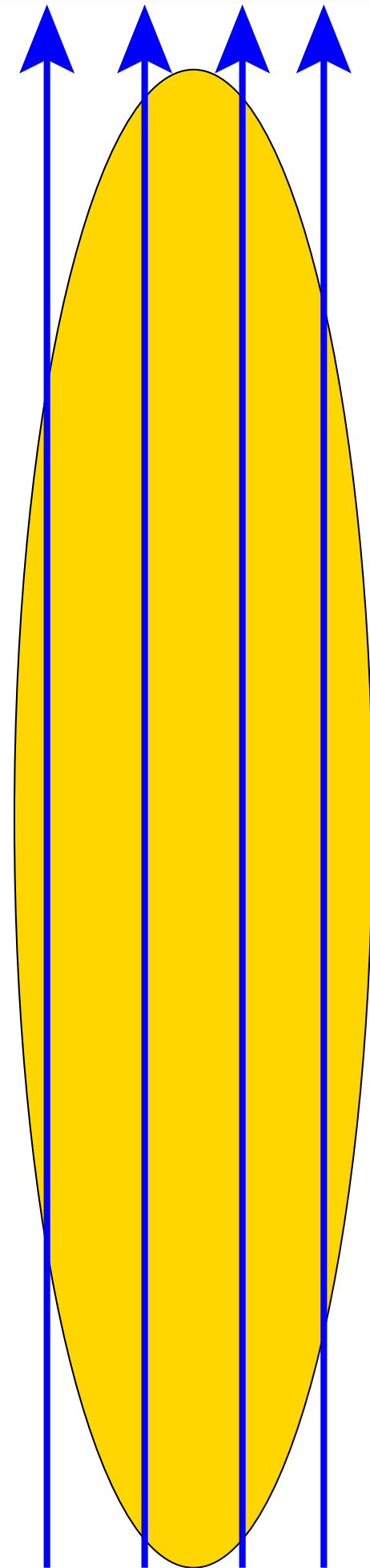
$$T > T_c$$
$$B = H$$



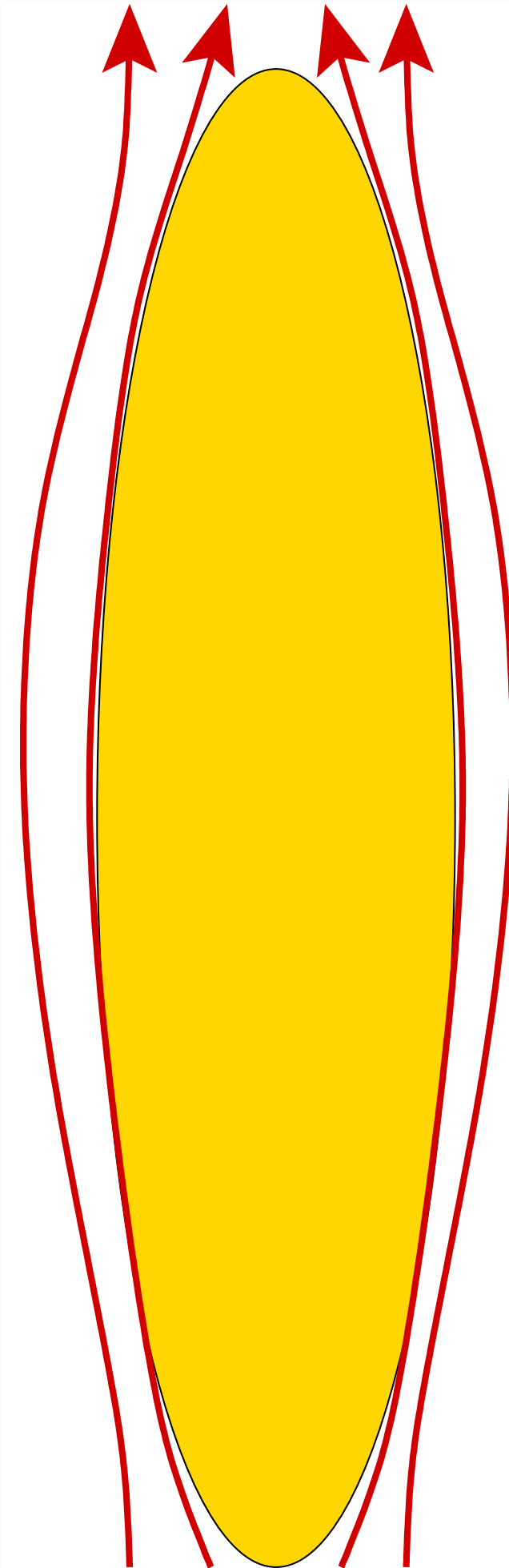
$$T < T_c$$
$$B = 0$$

Perfect Diamagnetism

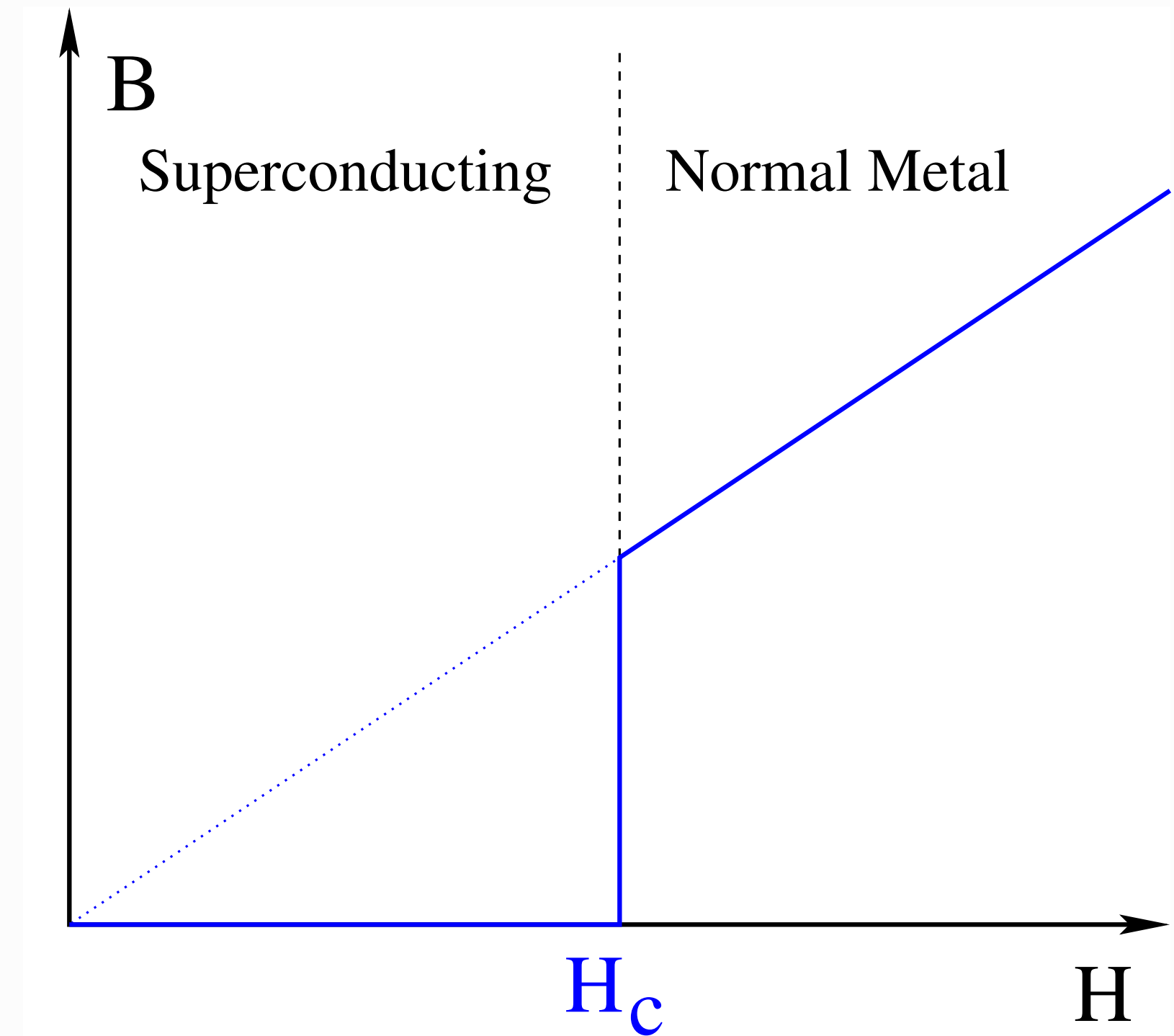
1933 - Walther Meissner & Robert Ochsenfeld, T.U. Munich



$$T > T_c$$
$$B = H$$

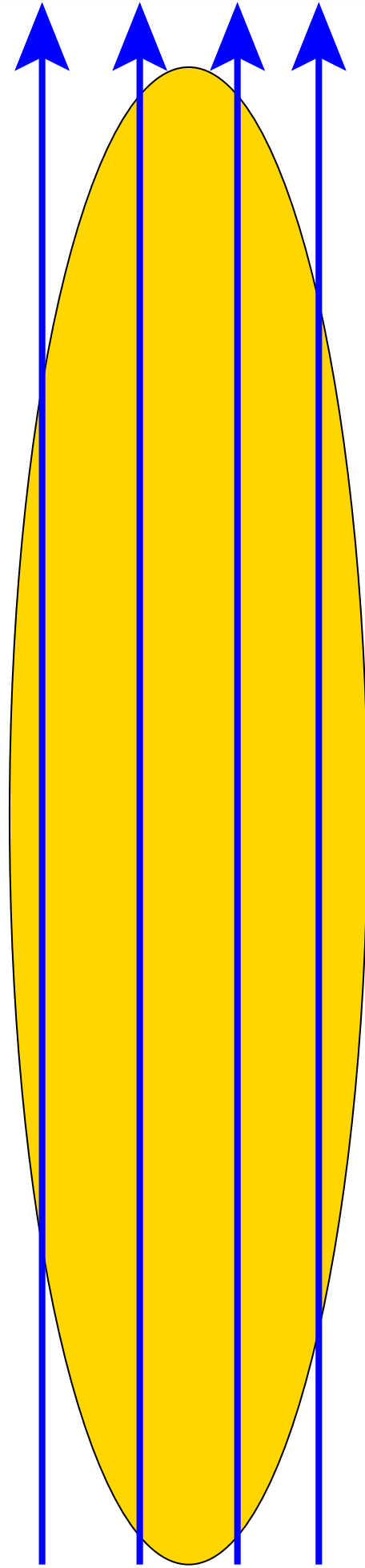


$$T < T_c$$
$$B = 0$$

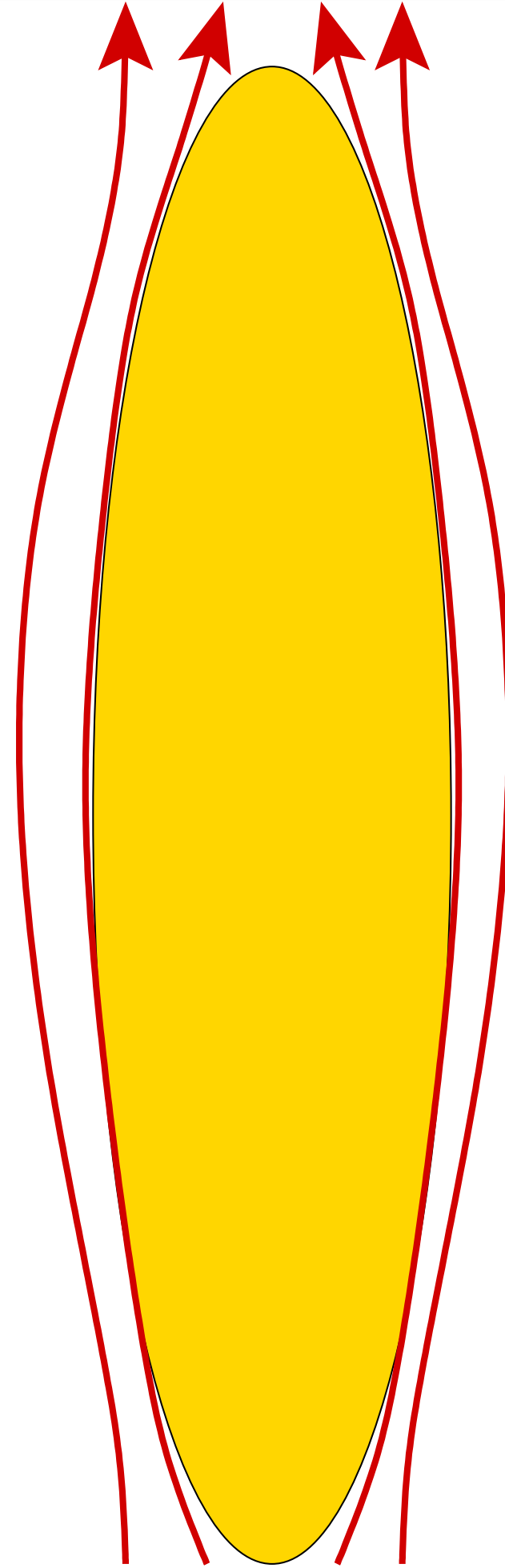


Perfect Diamagnetism

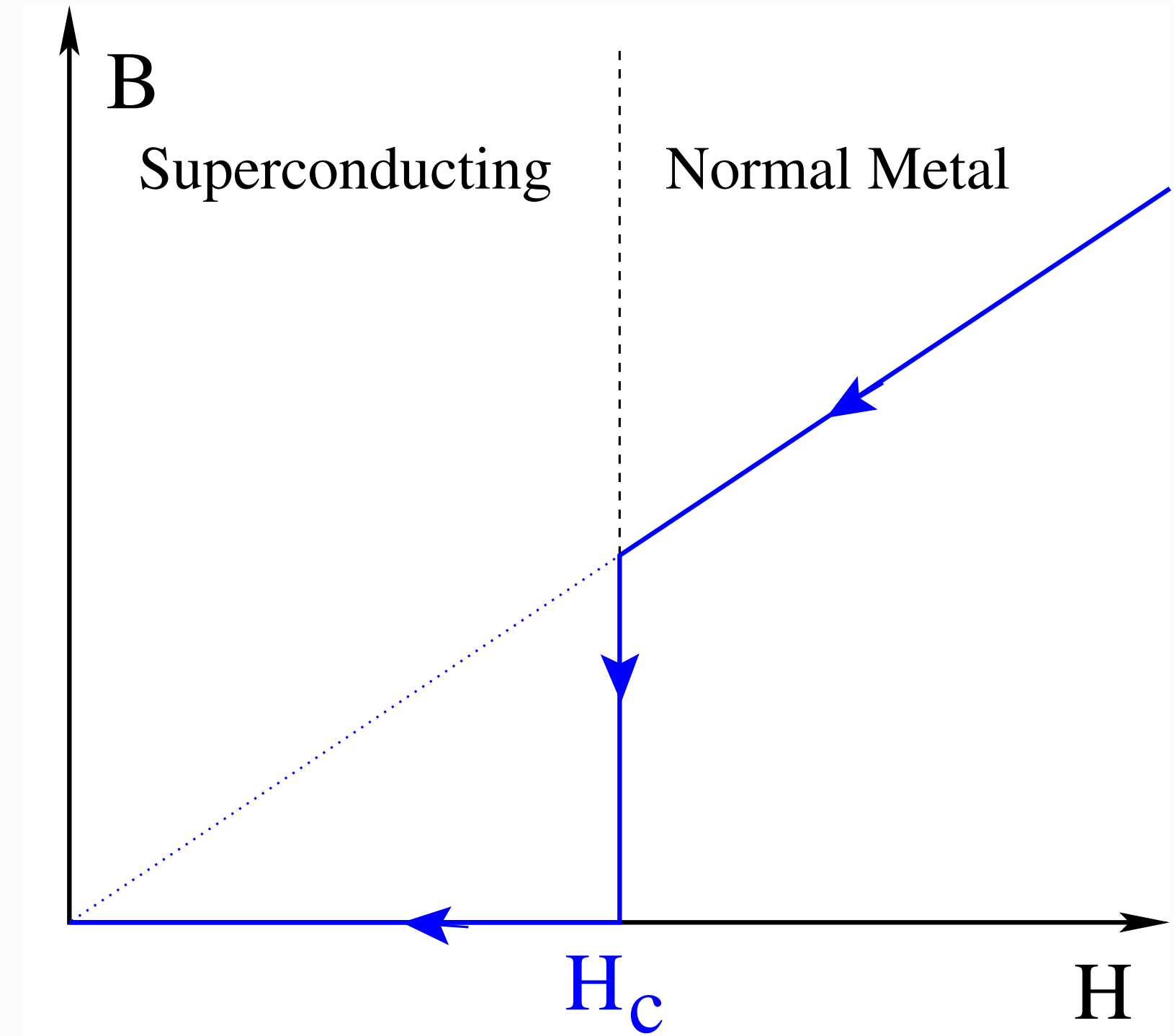
1933 - Walther Meissner & Robert Ochsenfeld, T.U. Munich



$$T > T_c$$
$$B = H$$



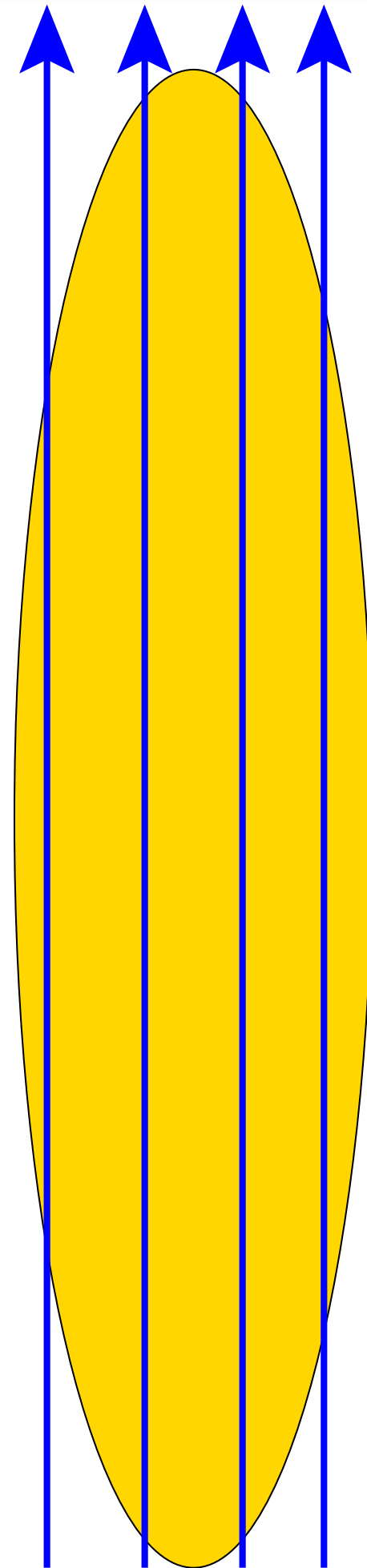
$$T < T_c$$
$$B = 0$$



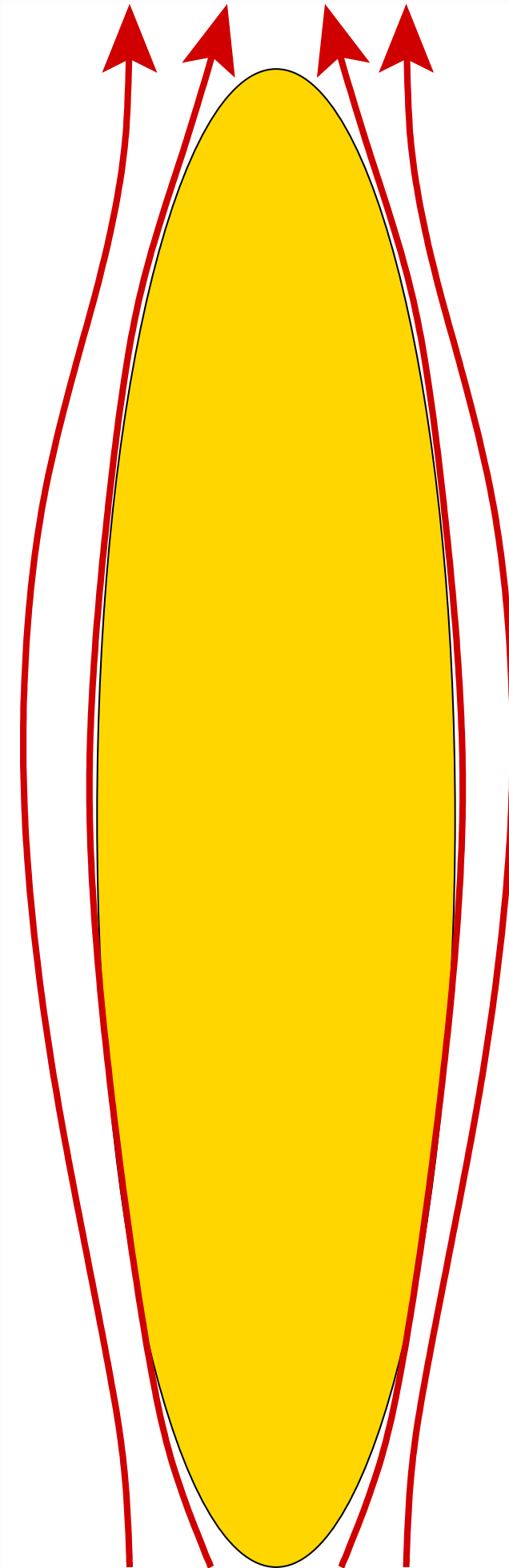
Perfect Diamagnetism

Equilibrium Current Carrying State of Supercurrents

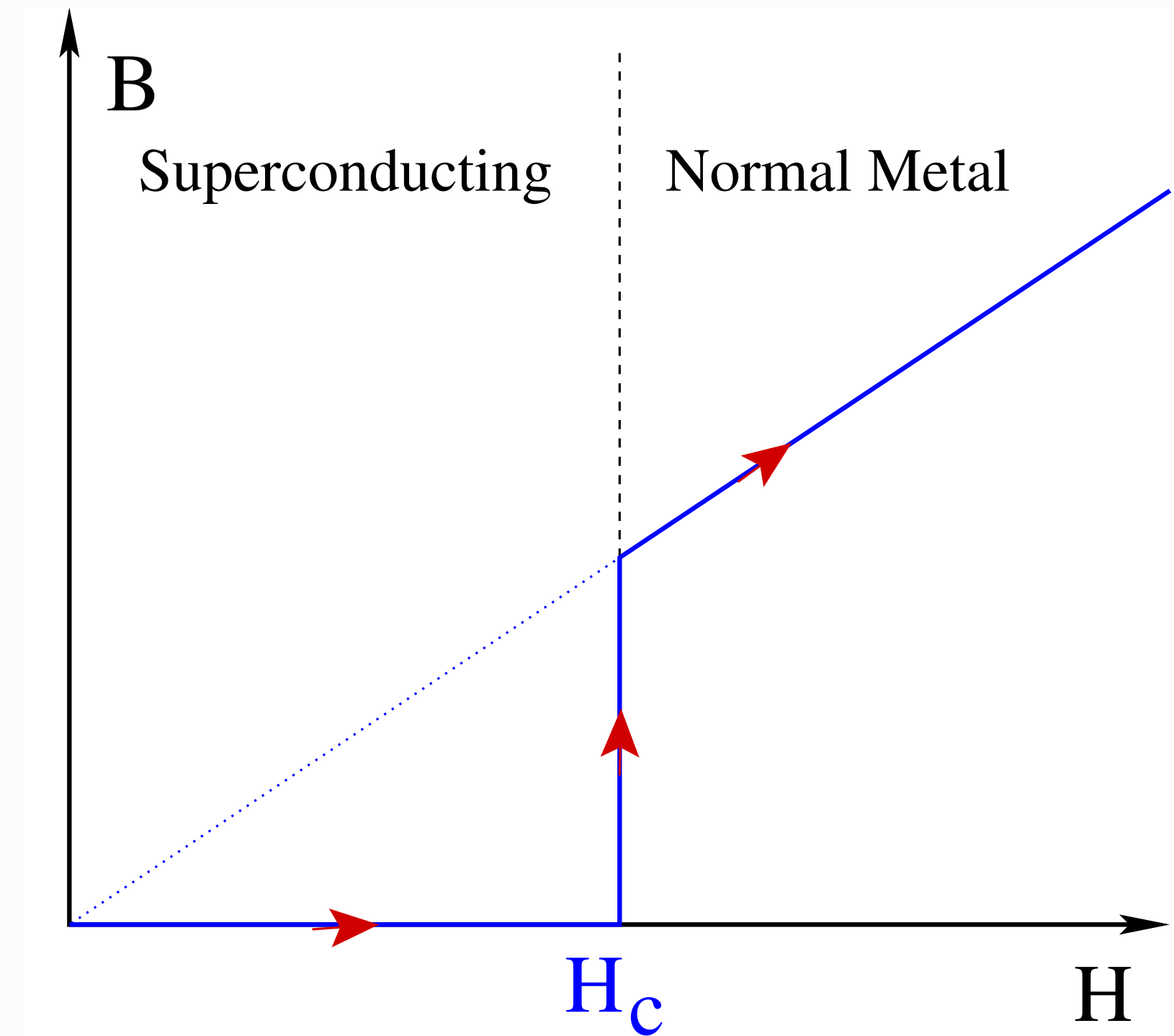
1933 - Walther Meissner & Robert Ochsenfeld, T.U. Munich



$T > T_c$
 $B = H$



$T < T_c$
 $B = 0$



$$B = H + 4\pi M = 0$$

► Screening Currents on the Boundary!

Electrodynamics of Superconductors

Electrodynamics of Superconductors

Fritz London's Theory c.a. 1935

Two Fluid Theory: n_n normal e^- and n_s super e^-

Electrodynamics of Superconductors

Fritz London's Theory c.a. 1935

Two Fluid Theory: n_n normal e^- and n_s super e^-

Low Temperatures: $T \ll T_c$

$$n_s \rightarrow n \quad n_n \sim e^{-\Delta/T} \rightarrow 0$$

Electrodynamics of Superconductors



Fritz London (1900–1954). (AIP Niels Bohr Library, Francis Simon Collection)

$$T \ll T_c$$
$$-\Delta/T \rightarrow 0$$

Electrodynamics of Superconductors

Fritz London's Theory c.a. 1935

Two Fluid Theory: n_n normal e^- and n_s super e^-

$$\frac{c}{4\pi} \nabla \times \mathbf{B} = \mathbf{J}$$

Low Temperatures: $T \ll T_c$
 $n_s \rightarrow n$ $n_n \sim e^{-\Delta/T} \rightarrow 0$

Electrodynamics of Superconductors

Fritz London's Theory c.a. 1935

Two Fluid Theory: n_n normal e^- and n_s super e^-

$$\frac{c}{4\pi} \nabla \times \mathbf{B} = \sigma_n \mathbf{E}$$

Low Temperatures: $T \ll T_c$
 $n_s \rightarrow n$ $n_n \sim e^{-\Delta/T} \rightarrow 0$

Electrodynamics of Superconductors

Fritz London's Theory c.a. 1935

Two Fluid Theory: n_n normal e^- and n_s super e^-

$$\frac{c}{4\pi} \nabla \times \mathbf{B} = \sigma_n \mathbf{E} - n_s \left(\frac{e^2}{c} \right) \mathbf{A}$$

Low Temperatures: $T \ll T_c$
 $n_s \rightarrow n$ $n_n \sim e^{-\Delta/T} \rightarrow 0$

★ Macroscopic Quantum State of $n_s \sim \mathcal{O}(n)$ electrons

Electrodynamics of Superconductors

Fritz London's Theory c.a. 1935

Two Fluid Theory: n_n normal e^- and n_s super e^-

$$\frac{c}{4\pi} \nabla \times \mathbf{B} = \sigma_n \mathbf{E} - n_s \left(\frac{e^2}{c} \right) \mathbf{A}$$

Low Temperatures: $T \ll T_c$
 $n_s \rightarrow n$ $n_n \sim e^{-\Delta/T} \rightarrow 0$

Screening of Magnetic Fields

★ Macroscopic Quantum State of $n_s \sim \mathcal{O}(n)$ electrons

Electrodynamics of Superconductors

Fritz London's Theory c.a. 1935

Two Fluid Theory: n_n normal e^- and n_s super e^-

$$\frac{c}{4\pi} \nabla \times \mathbf{B} = \sigma_n \mathbf{E} - n_s \left(\frac{e^2}{c} \right) \mathbf{A}$$

Low Temperatures: $T \ll T_c$
 $n_s \rightarrow n$ $n_n \sim e^{-\Delta/T} \rightarrow 0$

Screening of Magnetic Fields

$$\left(-\nabla^2 \mathbf{B} + \frac{1}{\lambda_L^2} \right) \mathbf{B} = 0$$

★ Macroscopic Quantum State of $n_s \sim \mathcal{O}(n)$ electrons

Electrodynamics of Superconductors

Fritz London's Theory c.a. 1935

Two Fluid Theory: n_n normal e^- and n_s super e^-

$$\frac{c}{4\pi} \nabla \times \mathbf{B} = \sigma_n \mathbf{E} - n_s \left(\frac{e^2}{c} \right) \mathbf{A}$$

Low Temperatures: $T \ll T_c$
 $n_s \rightarrow n$ $n_n \sim e^{-\Delta/T} \rightarrow 0$

Screening of Magnetic Fields

$$\left(-\nabla^2 \mathbf{B} + \frac{1}{\lambda_L^2} \right) \mathbf{B} = 0$$
$$\lambda_L = \sqrt{\frac{c^2}{4\pi n_s e^2}} \approx 50 - 100 \text{ nm}$$

★ Macroscopic Quantum State of $n_s \sim \mathcal{O}(n)$ electrons

Electrodynamics of Superconductors

Fritz London's Theory c.a. 1935

Two Fluid Theory: n_n normal e^- and n_s super e^-

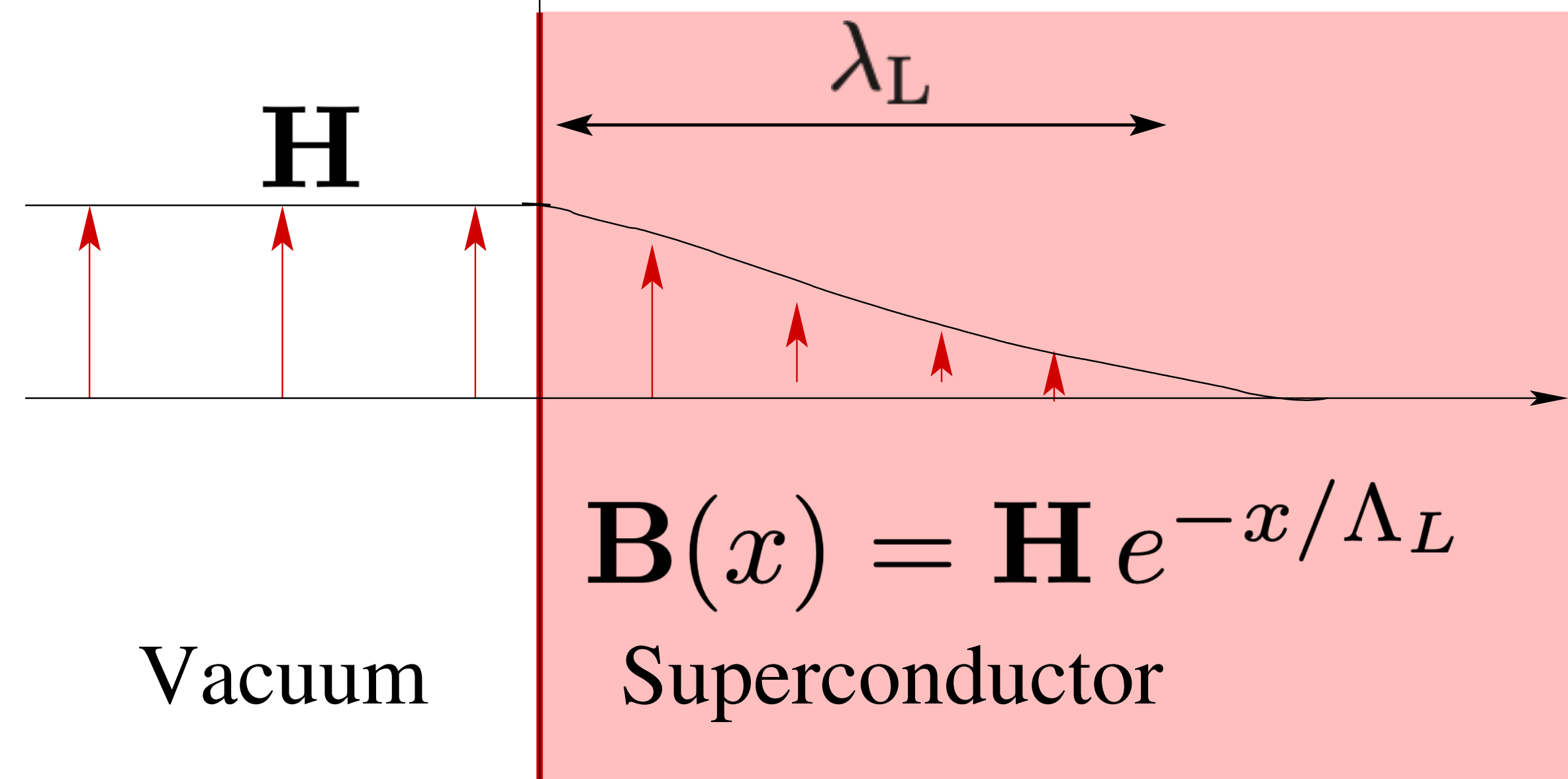
$$\frac{c}{4\pi} \nabla \times \mathbf{B} = \sigma_n \mathbf{E} - n_s \left(\frac{e^2}{c} \right) \mathbf{A}$$

Low Temperatures: $T \ll T_c$
 $n_s \rightarrow n$ $n_n \sim e^{-\Delta/T} \rightarrow 0$

Screening of Magnetic Fields

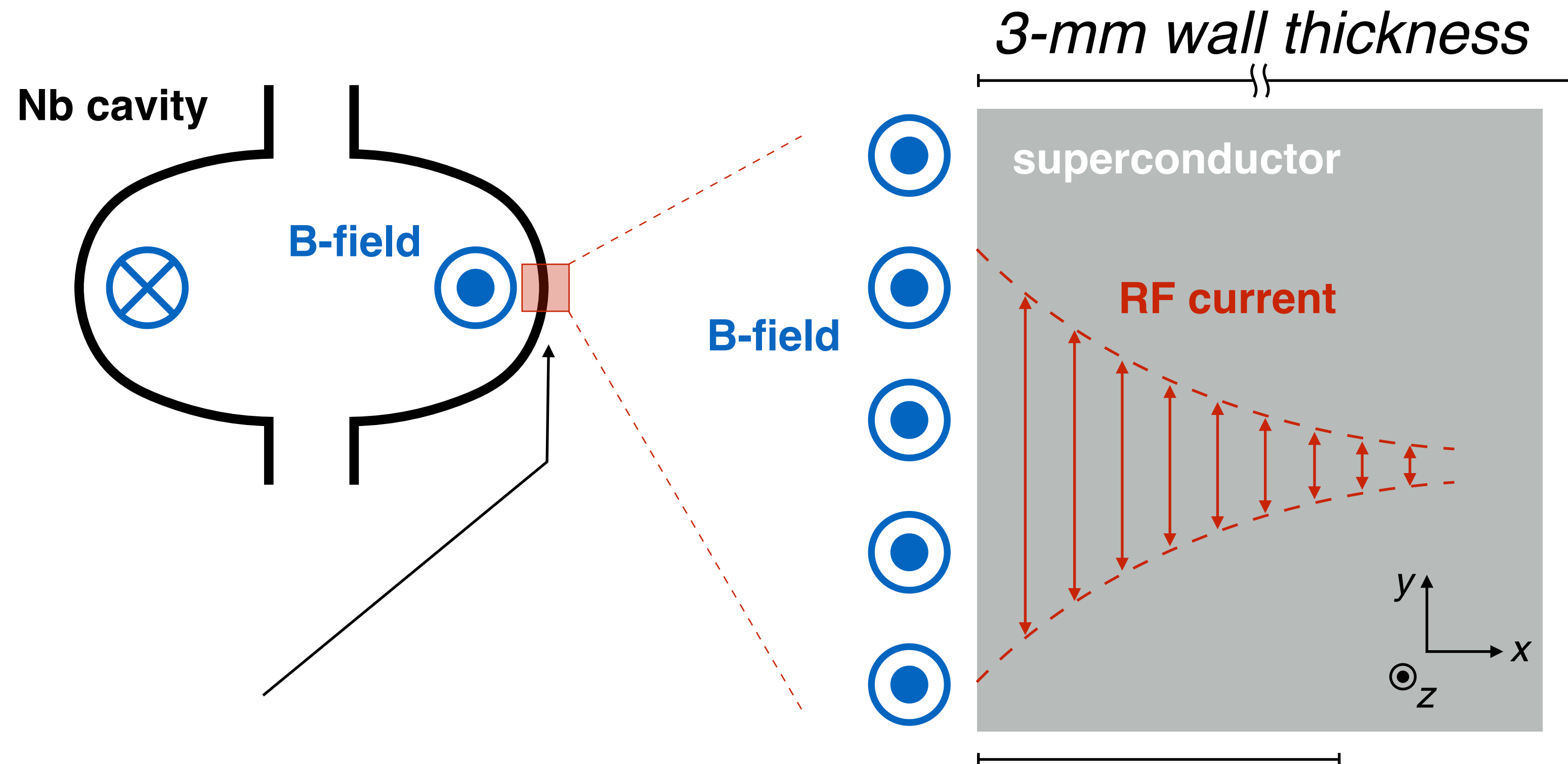
$$\left(-\nabla^2 \mathbf{B} + \frac{1}{\lambda_L^2} \right) \mathbf{B} = 0$$

$$\lambda_L = \sqrt{\frac{c^2}{4\pi n_s e^2}} \approx 50 - 100 \text{ nm}$$



★ Macroscopic Quantum State of $n_s \sim \mathcal{O}(n)$ electrons

SRF Cavities with High Q work because of a 100-nm layer of superconductor!!



This region on screening currents confines the EM field to the cavity and a small layer of superconductor

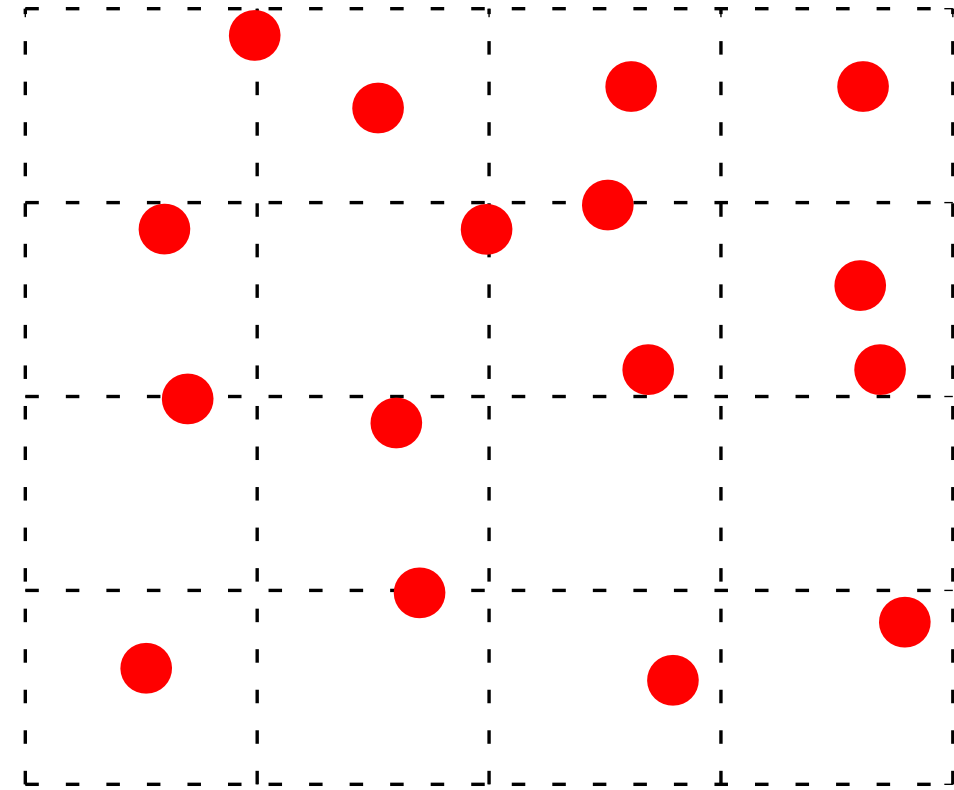
RF field penetrates only ~100nm (London penetration depth of Nb)

Broken Symmetry & Ordered Phases

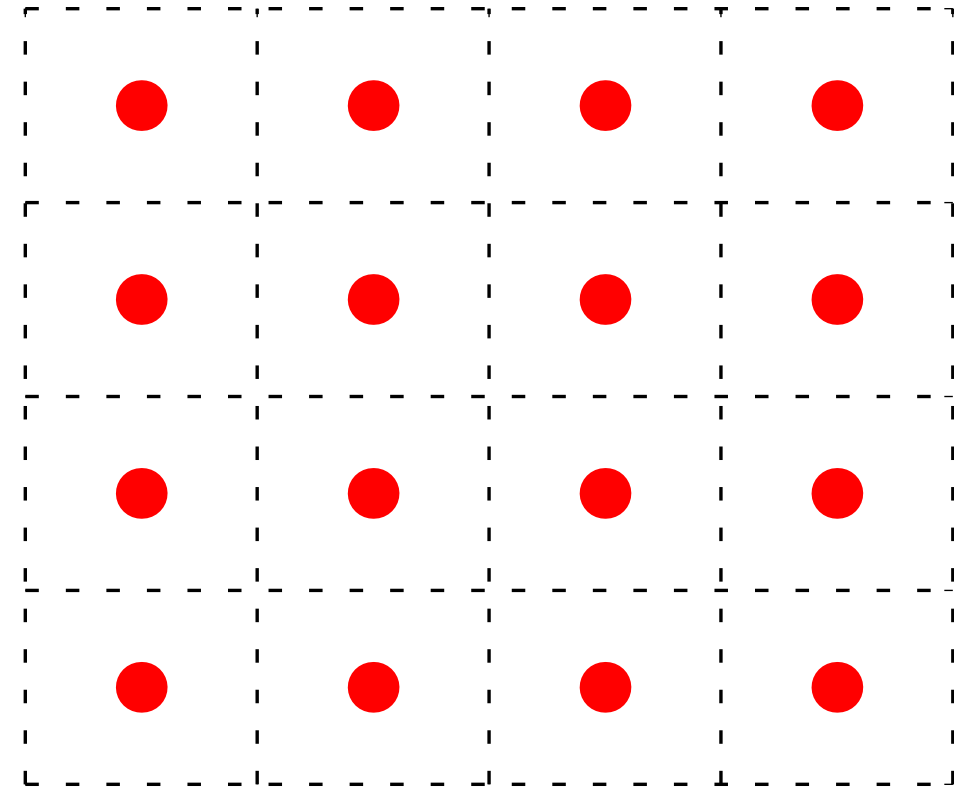


Broken Symmetry & Ordered Phases

Liquid



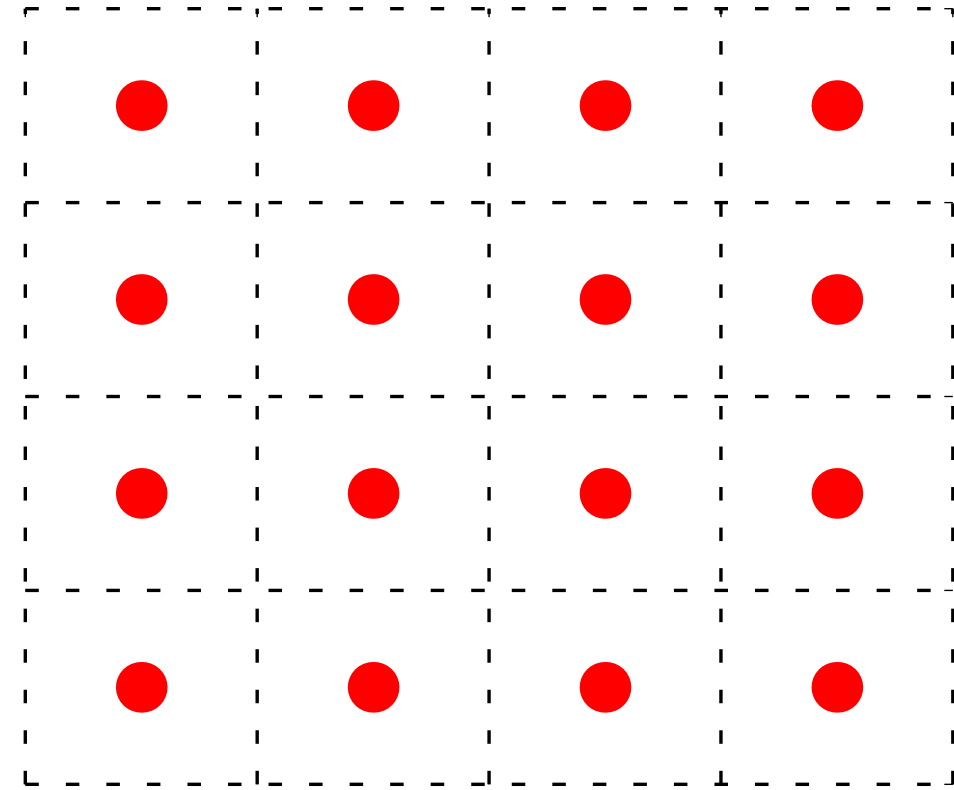
Broken Symmetry & Ordered Phases



Solid



Broken Symmetry & Ordered Phases



Solid

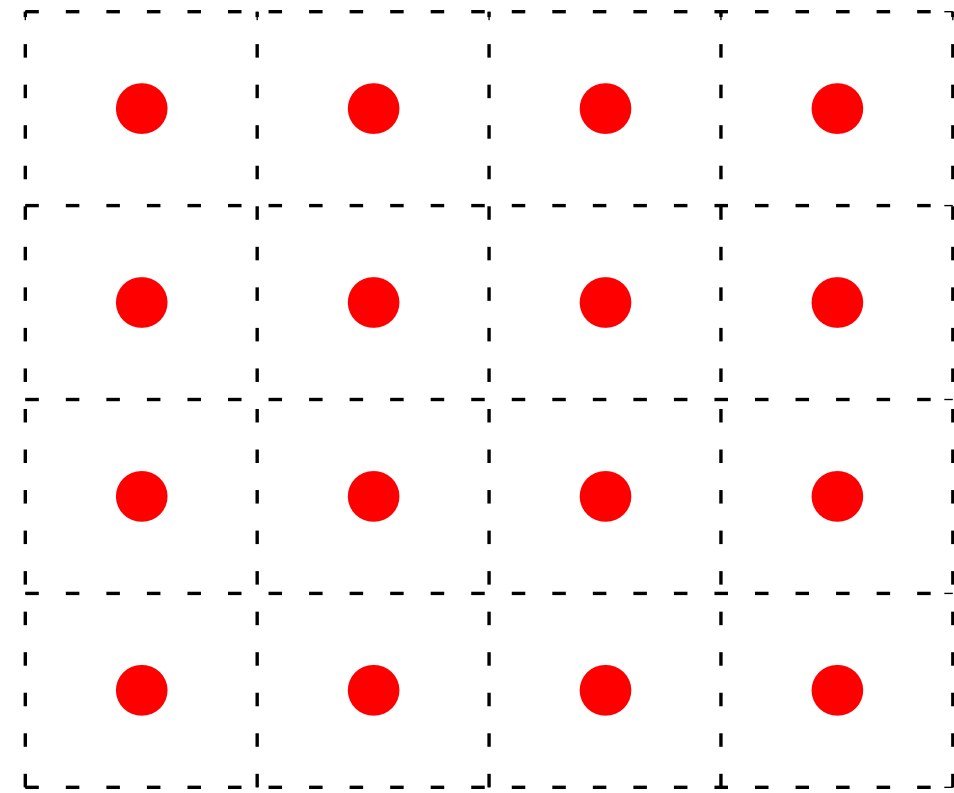
Translations

$$\rho(\mathbf{q}) = \int d\mathbf{r} e^{-i\mathbf{q}\cdot\mathbf{r}} \delta n(\mathbf{r})$$

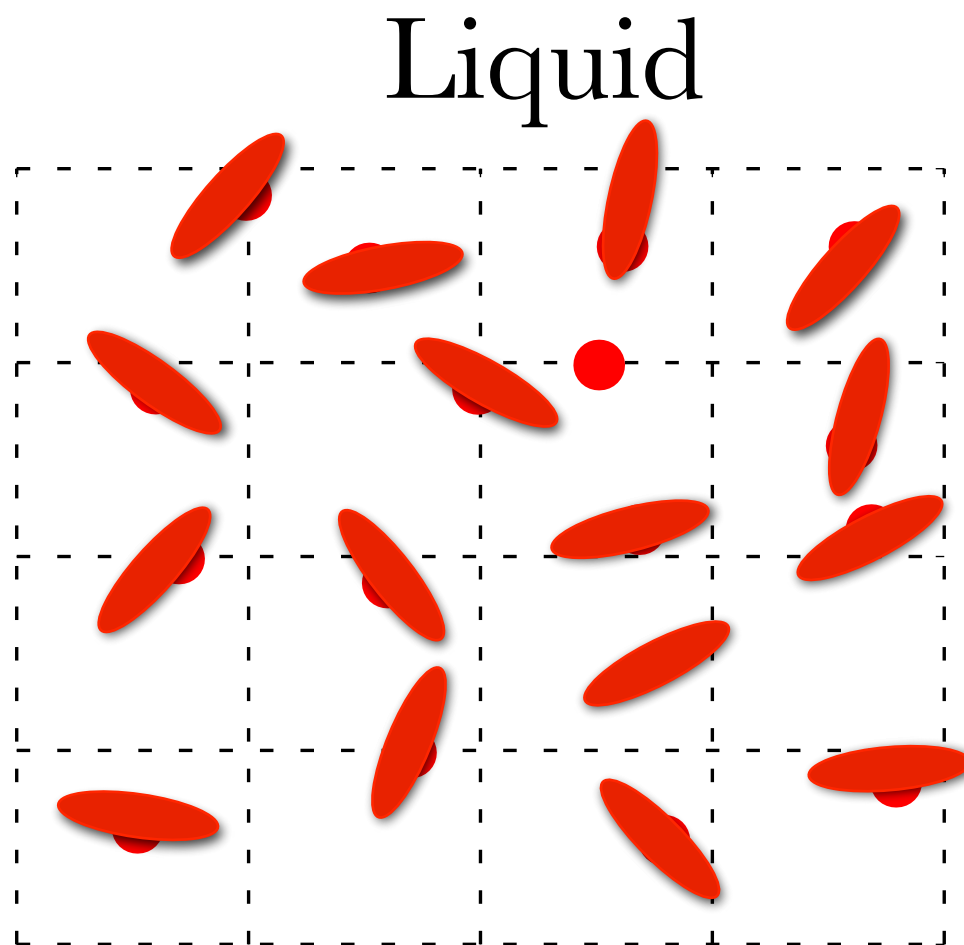
X-ray diffraction
peaks



Broken Symmetry & Ordered Phases



Solid



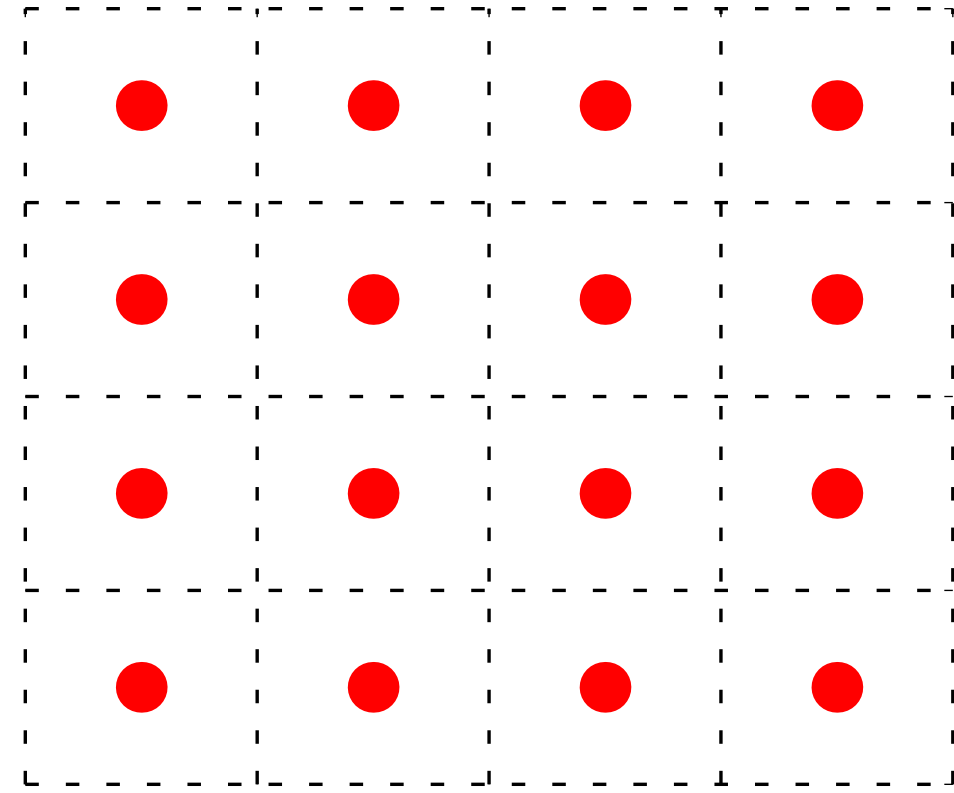
Translations

$$\rho(\mathbf{q}) = \int d\mathbf{r} e^{-i\mathbf{q}\cdot\mathbf{r}} \delta n(\mathbf{r})$$

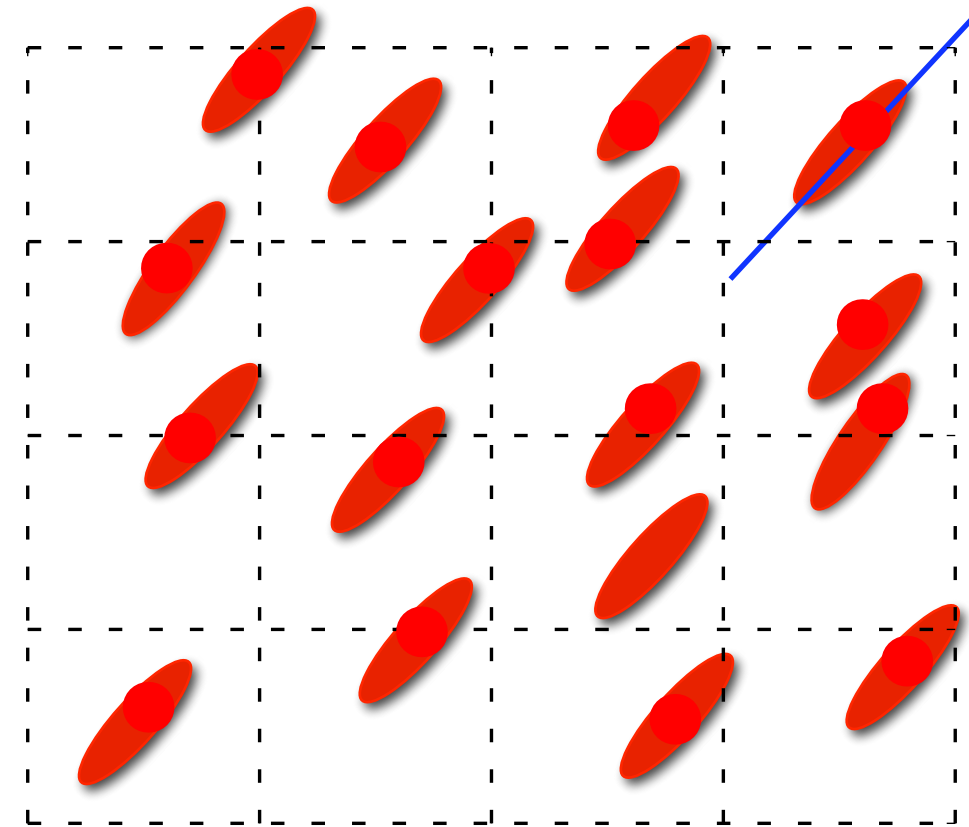
X-ray diffraction
peaks



Broken Symmetry & Ordered Phases



Solid



Nematic

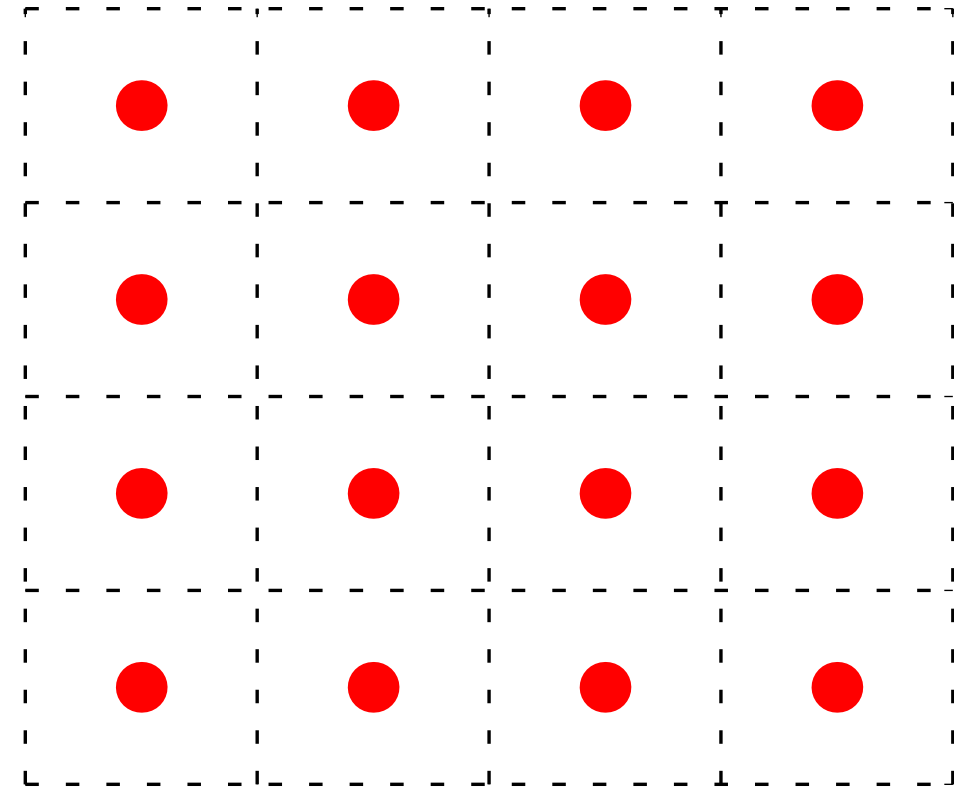
Translations

$$\rho(\mathbf{q}) = \int d\mathbf{r} e^{-i\mathbf{q}\cdot\mathbf{r}} \delta n(\mathbf{r})$$

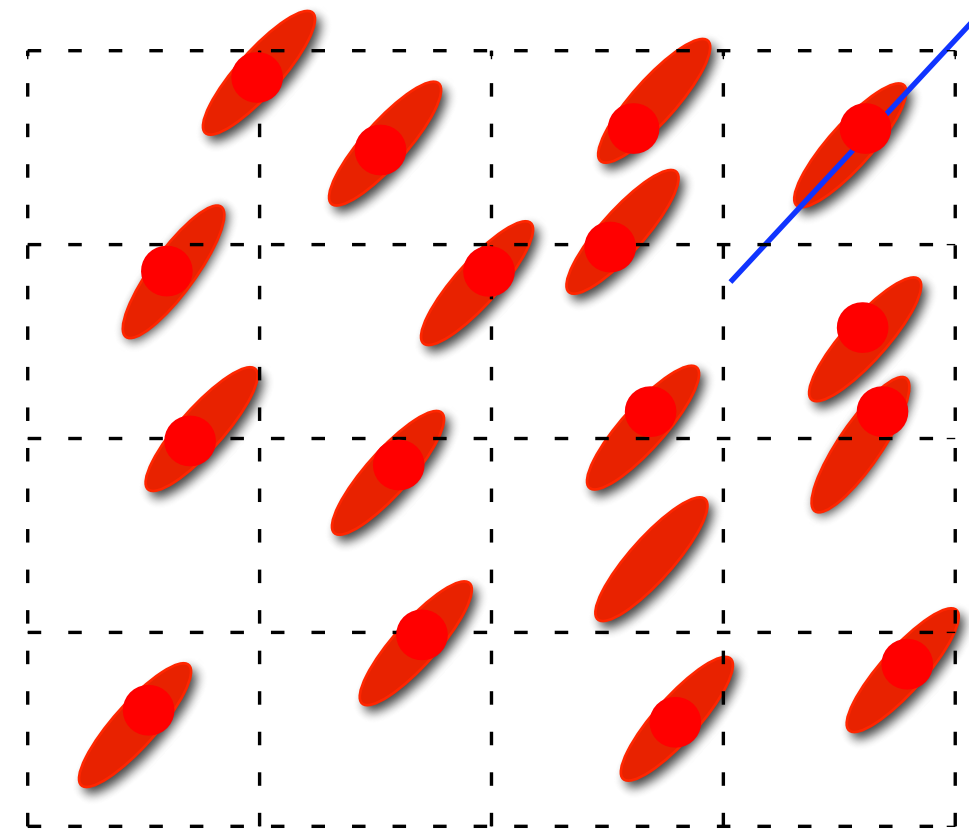
X-ray diffraction
peaks



Broken Symmetry & Ordered Phases



Solid



Nematic

Translations

$$\rho(\mathbf{q}) = \int d\mathbf{r} e^{-i\mathbf{q}\cdot\mathbf{r}} \delta n(\mathbf{r})$$

X-ray diffraction
peaks

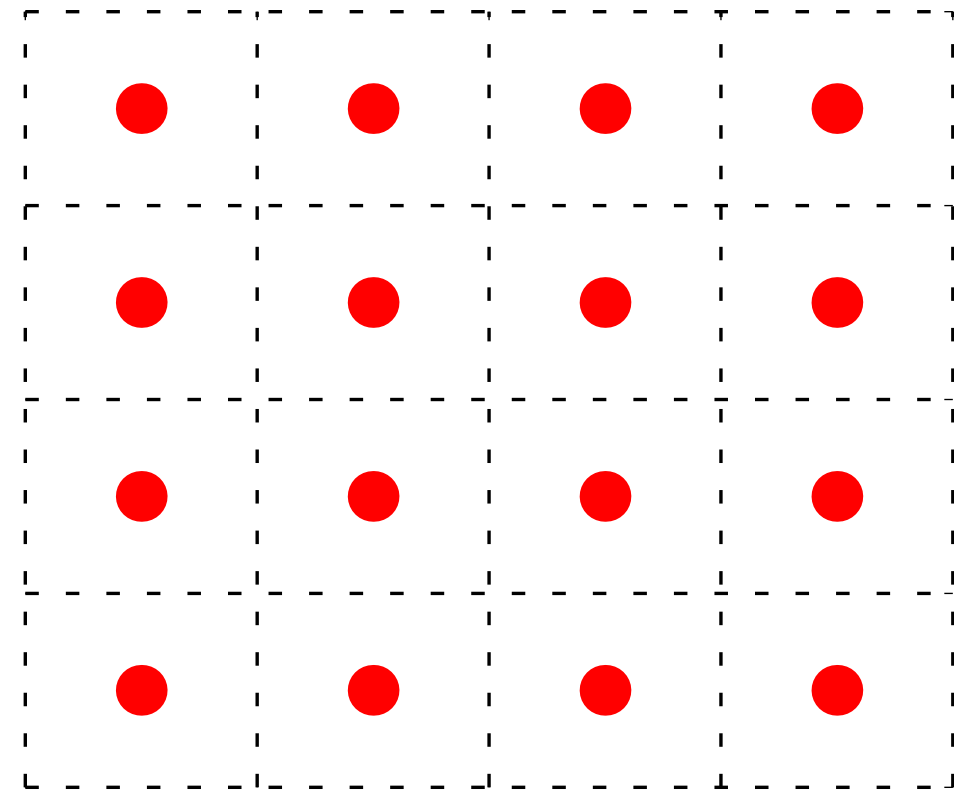
Space Rotations

$$\Delta\varepsilon_{ij} = \varepsilon(T) \hat{\mathbf{n}}_i \hat{\mathbf{n}}_j$$

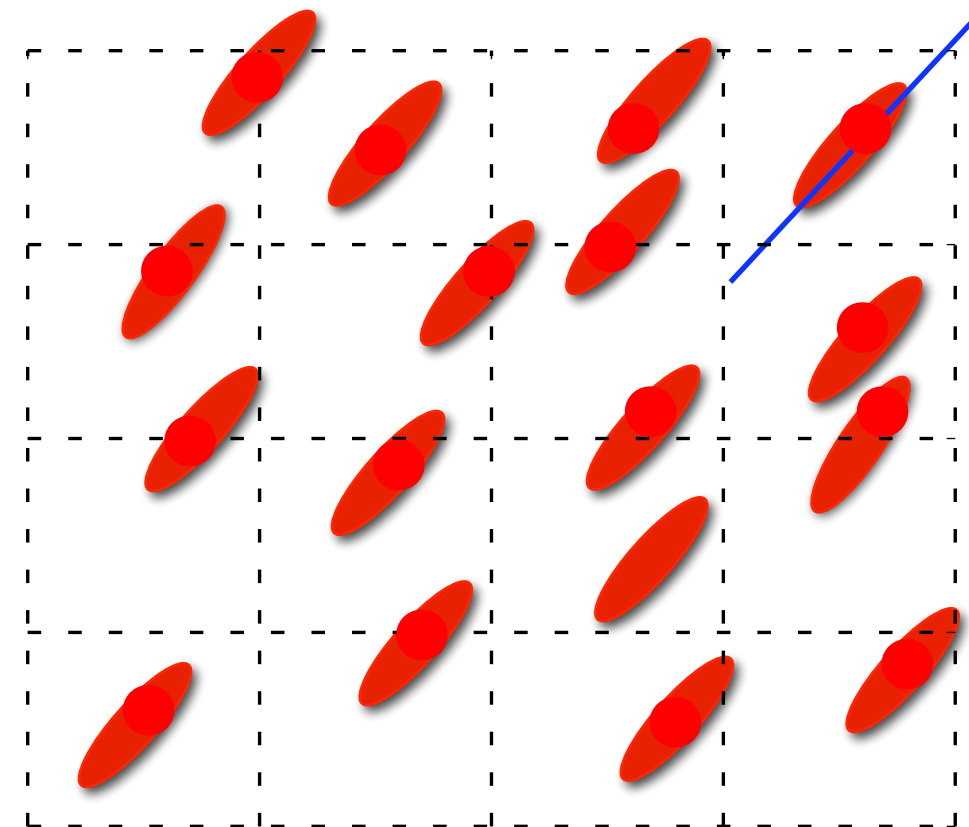
Anisotropic
dielectric function



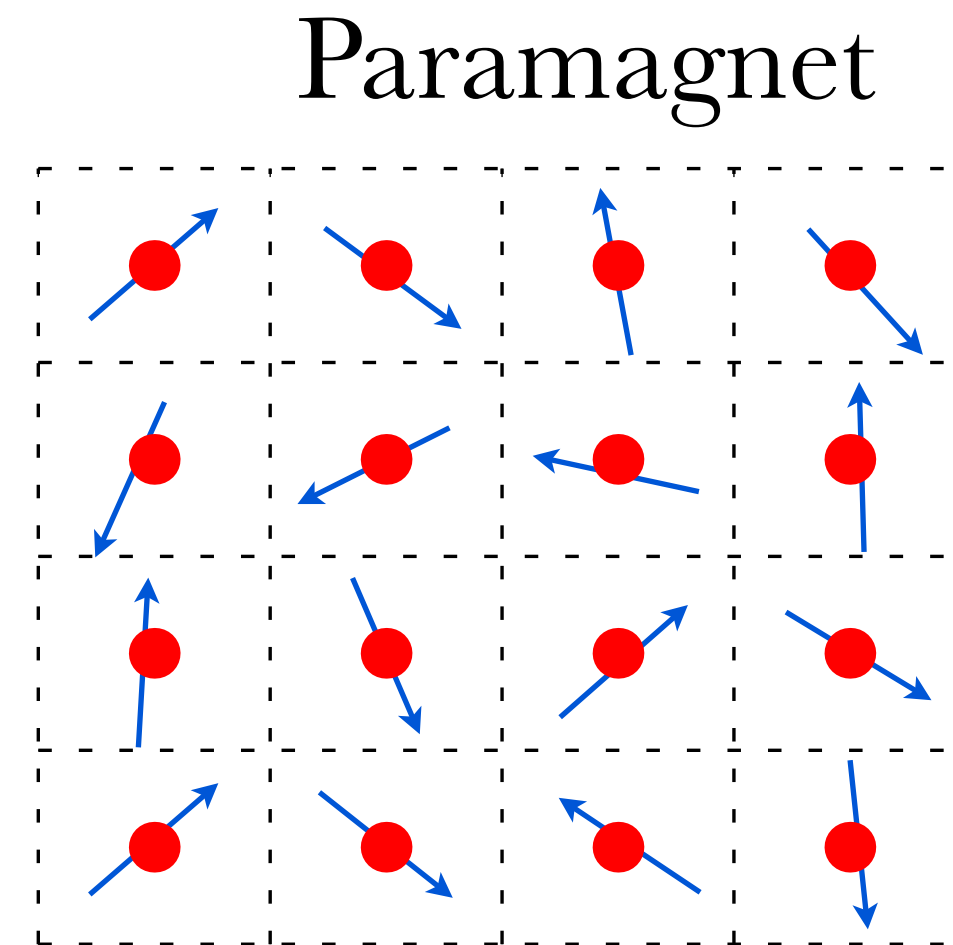
Broken Symmetry & Ordered Phases



Solid



Nematic



Translations

$$\rho(\mathbf{q}) = \int d\mathbf{r} e^{-i\mathbf{q}\cdot\mathbf{r}} \delta n(\mathbf{r})$$

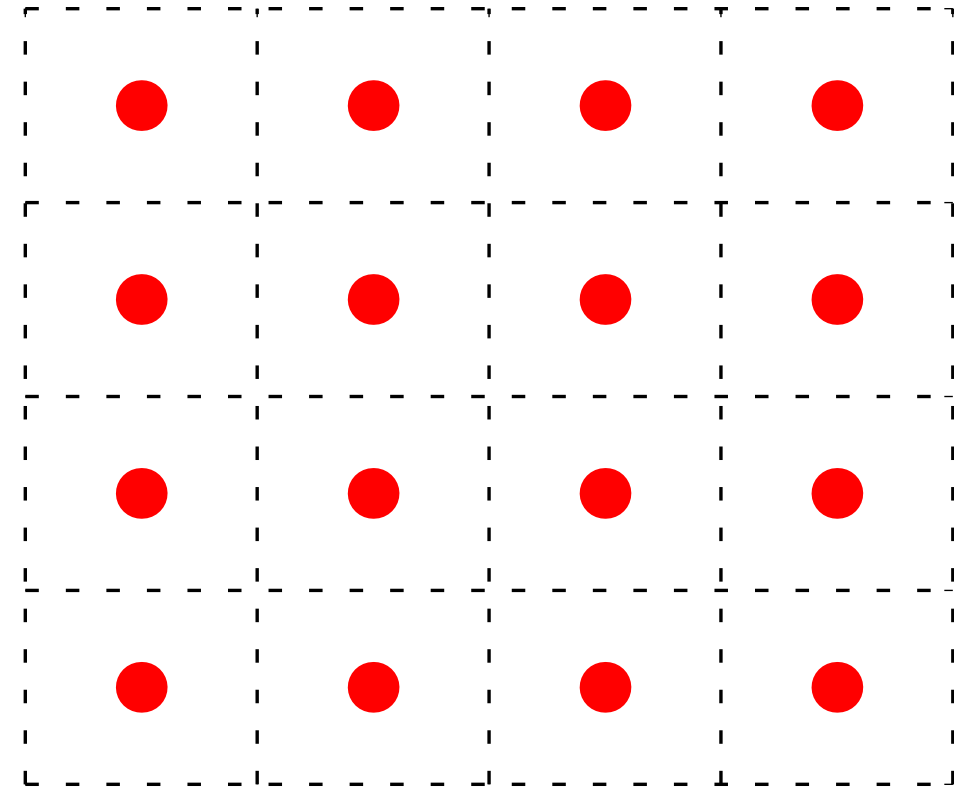
X-ray diffraction
peaks

Space Rotations

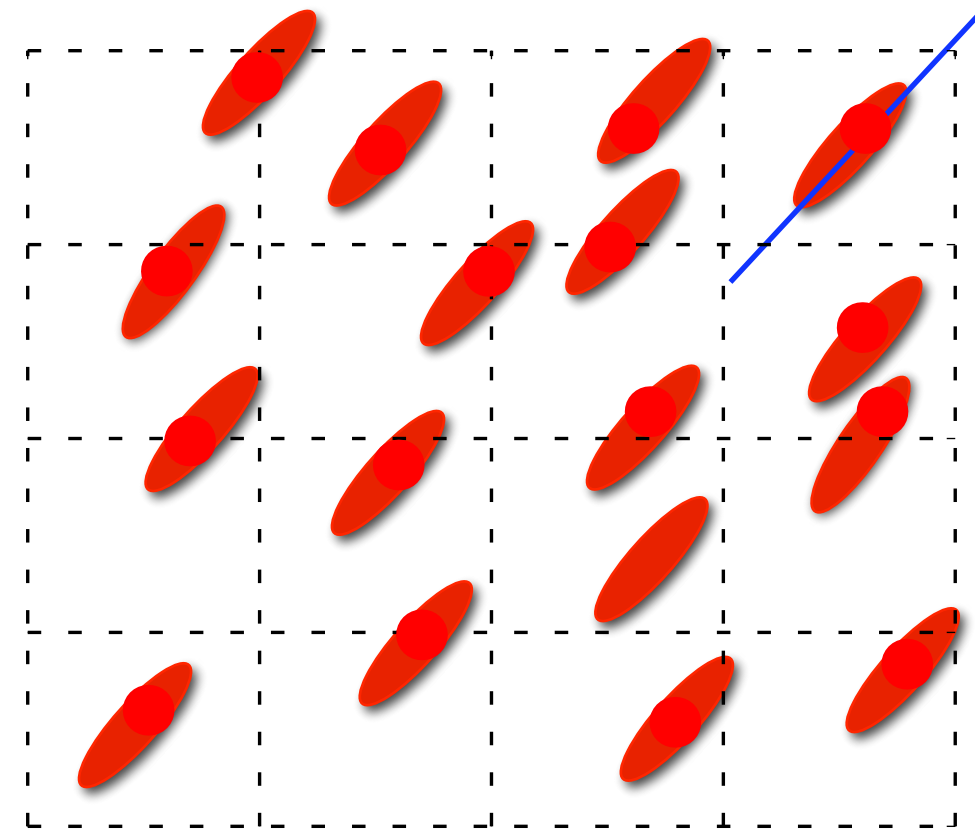
$$\Delta\varepsilon_{ij} = \varepsilon(T) \hat{\mathbf{n}}_i \hat{\mathbf{n}}_j$$

Anisotropic
dielectric function

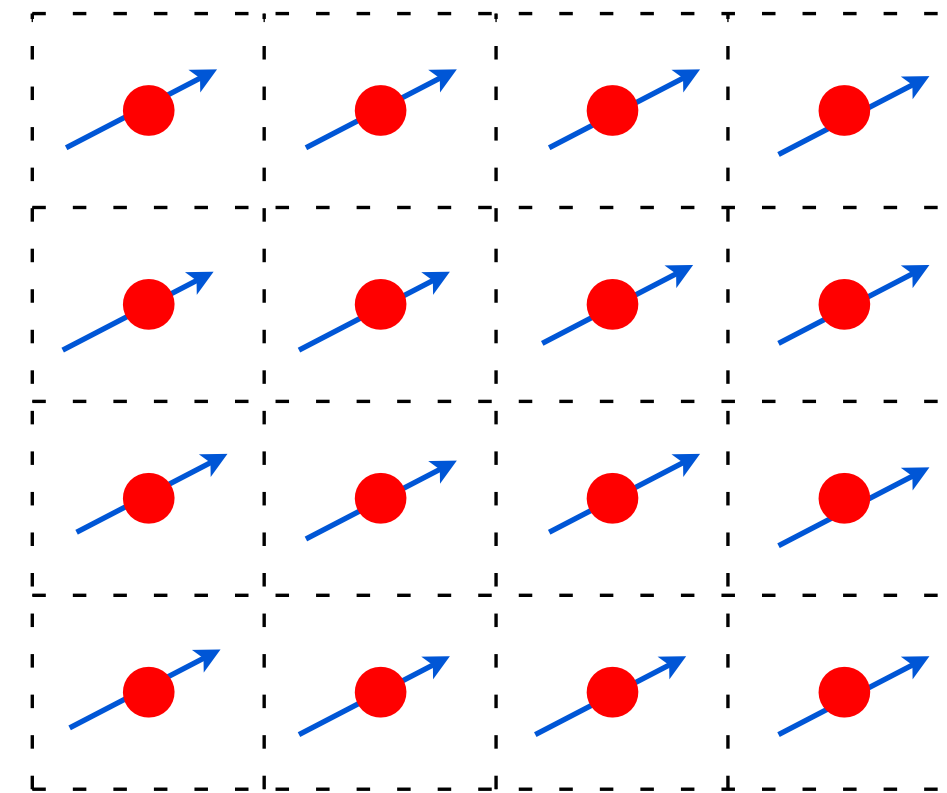
Broken Symmetry & Ordered Phases



Solid



Nematic



Ferromagnet

Translations

$$\rho(\mathbf{q}) = \int d\mathbf{r} e^{-i\mathbf{q}\cdot\mathbf{r}} \delta n(\mathbf{r})$$

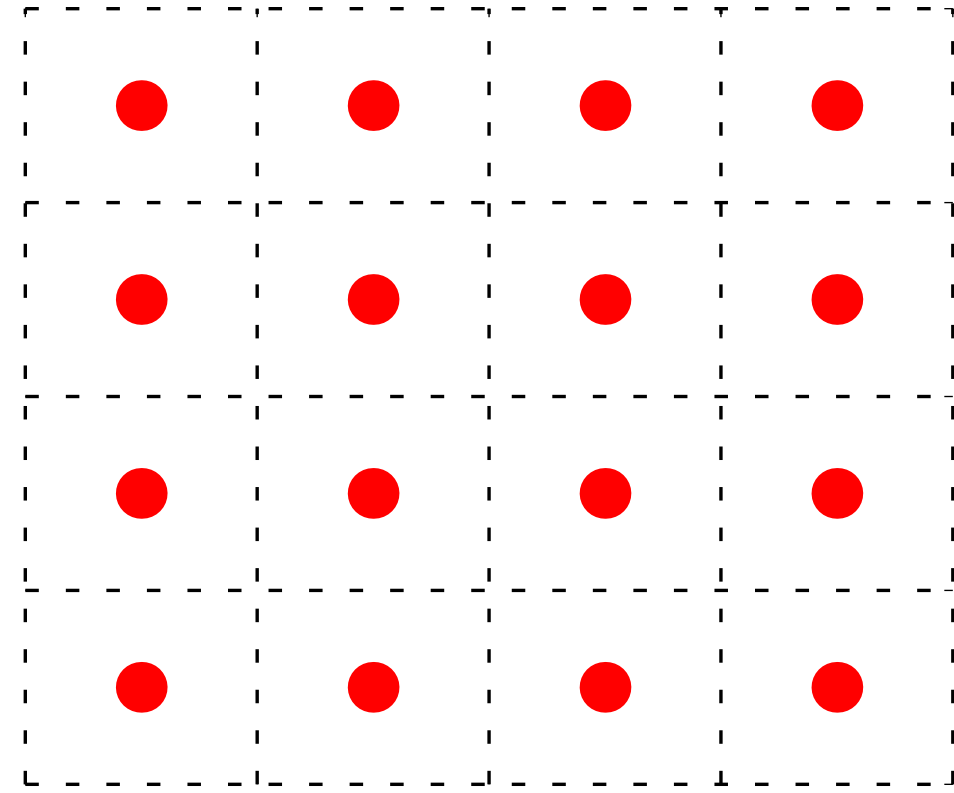
X-ray diffraction
peaks

Space Rotations

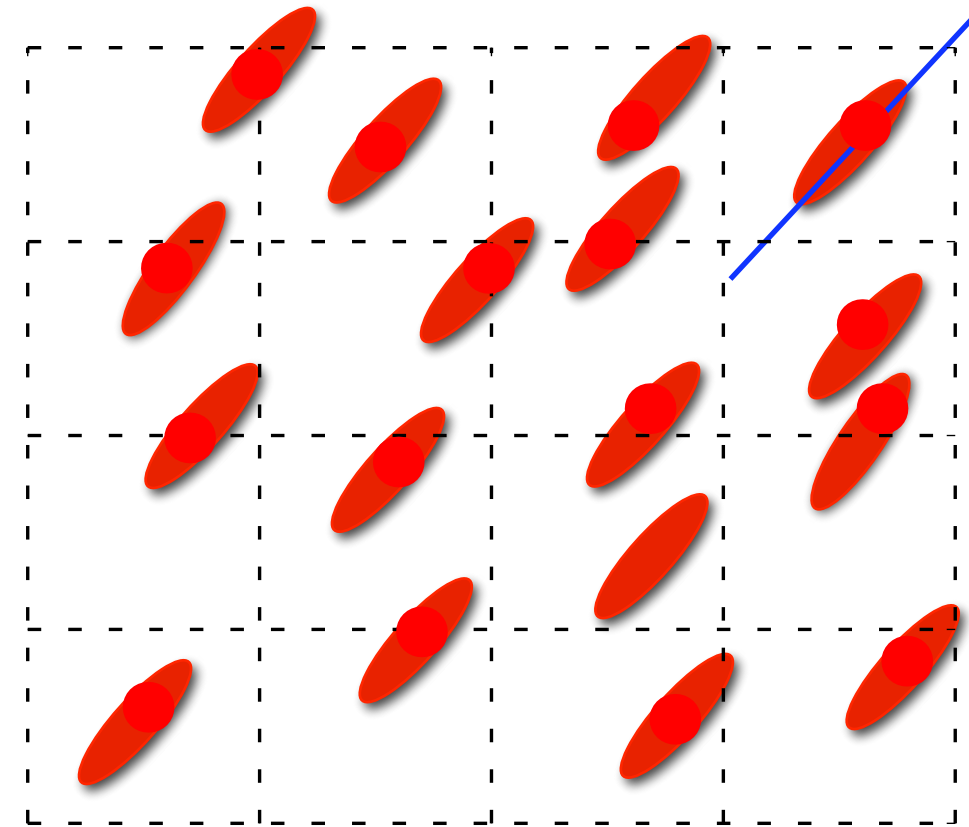
$$\Delta\varepsilon_{ij} = \varepsilon(T) \hat{\mathbf{n}}_i \hat{\mathbf{n}}_j$$

Anisotropic
dielectric function

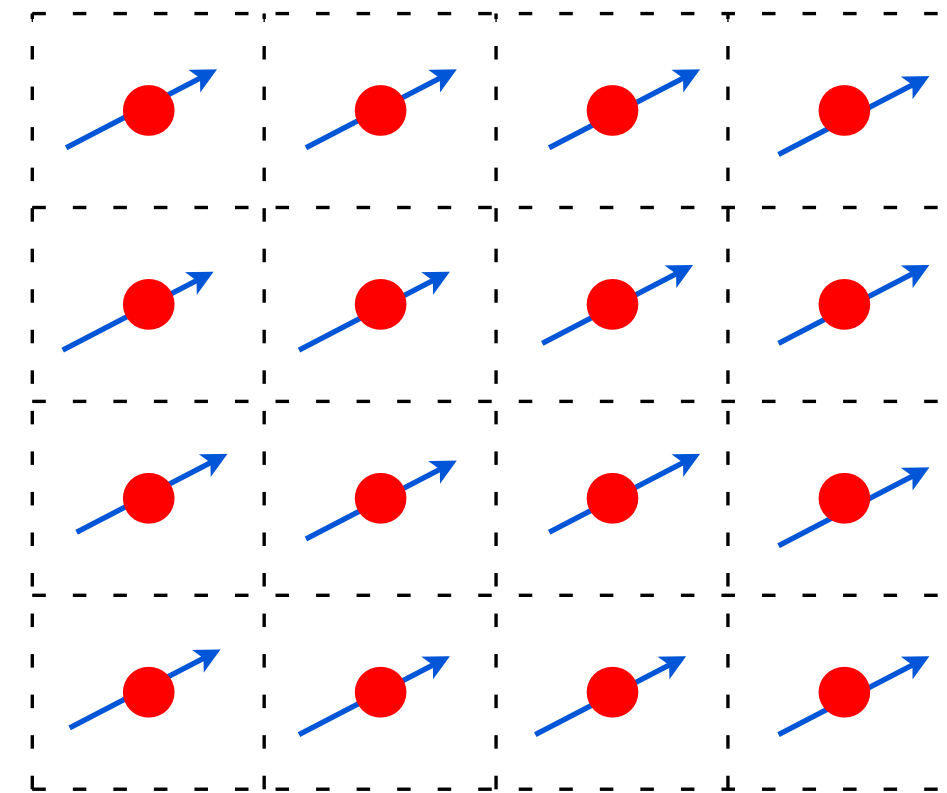
Broken Symmetry & Ordered Phases



Solid



Nematic



Ferromagnet

Translations

Space Rotations

Spin Rotation

$$\rho(\mathbf{q}) = \int d\mathbf{r} e^{-i\mathbf{q}\cdot\mathbf{r}} \delta n(\mathbf{r})$$

X-ray diffraction
peaks

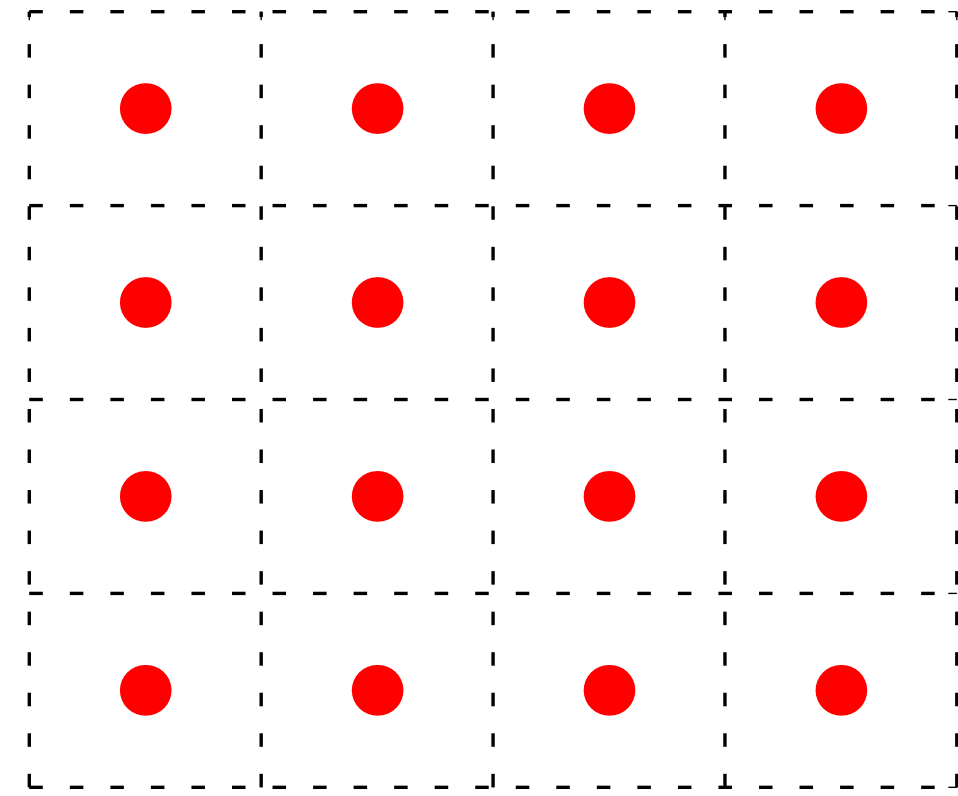
$$\Delta\varepsilon_{ij} = \varepsilon(T) \hat{\mathbf{n}}_i \hat{\mathbf{n}}_j$$

Anisotropic
dielectric function

$$\mathbf{M} = \gamma \langle \mathbf{S} \rangle$$

Spontaneous
Magnetization

Broken Symmetry & Ordered Phases

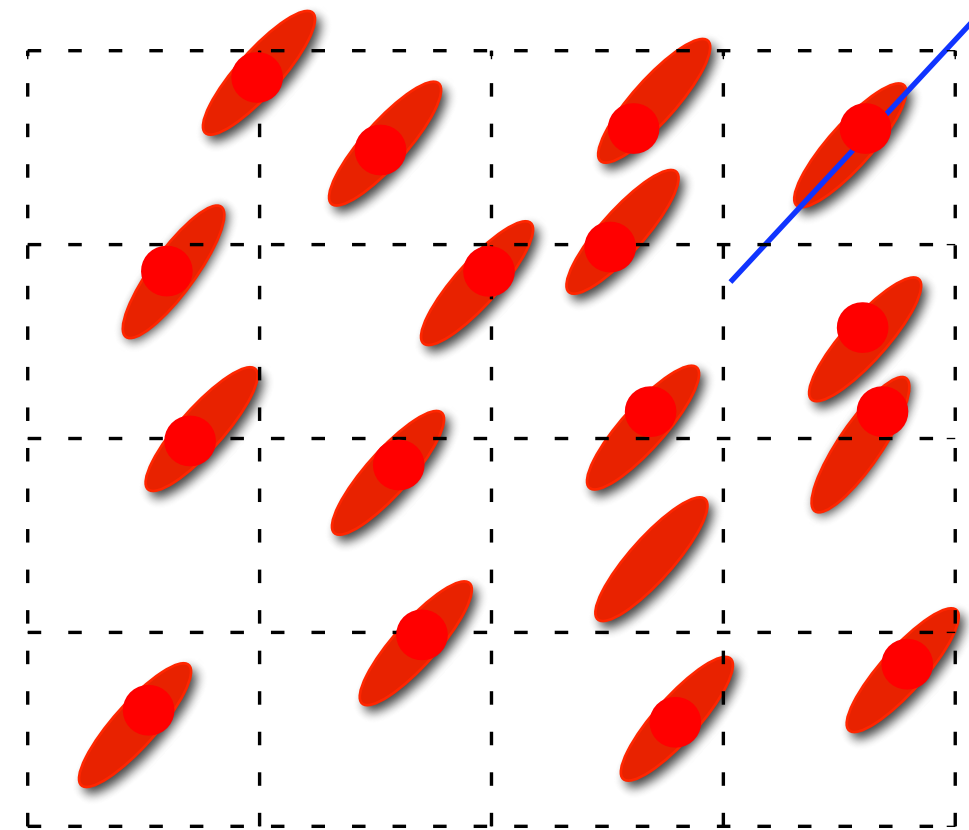


Solid

Translations

$$\rho(\mathbf{q}) = \int d\mathbf{r} e^{-i\mathbf{q}\cdot\mathbf{r}} \delta n(\mathbf{r})$$

X-ray diffraction
peaks

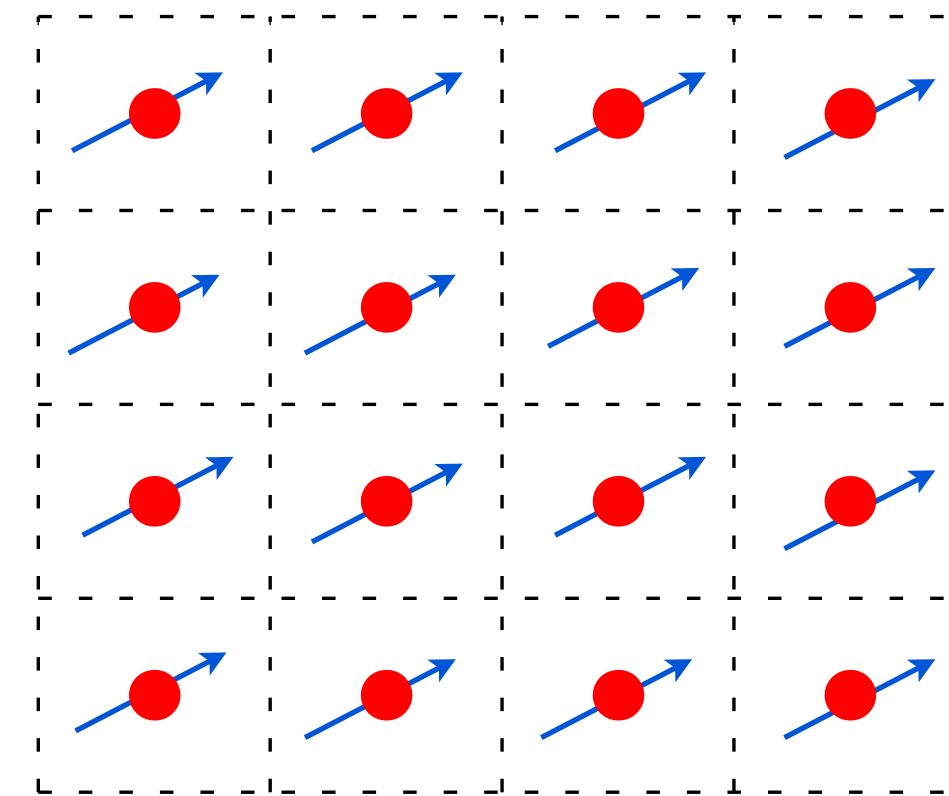


Nematic

Space Rotations

$$\Delta\varepsilon_{ij} = \varepsilon(T) \hat{\mathbf{n}}_i \hat{\mathbf{n}}_j$$

Anisotropic
dielectric function



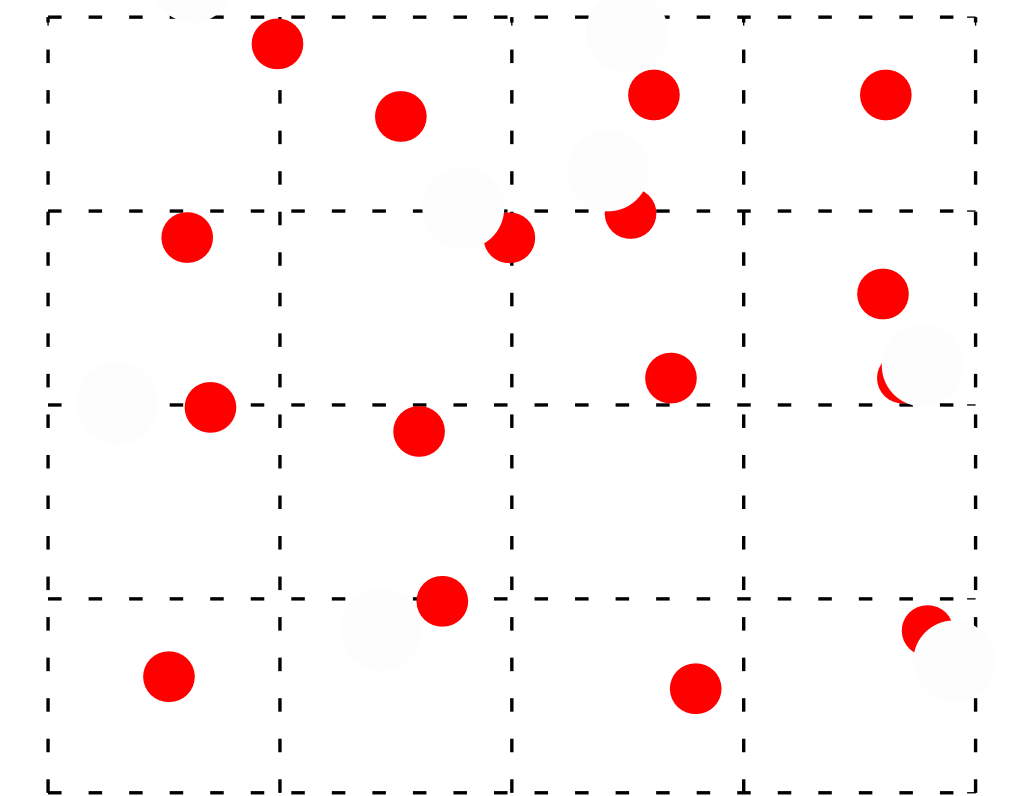
Ferromagnet

Spin Rotation

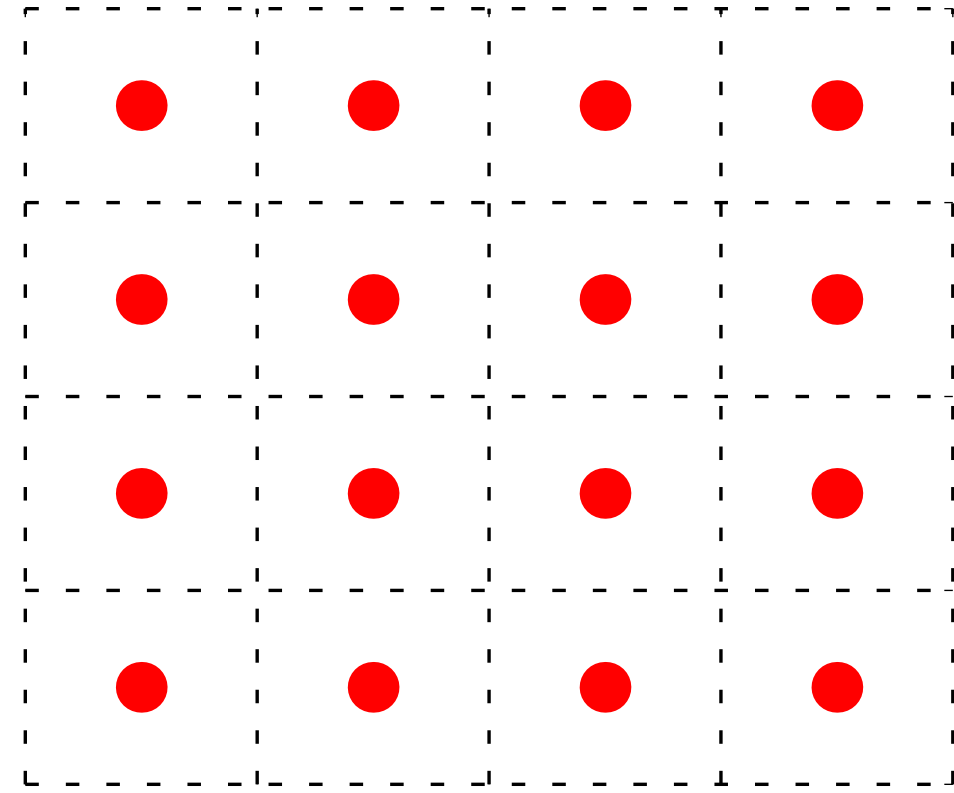
$$\mathbf{M} = \gamma \langle \mathbf{S} \rangle$$

Spontaneous
Magnetization

Helium & Metals



Broken Symmetry & Ordered Phases

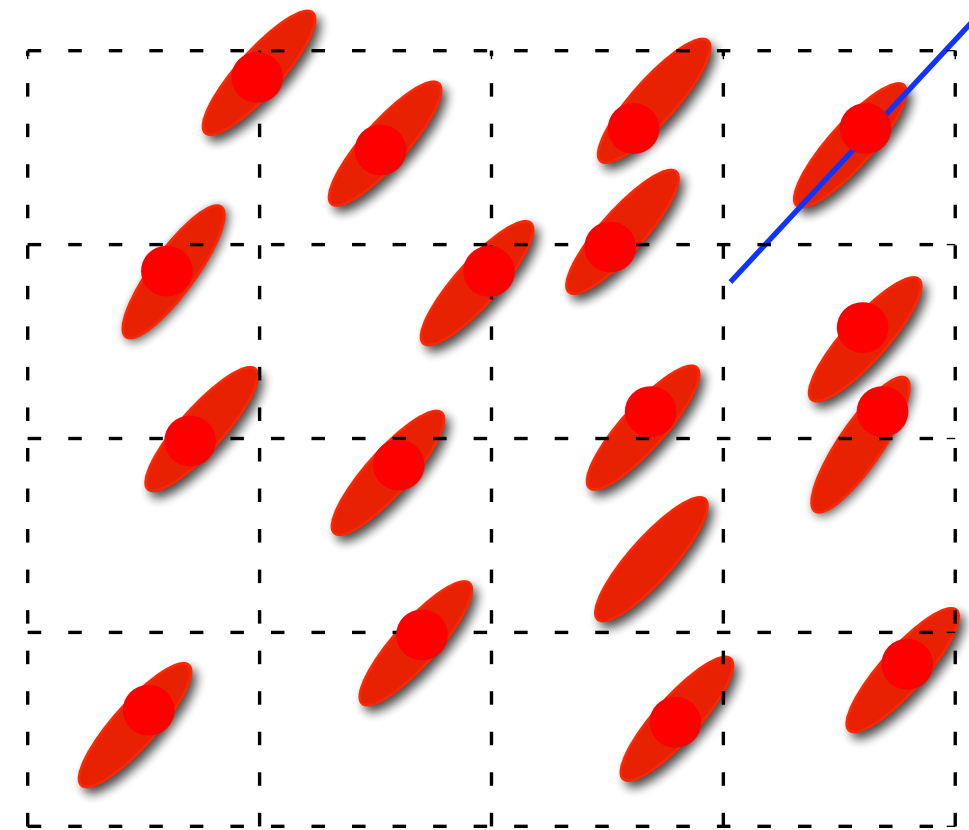


Solid

Translations

$$\rho(\mathbf{q}) = \int d\mathbf{r} e^{-i\mathbf{q}\cdot\mathbf{r}} \delta n(\mathbf{r})$$

X-ray diffraction
peaks

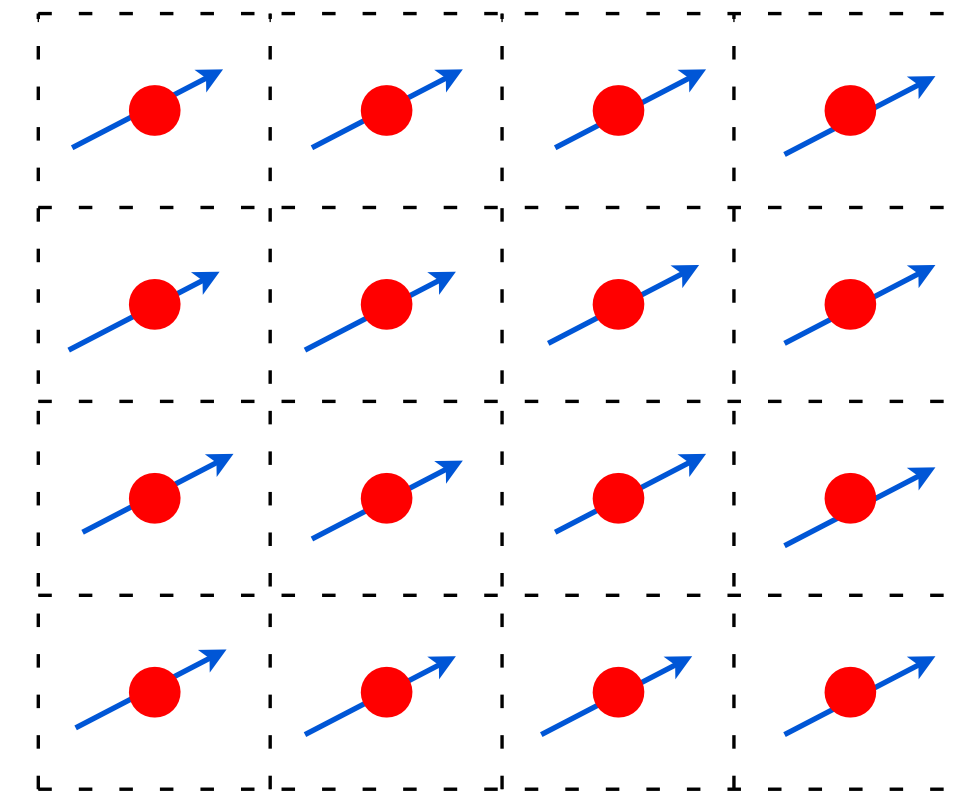


Nematic

Space Rotations

$$\Delta\varepsilon_{ij} = \varepsilon(T) \hat{\mathbf{n}}_i \hat{\mathbf{n}}_j$$

Anisotropic
dielectric function

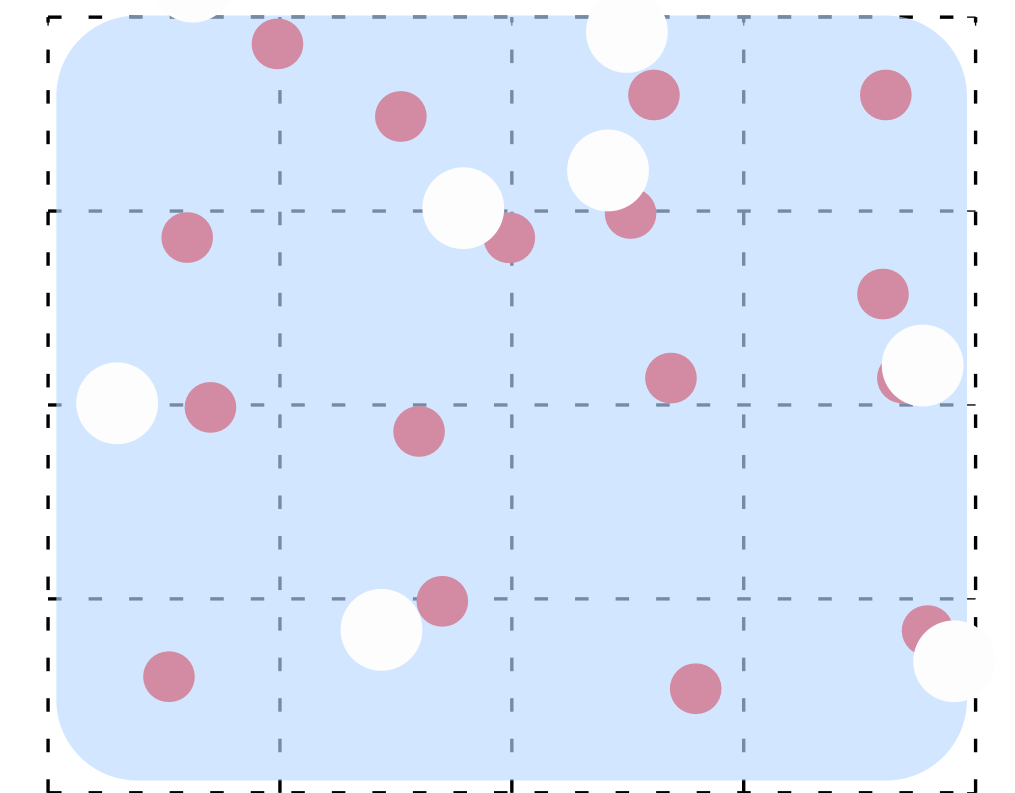


Ferromagnet

Spin Rotation

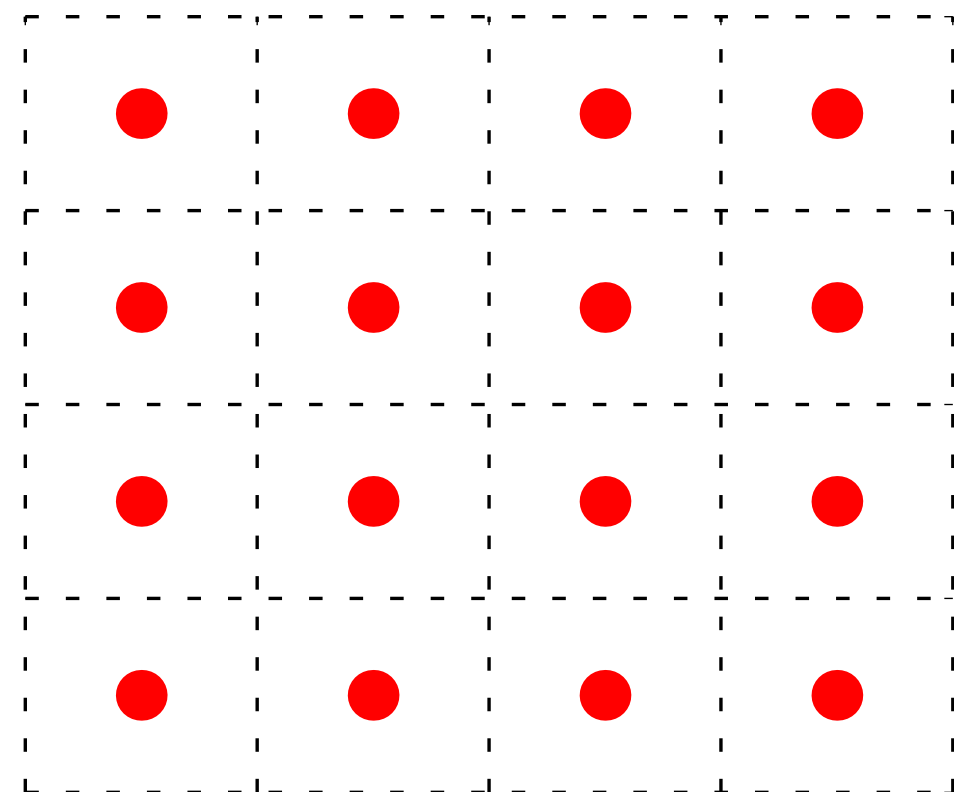
$$\mathbf{M} = \gamma \langle \mathbf{S} \rangle$$

Spontaneous
Magnetization



Superfluids
Superconductors

Broken Symmetry & Ordered Phases

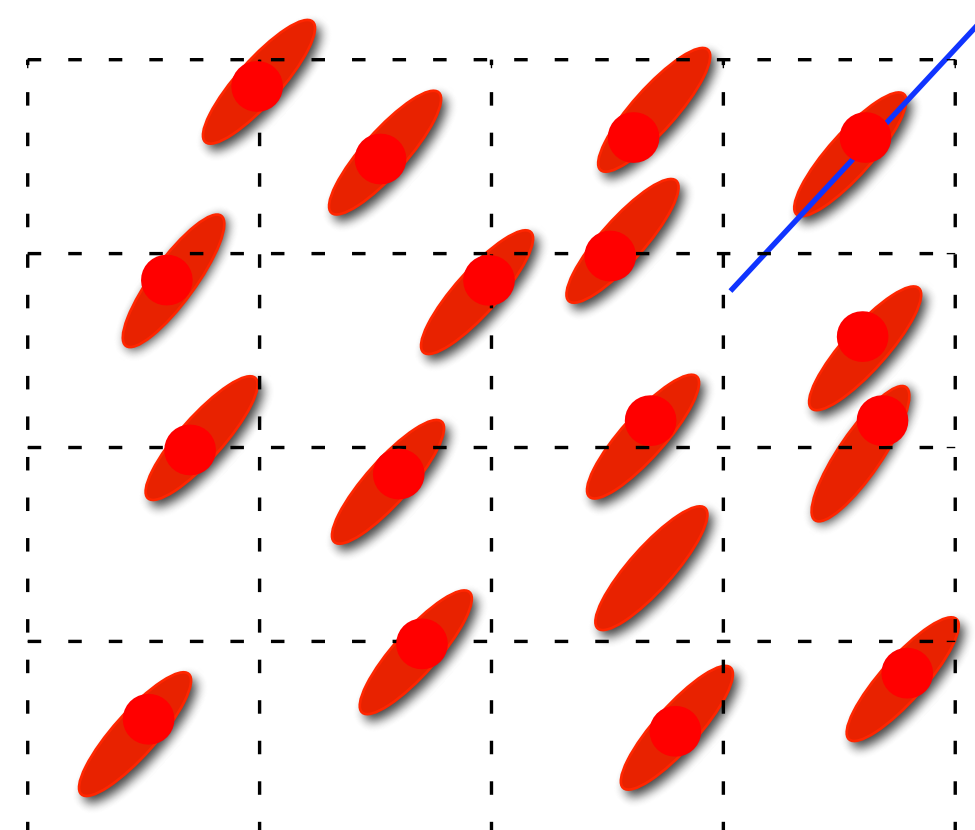


Solid

Translations

$$\rho(\mathbf{q}) = \int d\mathbf{r} e^{-i\mathbf{q}\cdot\mathbf{r}} \delta n(\mathbf{r})$$

X-ray diffraction peaks

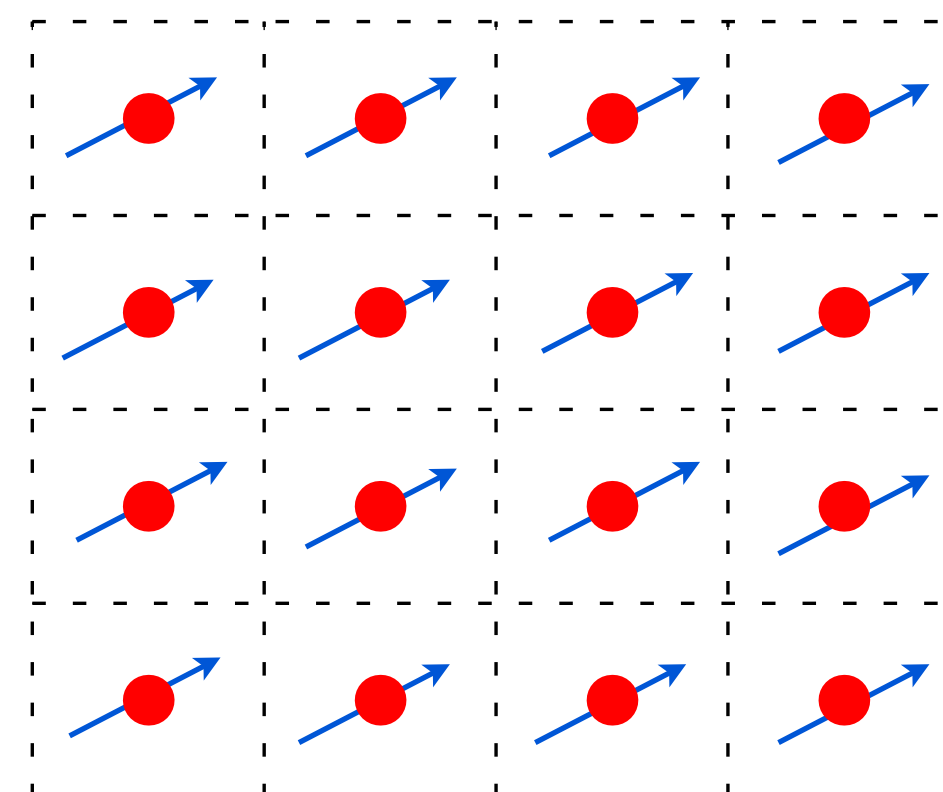


Nematic

Space Rotations

$$\Delta\varepsilon_{ij} = \varepsilon(T) \hat{\mathbf{n}}_i \hat{\mathbf{n}}_j$$

Anisotropic dielectric function

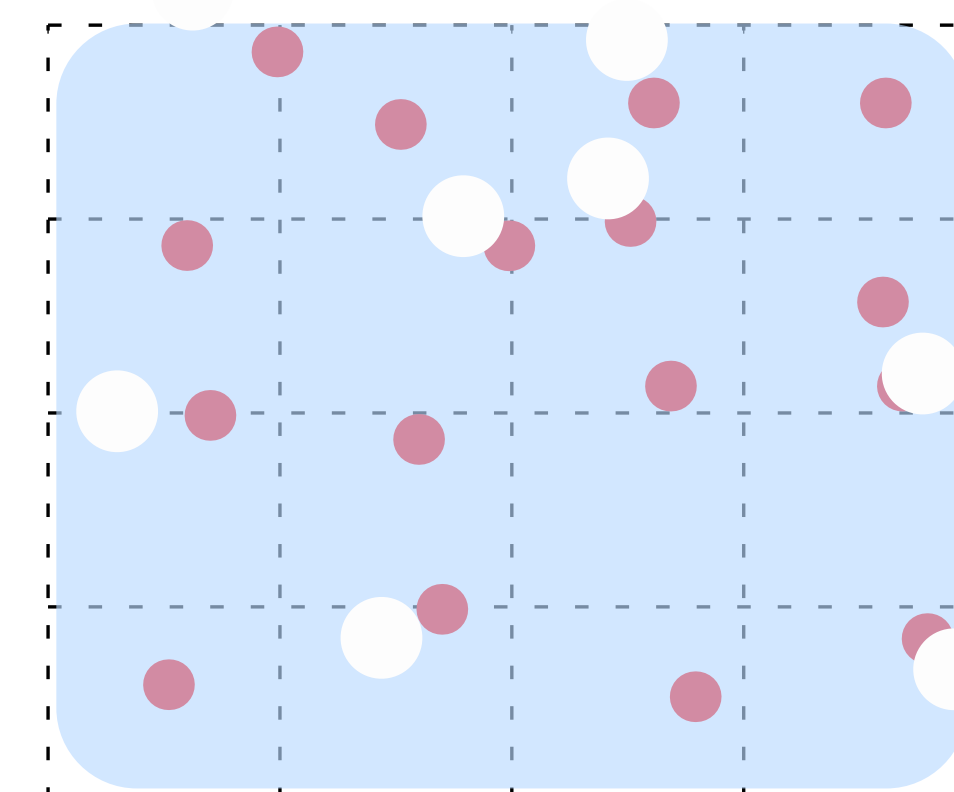


Ferromagnet

Spin Rotation

$$\mathbf{M} = \gamma \langle \mathbf{S} \rangle$$

Spontaneous Magnetization



Superfluids
Superconductors

Gauge

$$\begin{aligned} \Psi &= \langle \psi(\mathbf{r}) \rangle \\ &\simeq \sqrt{N/V} e^{i\vartheta} \end{aligned}$$

Condensate
Wave function

Ginzburg-Landau Theory August 6, 2023

V. L. Ginzburg and L. D. Landau, JETP ... (1950).

- ▶ Superconductivity originates from a macroscopic quantum state, $\Psi(\mathbf{r})$ with,

$$n_S \equiv |\Psi(\mathbf{r})|^2 = \text{density of "super" electrons}$$

- ▶ $\Psi(\mathbf{r}) = |\Psi(\mathbf{r})| e^{i\vartheta(\mathbf{r})} \rightsquigarrow \vec{J}(\mathbf{r}) \propto |\Psi(\mathbf{r})|^2 \nabla \vartheta(\mathbf{r}) = \text{"supercurrents"}$

- ▶ $\Psi(\mathbf{r})$ is a thermodynamic variable of state at finite T and p

Ginzburg-Landau Theory August 6, 2023

V. L. Ginzburg and L. D. Landau, JETP ... (1950).

- ▶ Superconductivity originates from a macroscopic quantum state, $\Psi(\mathbf{r})$ with,

$$n_S \equiv |\Psi(\mathbf{r})|^2 = \text{density of "super" electrons}$$

- ▶ $\Psi(\mathbf{r}) = |\Psi(\mathbf{r})| e^{i\vartheta(\mathbf{r})} \rightsquigarrow \vec{J}(\mathbf{r}) \propto |\Psi(\mathbf{r})|^2 \nabla \vartheta(\mathbf{r}) = \text{"supercurrents"}$

- ▶ $\Psi(\mathbf{r})$ is a thermodynamic variable of state at finite T and p

- ▶ Equilibrium: Landau's theory of symmetry breaking phase transitions

- ▶ Continuous Transition: $\Psi \rightarrow 0$ for $T \rightarrow T_c - 0^+$
- ▶ Discontinuous Change in Symmetry: $G' \subset G$

Ginzburg-Landau Theory August 6, 2023

V. L. Ginzburg and L. D. Landau, JETP ... (1950).

- ▶ Superconductivity originates from a macroscopic quantum state, $\Psi(\mathbf{r})$ with,

$$n_S \equiv |\Psi(\mathbf{r})|^2 = \text{density of "super" electrons}$$

- ▶ $\Psi(\mathbf{r}) = |\Psi(\mathbf{r})| e^{i\vartheta(\mathbf{r})} \rightsquigarrow \vec{J}(\mathbf{r}) \propto |\Psi(\mathbf{r})|^2 \nabla \vartheta(\mathbf{r}) = \text{"supercurrents"}$

- ▶ $\Psi(\mathbf{r})$ is a thermodynamic variable of state at finite T and p

- ▶ Equilibrium: Landau's theory of symmetry breaking phase transitions

- ▶ Continuous Transition: $\Psi \rightarrow 0$ for $T \rightarrow T_c - 0^+$
- ▶ Discontinuous Change in Symmetry: $G' \subset G$

- ▶ Ginzburg-Landau: $U(1)_N$ gauge symmetry is broken: $\Psi \xrightarrow{\alpha \in U(1)_N} \Psi e^{i\alpha} \neq \Psi$

- ▶ Taylor Expansion of the Free Energy in Maximal Symmetry Invariants: $\Psi\Psi^* = |\Psi|^2$ $\Psi\Psi\Psi^*\Psi^* = |\Psi|^4$

$$\nabla_i \Psi \nabla_i \Psi^* = |\nabla \Psi|^2$$

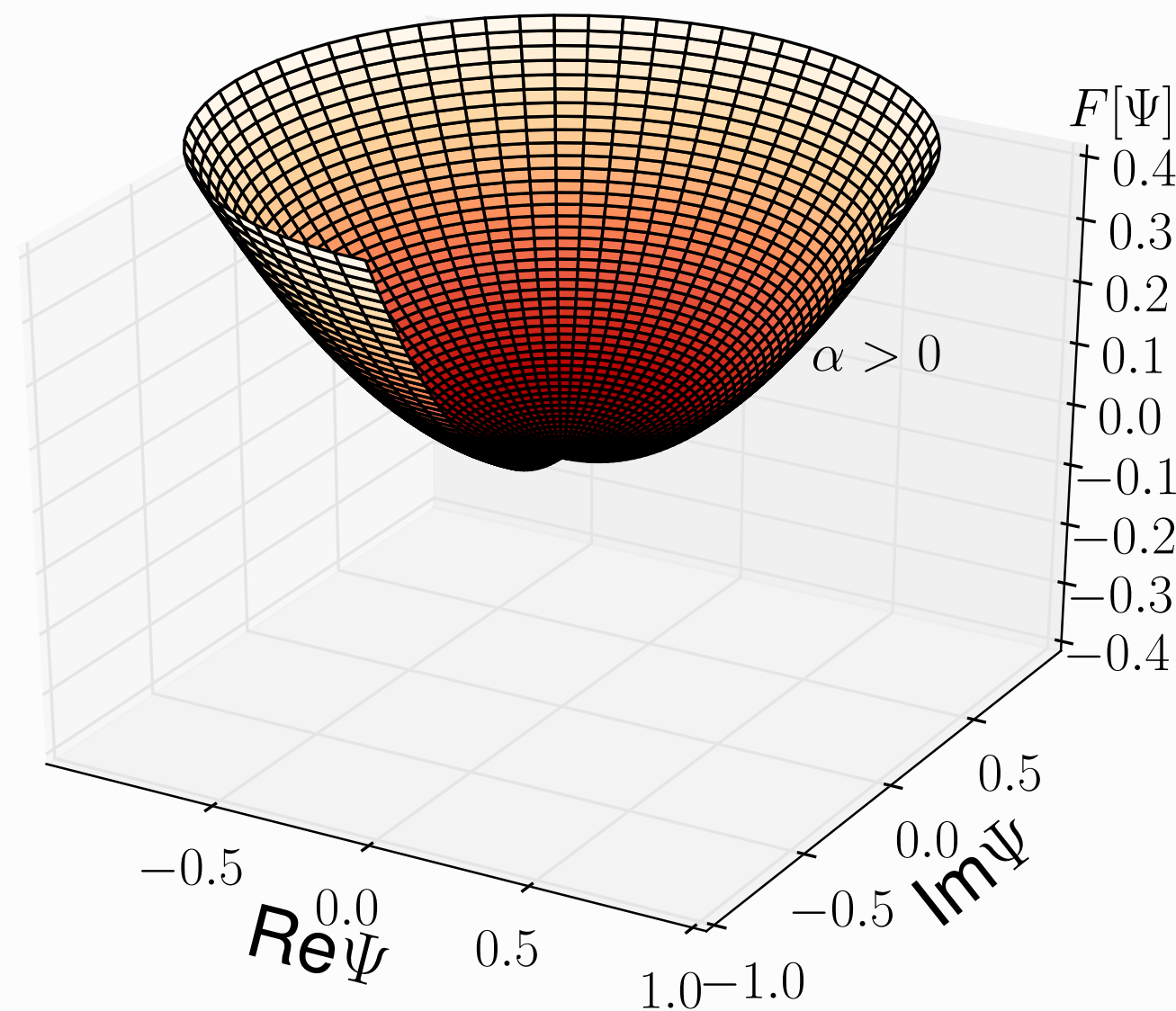
Ginzburg-Landau Free Energy Functional August 6, 2023

▶ $F = E - TS$ for a homogeneous Superconductor ($\vec{B} = 0$):

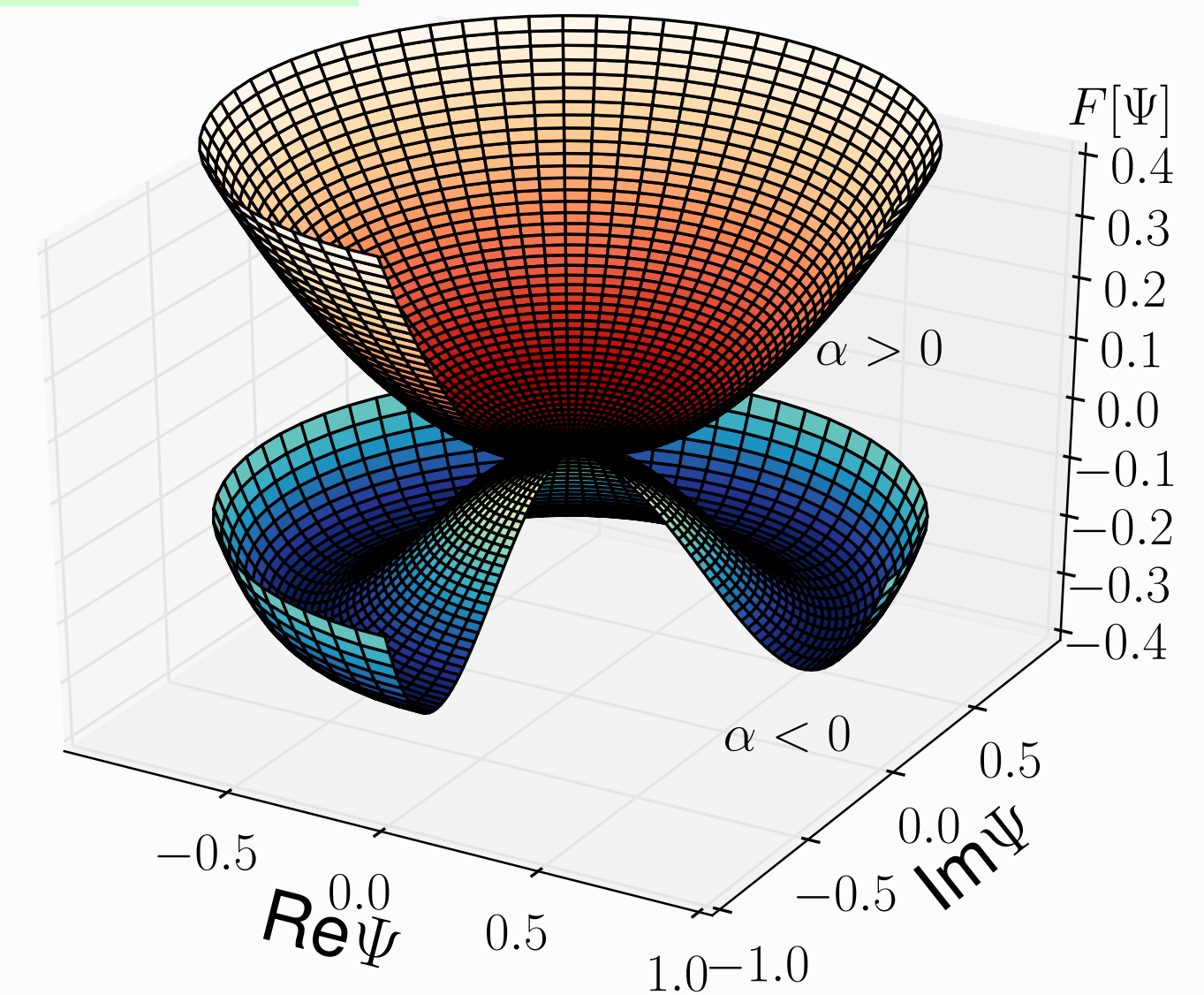
$$F[\Psi; T, p] = \overbrace{F_N(p, T)}^{\text{Normal State}} + \int dV \left\{ \alpha(p, T) |\Psi|^2 + \beta(p, T) |\Psi|^4 \right\} \quad (1)$$

▶ Equilibrium: Minimum of F with respect to Ψ

▶ Global Stability: $\beta > 0$ ▶ Transition: $\alpha(T_c, p) \equiv 0 \rightsquigarrow \alpha(T, p) \approx \alpha'(T - T_c)$



▶ $T > T_c$: $\Psi = 0$ (normal state)

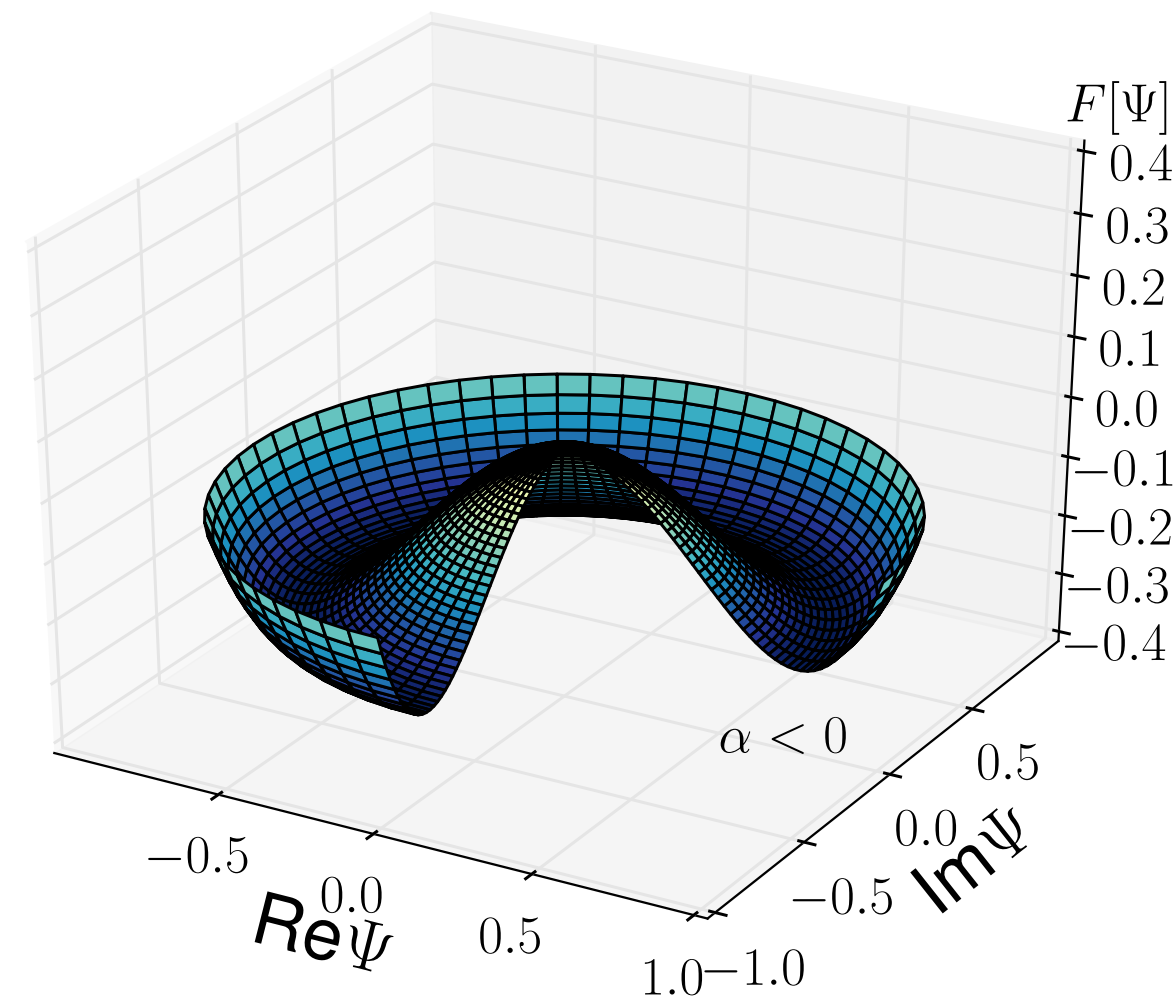


▶ $T < T_c$: $|\Psi| = \sqrt{\frac{|\alpha(T, p)|}{2\beta}} \sim (1 - T/T_c)^{\frac{1}{2}}$

Ginzburg-Landau Thermodynamics August 6, 2023

▶ Condensate Amplitude for $T < T_c$:

$$\Psi_{\text{eq}} = \sqrt{\frac{\alpha' T_c}{2\beta}} (1 - T/T_c)^{\frac{1}{2}}$$



▶ Condensation Energy Density:

$$\Delta F_{\text{eq}} = \frac{1}{2} \alpha(T, p) \Psi_{\text{eq}}^2 \quad (2)$$

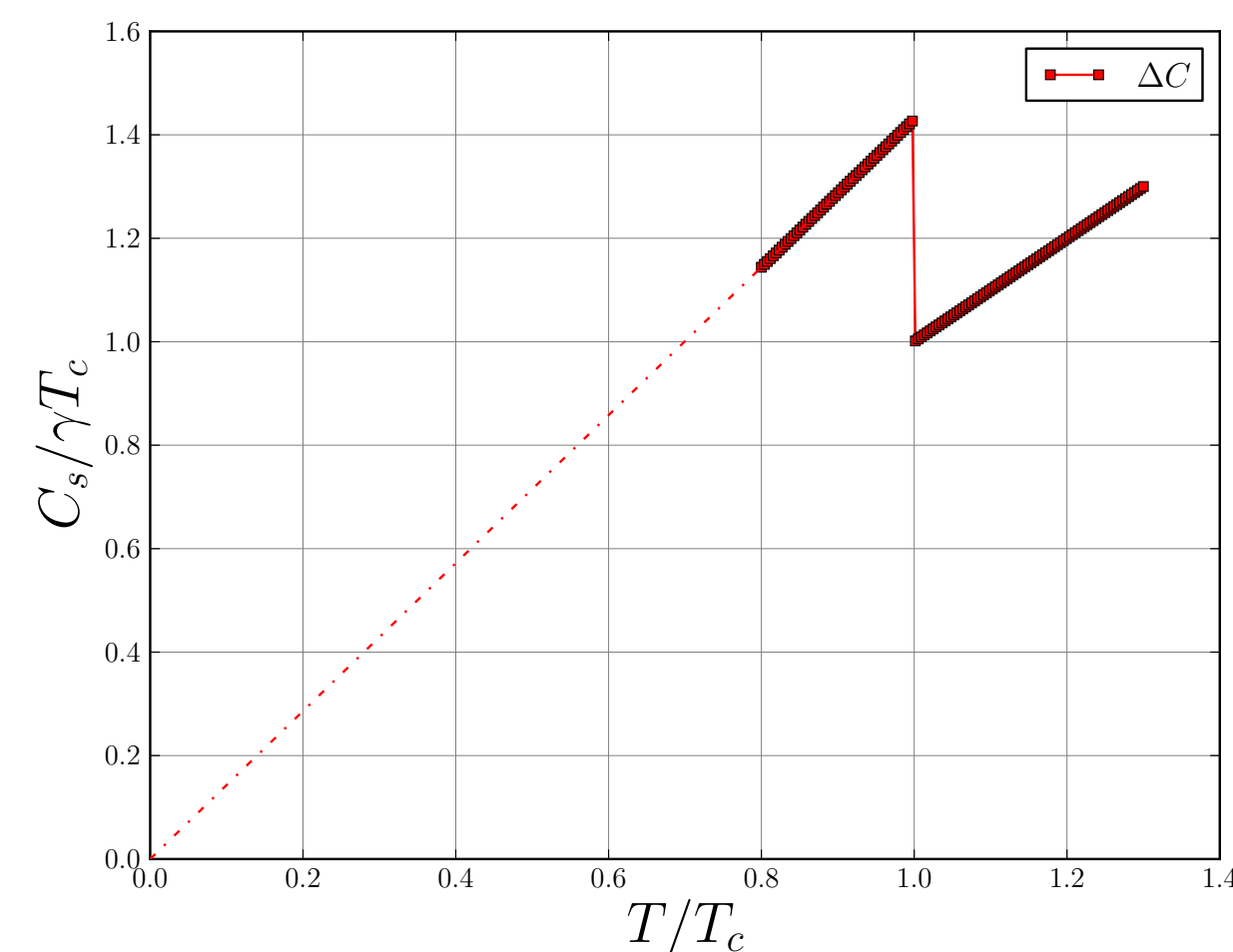
$$= -\frac{(\alpha')^2}{4\beta} (T - T_c)^2 \quad (3)$$

▶ Entropy Reduction:

$$\Delta S = -\frac{\partial \Delta F}{\partial T} = \frac{(\alpha')^2}{2\beta} (T - T_c) \quad (4)$$

▶ Heat Capacity Jump:

$$\Delta C = T \frac{\partial \Delta S}{\partial T} = T \frac{(\alpha')^2}{2\beta} \quad (5)$$



Ginzburg-Landau Theory - Coupling to Static Magnetic Fields August 6, 2023

- ▶ External Field - \vec{H} , Magnetization \vec{M} and Total Field $\vec{B} = \nabla \times \vec{A}$ (Vector Potential)
- ▶ $\Psi(\mathbf{r})$ is the wave function for “super” electrons of charge e^*
- ▶ BCS theory: $e^* = 2e$ (Cooper Pairs of Electrons)

Local

- ▶ Gauge Invariant Coupling: $\frac{\hbar}{i} \nabla \Psi \rightsquigarrow \left(\frac{\hbar}{i} \nabla - \frac{e^*}{c} \vec{A} \right) \Psi$

GL Functional with Coupling to \vec{A} plus Field Energy

$$F[\Psi, \vec{A}] = \int dV \left\{ \alpha(T) |\Psi|^2 + \frac{1}{2} \beta |\Psi|^4 + \frac{1}{2M^*} \left| \left(\frac{\hbar}{i} \nabla - \frac{e^*}{c} \vec{A} \right) \Psi \right|^2 + \frac{1}{8\pi} \left(\nabla \times \vec{A} - \vec{H} \right)^2 \right\}$$

Ginzburg-Landau Theory - Coupling to Static Magnetic Fields August 6, 2023

- ▶ External Field - \vec{H} , Magnetization \vec{M} and Total Field $\vec{B} = \nabla \times \vec{A}$ (Vector Potential)
- ▶ $\Psi(\mathbf{r})$ is the wave function for “super” electrons of charge e^*
- ▶ BCS theory: $e^* = 2e$ (Cooper Pairs of Electrons)

Local

- ▶ Gauge Invariant Coupling: $\frac{\hbar}{i} \nabla \Psi \rightsquigarrow \left(\frac{\hbar}{i} \nabla - \frac{e^*}{c} \vec{A} \right) \Psi$

GL Functional with Coupling to \vec{A} plus Field Energy

$$F[\Psi, \vec{A}] = \int dV \left\{ \alpha(T) |\Psi|^2 + \frac{1}{2} \beta |\Psi|^4 + \frac{1}{2M^*} \left| \left(\frac{\hbar}{i} \nabla - \frac{e^*}{c} \vec{A} \right) \Psi \right|^2 + \frac{1}{8\pi} \left(\nabla \times \vec{A} - \vec{H} \right)^2 \right\}$$

Ginzburg-Landau Field Equations

Euler-Lagrange
Equations of GL Theory

$$\frac{1}{2M^*} \left(\frac{\hbar}{i} \nabla - \frac{e^*}{c} \vec{A} \right)^2 \Psi + \beta |\Psi|^2 \Psi = -\alpha(T) \Psi$$

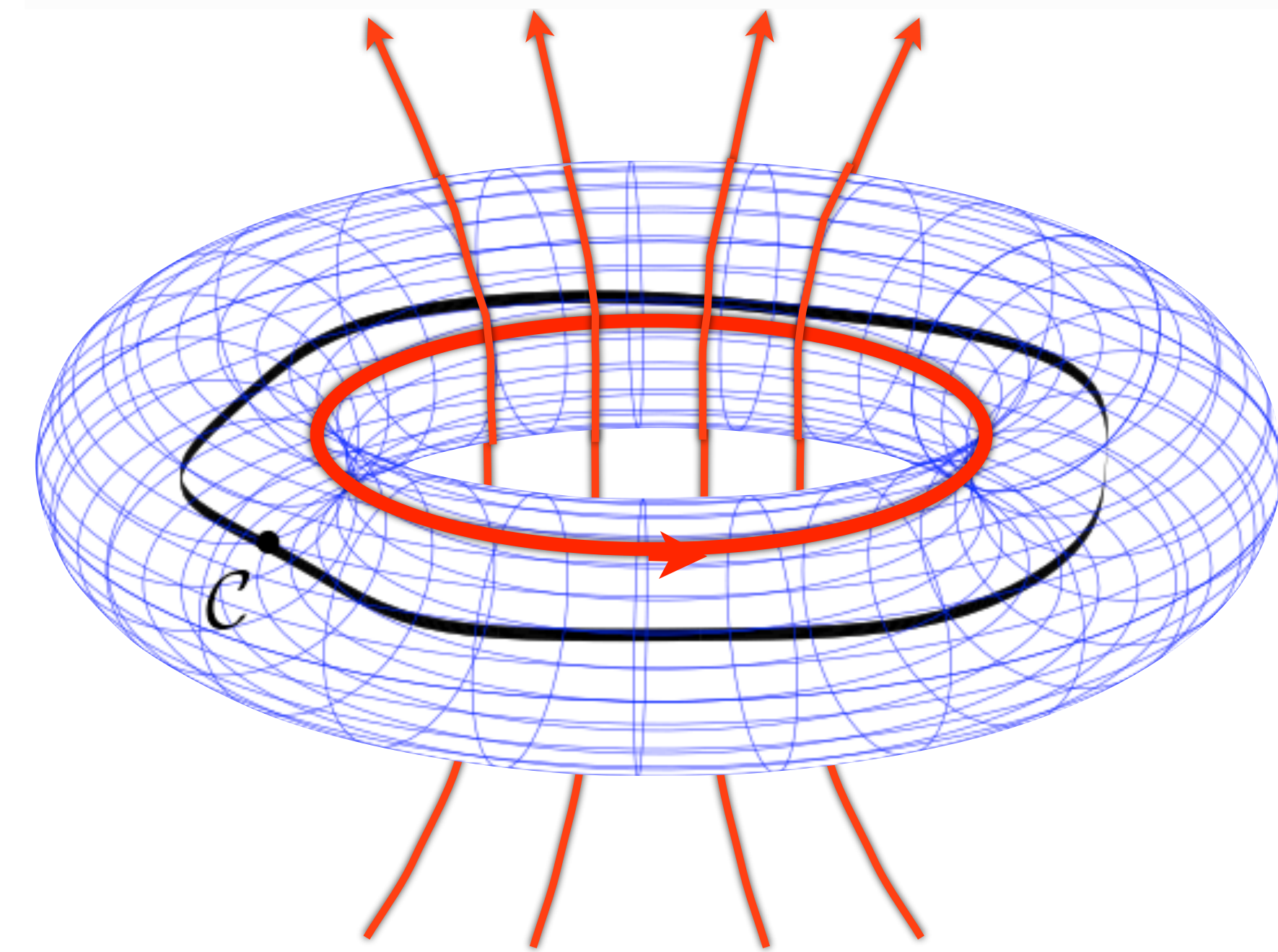
Local Gauge Invariance

$$\nabla \times \nabla \times \vec{A} = \frac{4\pi}{c} \vec{J} = \frac{4\pi}{c} \frac{e^*}{2M^*} \left[\Psi^* \left(\frac{\hbar}{i} \nabla - \frac{e^*}{c} \vec{A} \right) \Psi + c.c. \right] = \frac{4\pi}{c} \frac{e^*}{M^*} |\Psi(\mathbf{r})|^2 \left(\hbar \nabla \vartheta - \frac{e^*}{c} \vec{A} \right)$$

- ▶ Gauge change: $\vec{A} \rightarrow \vec{A} + \nabla \Lambda \rightsquigarrow \vartheta \rightarrow \vartheta + \frac{e^*}{\hbar c} \Lambda$ (broken $U(1)_N$ symmetry)

Quantization of Magnetic Flux (F. London, *Superfluids*, 1950) August 6, 2023

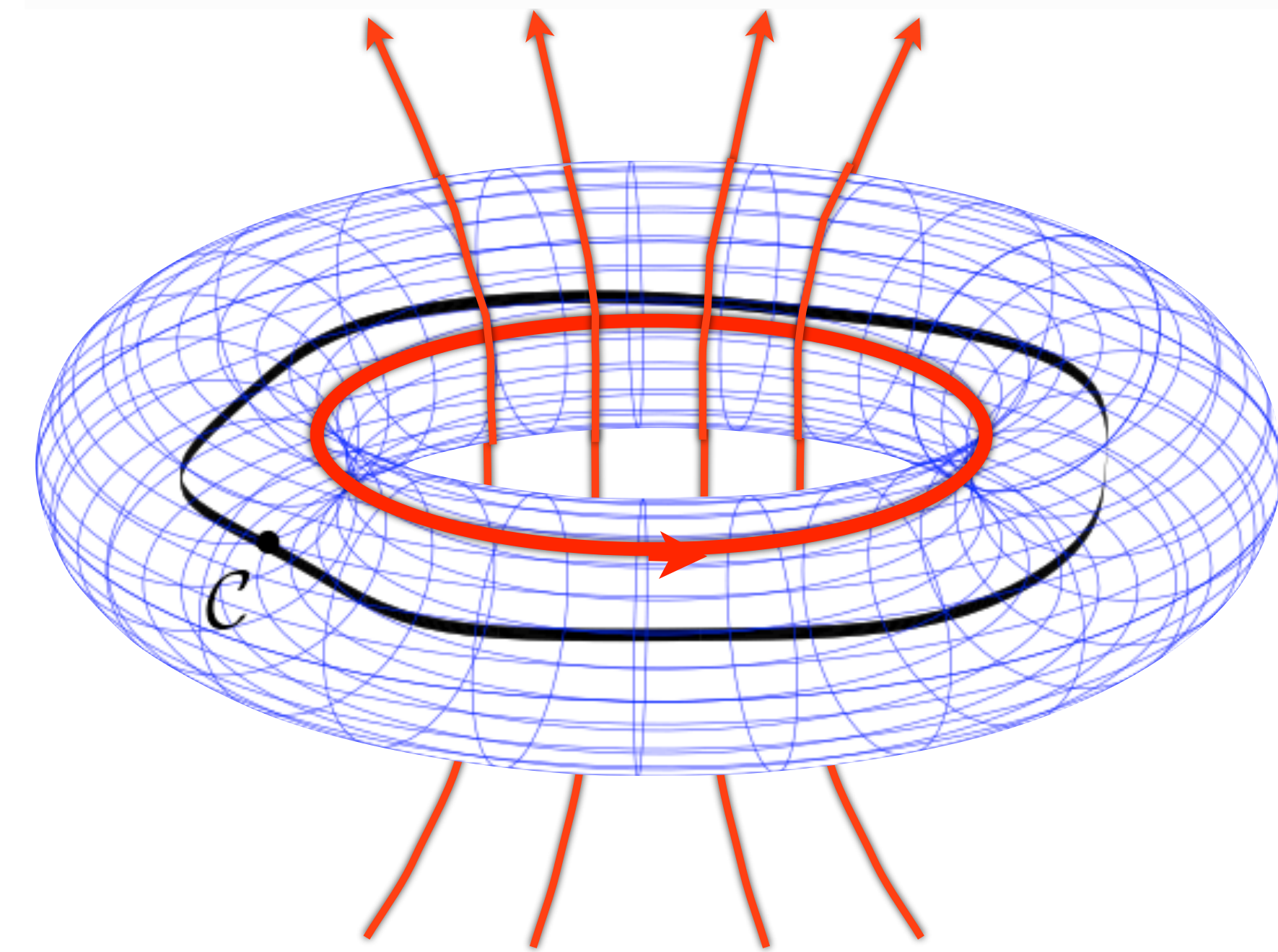
- ▶ $T < T_c$ in an External Magnetic Field
- ▶ $T < T_c$ Turn off External Field
- ▶ Trapped \vec{B} threads the hole in the Torus



- ▶ $\vec{B} = 0$ inside the Superconductor

Quantization of Magnetic Flux (F. London, *Superfluids*, 1950) August 6, 2023

- ▶ $T < T_c$ in an External Magnetic Field
- ▶ $T < T_c$ Turn off External Field
- ▶ Trapped \vec{B} threads the hole in the Torus



- ▶ $\vec{B} = 0$ inside the Superconductor

$$\text{▶ } \vec{J} = \frac{e^*}{M^*} |\Psi_0|^2 \left(\hbar \nabla \vartheta - \frac{e^*}{c} \vec{A} \right)$$

- ▶ $\vec{J} \neq 0$ on the Inner surface

- ▶ Meissner Screening inside the SC

$$\rightsquigarrow \vec{J} = 0 \quad \therefore \oint_{\mathcal{C}} \vec{J} \cdot d\vec{l} \equiv 0$$

Quantization of Magnetic Flux (F. London, *Superfluids*, 1950) August 6, 2023

- ▶ $T < T_c$ in an External Magnetic Field
- ▶ $T < T_c$ Turn off External Field
- ▶ Trapped \vec{B} threads the hole in the Torus

$$\vec{J} = \frac{e^*}{M^*} |\Psi_0|^2 \left(\hbar \nabla \vartheta - \frac{e^*}{c} \vec{A} \right)$$

- ▶ $\vec{J} \neq 0$ on the Inner surface

- ▶ Meissner Screening inside the SC

$$\rightsquigarrow \vec{J} = 0 \quad \therefore \oint_{\mathcal{C}} \vec{J} \cdot d\vec{l} \equiv 0$$

$$\therefore \oint_{\mathcal{C}} \vec{A} \cdot d\vec{l} = \frac{\hbar c}{e^*} \oint_{\mathcal{C}} \nabla \vartheta \cdot d\vec{l}$$

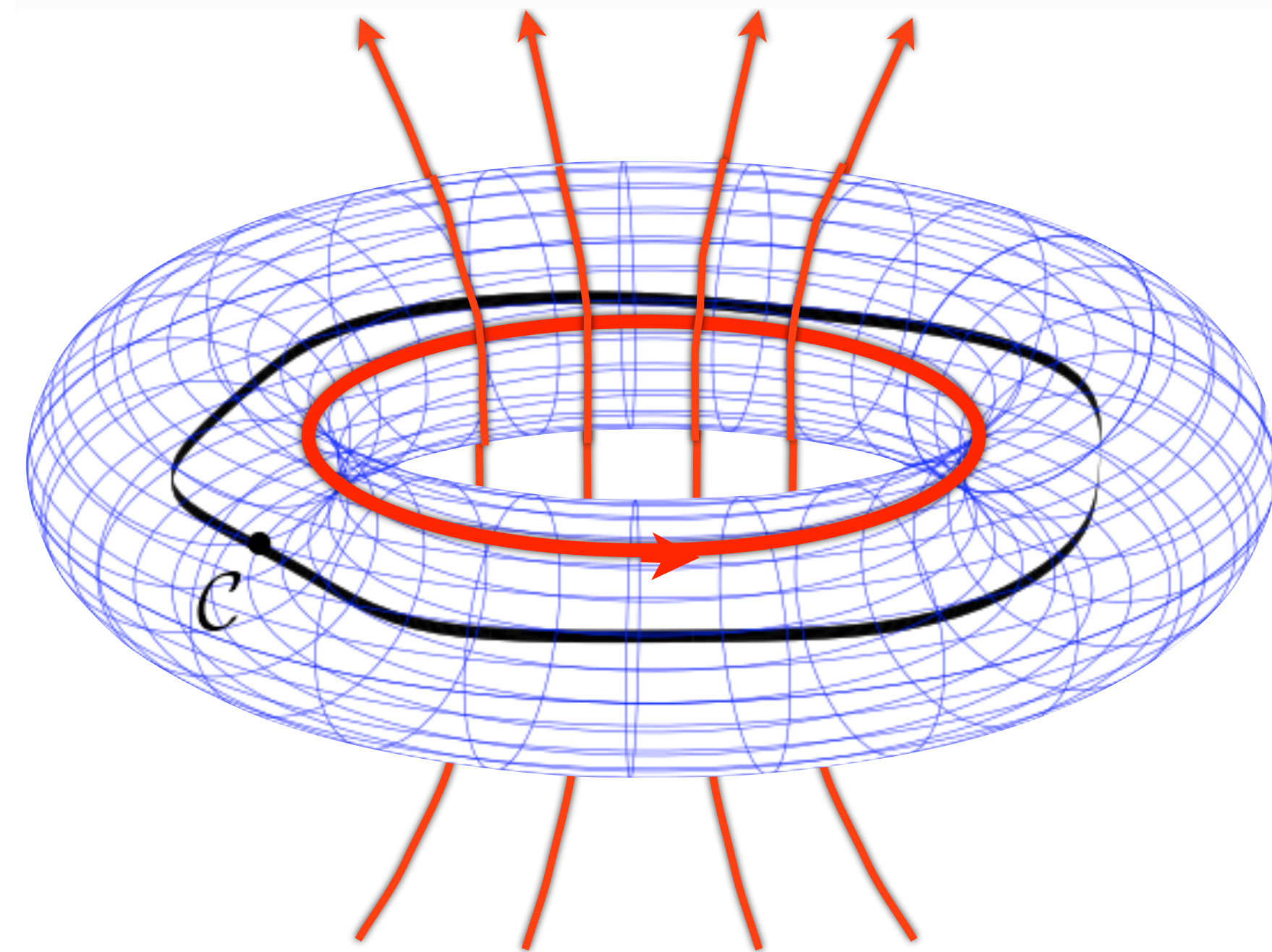
$$\text{▶ Phase Quantization: } \oint_{\mathcal{C}} \nabla \vartheta \cdot d\vec{l} = N 2\pi$$

$$N = 0, \pm 1, \pm 2, \dots$$

$$\text{▶ Flux Quantization: } \Phi \equiv \iint_{S_{\mathcal{C}}} \vec{B} \cdot d\vec{S} = \oint_{\mathcal{C}} \vec{A} \cdot d\vec{l} = N \frac{\hbar c}{e^*}$$

- ▶ Superconducting electrons are *bound electron pairs*: $\rightsquigarrow e^* = 2e$

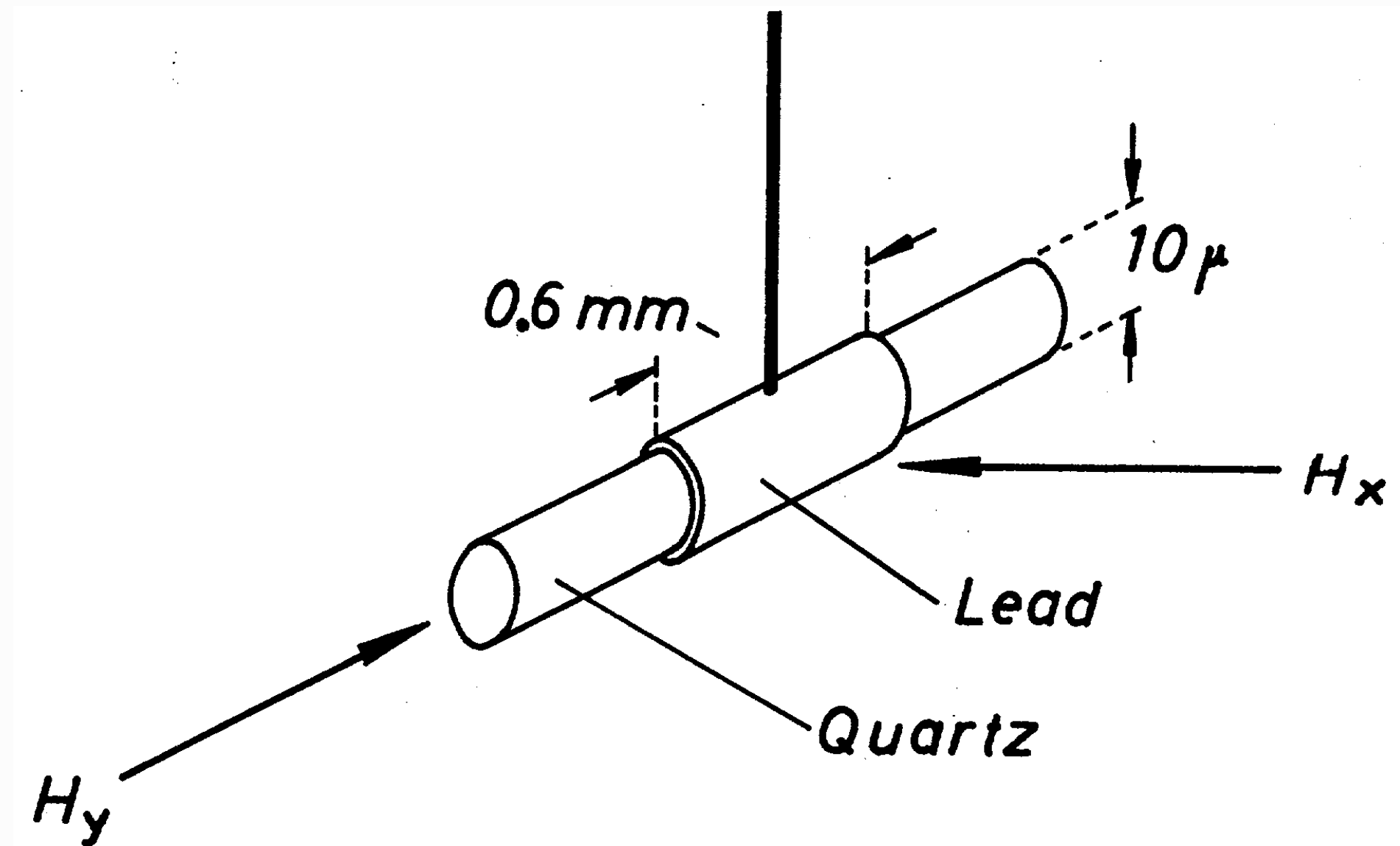
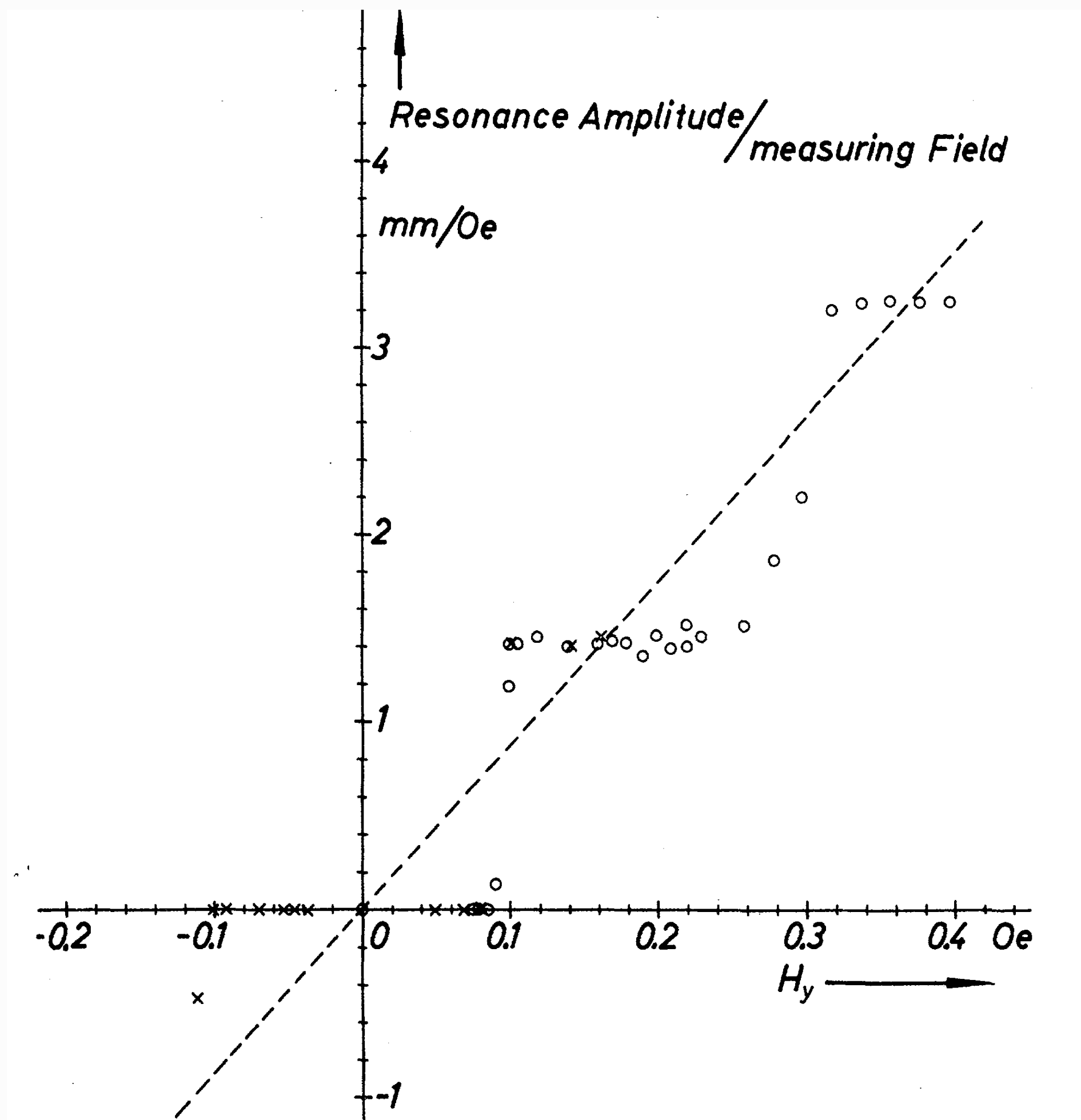
$$\therefore \Phi = N \frac{\hbar c}{2e} \text{ with Flux Quantum } \Phi_0 \equiv \frac{\hbar c}{2e} \approx 2 \times 10^{-7} \text{ G-cm}^2$$



- ▶ $\vec{B} = 0$ inside the Superconductor

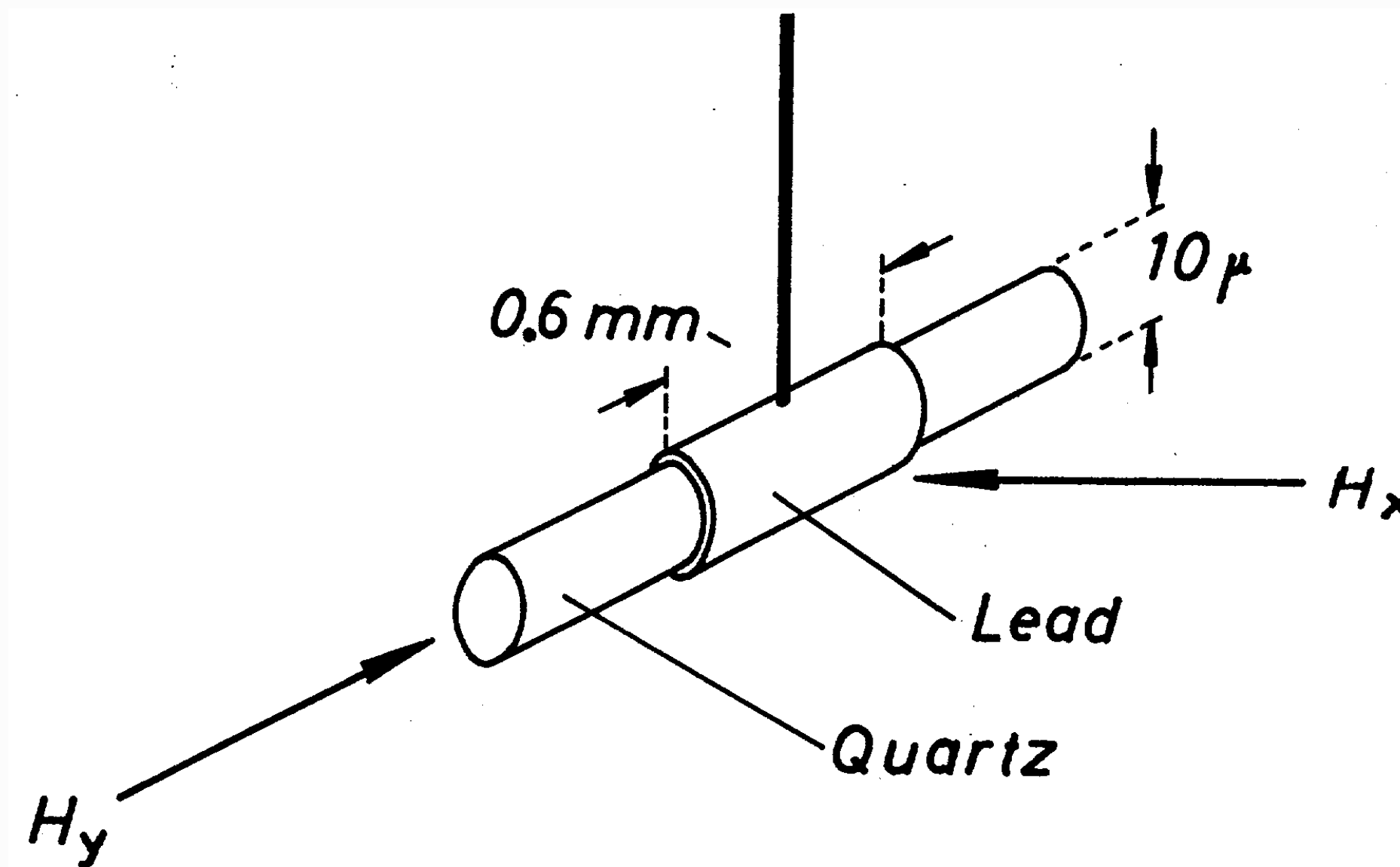
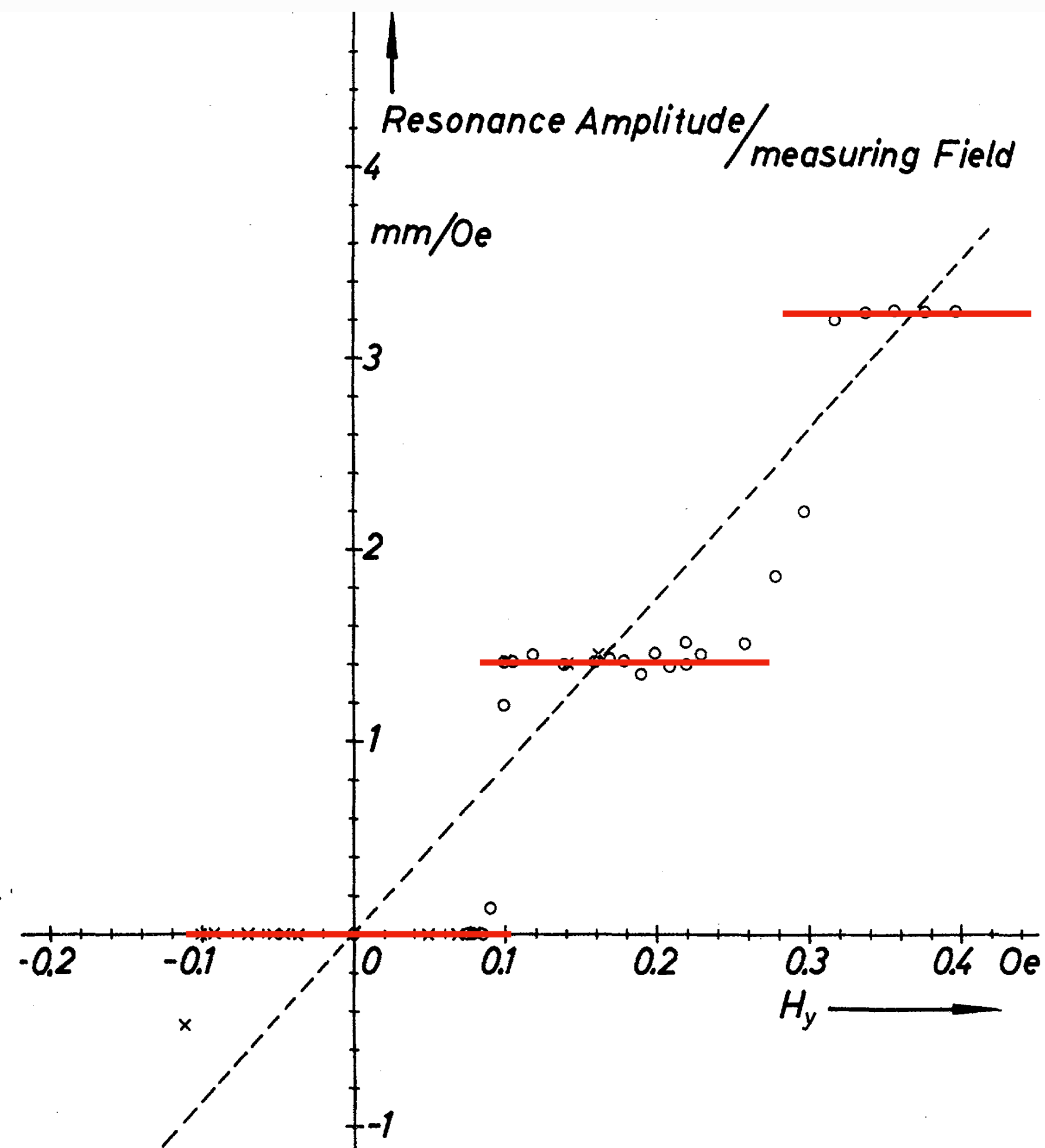
Observation of Magnetic Flux Quantization August 6, 2023

R. Doll and M. Nábauer, Physical Review Letters 7, 51 (1961)



Observation of Magnetic Flux Quantization August 6, 2023

R. Doll and M. Nābauer, Physical Review Letters 7, 51 (1961)



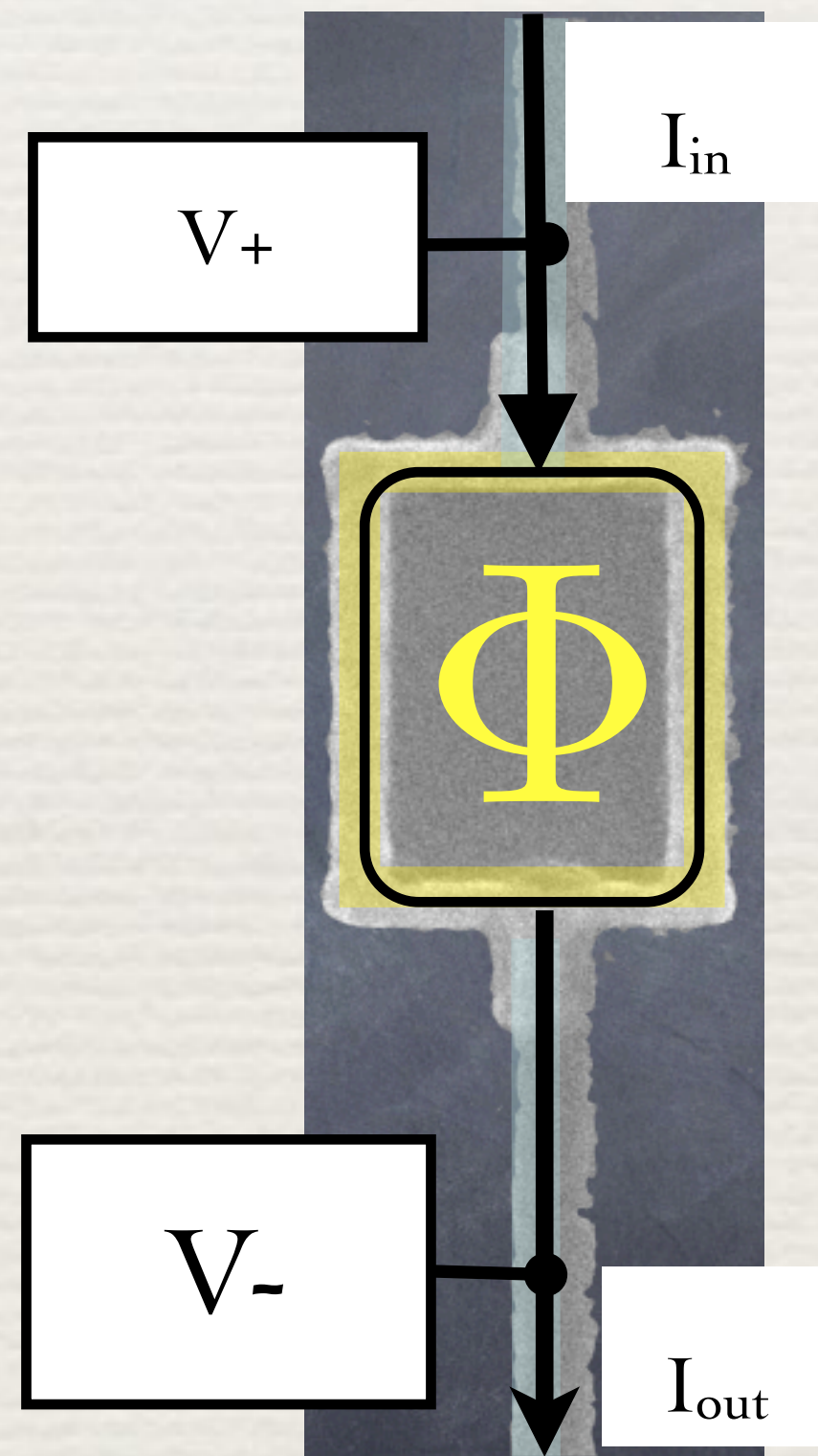
► Doll and Nābauer thought they had a systematic error (" $\approx \times 2$ ") as they were looking to find steps of size $\frac{hc}{e}$ - London's prediction prior to BCS theory!

Superconductor-Normal-Superconductor Quantum Interference Device

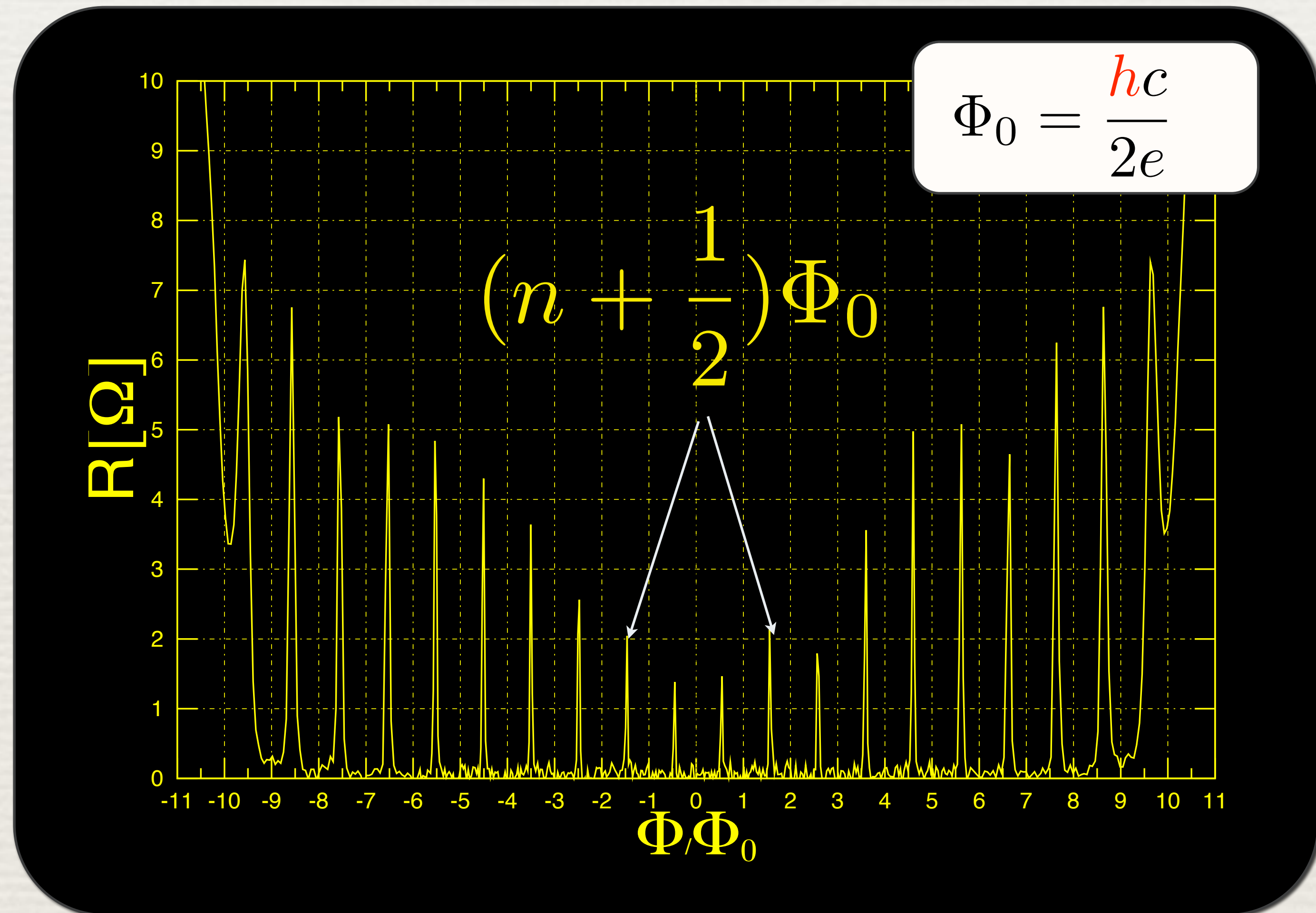
- Au – normal conductor (in *contact* to superconducting leads)
- Al – superconductor
- Silicon oxide substrate

V. Chandrasekhar's Lab
Northwestern University

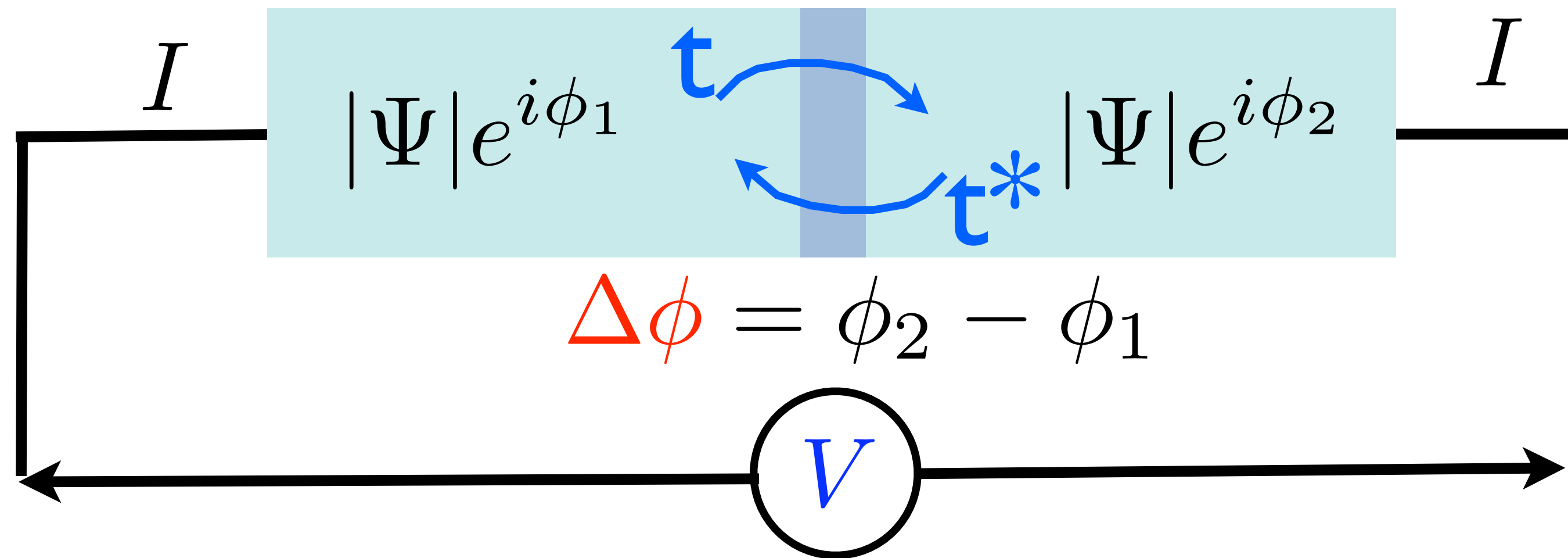
J. Wei, et al. 2008 (J. Appl. Phys.)



$$\Delta\vartheta = 2\pi\Phi/\Phi_0$$



Josephson Effect



d.c. Josephson current $I = I_c(T) \sin(\Delta\phi)$

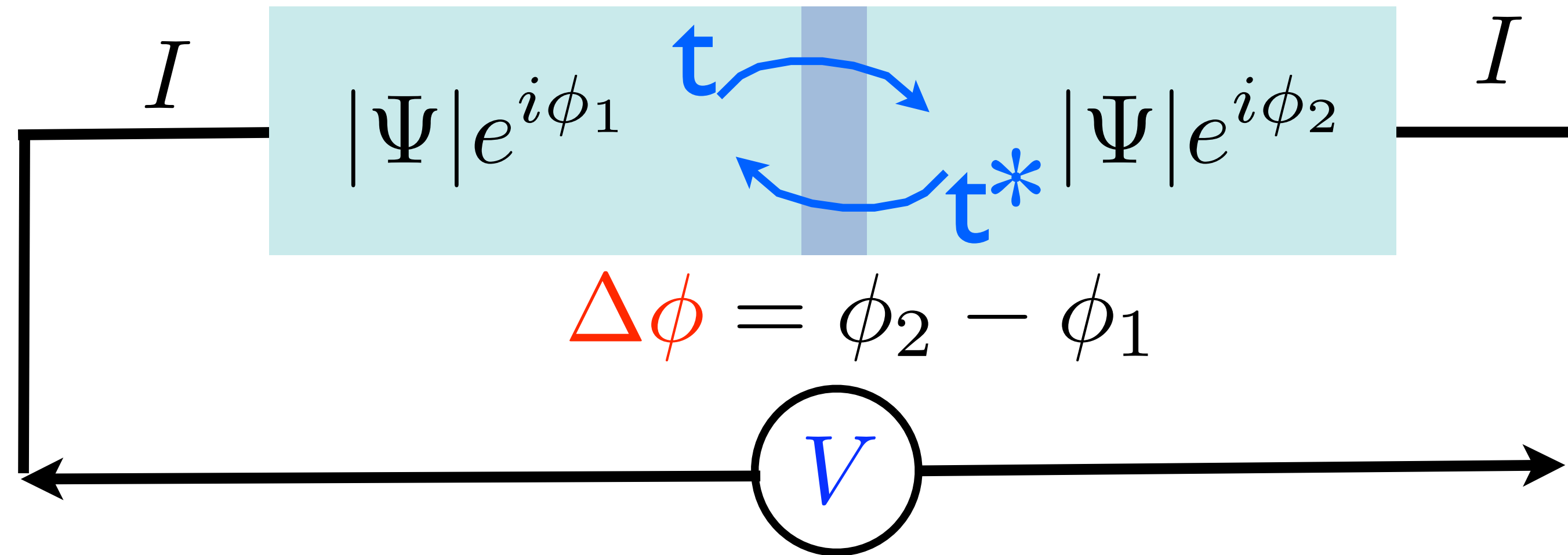
$I_c \propto |t|^2$

a.c. Josephson effect $I > I_c$

$\Delta\phi_t = \frac{2e}{\hbar} V t$

B. Josephson, Phys. Lett. 1, 251 (1962);
 Adv. Phys. 14, 419 (1965)

Josephson Effect



Key element of
quantum circuits
for qubits



Next Lecture by
Prof. Jens Koch

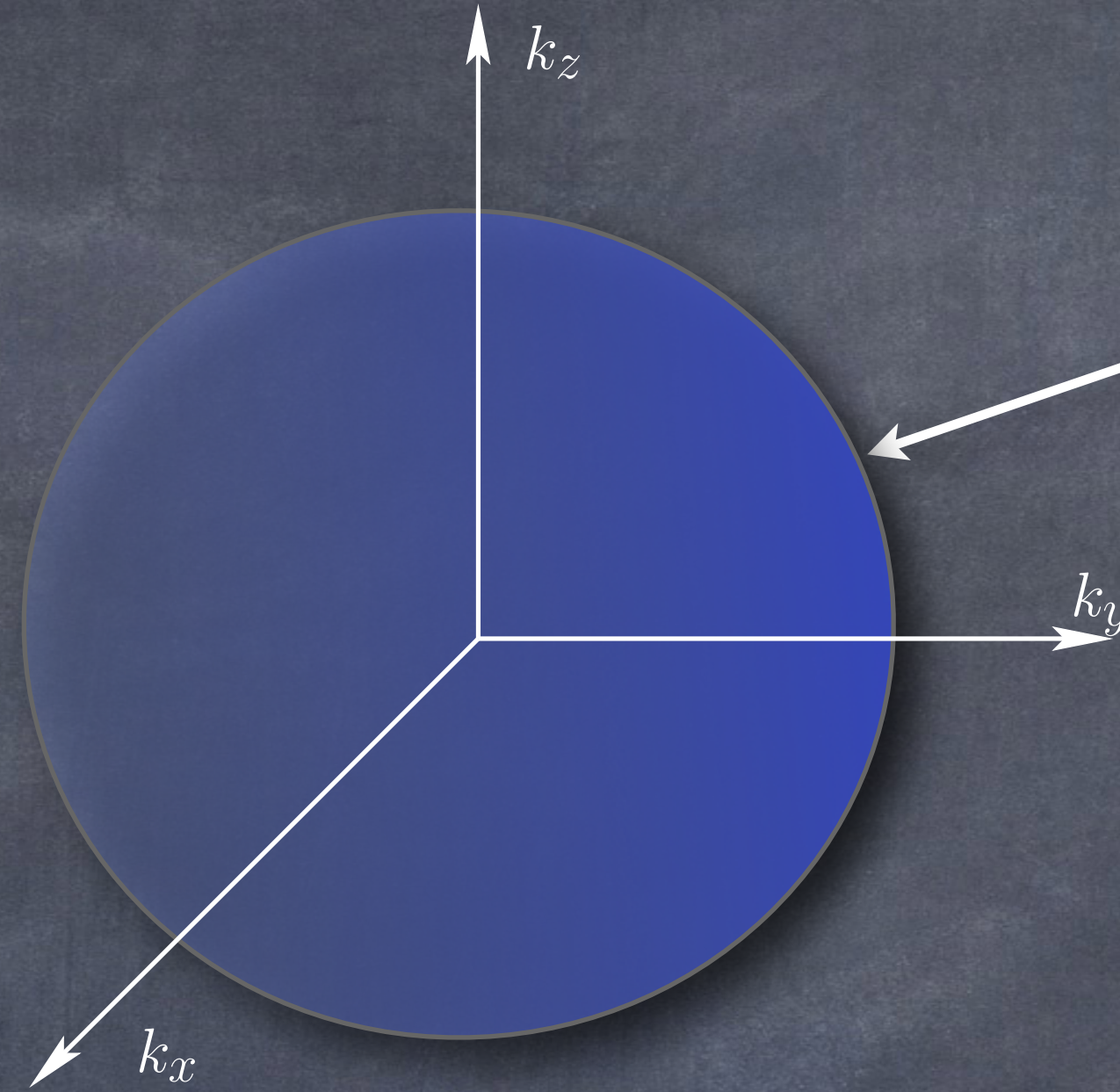
d.c. Josephson current $I = I_c(T) \sin(\Delta\phi)$
 $I_c \propto |t|^2$

a.c. Josephson effect $I > I_c$ $\Delta\phi_t = \frac{2e}{\hbar} V t$

B. Josephson, Phys. Lett. 1, 251 (1962);
 Adv. Phys. 14, 419 (1965)

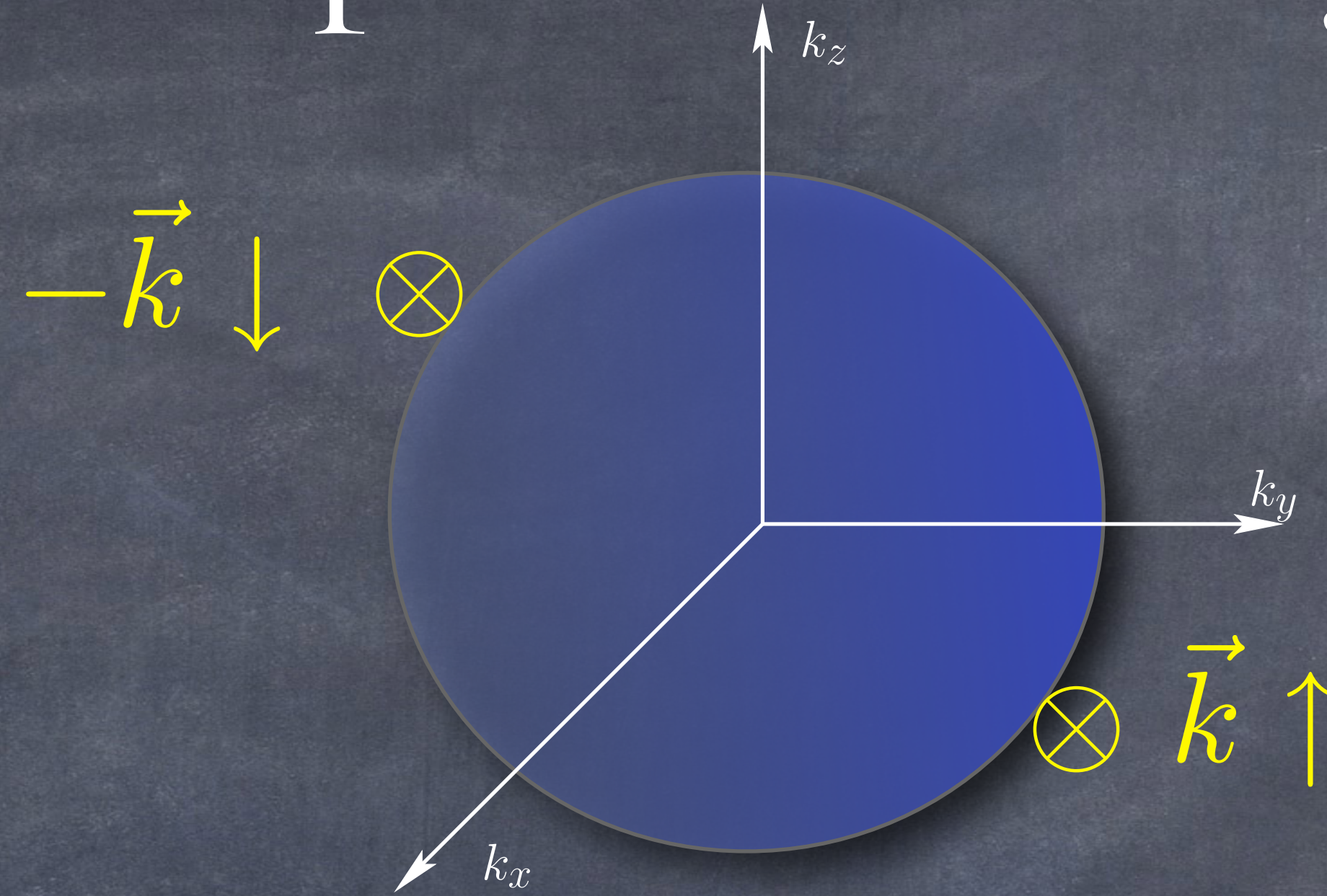
Cooper's Instability

Cooper's Instability

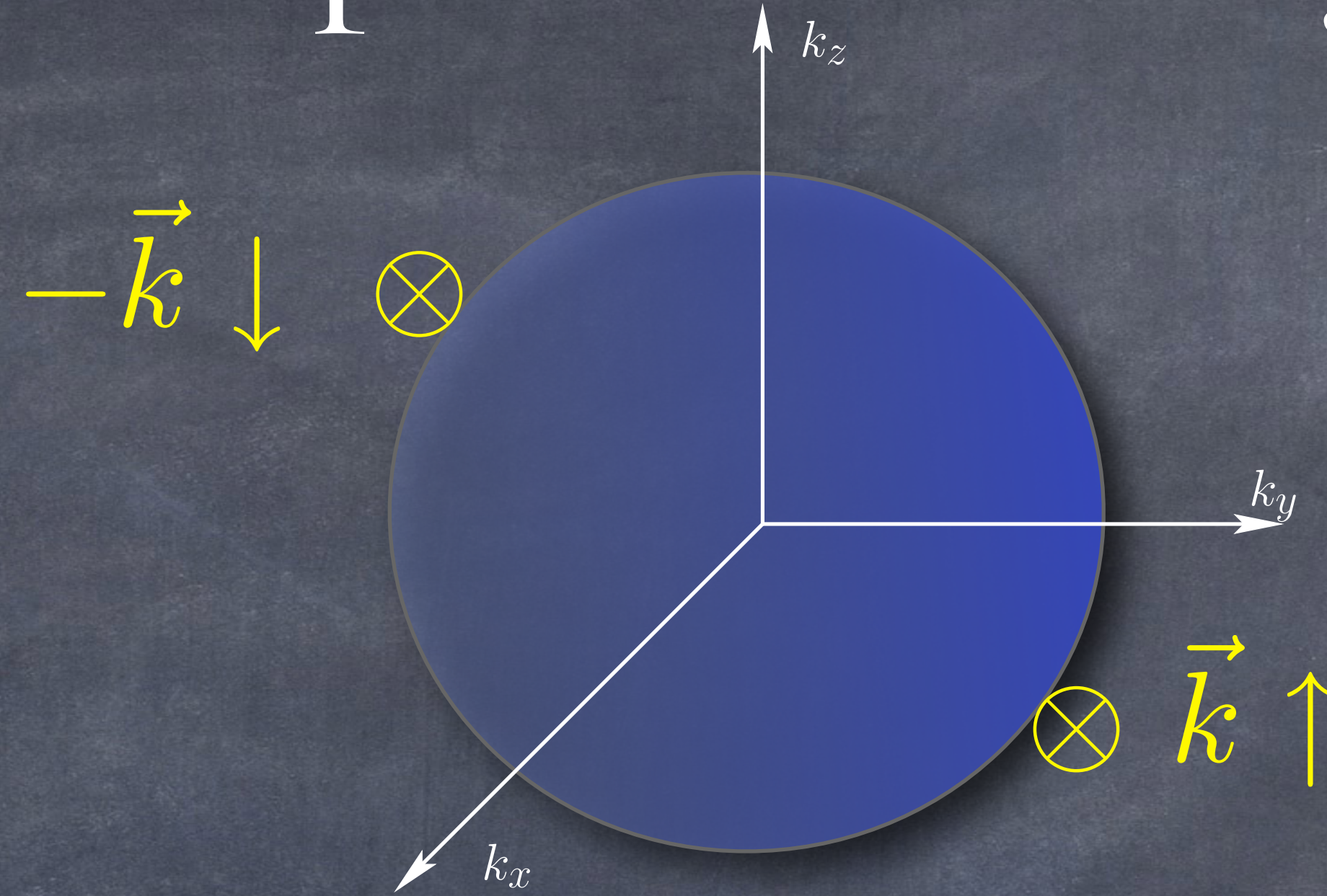


Normal Metal
Filled Fermi Sea

Cooper's Instability

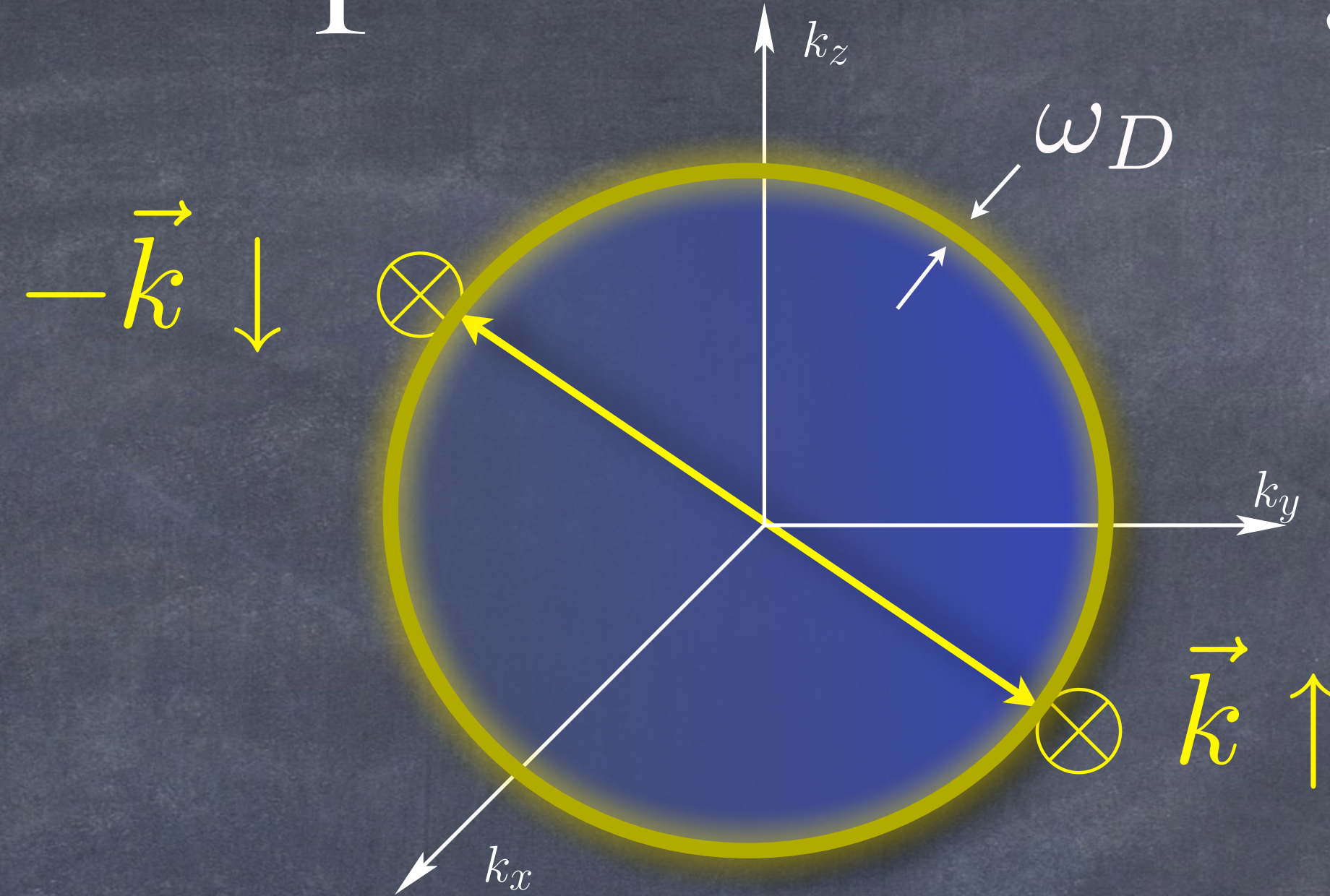


Cooper's Instability



$$2 \times \frac{\hbar^2 k^2}{2m} \varphi_{\vec{k}}$$

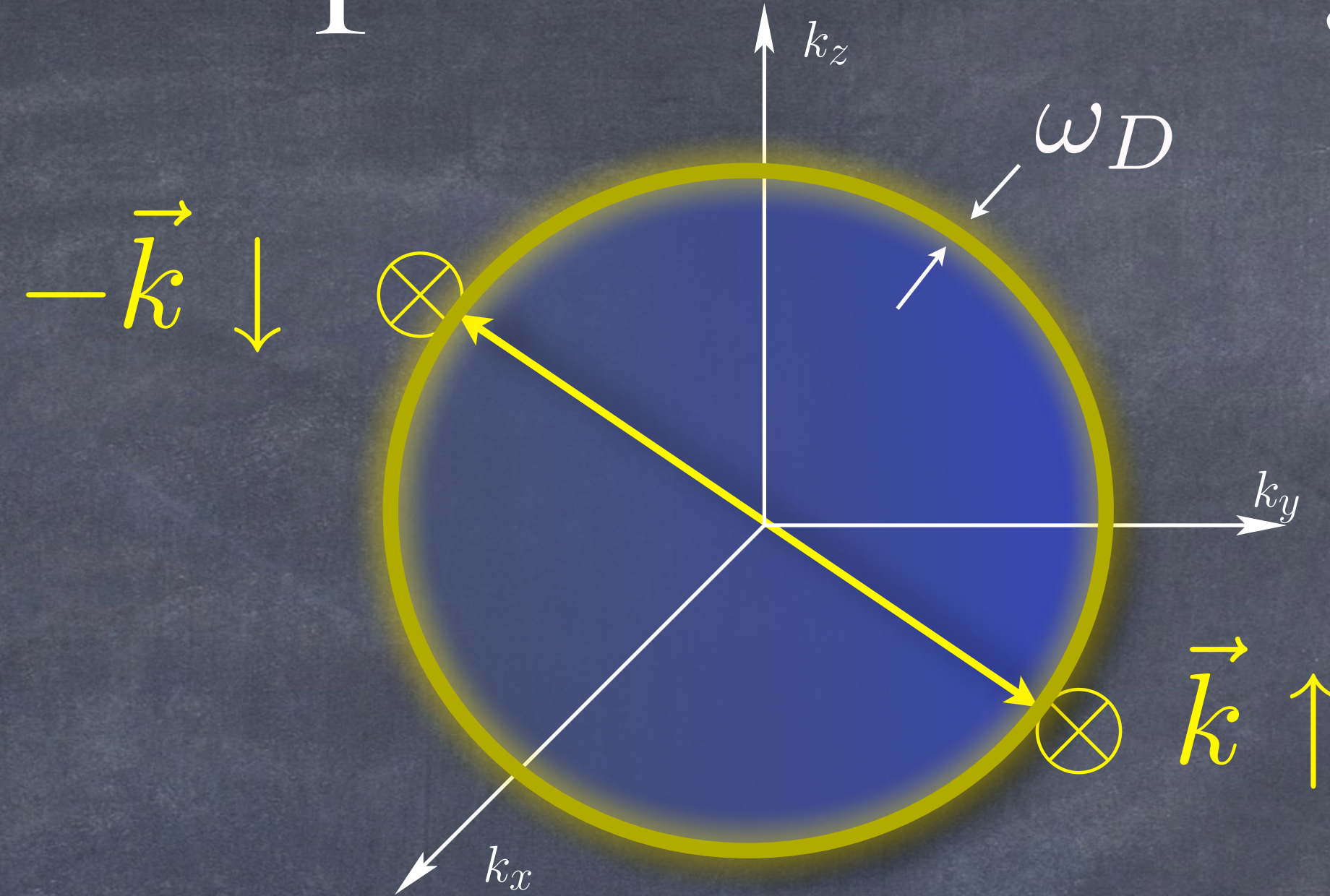
Cooper's Instability



$$2 \times \frac{\hbar^2 k^2}{2m} \varphi_{\vec{k}}$$

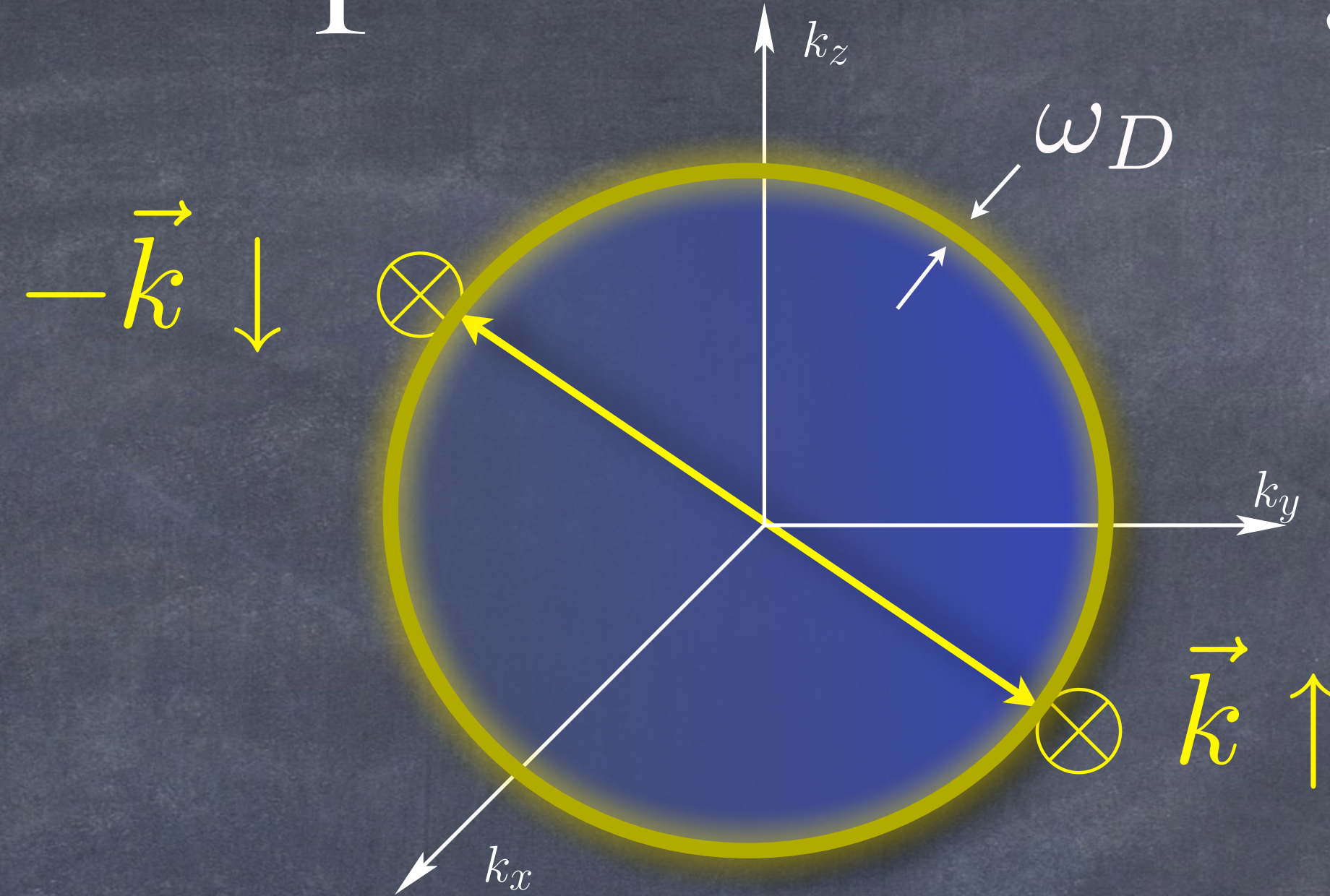
$$V_{\vec{k}, \vec{k}'} \varphi_{\vec{k}'}$$

Cooper's Instability



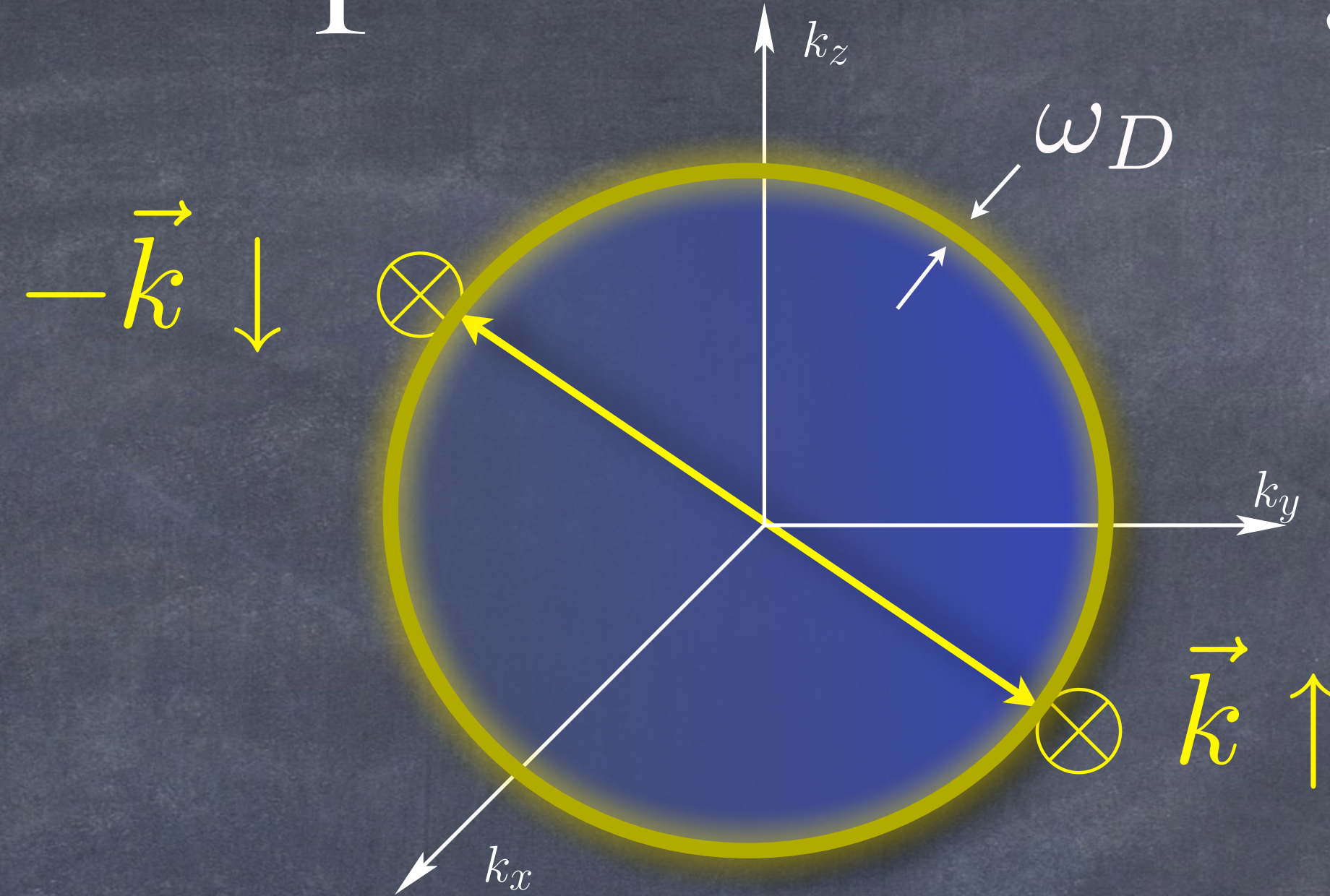
$$2 \times \frac{\hbar^2 k^2}{2m} \varphi_{\vec{k}} - \int \frac{d^3 k'}{8\pi^3} \boxed{V_{\vec{k}, \vec{k}'} \varphi_{\vec{k}'}}$$

Cooper's Instability



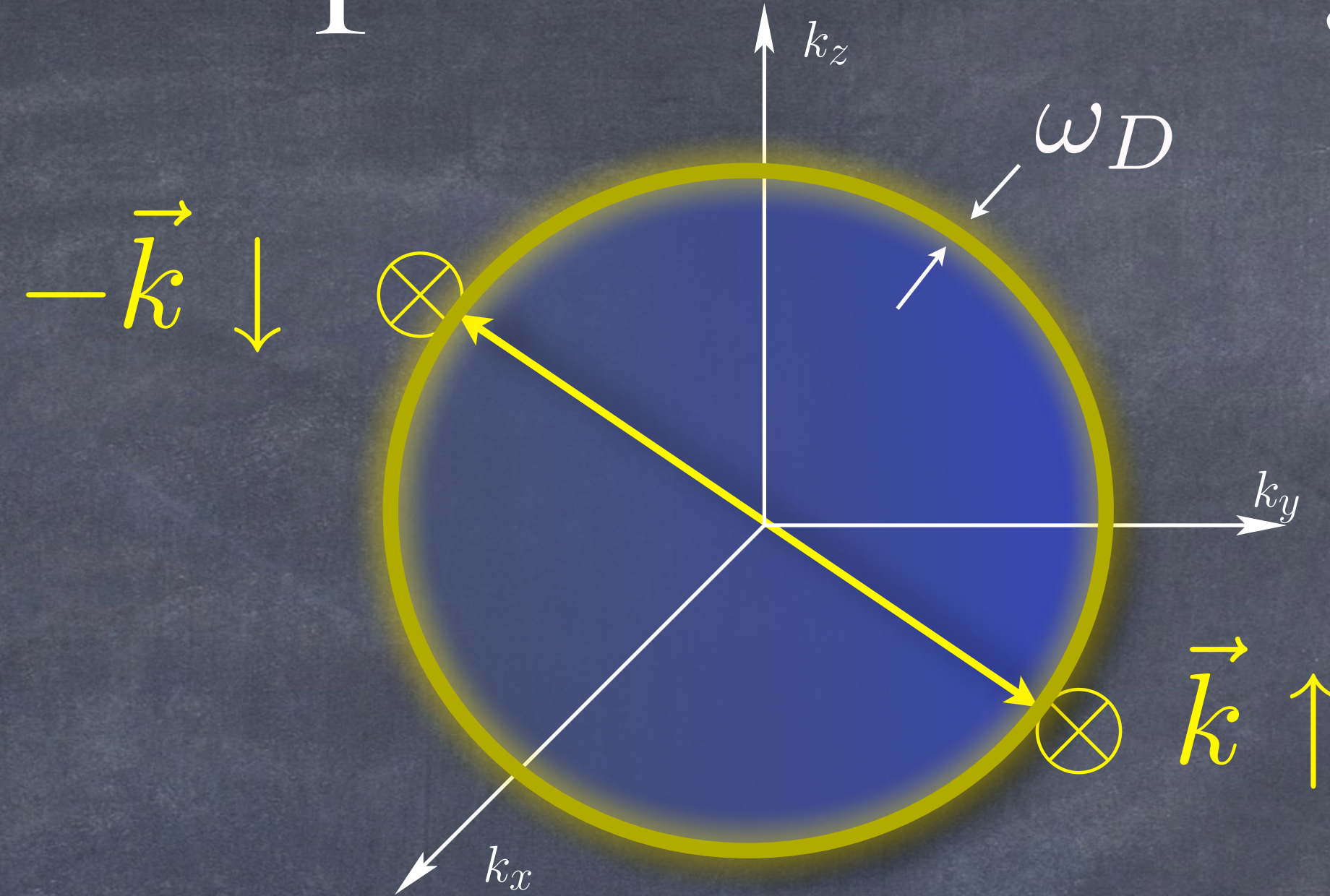
$$2 \times \frac{\hbar^2 k^2}{2m} \varphi_{\vec{k}} - \int \frac{d^3 k'}{8\pi^3} \boxed{V_{\vec{k}, \vec{k}'} \varphi_{\vec{k}'}} = \left(2 \frac{\hbar^2 k_f^2}{2m} + \epsilon \right) \varphi_{\vec{k}}$$

Cooper's Instability



$$2 \times \frac{\hbar^2 k^2}{2m} \varphi_{\vec{k}} - \int \frac{d^3 k'}{8\pi^3} \boxed{V_{\vec{k}, \vec{k}'} \varphi_{\vec{k}'}} = \left(2 \frac{\hbar^2 k_f^2}{2m} + \epsilon \right) \varphi_{\vec{k}}$$

Cooper's Instability



$$2 \times \frac{\hbar^2 k^2}{2m} \varphi_{\vec{k}} - \int \frac{d^3 k'}{8\pi^3} \boxed{V_{\vec{k}, \vec{k}'} \varphi_{\vec{k}'}} = \left(2 \frac{\hbar^2 k_f^2}{2m} + \epsilon \right) \varphi_{\vec{k}}$$

Bound-State of 2 electrons on the Fermi Sea

$$\epsilon_{bs} = -\omega_D e^{-1/N(0)V}$$

$$|BCS\rangle = \left[\sum_k \Phi_k a_{k\uparrow}^\dagger a_{-k\downarrow}^\dagger \right]^{N/2} |Fermi\rangle$$

Theory of Superconductivity*

J. BARDEEN, L. N. COOPER,[†] AND J. R. SCHRIEFFER[‡]
Department of Physics, University of Illinois, Urbana, Illinois

(Received July 8, 1957)

$$|BCS\rangle = \left[\sum_k \Phi_k a_{k\uparrow}^\dagger a_{-k\downarrow}^\dagger \right]^{N/2} |Fermi\rangle$$

Theory of Superconductivity*

J. BARDEEN, L. N. COOPER,[†] AND J. R. SCHRIEFFER[‡]
Department of Physics, University of Illinois, Urbana, Illinois

(Received July 8, 1957)

$$|BCS\rangle = \left[\sum_k \Phi_k a_{k\uparrow}^\dagger a_{-k\downarrow}^\dagger \right]^{N/2} |Fermi\rangle$$

Electron Pairs - charge = $2e$

BCS Condensation:

Macroscopic State of Fermion Pairs

Theory of Superconductivity*

J. BARDEEN, L. N. COOPER,[†] AND J. R. SCHRIEFFER[‡]
Department of Physics, University of Illinois, Urbana, Illinois

(Received July 8, 1957)

$$|BCS\rangle = \left[\sum_k \Phi_k a_{k\uparrow}^\dagger a_{-k\downarrow}^\dagger \right]^{N/2} |Fermi\rangle$$

Electron Pairs - charge = $2e$

BCS Condensation:

Macroscopic State of Fermion Pairs

- ❖ Condensation Energy
- ❖ Supercurrents
- ❖ Energy Gap for Excitations
- ❖ Josephson Effect
- ❖ Meissner Effect
- ❖ Flux Quantization

Reduced to London &
 Ginzburg-Landau Theories
 in appropriate limits

Theory of Superconductivity*

J. BARDEEN, L. N. COOPER,[†] AND J. R. SCHRIEFFER[‡]
Department of Physics, University of Illinois, Urbana, Illinois

(Received July 8, 1957)

$$|BCS\rangle = \left[\sum_k \Phi_k a_{k\uparrow}^\dagger a_{-k\downarrow}^\dagger \right]^{N/2} |Fermi\rangle$$

Electron Pairs - charge = 2e

BCS Condensation:

Macroscopic State of Fermion Pairs

- ❖ Condensation Energy
- ❖ Supercurrents
- ❖ Energy Gap for Excitations
- ❖ Josephson Effect
- ❖ Meissner Effect
- ❖ Flux Quantization

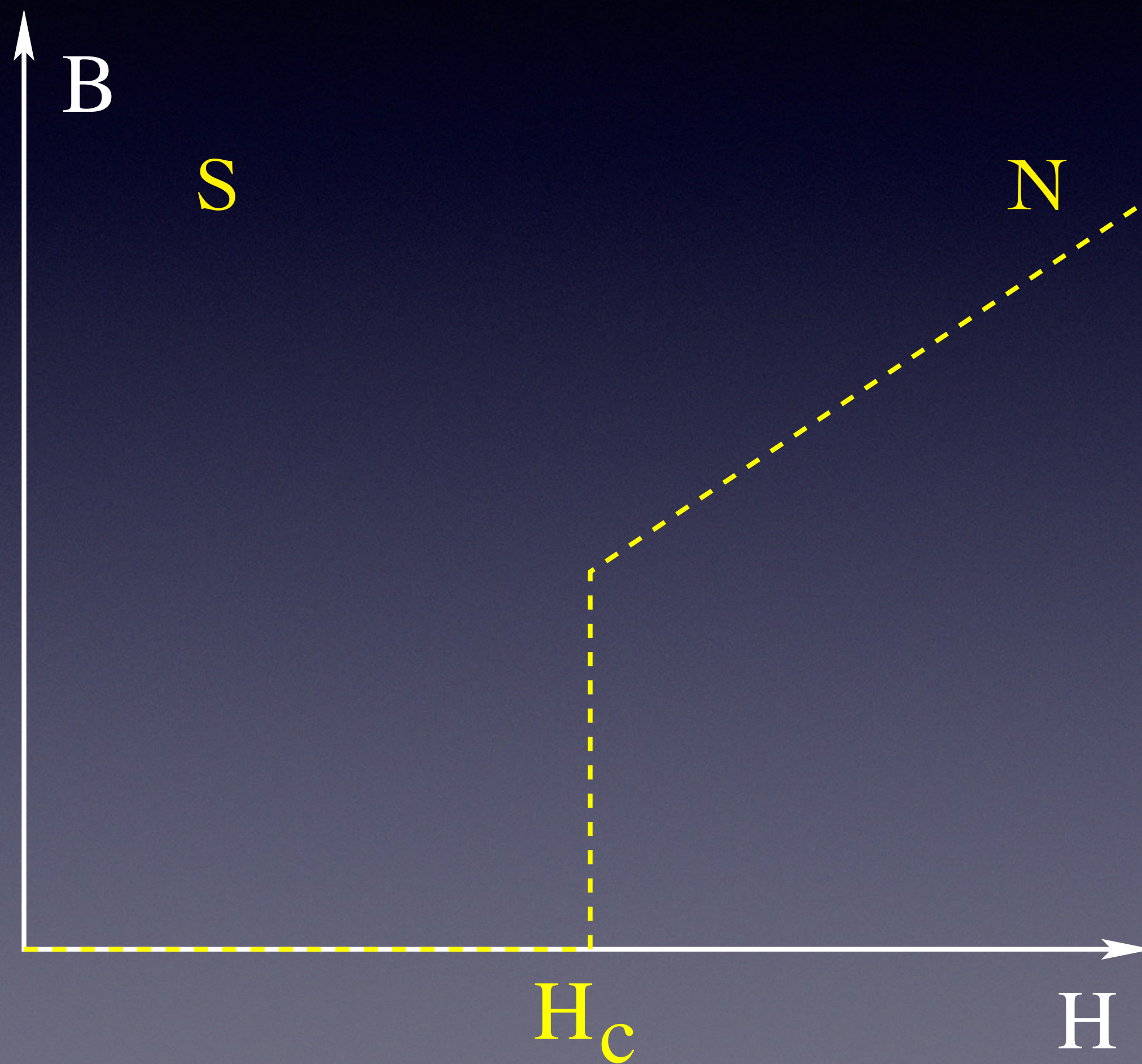
Reduced to London &
 Ginzburg-Landau Theories
 in appropriate limits

”It would have been very difficult to have arrived at the theory [of superconductivity] by purely deductive reasoning from the basic equations of quantum mechanics. Even if someone had done so, no one would have believed that such remarkable properties would really occur in nature.”

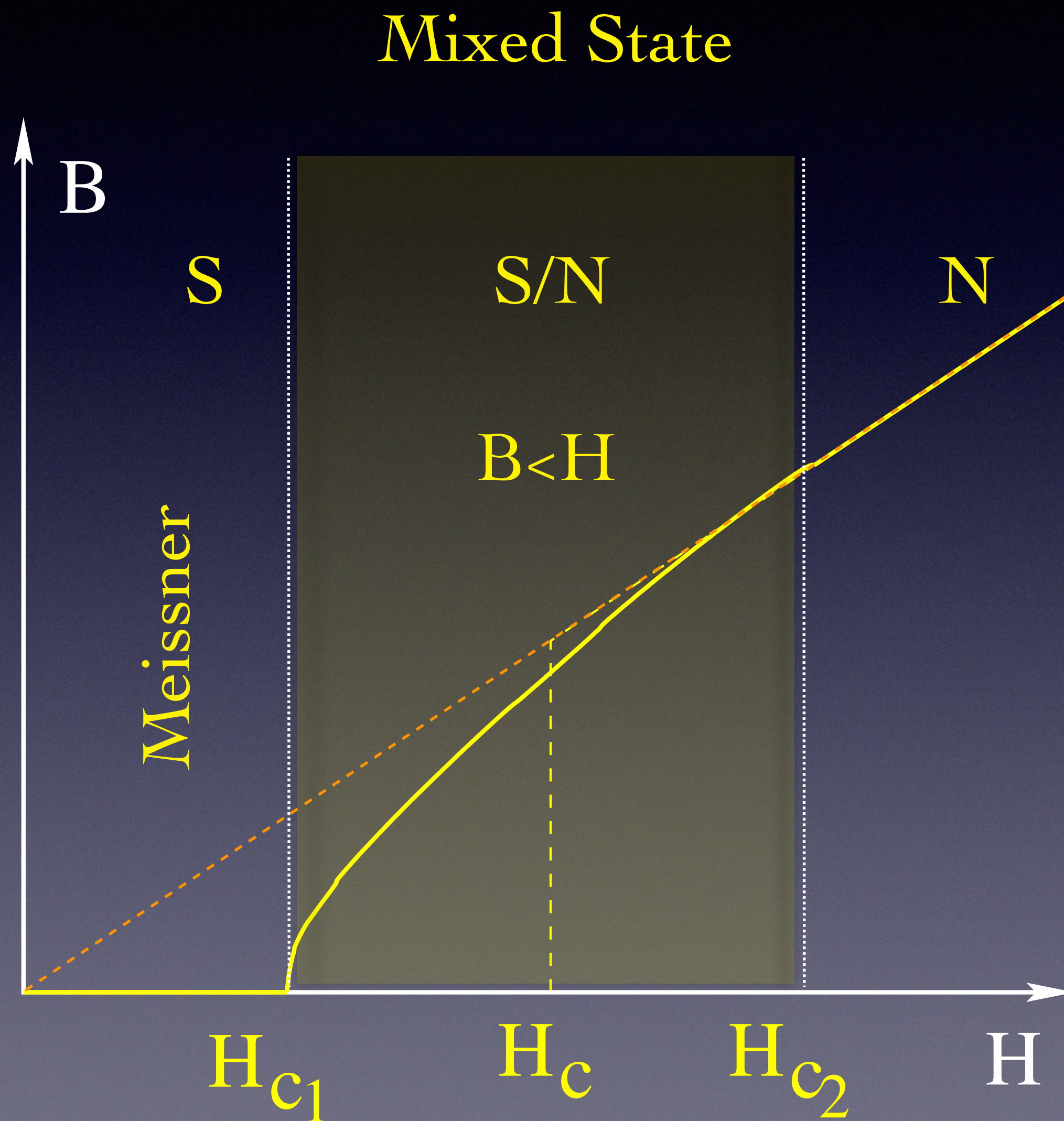
John Bardeen Nobel Lecture, Stockholm, December 11, 1972

Type I Superconductors

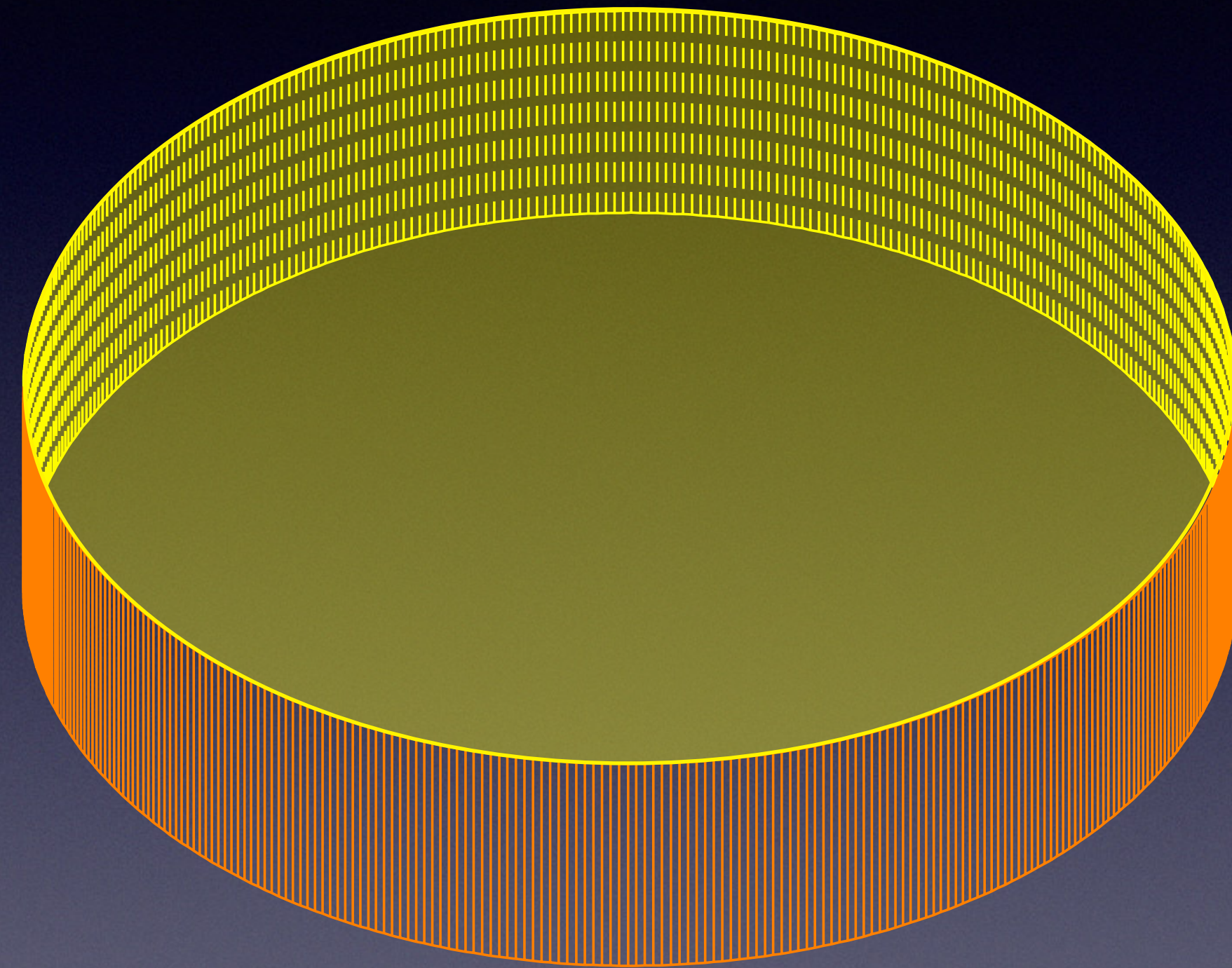
Type I Superconductors



Type II Superconductors

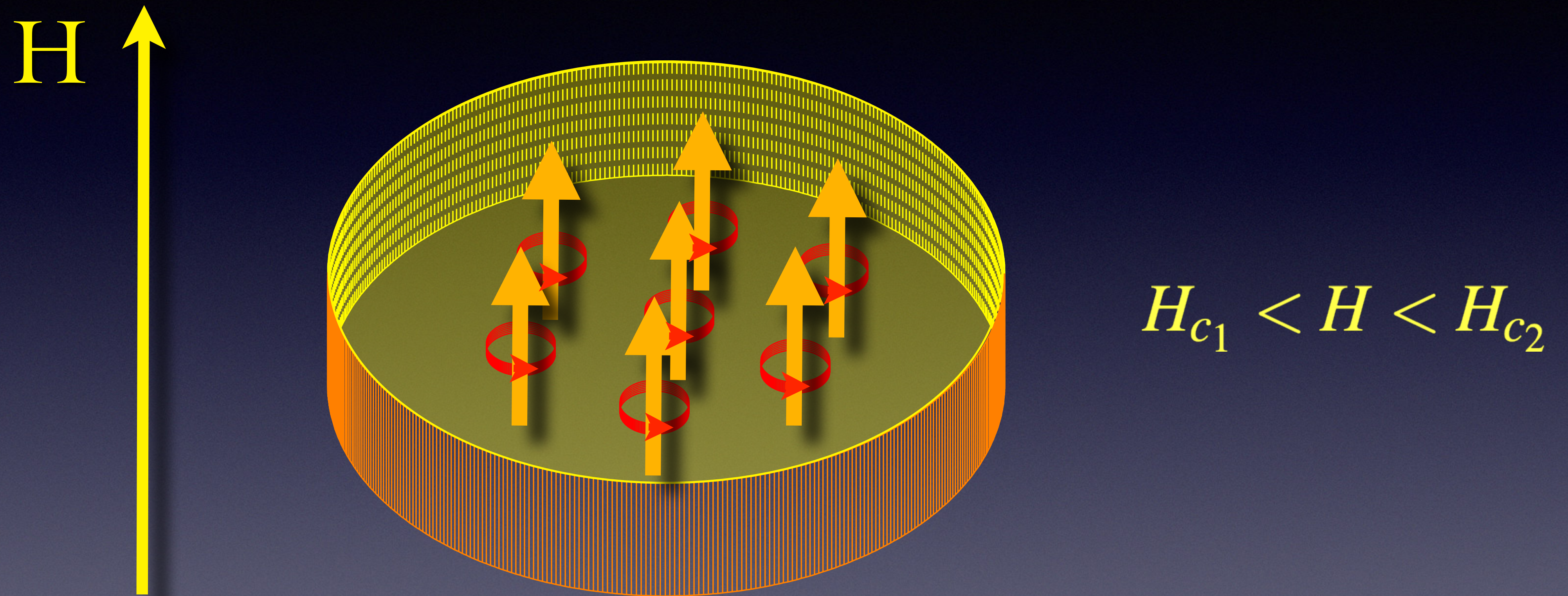


Abrikosov Vortices



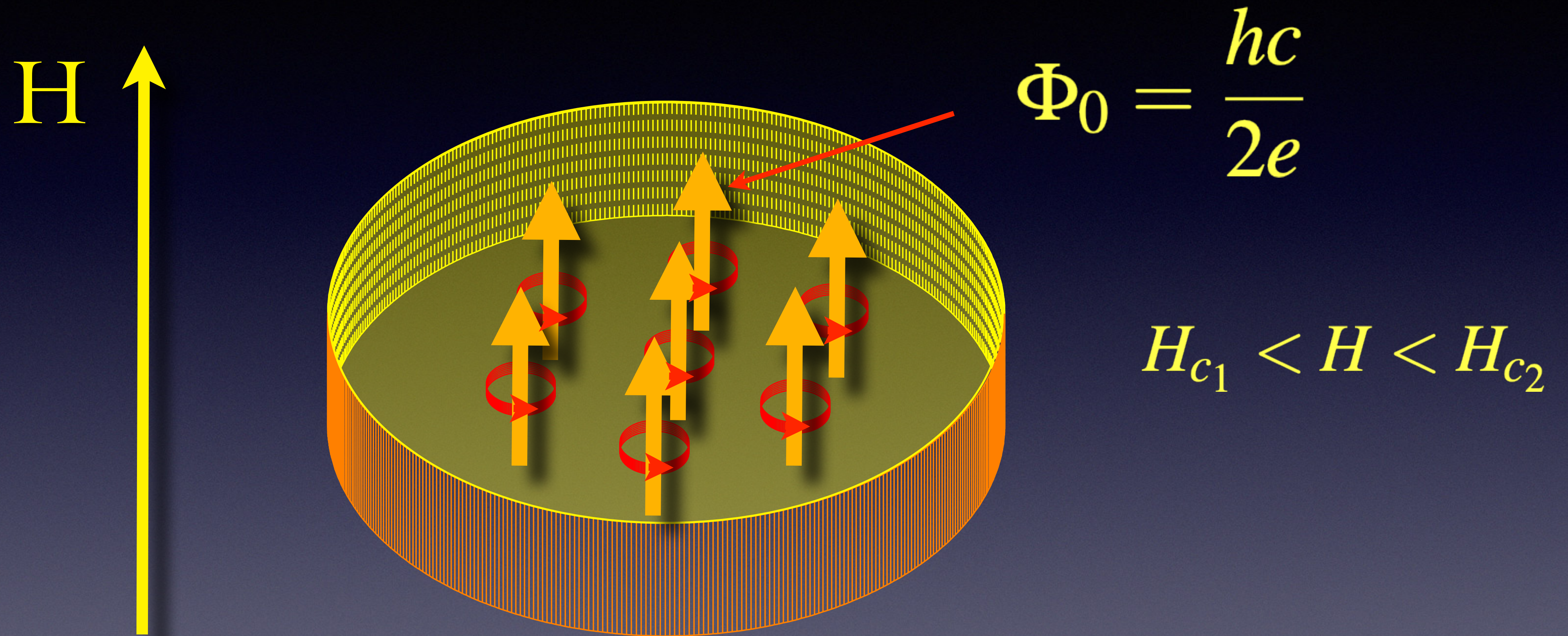
A.A. Abrikosov "On the magnetic properties of... ", Soviet Physics JETP 5, 1174 (1957)

Abrikosov Vortices



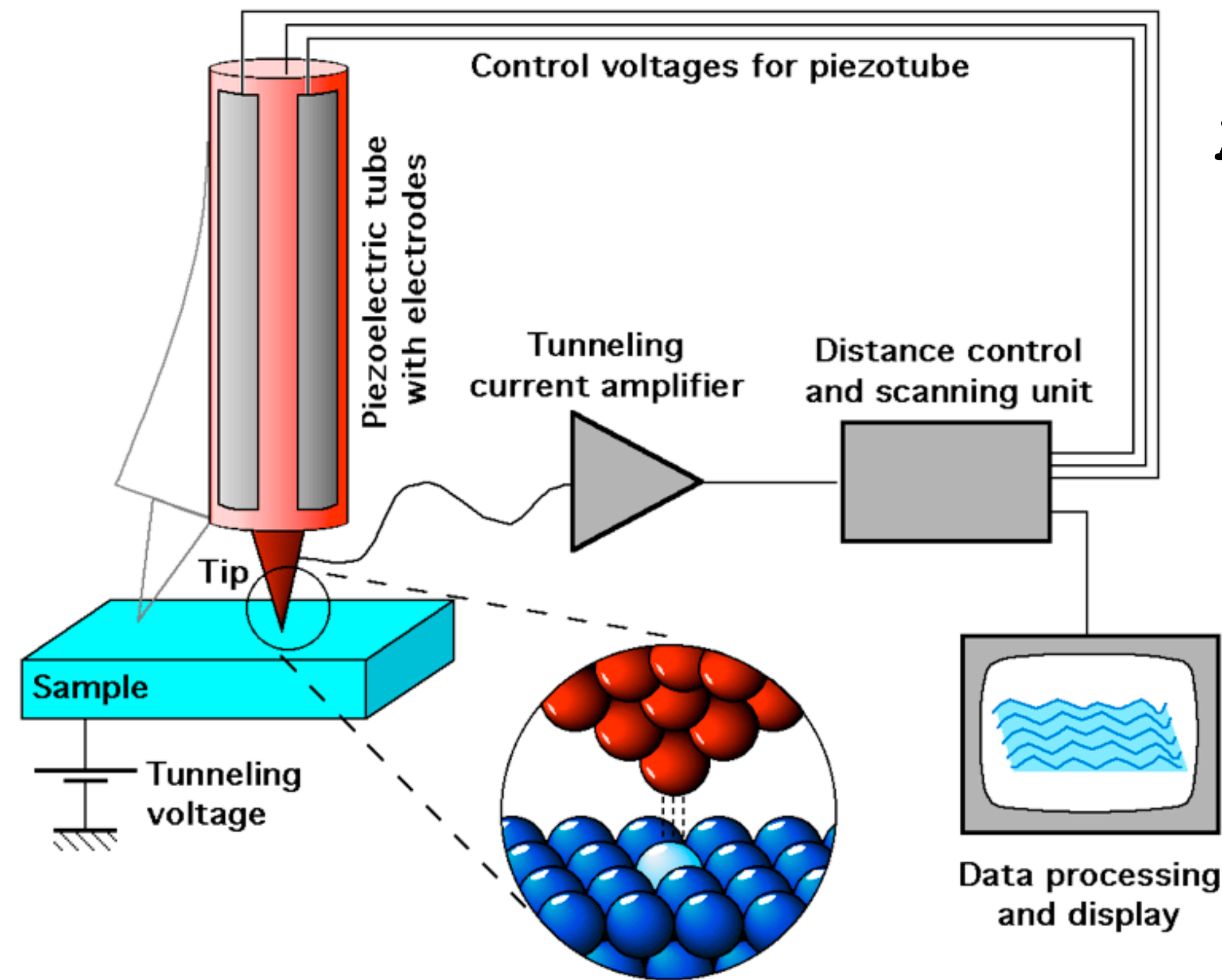
A.A. Abrikosov "On the magnetic properties of...", Soviet Physics JETP 5, 1174 (1957)

Abrikosov Vortices



A.A. Abrikosov "On the magnetic properties of...", Soviet Physics JETP 5, 1174 (1957)

Scanning Tunneling Microscope

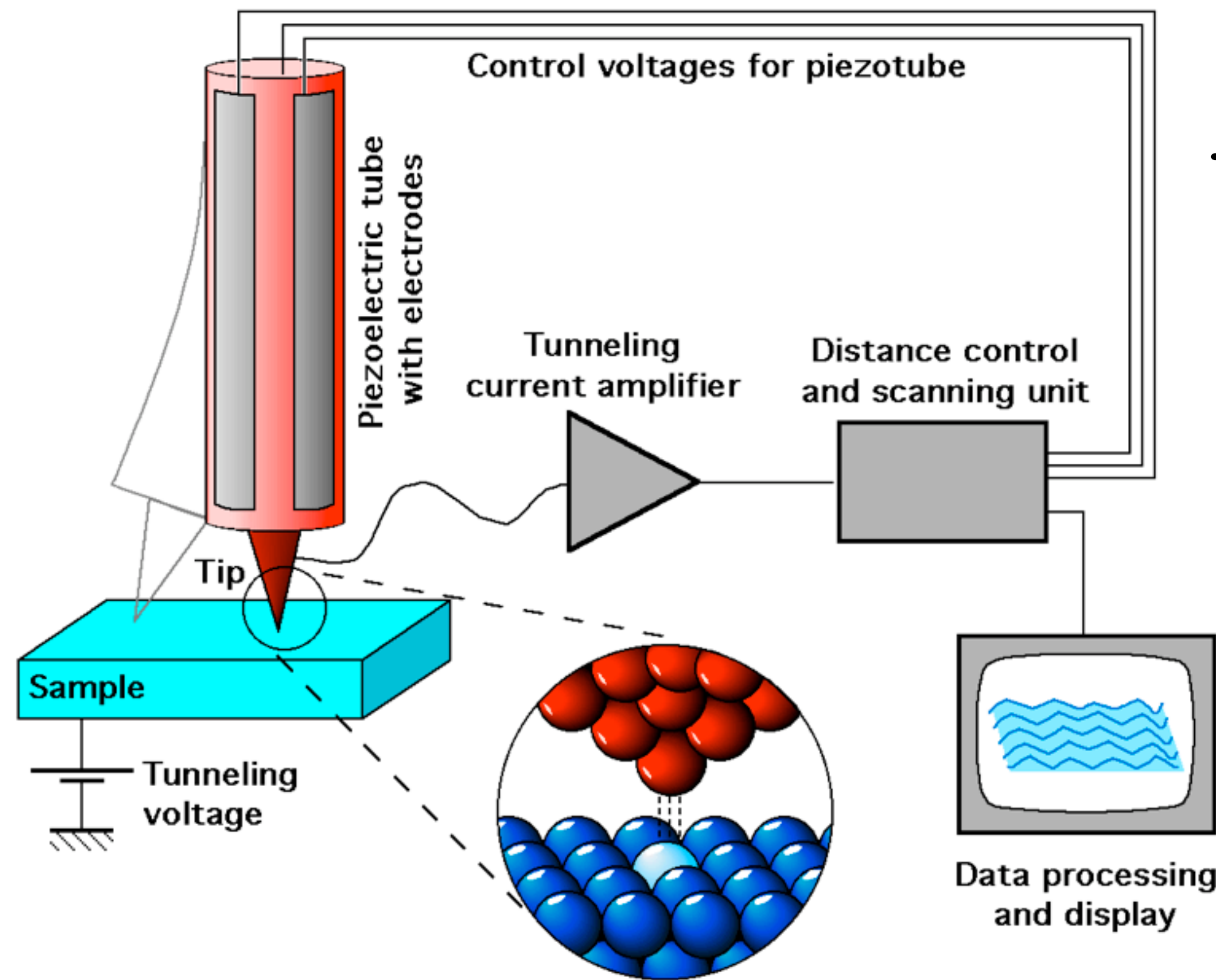


Atomic Scale Positioning

x y z
directions

Tunnel Current

Scanning Tunneling Microscope



Atomic Scale Positioning

x y z
directions

Local Spectroscopy

$$\frac{dI}{dV} \propto N(E = eV, x, y)$$

Tunnel Current

Abrikosov Vortex Lattices

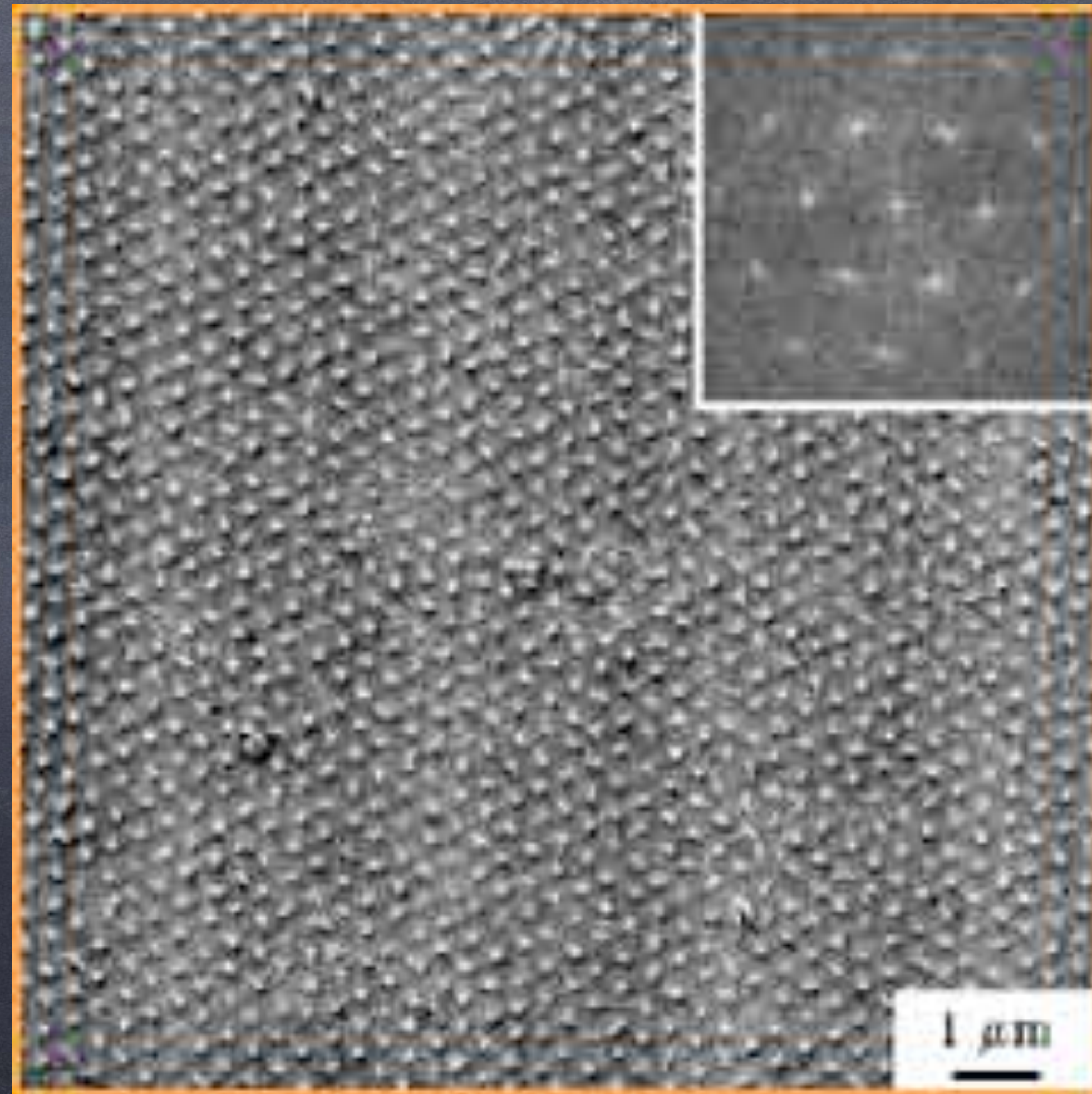
Abrikosov Vortex Lattices

MgB₂ crystal, 200G

L. Ya. Vinnikov et al.

Phys. Rev. (2003)

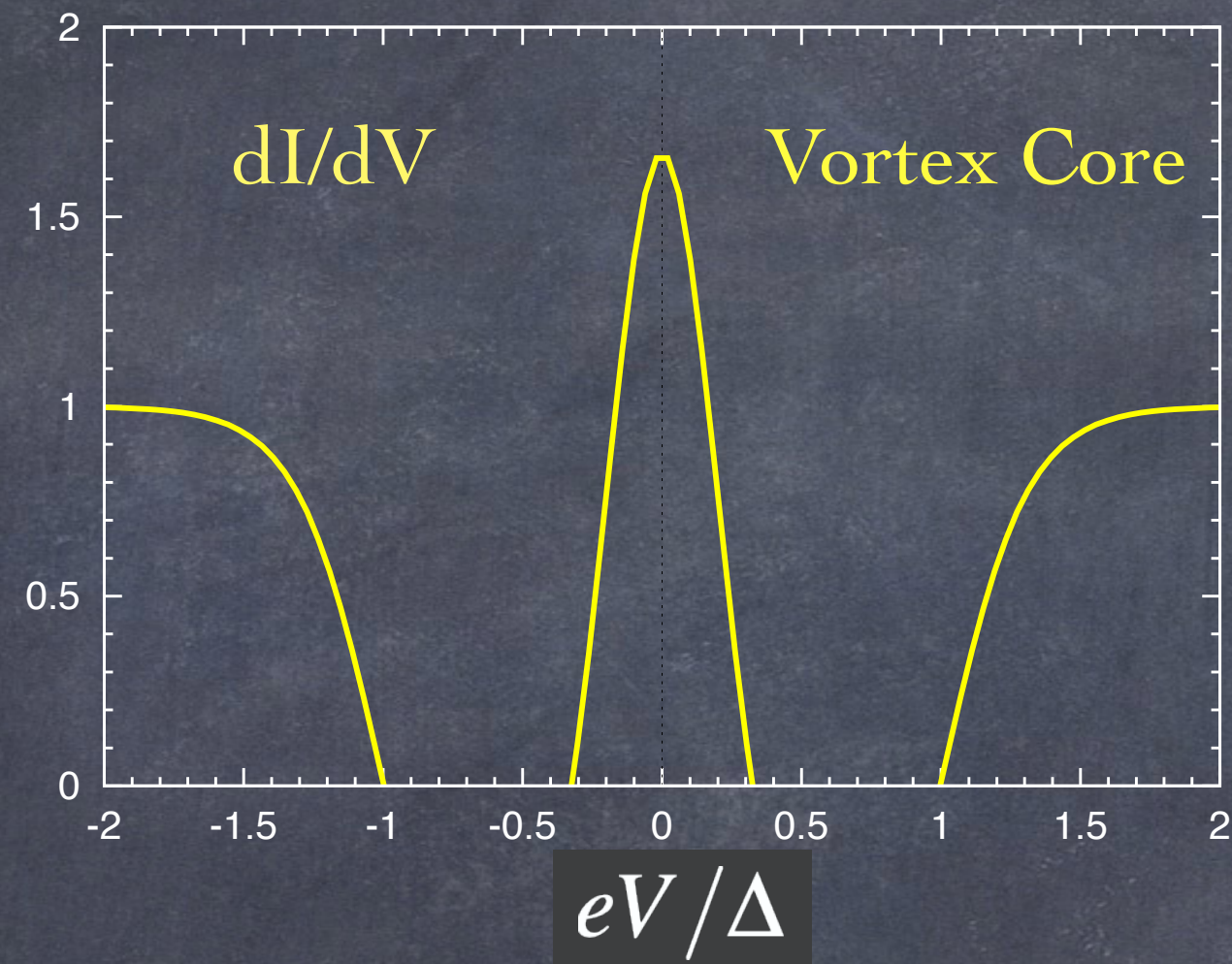
Magnetic Decoration



Abrikosov Vortex Lattices

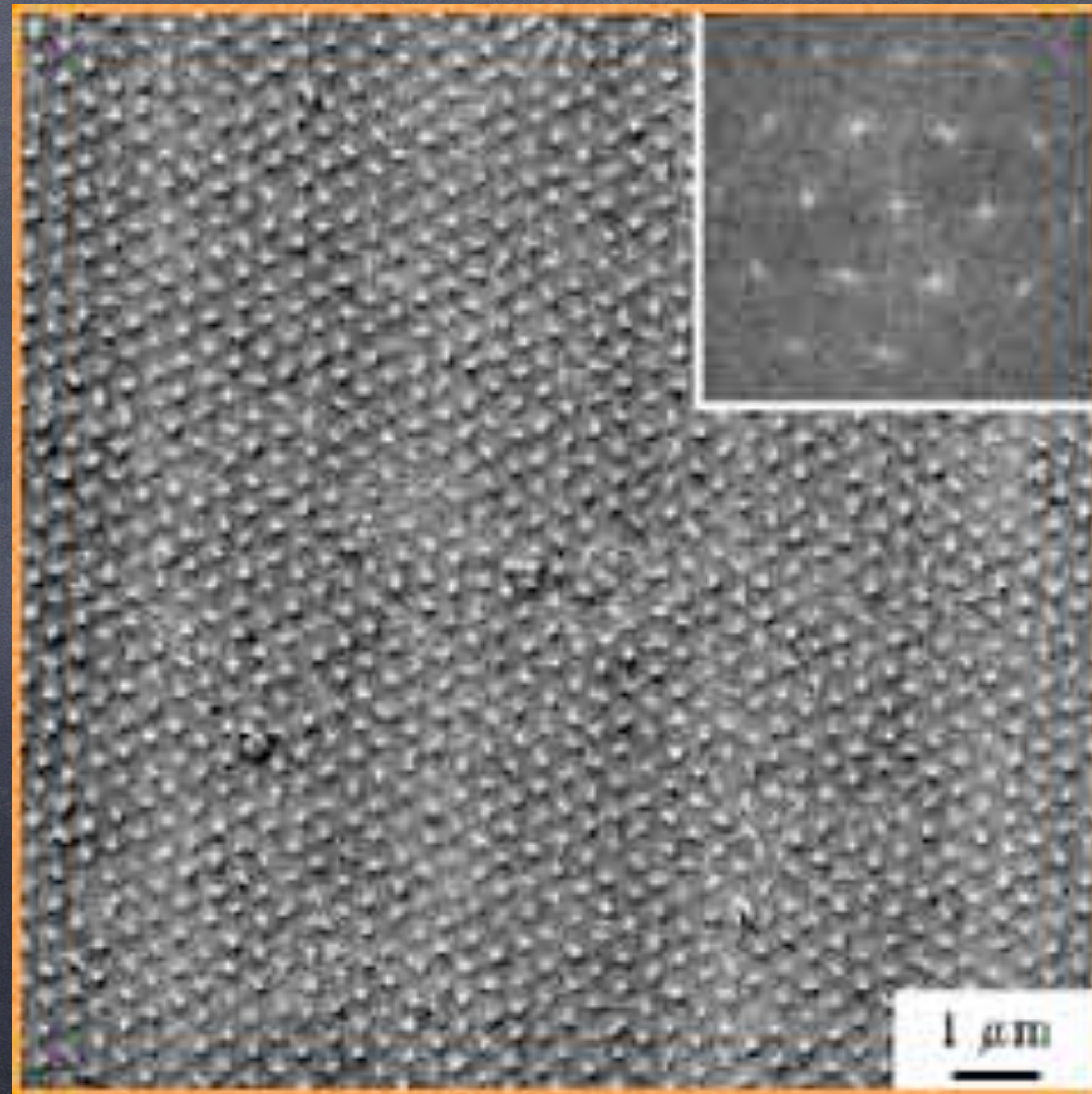
Scanning Tunneling
Microscope Spectroscopy

NbSe₂ T_c=5K, Hess et al. PRL (1989)



MgB₂ crystal, 200G
L. Ya. Vinnikov et al.
Phys. Rev. (2003)

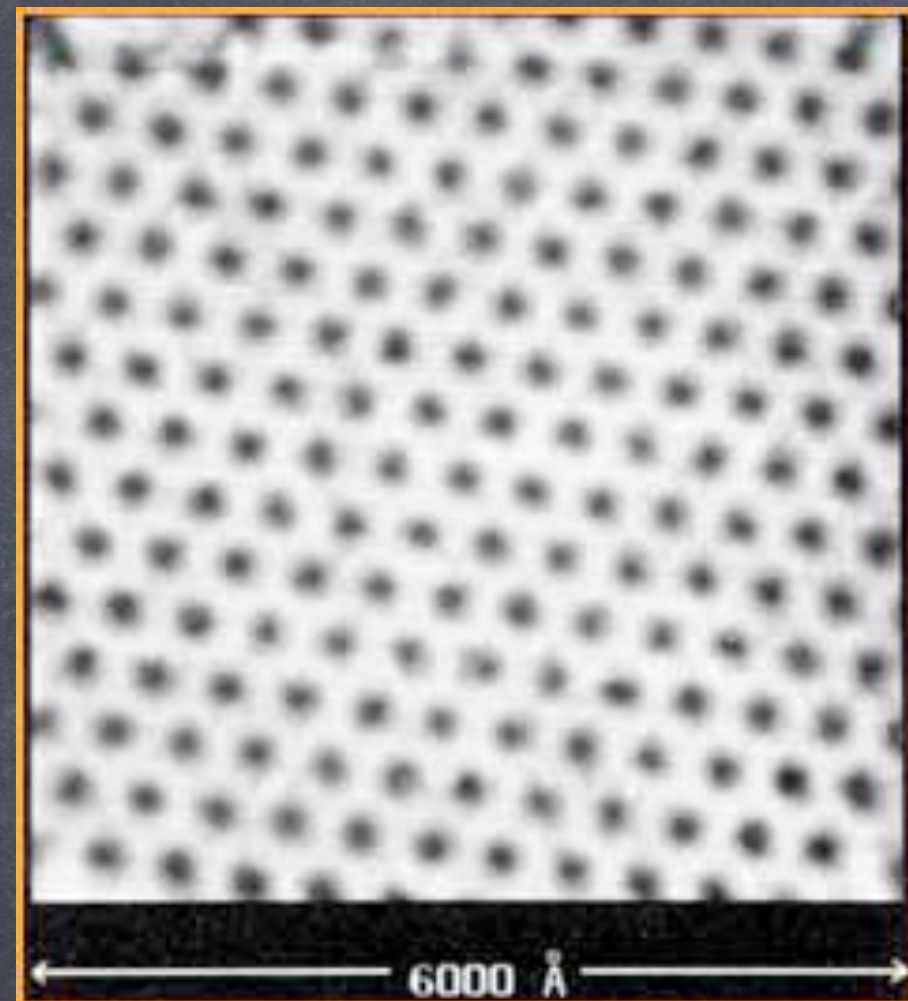
Magnetic Decoration



Abrikosov Vortex Lattices

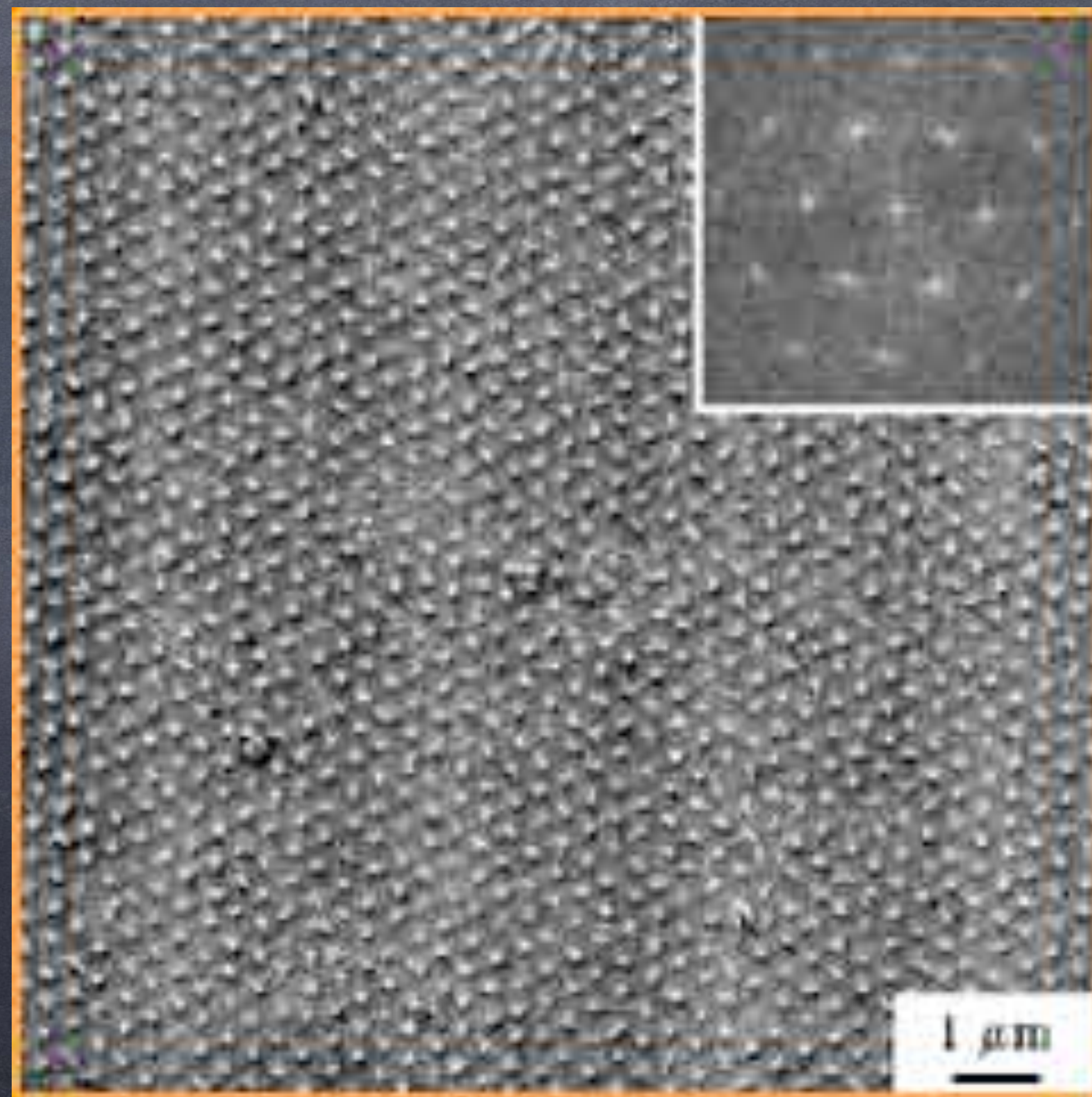
Scanning Tunneling
Microscope Spectroscopy

NbSe₂ T_c=5K, Hess et al. PRL (1989)



Magnetic Decoration

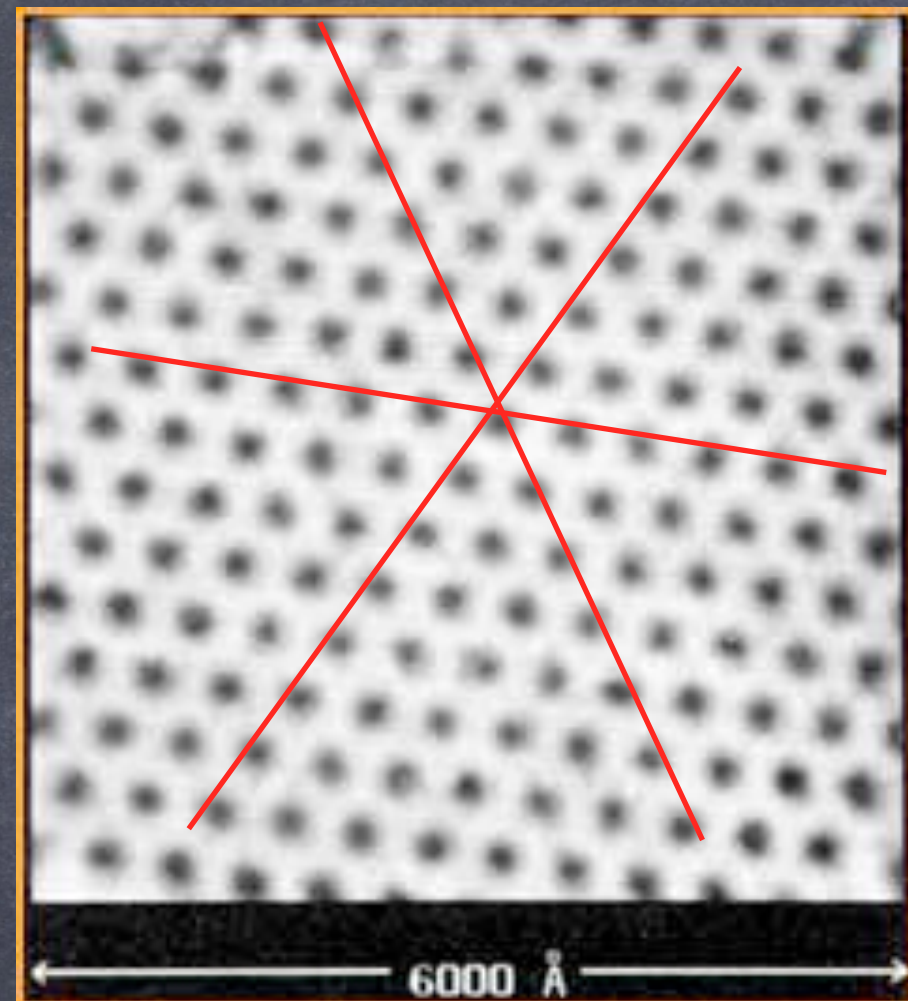
MgB₂ crystal, 200G
L. Ya. Vinnikov et al.
Phys. Rev. (2003)



Abrikosov Vortex Lattices

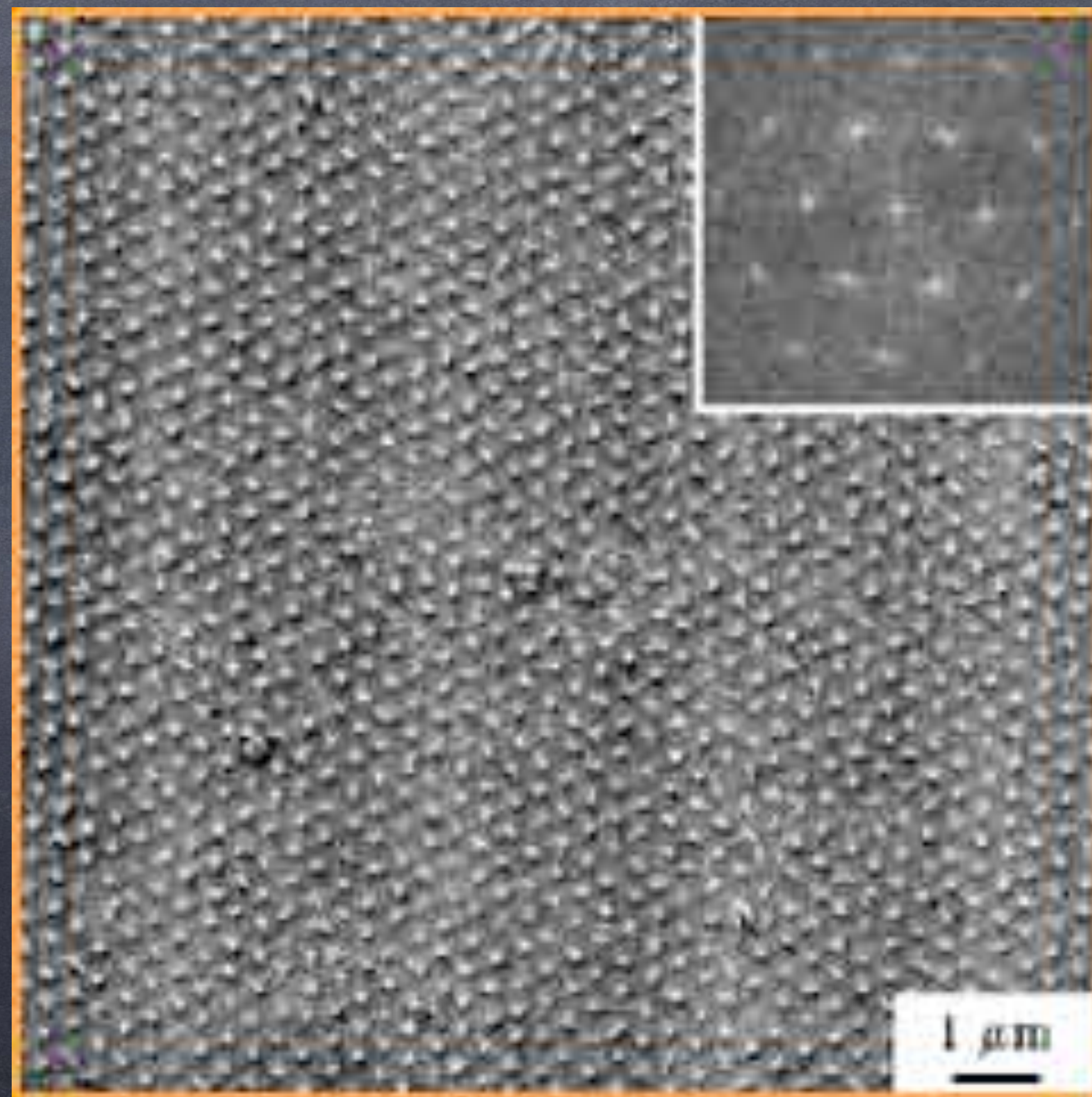
Scanning Tunneling
Microscope Spectroscopy

NbSe₂ T_c=5K, Hess et al. PRL (1989)



Magnetic Decoration

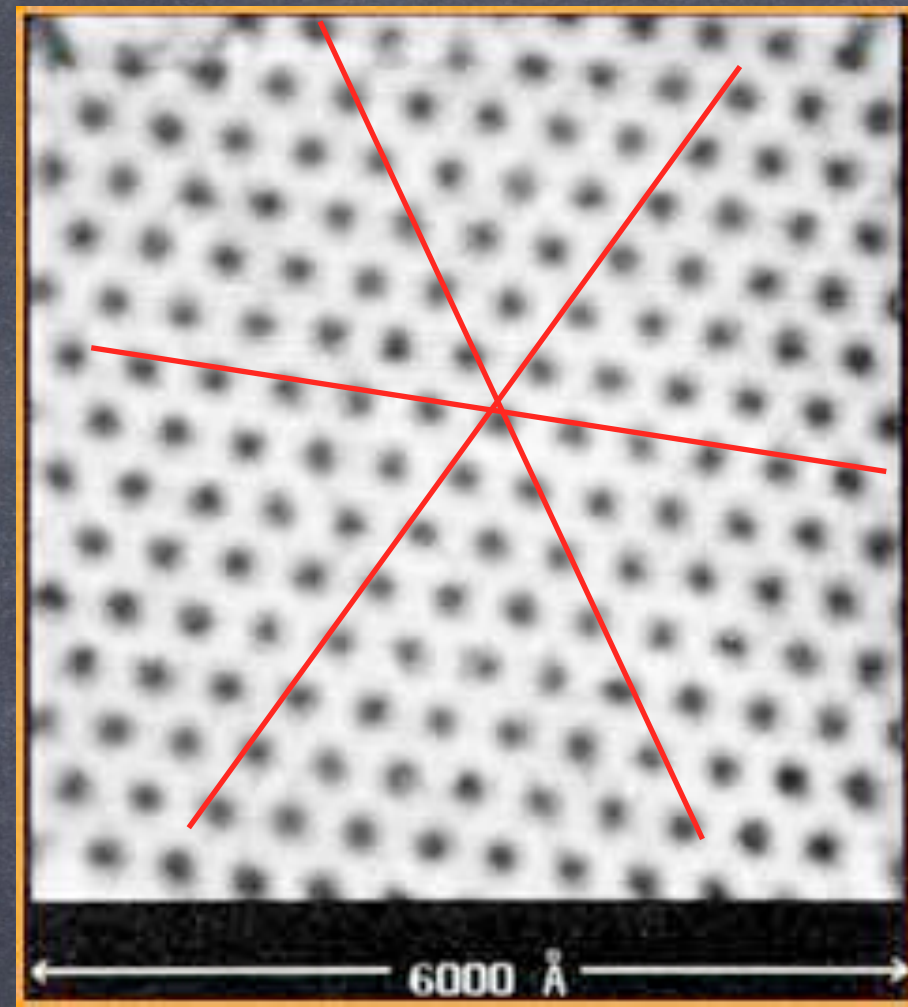
MgB₂ crystal, 200G
L. Ya. Vinnikov et al.
Phys. Rev. (2003)



Abrikosov Vortex Lattices

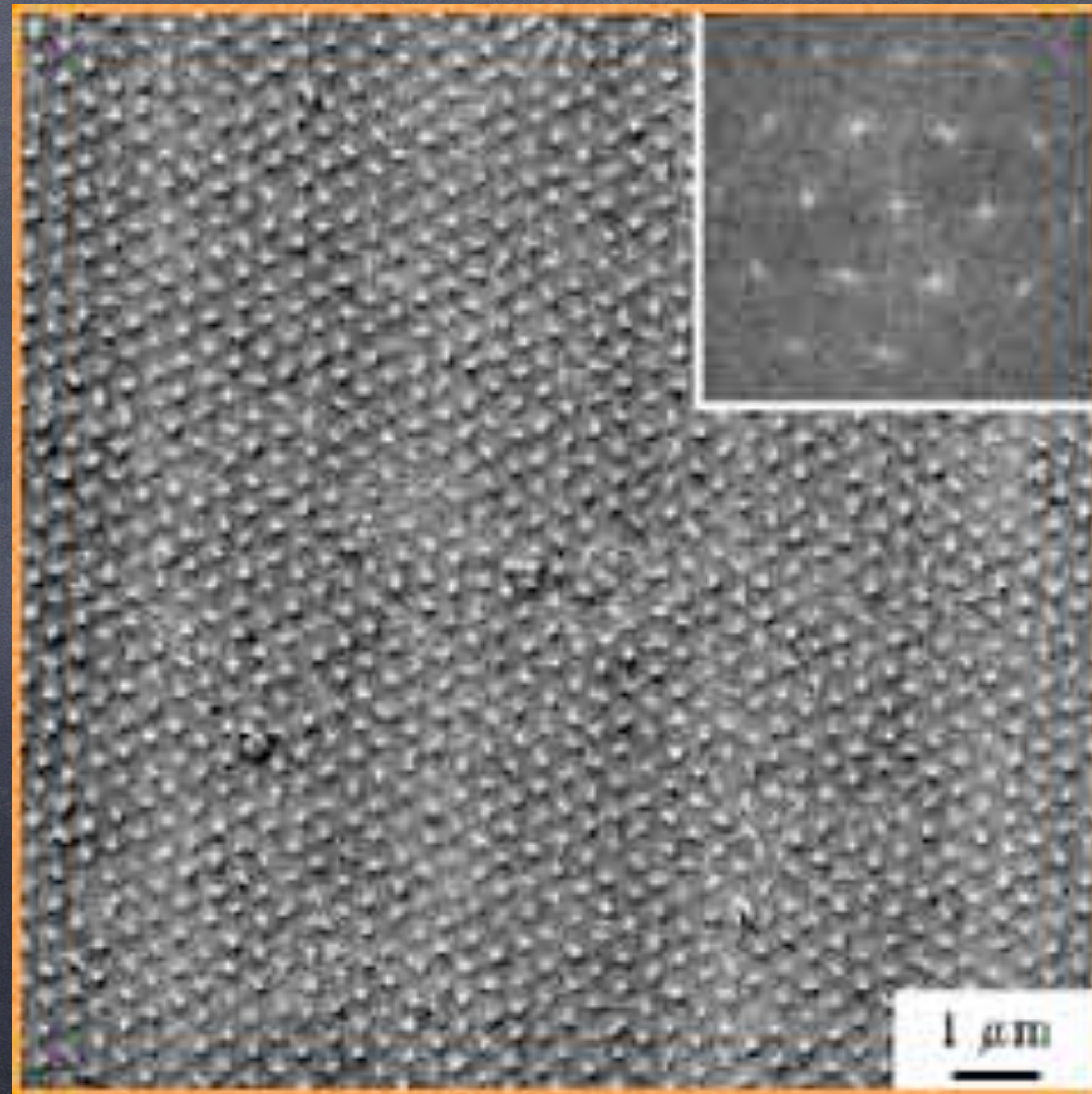
Scanning Tunneling
Microscope Spectroscopy

NbSe₂ T_c=5K, Hess et al. PRL (1989)

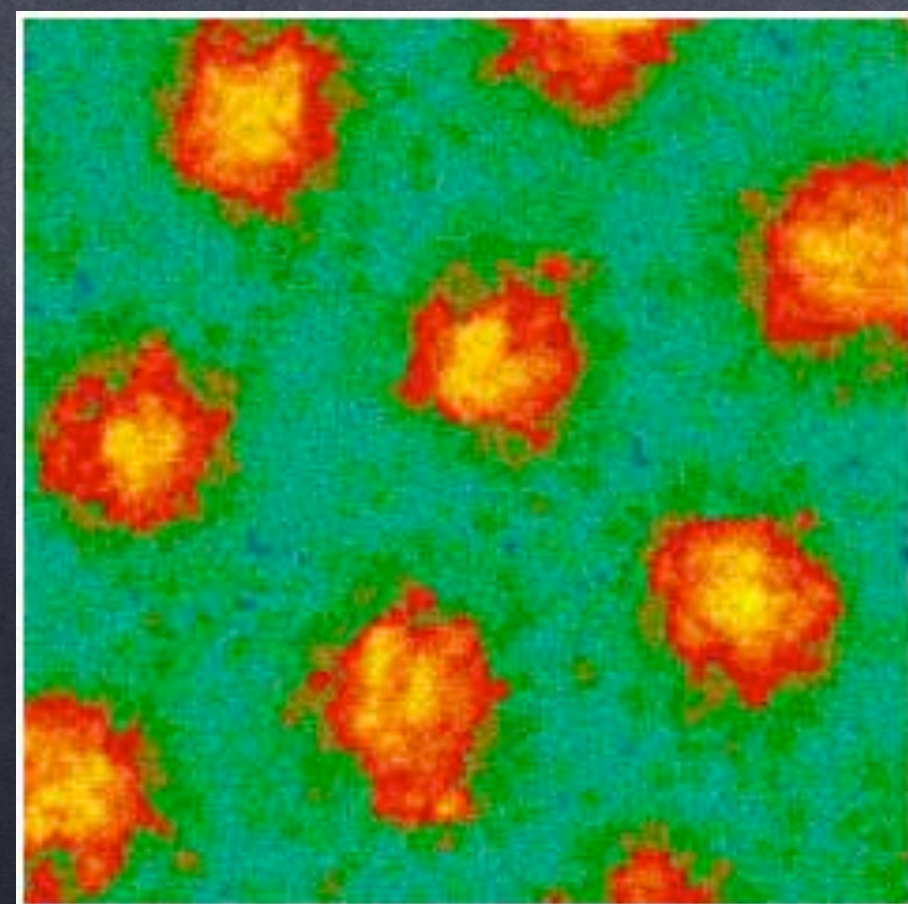


MgB₂ crystal, 200G
L. Ya. Vinnikov et al.
Phys. Rev. (2003)

Magnetic Decoration



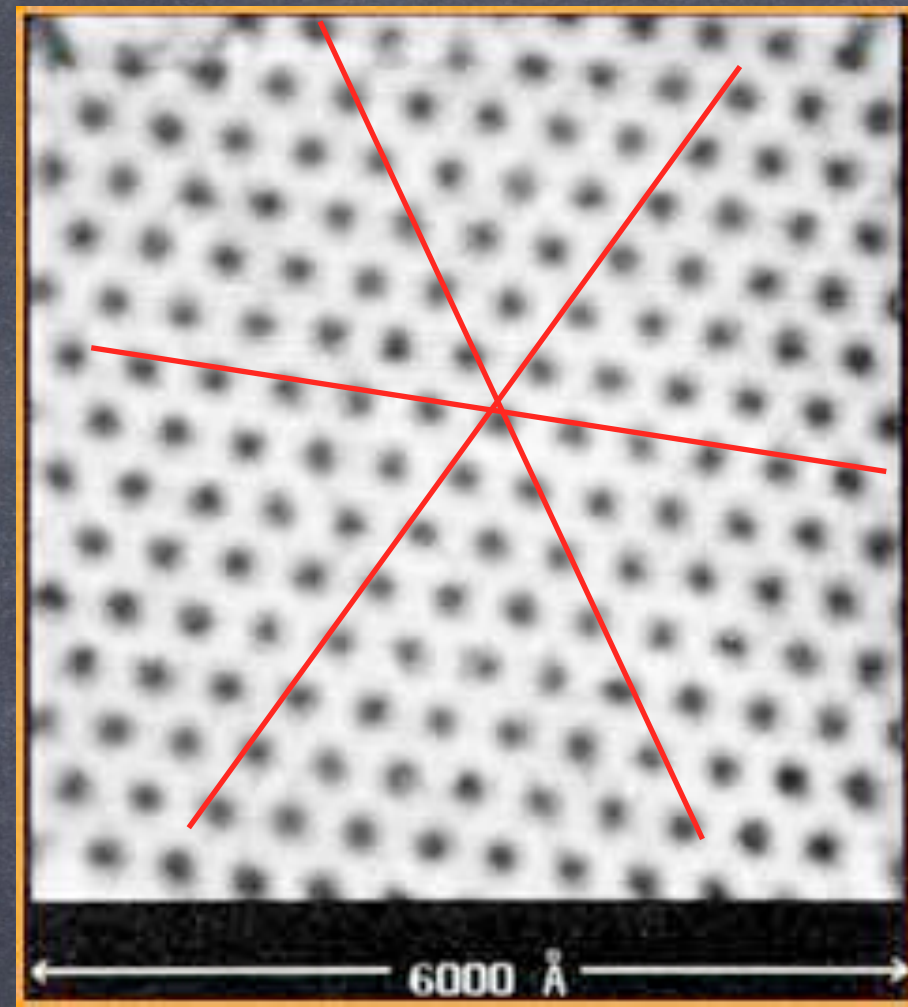
Small Angle
Neutron Diffraction
By the Magnetic field of
Flux Lines



Abrikosov Vortex Lattices

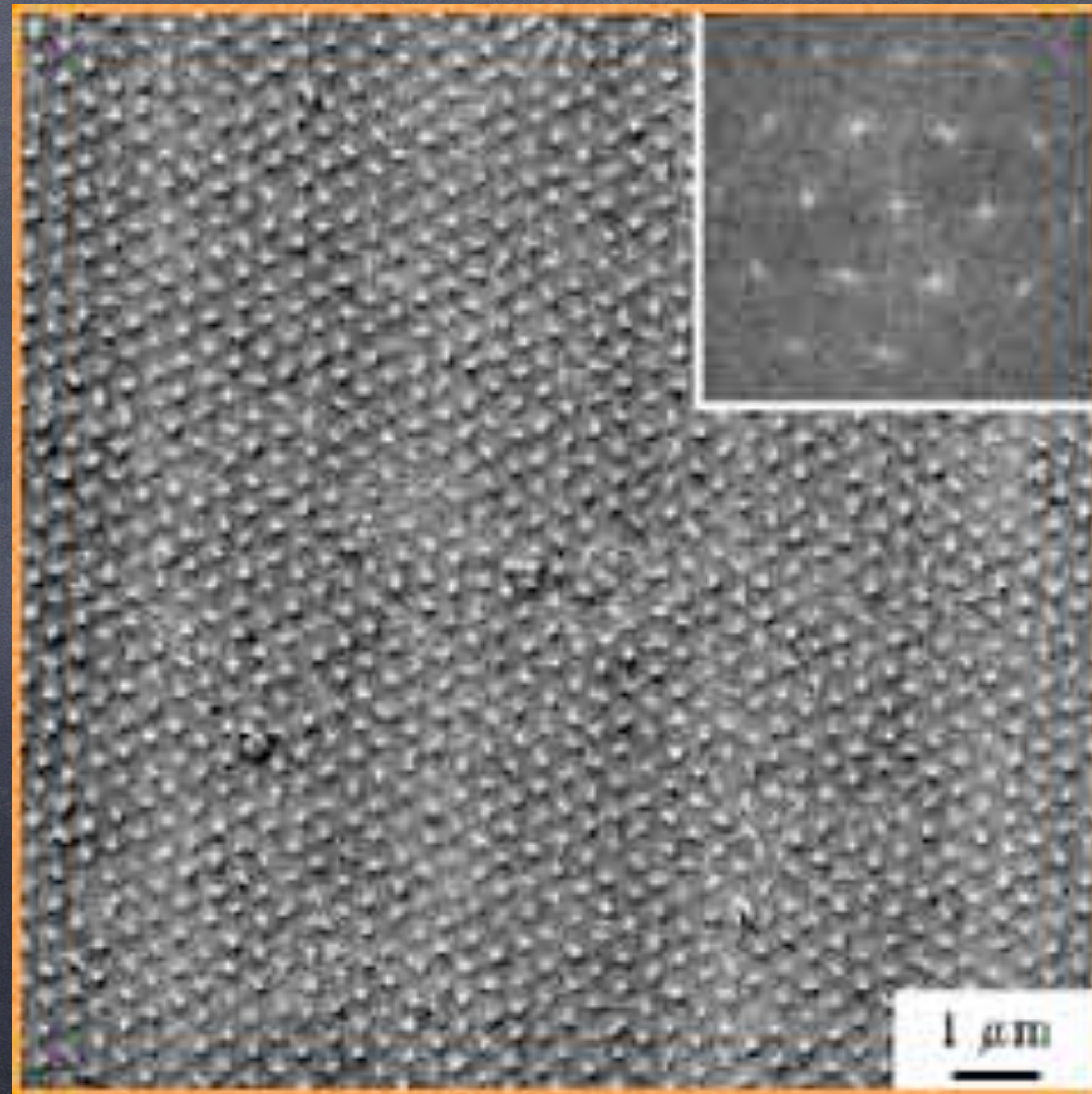
Scanning Tunneling
Microscope Spectroscopy

NbSe₂ T_c=5K, Hess et al. PRL (1989)

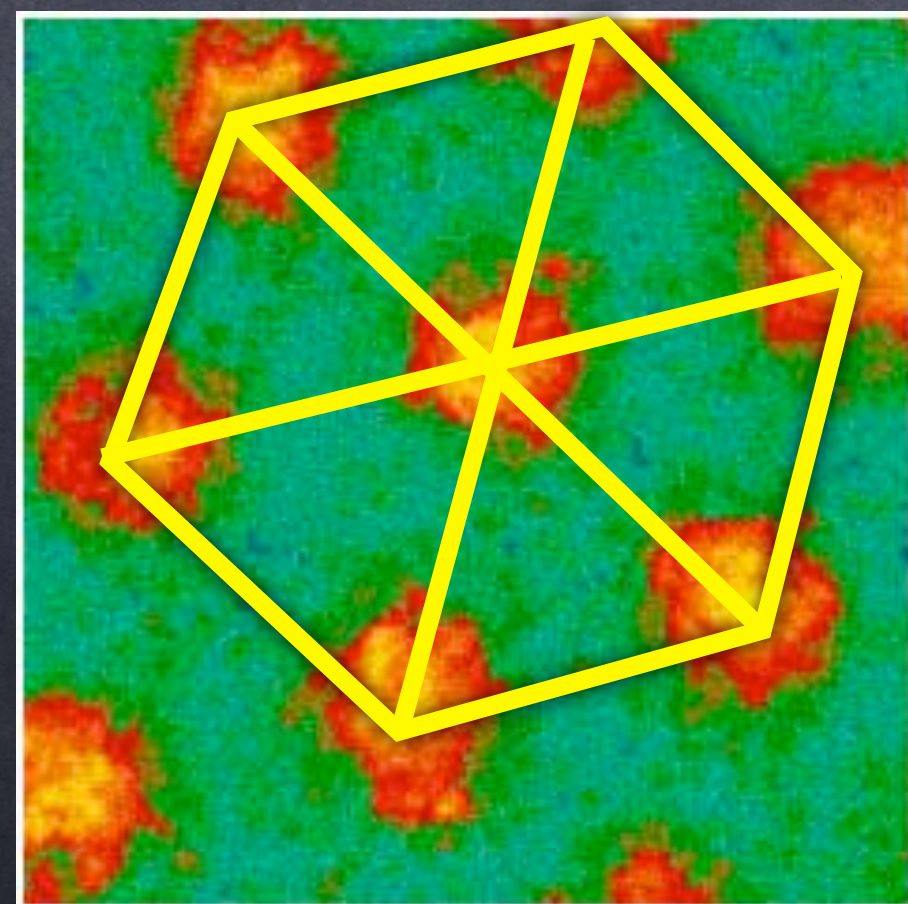


MgB₂ crystal, 200G
L. Ya. Vinnikov et al.
Phys. Rev. (2003)

Magnetic Decoration



Small Angle
Neutron Diffraction
By the Magnetic field of
Flux Lines



Other Imaging
Methods

MgB₂ T=2K, B=2 kG M. R. Eskildsen et al. PRL (2002)

Abrikosov Vortices are Often Pinned to Impurities or
Structural Defects in the Superconductor \rightsquigarrow
Disordered and complex Flux pattern

Abrikosov Vortices are Often Pinned to Impurities or
Structural Defects in the Superconductor \rightsquigarrow
Disordered and complex Flux pattern

Levitation by *High- T_c* superconductors

A. B. Riise, et al.

Physical Review B 60, 9855 (1998)

Abrikosov Vortices are Often Pinned to Impurities or Structural Defects in the Superconductor \rightsquigarrow
Disordered and complex Flux pattern

Levitation by High- T_c superconductors

A. B. Riise, et al.

Physical Review B 60, 9855 (1998)



❖ NdFeB - Magnet

❖ YBCO - Superconductor

❖ Flux Pinning

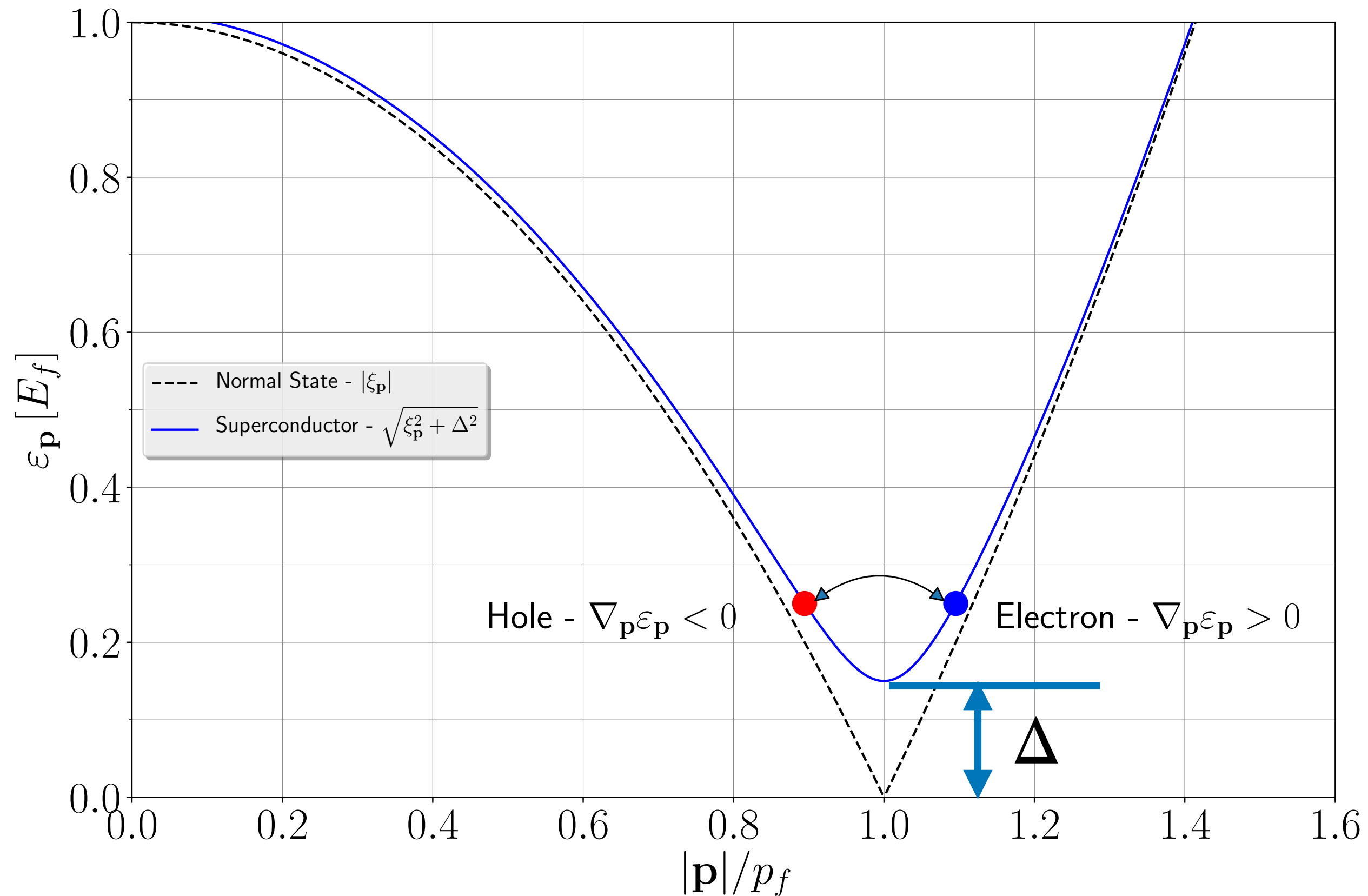
❖ Flux Creep on warming

The Energy Gap of BCS Superconductors

Normal metal $\xi_{\mathbf{p}} = \frac{|\mathbf{p}|^2}{2m} - \frac{p_f^2}{2m} \approx v_f(|\mathbf{p}| - p_f)$

Superconductor $E_{\mathbf{p}} = \sqrt{\xi_{\mathbf{p}}^2 + \Delta^2}$

Two types of Excitations



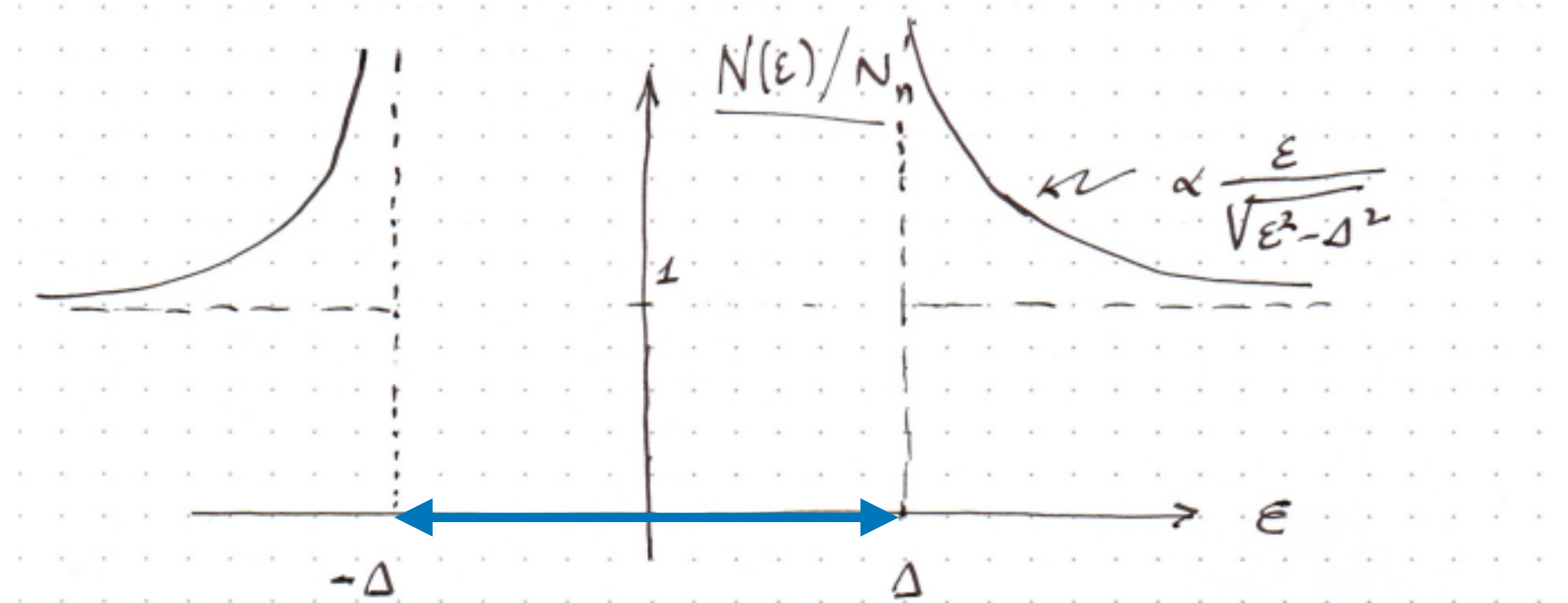
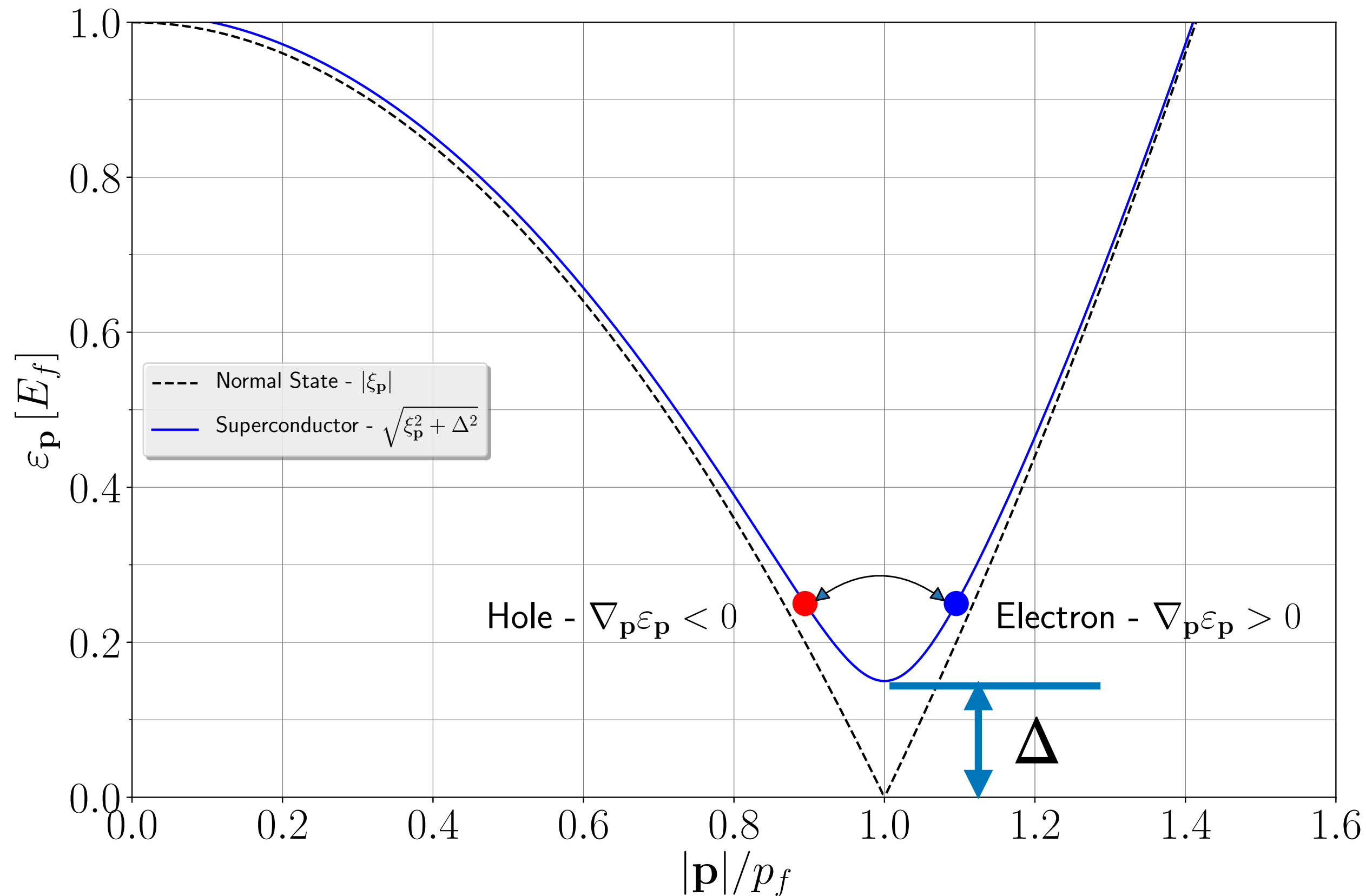
The Energy Gap of BCS Superconductors

Normal metal $\xi_{\mathbf{p}} = \frac{|\mathbf{p}|^2}{2m} - \frac{p_f^2}{2m} \approx v_f(|\mathbf{p}| - p_f)$

Superconductor $E_{\mathbf{p}} = \sqrt{\xi_{\mathbf{p}}^2 + \Delta^2}$

Number of States per unit Energy in $(\varepsilon, \varepsilon + d\varepsilon)$

Two types of Excitations



BCS Quasiparticle Density of States

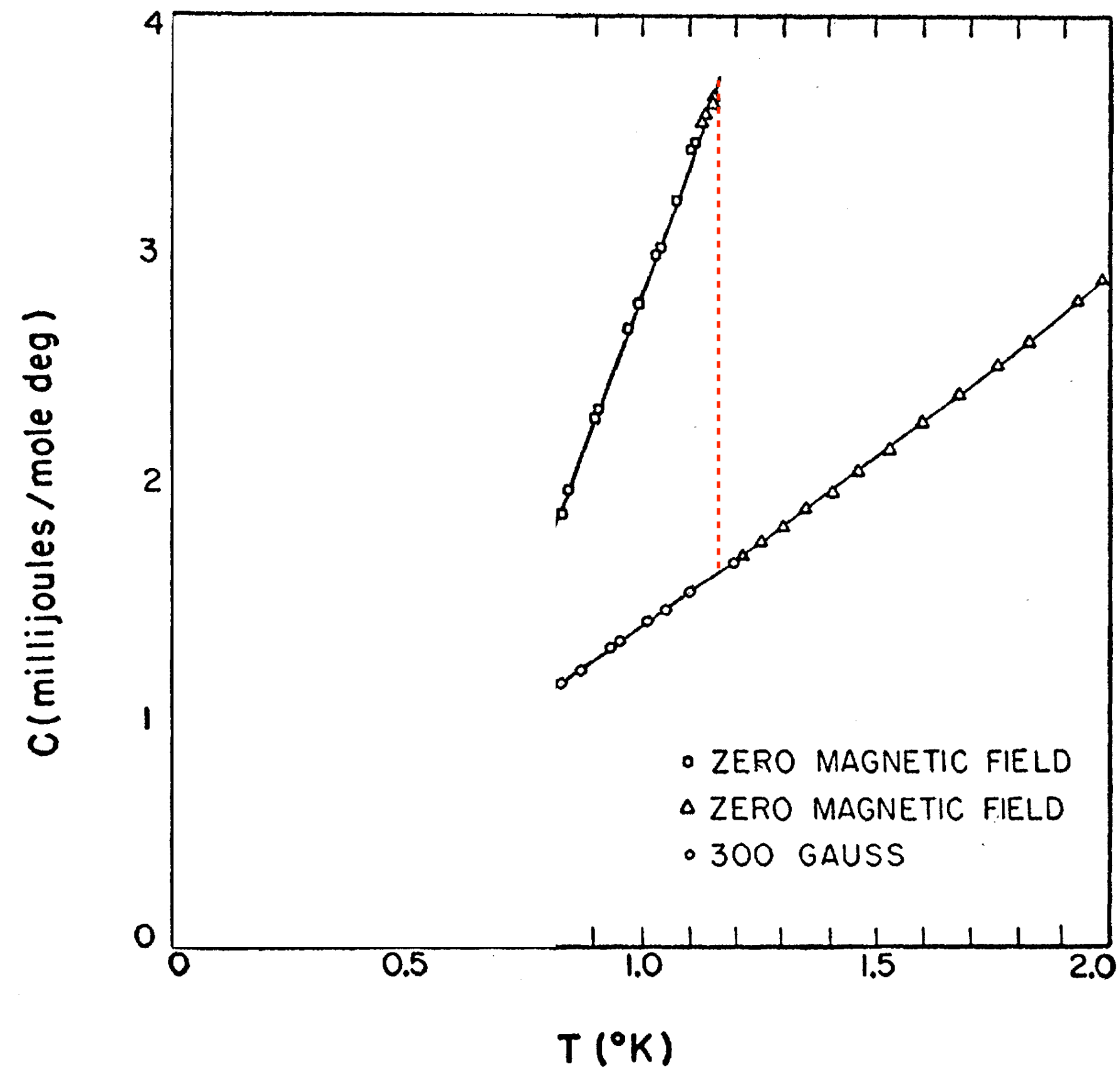
- ▣ $N_n = \frac{3}{2} n / E_F = \text{Normal Metal DOS @ } E_F$.
- ▣ $\Delta = \text{Excitation Gap for Quasiparticles/Q-holes}$

$$\Delta(Nb) \cong 2 \text{ meV}$$

$$\Delta(Al) \cong 0.2 \text{ meV}$$

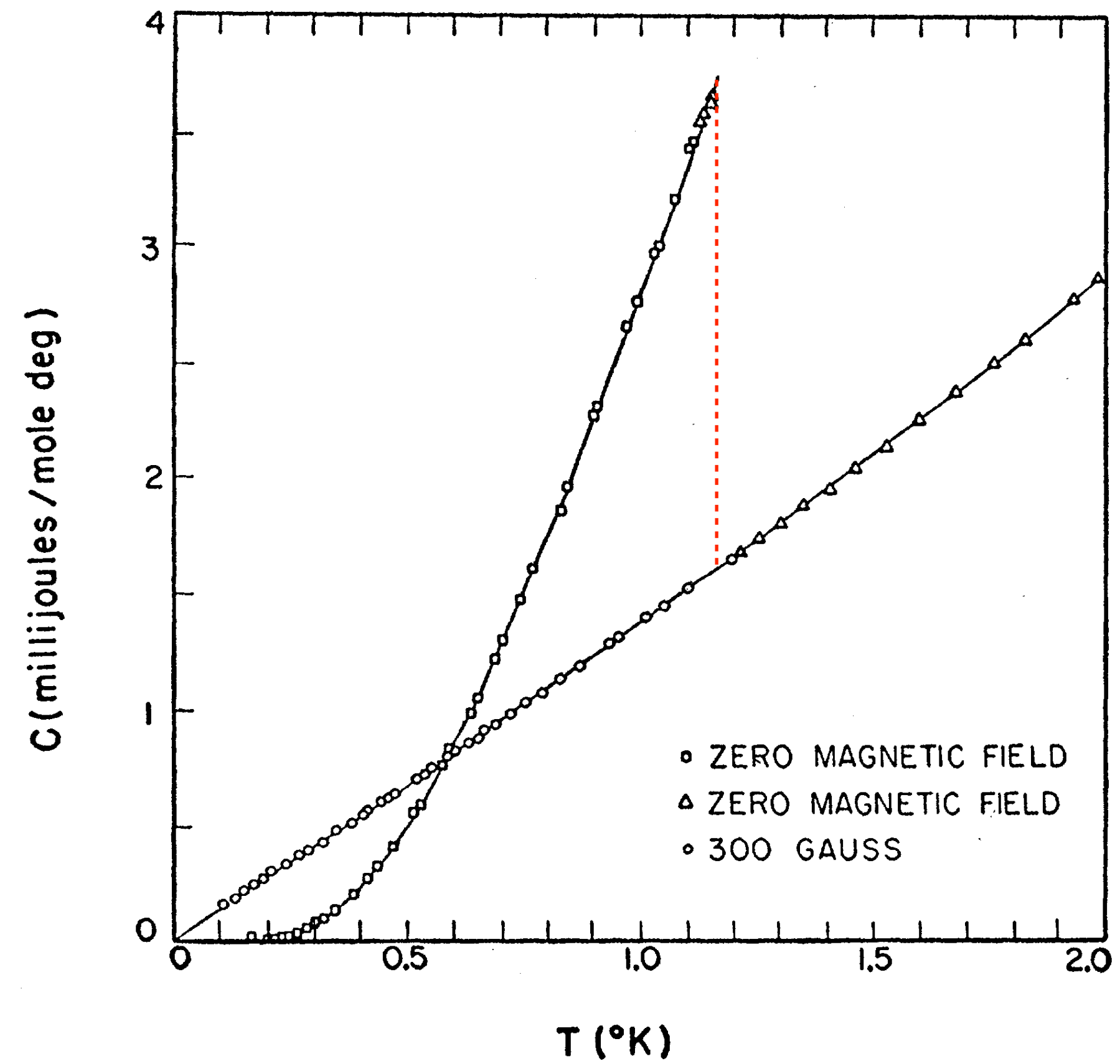
Thermodynamics - Heat Capacity

Heat Capacity of Al, Phys. Rev. 114, 676 (1959), N.E. Phillips



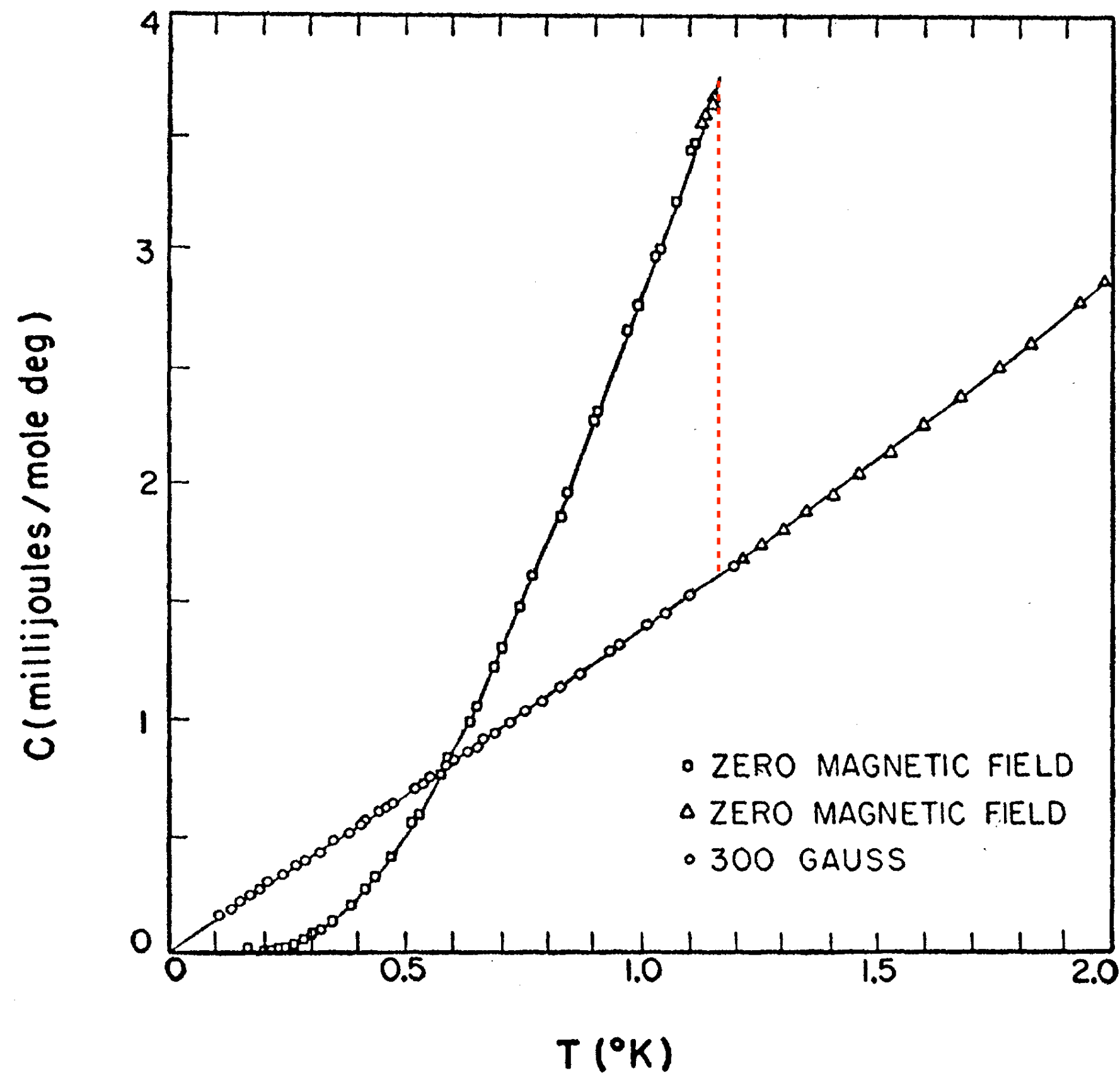
Thermodynamics - Heat Capacity

Heat Capacity of Al, Phys. Rev. 114, 676 (1959), N.E. Phillips



Thermodynamics - Heat Capacity

Heat Capacity of Al, Phys. Rev. 114, 676 (1959), N.E. Phillips



- ▶ Electronic Entropy: *Fermions* with $N(E) \approx N(E_f)$
- ▶ $T > T_c = 1.16K$: $C = \gamma T$
- ▶ 2nd Order Transition: $\Delta C / \gamma T_c \approx 1.6$
- ▶ $T < 0.5K$: $C \propto e^{-\Delta/k_B T}$?

Evidence of an Energy Gap for un-bound electrons in Superconductors

Rev. Mod. Phys. 30, 1109 (1958), M. Biondi et al.

Phys. Rev. 122, 1101 (1961), I. Gaiver et al.

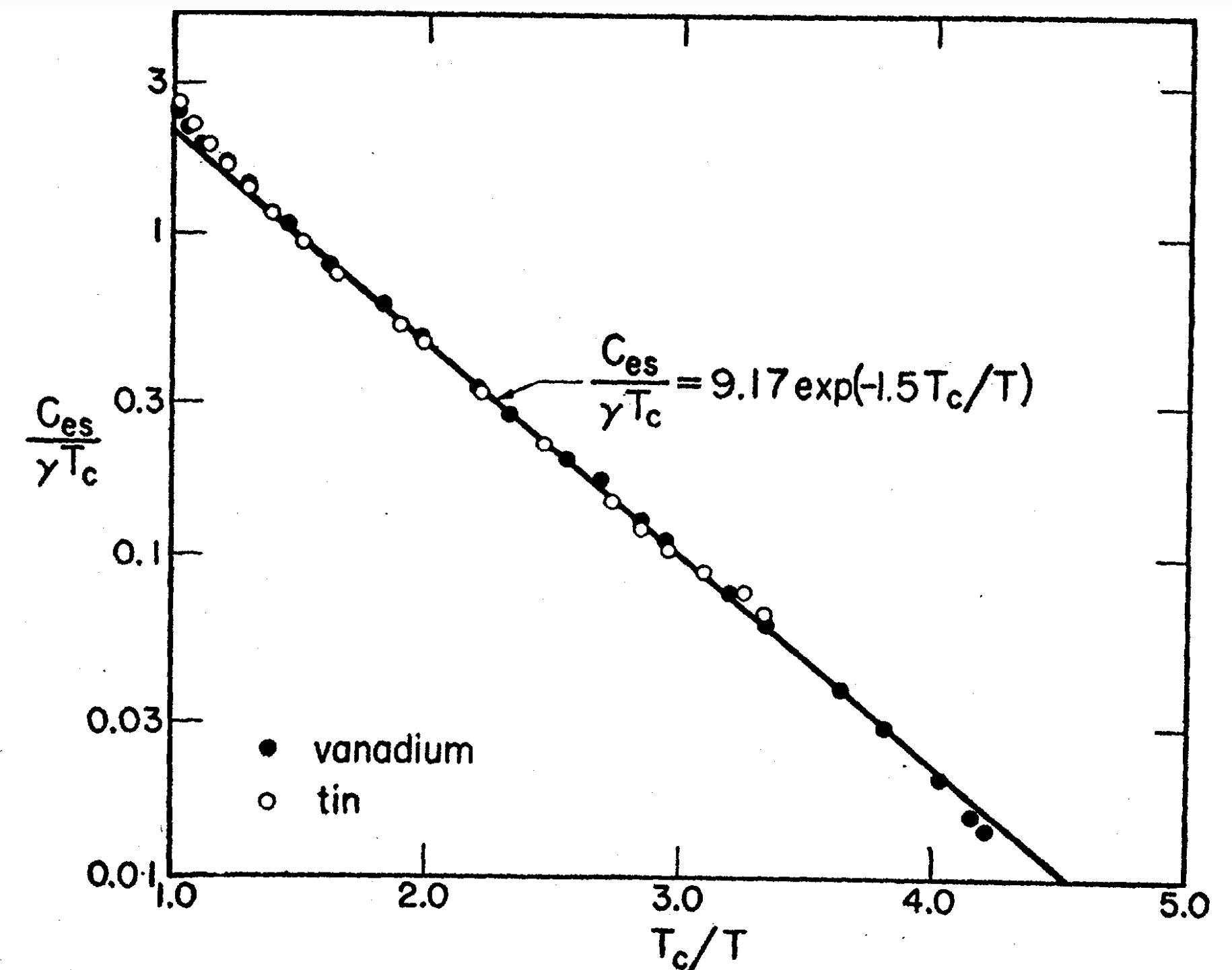
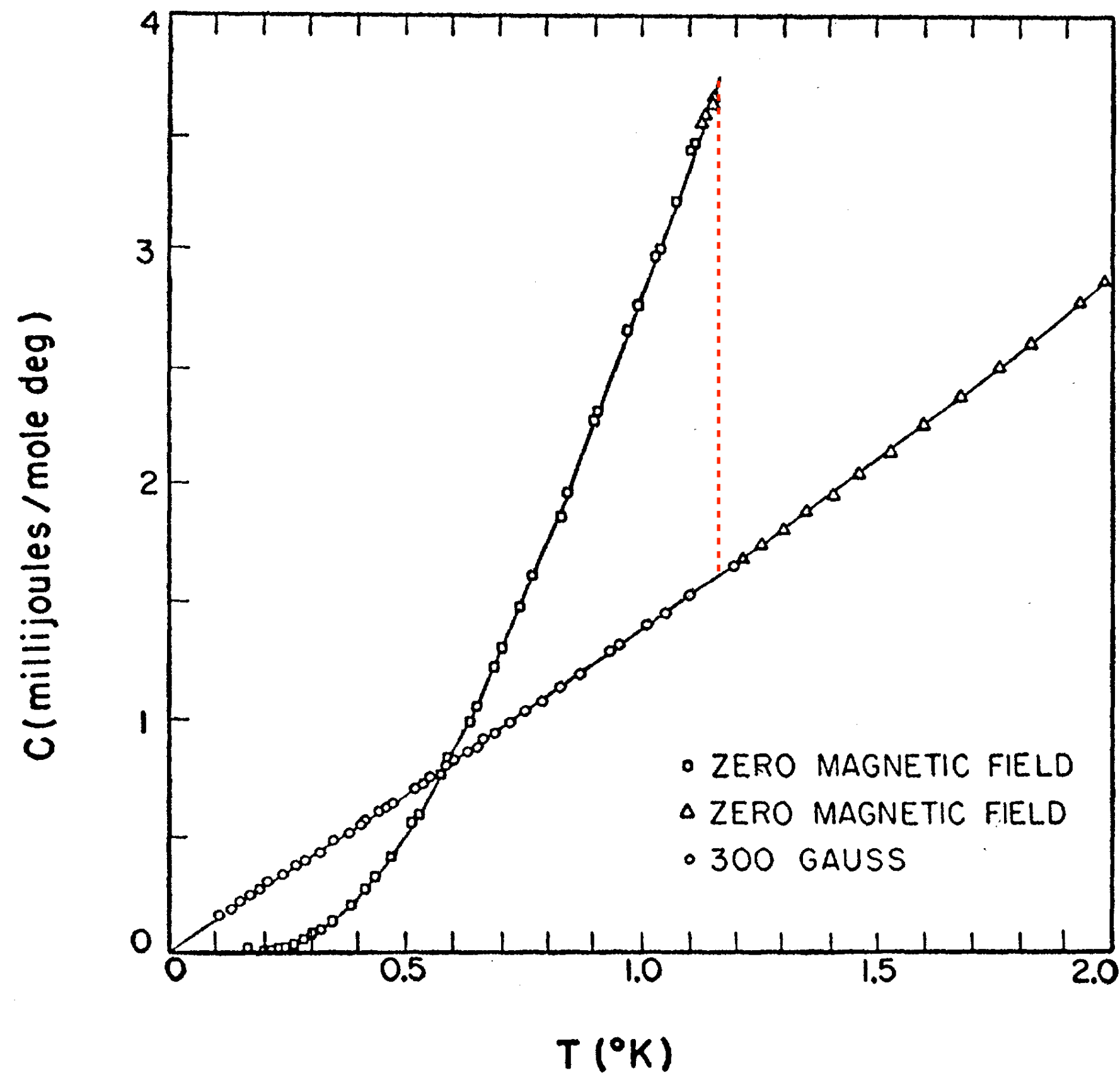


FIG. 6. Reduced electronic specific heat in the superconducting state for vanadium and tin.

Thermodynamics - Heat Capacity

Heat Capacity of Al, Phys. Rev. 114, 676 (1959), N.E. Phillips



- ▶ Electronic Entropy: *Fermions* with $N(E) \approx N(E_f)$
- ▶ $T > T_c = 1.16K$: $C = \gamma T$
- ▶ 2nd Order Transition: $\Delta C / \gamma T_c \approx 1.6$
- ▶ $T < 0.5K$: $C \propto e^{-\Delta/k_B T}$?

Evidence of an Energy Gap for un-bound electrons in Superconductors

Rev. Mod. Phys. 30, 1109 (1958), M. Biondi et al.

Phys. Rev. 122, 1101 (1961), I. Gaiver et al.

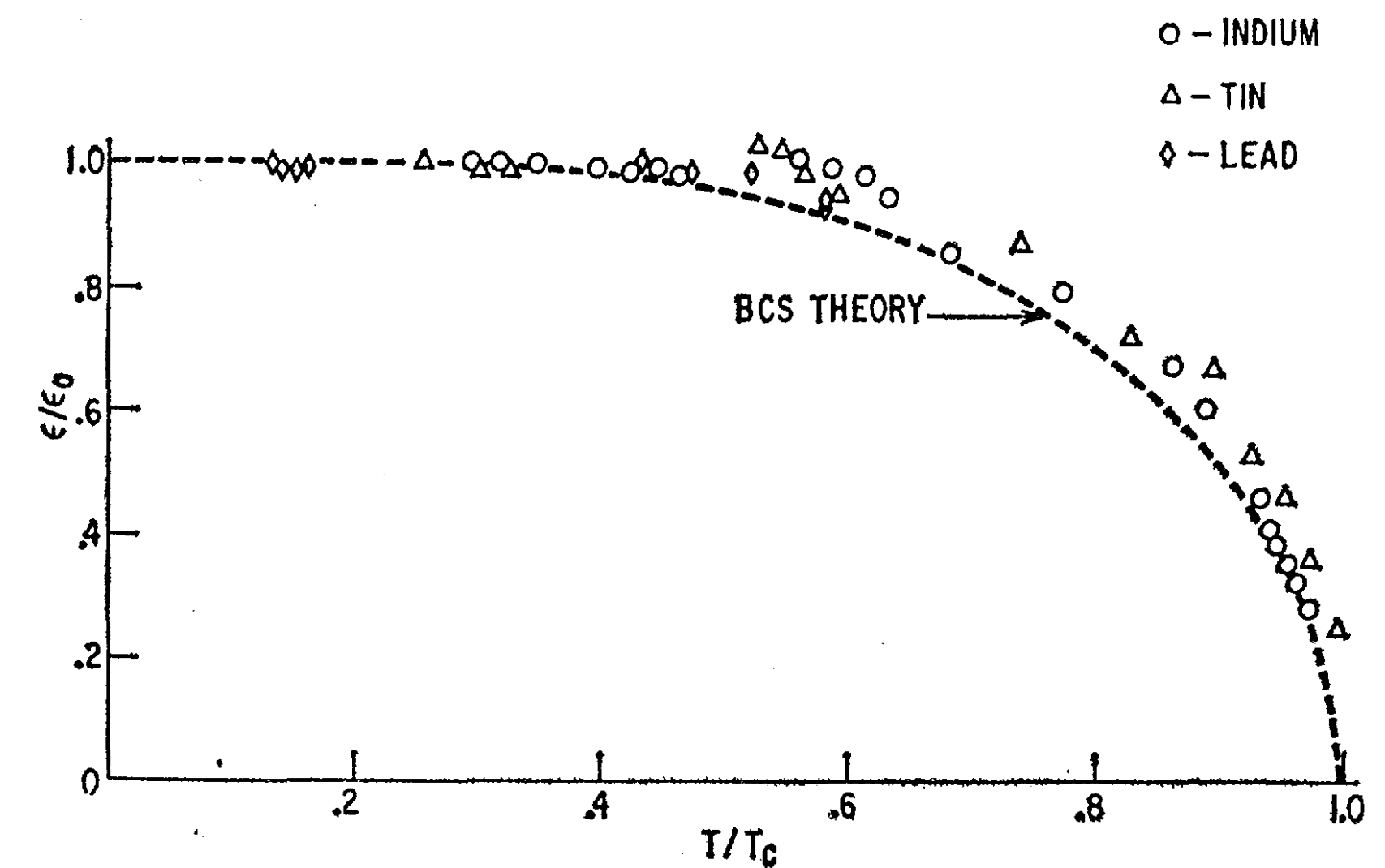


FIG. 11. The energy gap of Pb, Sn, and In films as a function of reduced temperature, compared with the Bardeen-Cooper-Schrieffer theory.

- ▶ Energy Gap: $\Delta \approx 1.5 - 1.8 k_B T_c$

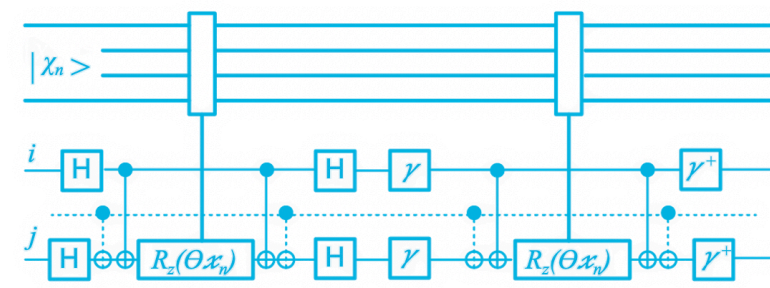
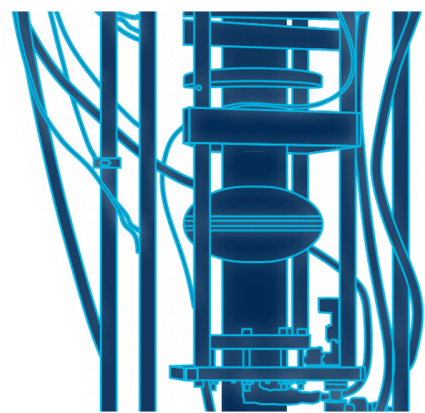
Heat Capacity Jumps & Energy Gaps for Elemental SCs

Element	$2\Delta/k_B T$	$\Delta C/\gamma T_c$	Element	$2\Delta/k_B T$	$\Delta C/\gamma T_c$
Al	2.5–4.2	1.3–1.6	Pb	4.0–4.4	2.7
Cd	3.2–3.4	1.3–1.4	Sn	2.8–4.0	1.6
Ga	3.5	1.4	Ta	3.5–3.7	1.6
Hg	4.0–4.6	2.4	Tl	3.6–3.9	1.5
In	3.4–3.7	1.7	V	3.4–3.5	1.5
La	1.7–3.2	1.5	Zn	3.2–3.4	1.2–1.3
Nb	3.6–3.8	1.9–2.0			
BCS	3.53	1.43			

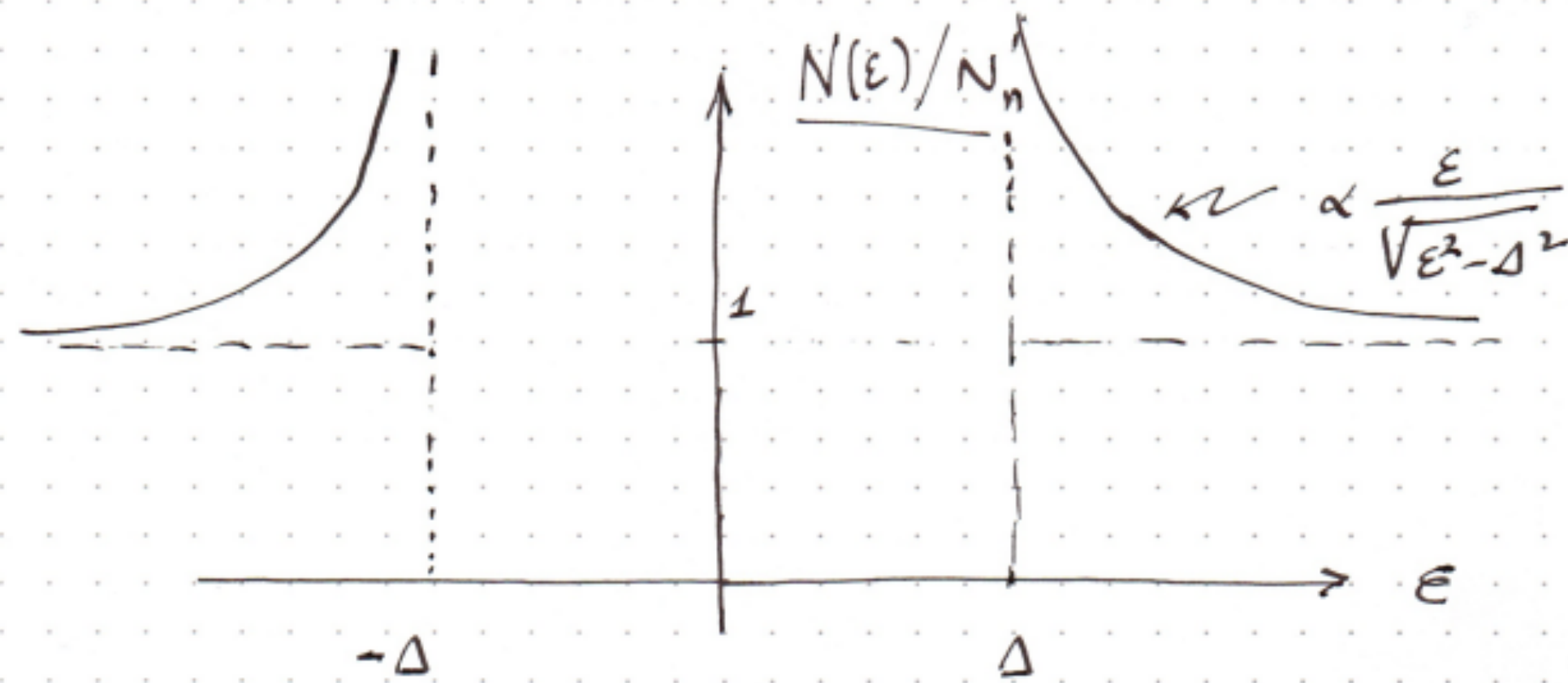
Table: Source: M. Marder, Condensed Matter Physics, Chapter 27, Wiley, 2010

Importance of understanding and controlling the excitation spectrum for superconducting quantum processors and sensor development

Quasiparticle Excitations – BCS Spectrum (Density of States)



Quasiparticle Excitations – BCS Spectrum (Density of States)



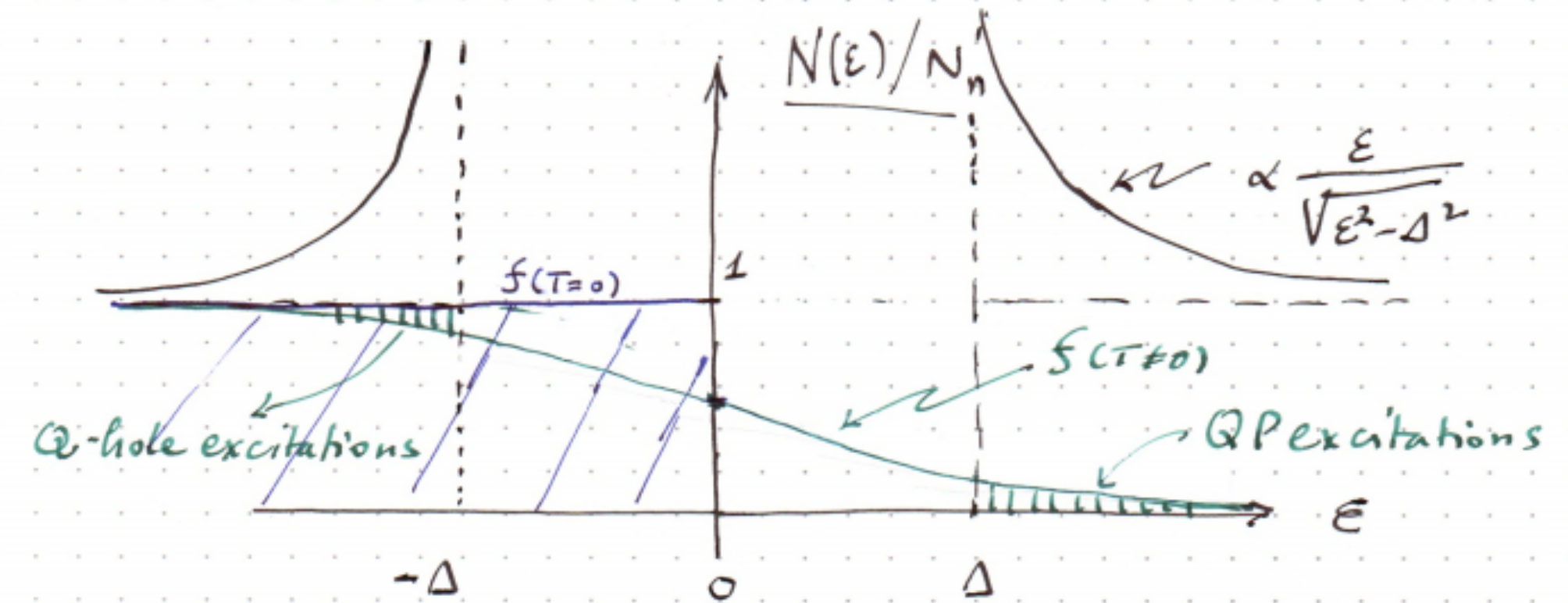
BCS Quasiparticle Density of States

• $N_n = \frac{3}{2} N / E_F$ = Normal Metal DOS @ E_F .

• Δ = Excitation Gap for Quasiparticles / Q-holes

$\Delta(Nb) \approx 2 \text{ meV}$

$\Delta(AL) \approx 0.2 \text{ meV}$

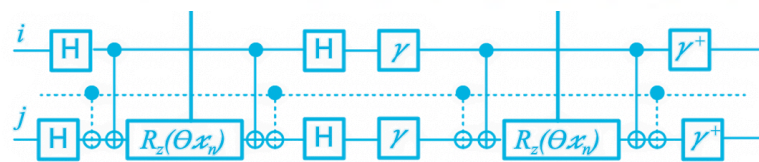


Thermal Excitations

$$f(\epsilon) = \frac{1}{e^{\epsilon/k_B T} + 1}$$

→ BCS Excitation Gap: $\Delta/k_B T$

$N_{QP} \propto \sqrt{k_B T / \Delta} e^{-\Delta/k_B T}$ → Expected Negligible @ 10^{-2} K Typical DR



Non-Equilibrium Quasiparticle Excitations in QIS devices

PHYSICAL REVIEW LETTERS **121**, 157701 (2018)

Hot Nonequilibrium Quasiparticles in Transmon Qubits

K. Serniak,^{1,*} M. Hays,¹ G. de Lange,^{1,2} S. Diamond,¹ S. Shankar,¹ L. D. Burkhardt,¹
L. Frunzio,¹ M. Houzet,³ and M. H. Devoret^{1,†}

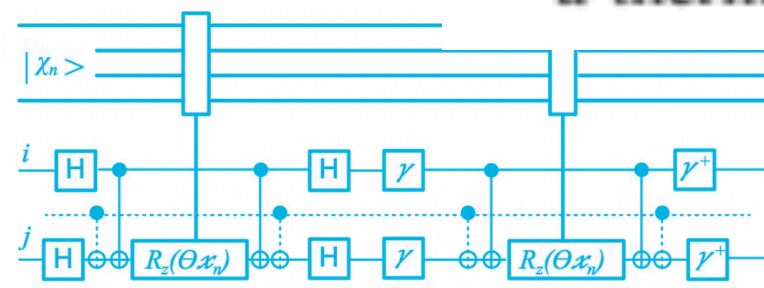
¹*Department of Applied Physics, Yale University, New Haven, Connecticut 06520, USA*

²*QuTech and Kavli Institute of Nanoscience, Delft University of Technology, 2600 GA Delft, Netherlands*

³*Univ. Grenoble Alpes, CEA, INAC-Pheligs, F-38000 Grenoble, France*

 (Received 2 April 2018; revised manuscript received 27 July 2018; published 10 October 2018)

Nonequilibrium quasiparticle excitations degrade the performance of a variety of superconducting circuits. Understanding the energy distribution of these quasiparticles will yield insight into their generation mechanisms, the limitations they impose on superconducting devices, and how to efficiently mitigate quasiparticle-induced qubit decoherence. To probe this energy distribution, we systematically correlate qubit relaxation and excitation with charge-parity switches in an offset-charge-sensitive transmon qubit, and find that quasiparticle-induced excitation events are the dominant mechanism behind the residual excited-state population in our samples. By itself, the observed quasiparticle distribution would limit T_1 to $\approx 200 \mu\text{s}$, which indicates that quasiparticle loss in our devices is on equal footing with all other loss mechanisms. Furthermore, the measured rate of quasiparticle-induced excitation events is greater than that of relaxation events, which signifies that the quasiparticles are more energetic than would be predicted from a thermal distribution describing their apparent density.



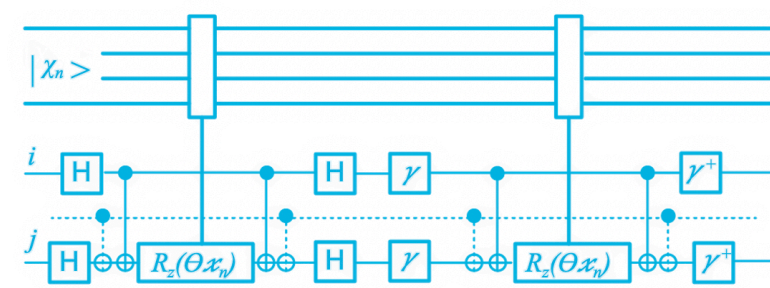
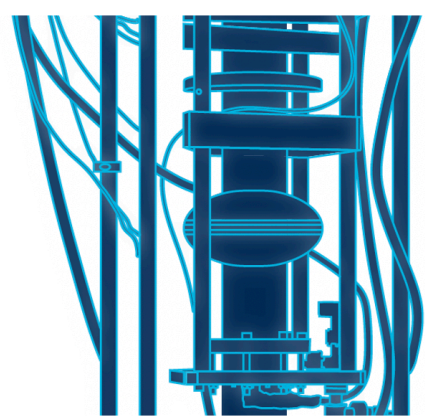
51

$$x_{QP}^{neq} \approx 10^{-7} \gg x_{QP}^{thermal}$$



SUPERCONDUCTING QUANTUM
MATERIALS & SYSTEMS CENTER

Quasiparticle Excitations – BCS theory vs Observation

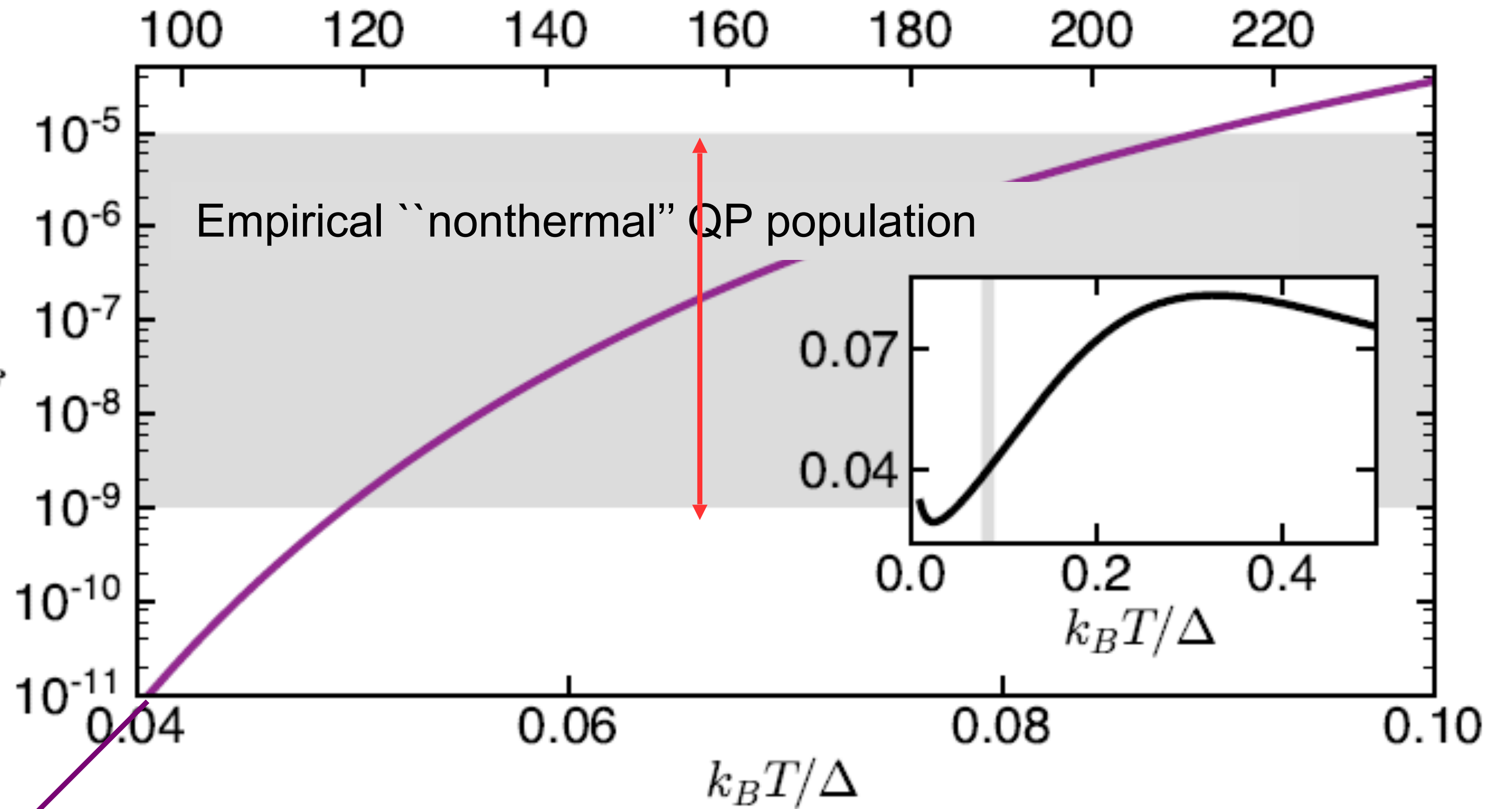


Quasiparticle Excitations – BCS theory vs Observation

Thermal population of Quasiparticles

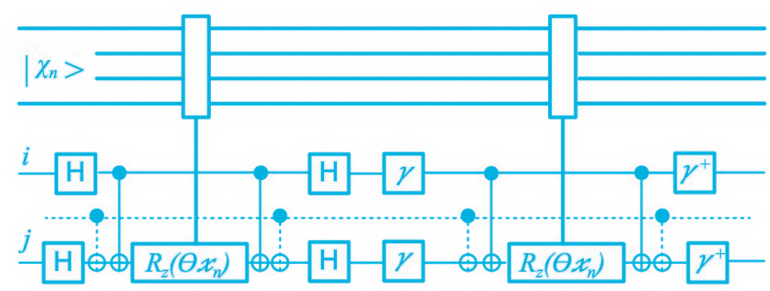
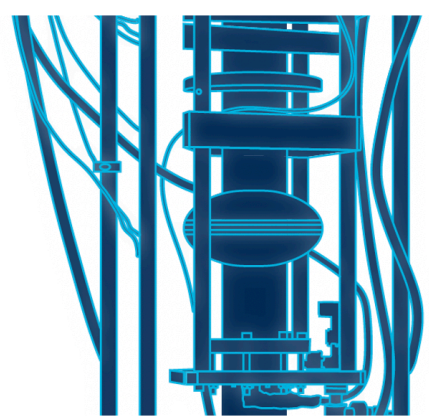
$$x_{QP}^{thermal} = \int_0^\infty d\varepsilon f(\varepsilon) N(\varepsilon) / N_n$$

T (mK) (assuming $\Delta_{Al} \approx 205 \mu\text{eV}$)

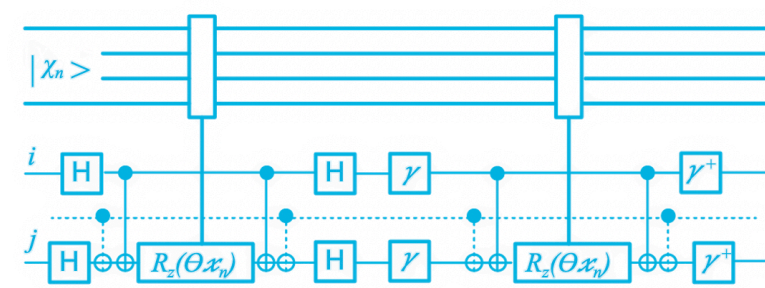
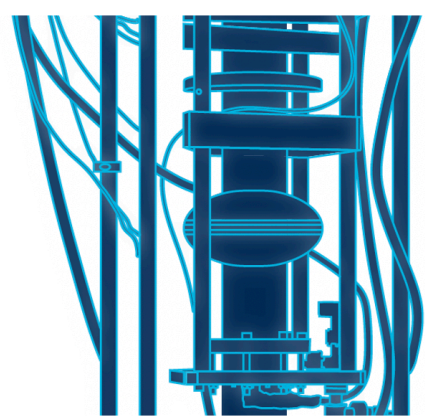


@ $T = 10$ mK

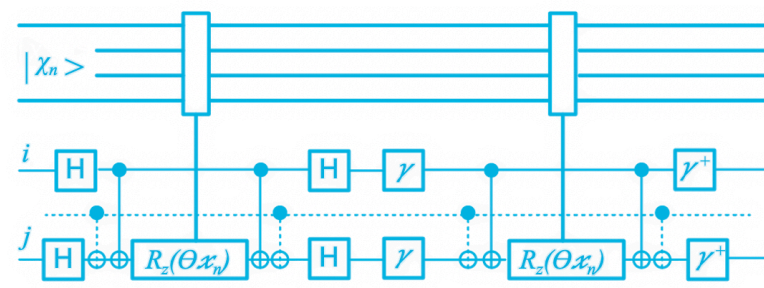
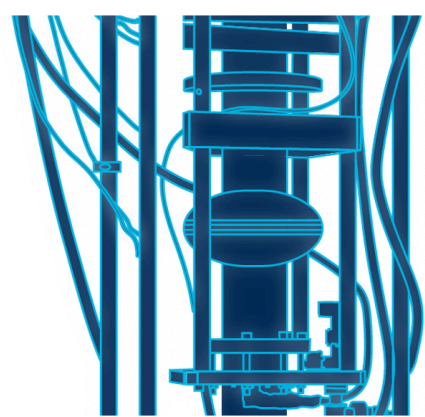
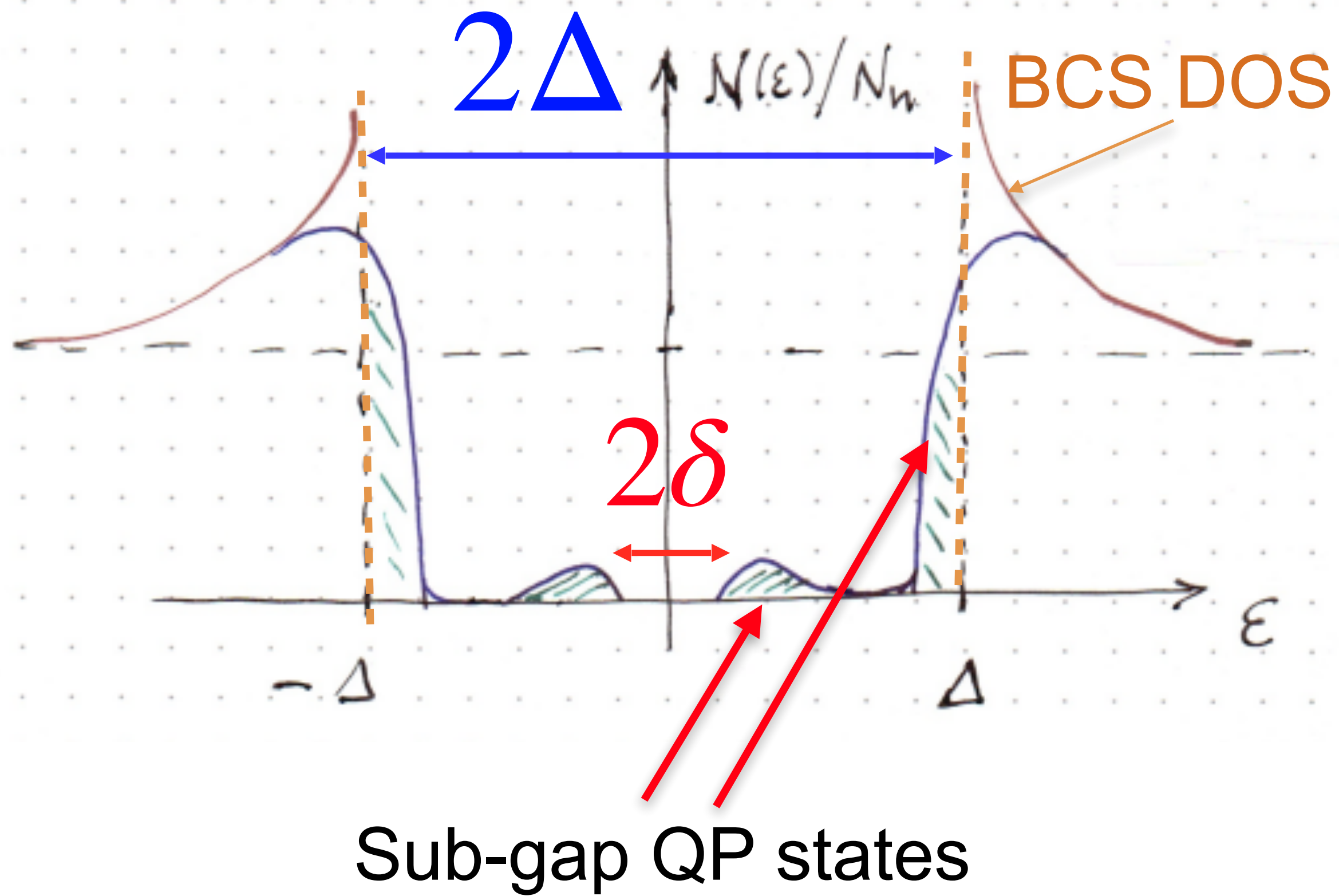
$$k_B T / \Delta_{Al} \approx 0.025$$



Quasiparticle Excitations (QPs) – Sources and Generation



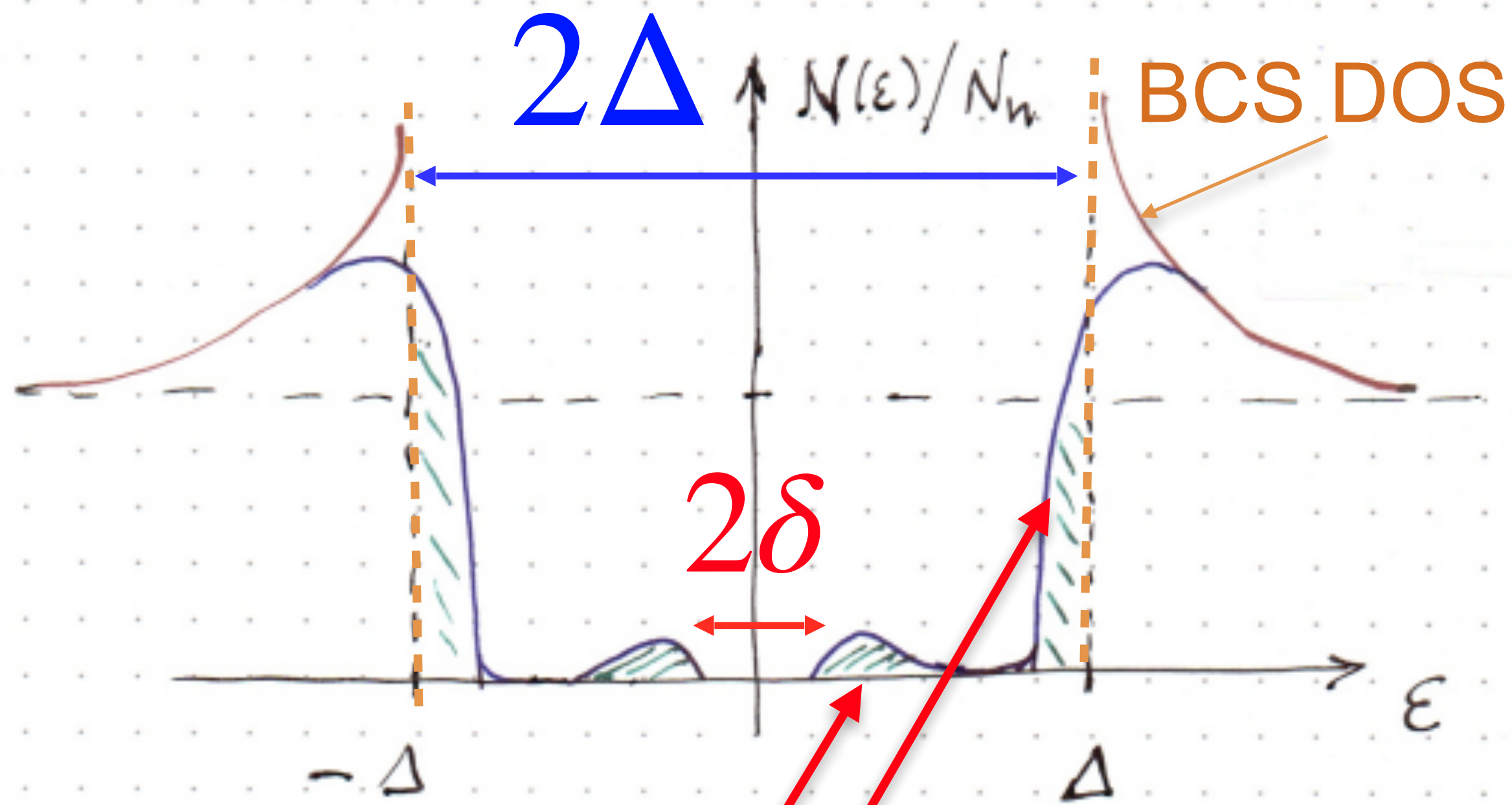
Quasiparticle Excitations (QPs) – Sources and Generation



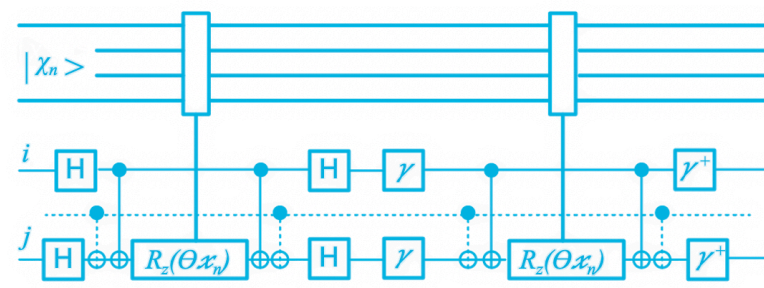
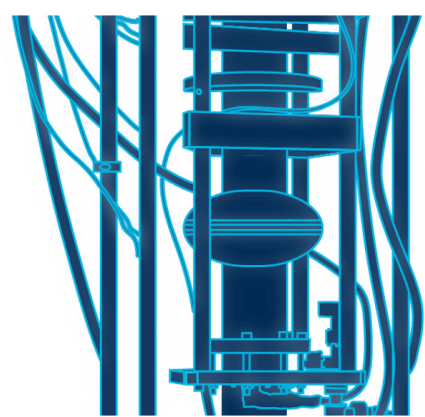
Quasiparticle Excitations (QPs) – Sources and Generation

Cooper Pair breaking Mechanisms

- Impurity scattering & $\Delta(\mathbf{p})$
 - Inhomogeneous $\Delta(\mathbf{r})$
- ↓
- Andreev Bound States



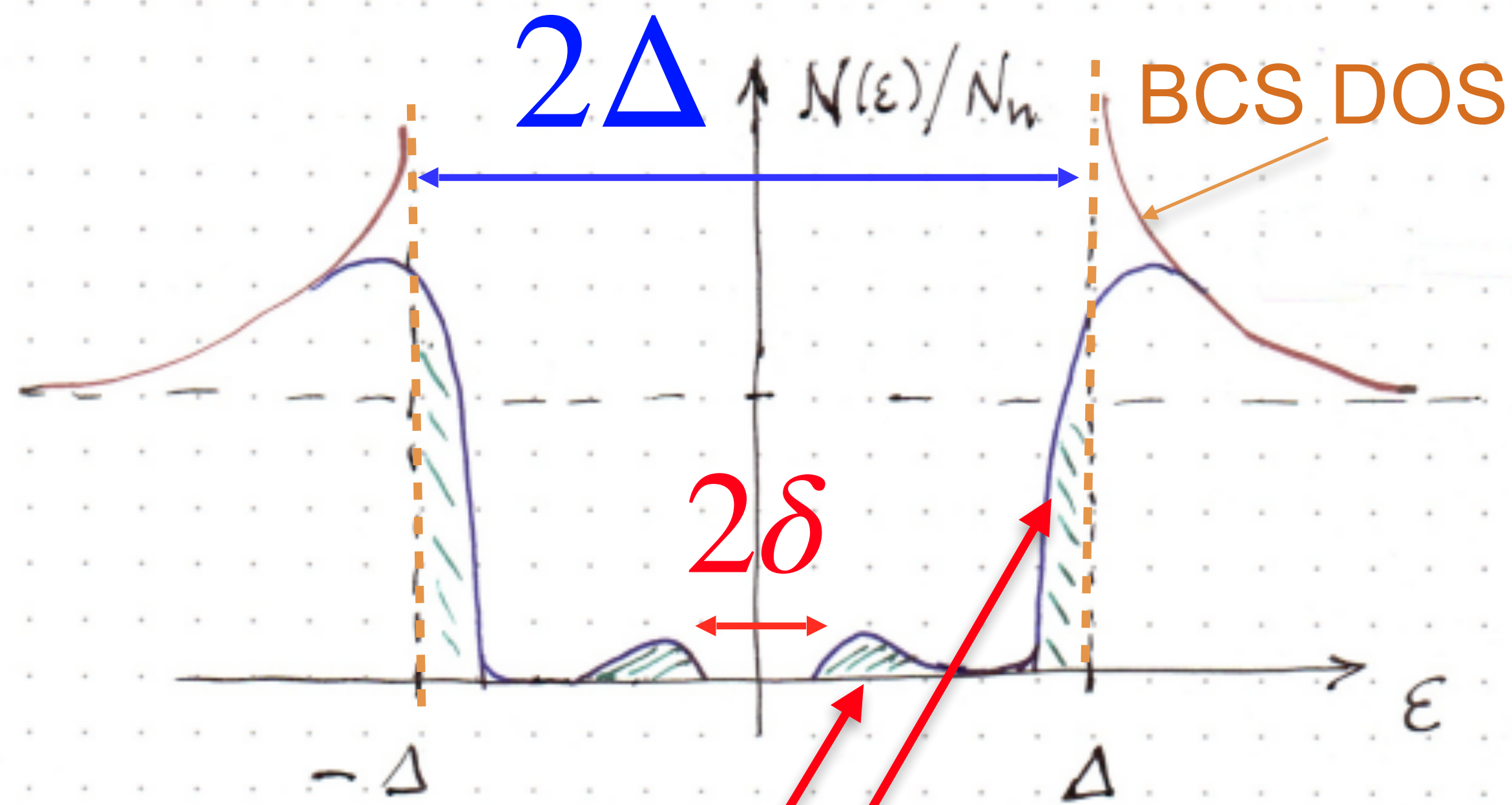
Sub-gap QP states



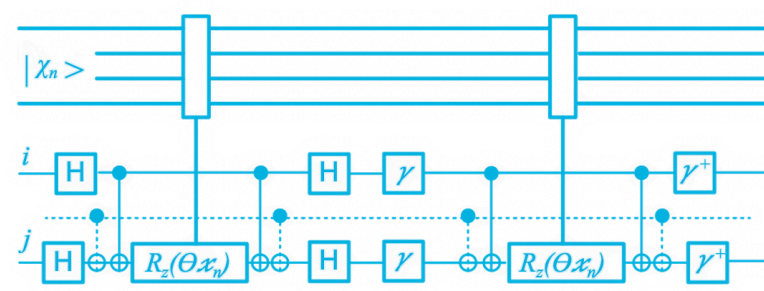
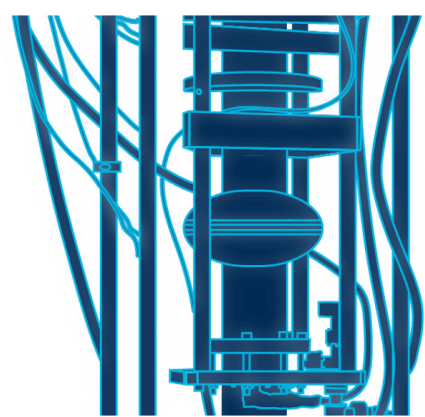
Quasiparticle Excitations (QPs) – Sources and Generation

Cooper Pair breaking Mechanisms

- Impurity scattering & $\Delta(\mathbf{p})$
- Inhomogeneous $\Delta(\mathbf{r})$
- ↓
- Andreev Bound States
- **Magnetic impurities**



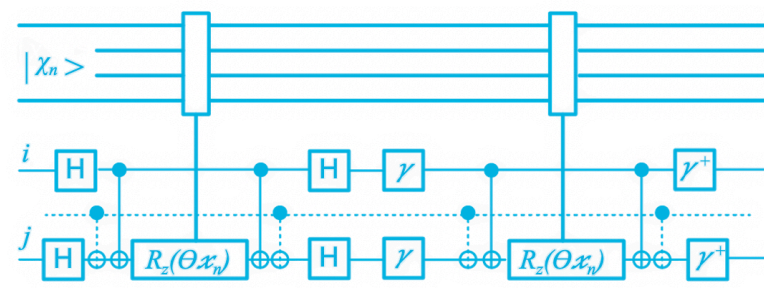
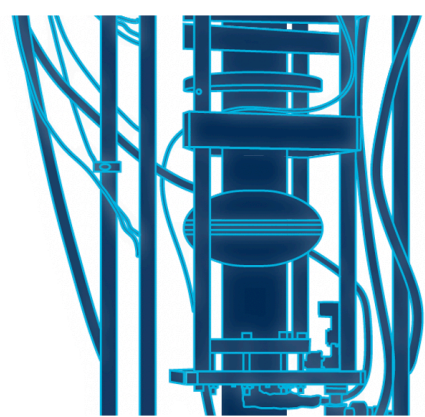
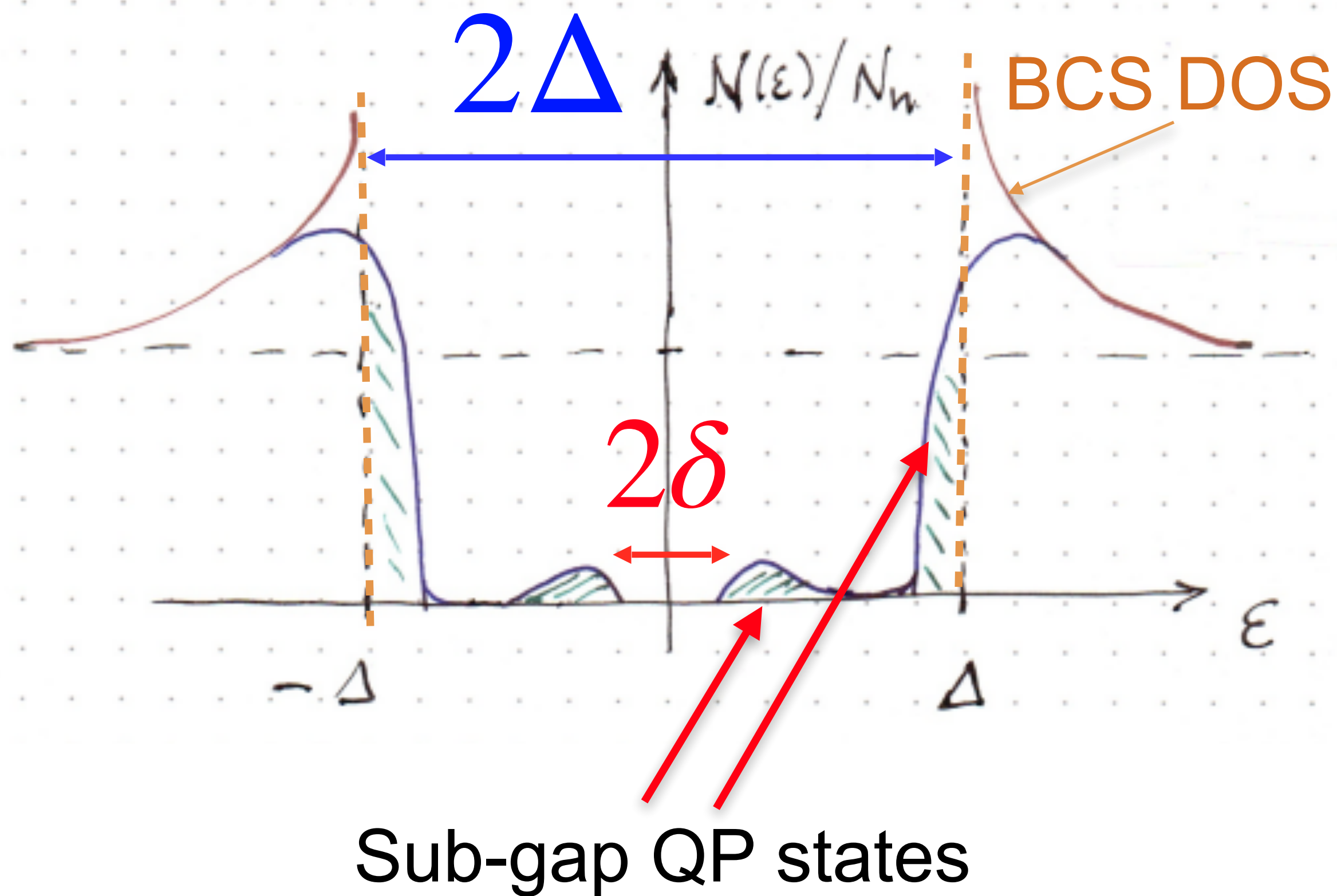
Sub-gap QP states



Quasiparticle Excitations (QPs) – Sources and Generation

Cooper Pair breaking Mechanisms

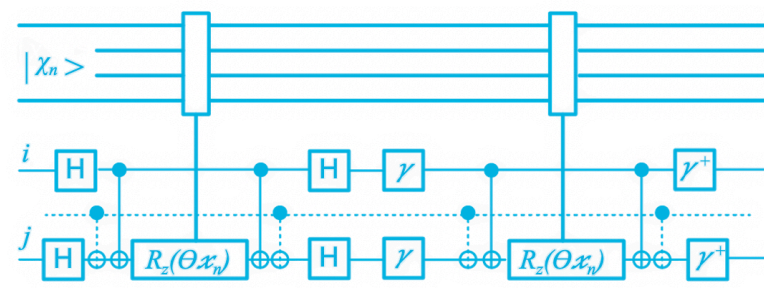
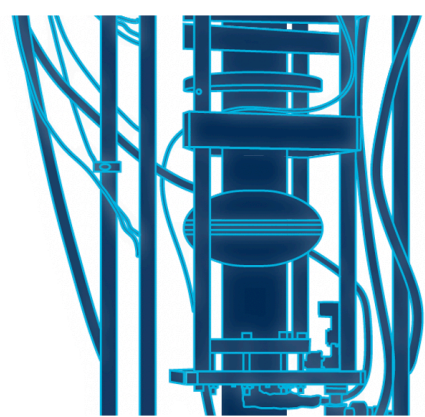
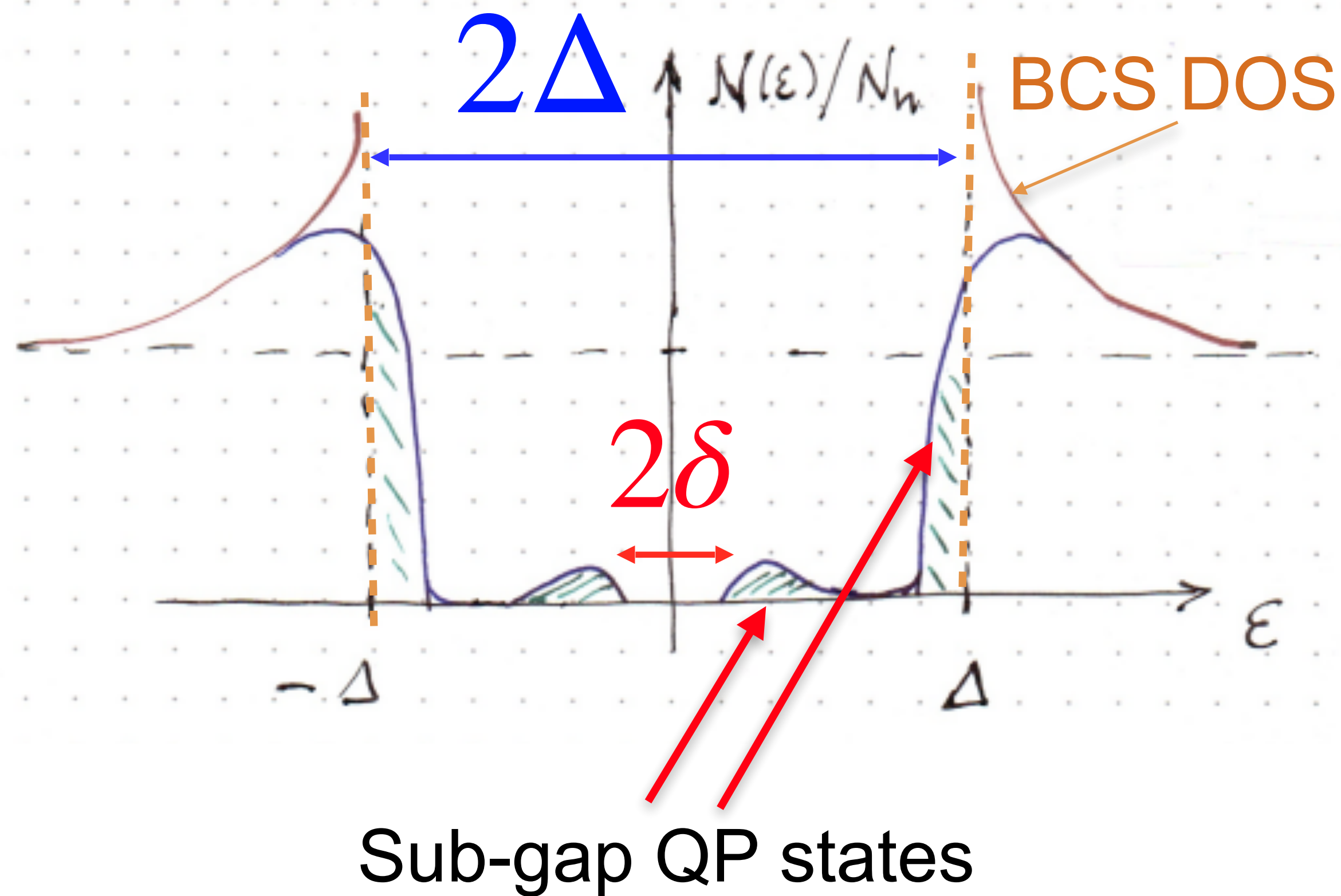
- Impurity scattering & $\Delta(\mathbf{p})$
 - Inhomogeneous $\Delta(\mathbf{r})$
- ↓
- Andreev Bound States
 - **Magnetic impurities**
 - **Dynamical Impurities (TLS[†])**



Quasiparticle Excitations (QPs) – Sources and Generation

Cooper Pair breaking Mechanisms

- Impurity scattering & $\Delta(\mathbf{p})$
 - Inhomogeneous $\Delta(\mathbf{r})$
- ↓
- Andreev Bound States
 - Magnetic impurities
 - Dynamical Impurities (TLS[†])
O, N, C, OH, NH ...



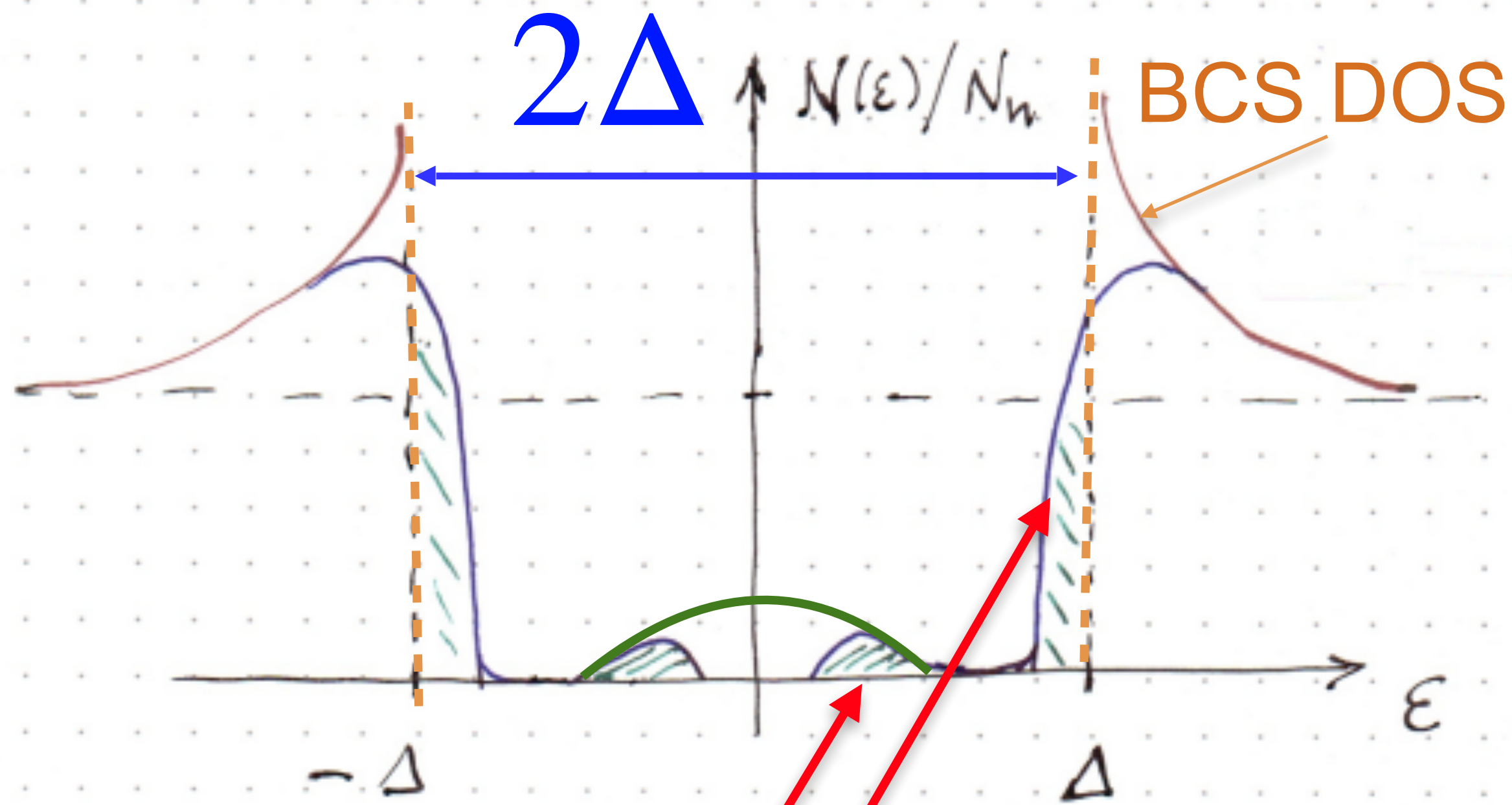
[†]impurity that tunnels between nearby sites



Quasiparticle Excitations (QPs) – Sources and Generation

Cooper Pair breaking Mechanisms

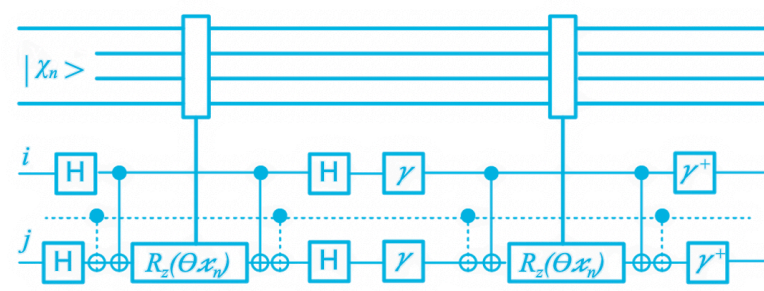
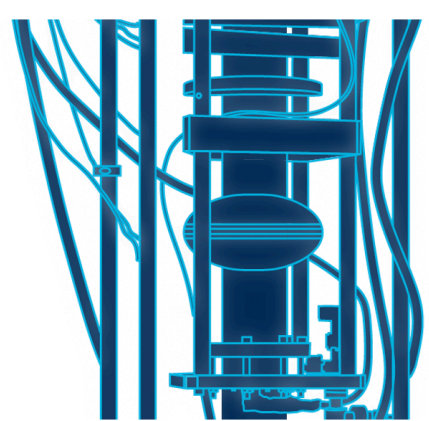
- Impurity scattering & $\Delta(\mathbf{p})$
 - Inhomogeneous $\Delta(\mathbf{r})$
- ↓
- Andreev Bound States
 - **Magnetic impurities**
 - **Dynamical Impurities (TLS[†])**
O, N, C, OH, NH ...



Sub-gap QP states

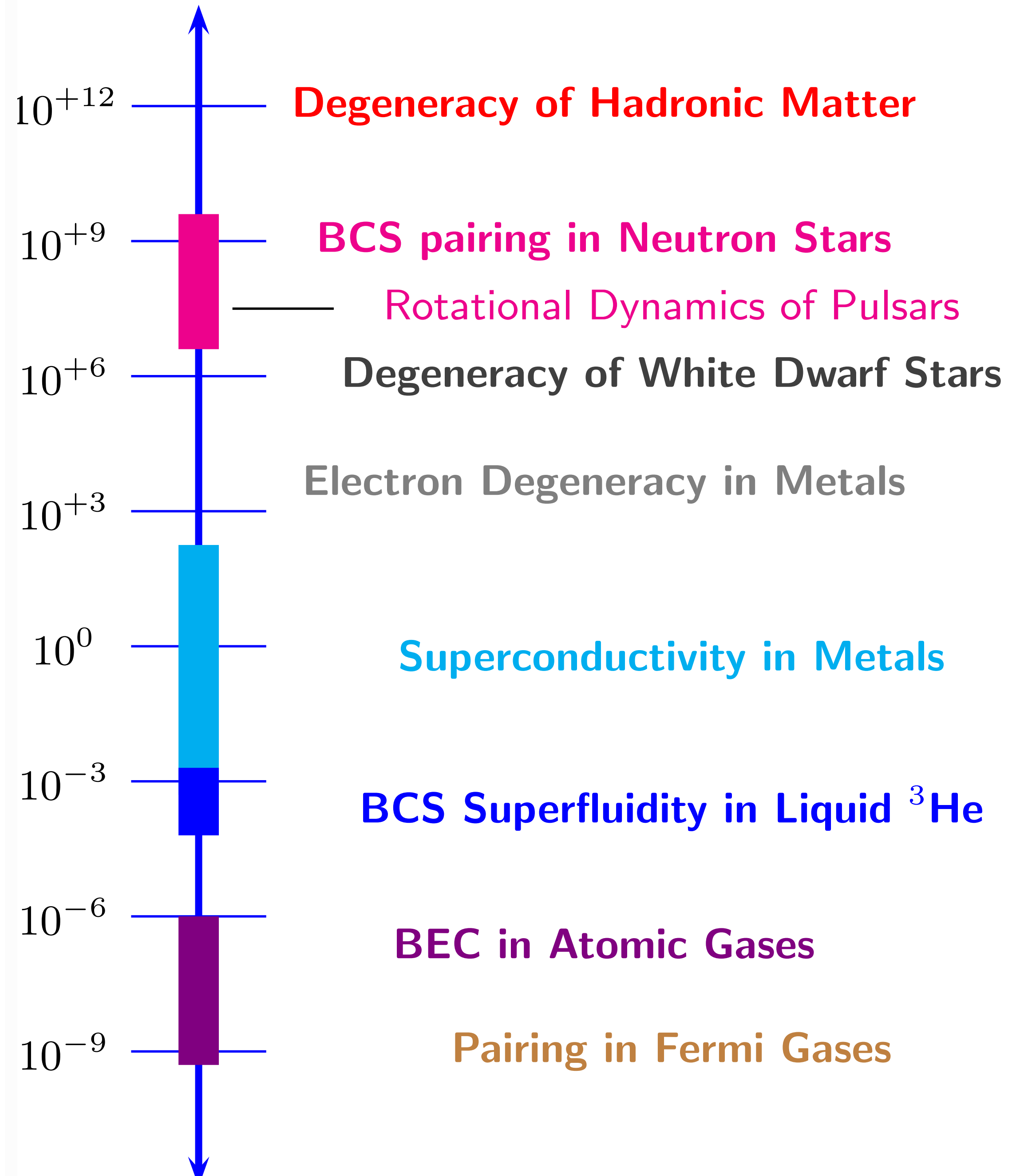
- Multi-photon (nonlinear μ -wave excitation)
- Radioactivity (INFN)
- **Nonequilibrium QP generation**

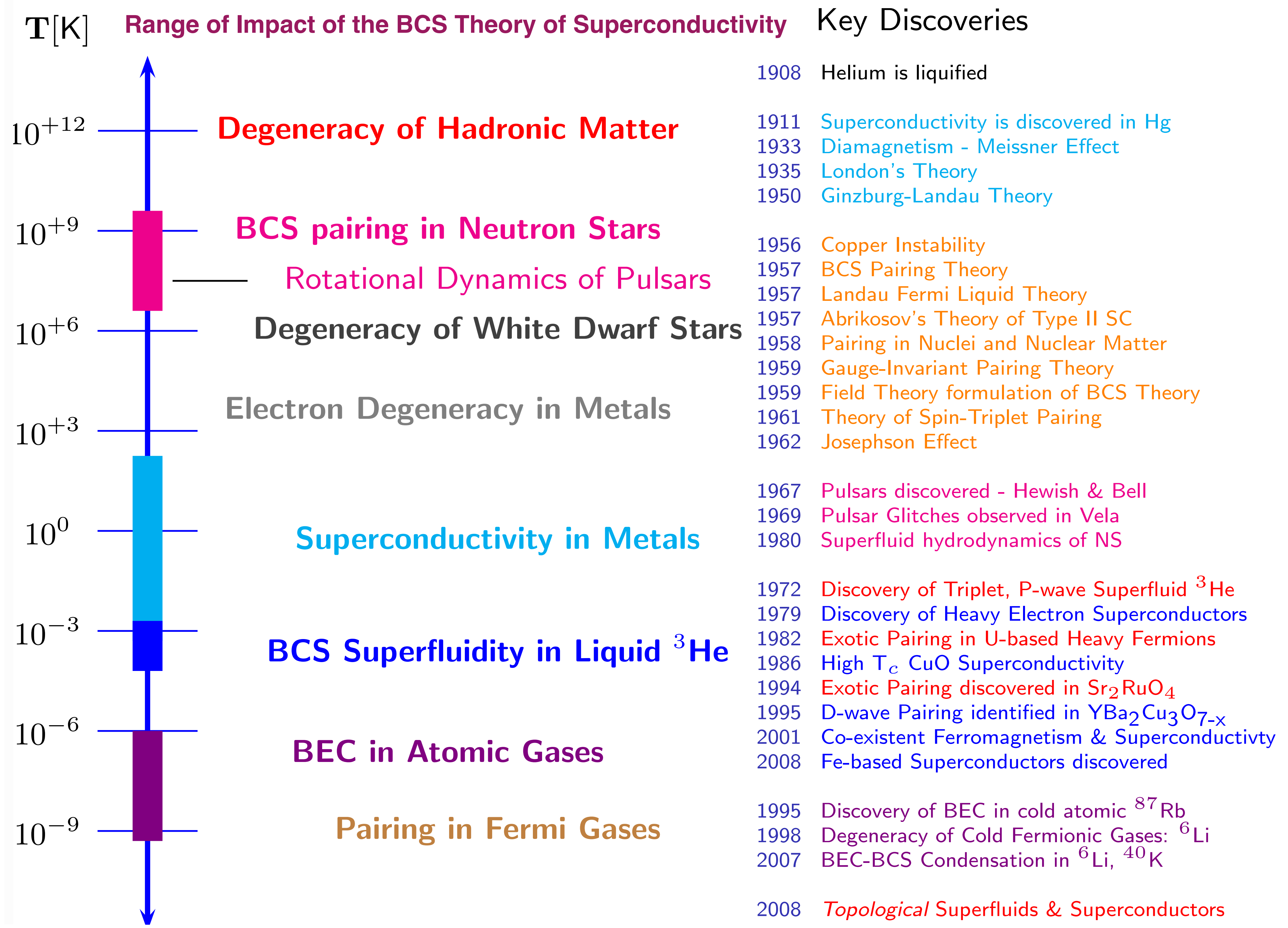
[†]impurity that tunnels between nearby sites



Range of Impact of the BCS Theory of Superconductivity

T[K] Range of Impact of the BCS Theory of Superconductivity





T[K]

10^{+12}

10^{+9}

10^{+6}

10^{+3}

10^0

10^{-3}

10^{-6}

10^{-9}

Degeneracy of Hadronic Matter

BCS pairing in Neutron Stars

Rotational Dynamics of Pulsars

Degeneracy of White Dwarf Stars

Electron Degeneracy in Metals

Superconductivity in Metals

BCS Superfluidity in Liquid ^3He

BEC in Atomic Gases

Pairing in Fermi Gases

1908 Helium is liquified

1911 Superconductivity is discovered in Hg

1933 Diamagnetism - Meissner Effect

1935 London's Theory

1950 Ginzburg-Landau Theory

1956 Copper Instability

1957 BCS Pairing Theory

1957 Landau Fermi Liquid Theory

1957 Abrikosov's Theory of Type II SC

1958 Pairing in Nuclei and Nuclear Matter

1959 Gauge-Invariant Pairing Theory

1959 Field Theory formulation of BCS Theory

1961 Theory of Spin-Triplet Pairing

1962 Josephson Effect

1967 Pulsars discovered - Hewish & Bell

1969 Pulsar Glitches observed in Vela

1980 Superfluid hydrodynamics of NS

1972 Discovery of Triplet, P-wave Superfluid ^3He

1979 Discovery of Heavy Electron Superconductors

1982 Exotic Pairing in U-based Heavy Fermions

1986 High T_c CuO Superconductivity

1994 Exotic Pairing discovered in Sr_2RuO_4

1995 D-wave Pairing identified in $\text{YBa}_2\text{Cu}_3\text{O}_{7-x}$

2001 Co-existent Ferromagnetism & Superconductivity

2008 Fe-based Superconductors discovered

1995 Discovery of BEC in cold atomic ^{87}Rb

1998 Degeneracy of Cold Fermionic Gases: ^6Li

2007 BEC-BCS Condensation in ^6Li , ^{40}K

2008 *Topological Superfluids & Superconductors*